Characterising Putative Effector Proteins of *Burkholderia pseudomallei*

Tanya Mary D'Cruze

B.Sc. (Biomed.) (Hons.)

A Thesis presented for the degree of

DOCTOR OF PHILOSOPHY

December 2011

Department of Biochemistry & Molecular Biology

Monash University

Clayton Campus, Melbourne 3800

Australia

“Education is the most powerful weapon which you can use to change the world”

Nelson Mandela

Notice 1

Under the Copyright Act 1968, this thesis must be used only under the normal conditions of scholarly fair dealing. In particular no results or conclusions should be extracted from it, nor should it be copied or closely paraphrased in whole or in part without the written consent of the author. Proper written acknowledgment should be made for any assistance obtained from this thesis.

Notice 2

I certify that I have made all reasonable efforts to secure copyright permissions for third-party content included in this thesis and have not knowingly added copyright content to my work without the owner's permission.

Table of Contents

Summary

Burkholderia pseudomallei, the aetiological agent of melioidosis, is classified as a category B bioterrorism agent (Stevens et al., 2004) by the United States Centre for Disease Control and Prevention. *B. pseudomallei* is an aerobic gram-negative saprophytic bacterium (Stevens et al., 2002), capable of dwelling in soil, stagnant water and rice paddies (Jones et al., 1996), in tropical climates. The bacterium is therefore endemic in parts of Thailand, northern Australia, Malaysia, Singapore, Vietnam and Burma (Wiersinga et al., 2006). Melioidosis was first described in Burma some 100 years ago (Whitmore and Krishnaswami, 1912). Infection is usually acquired through cutaneous inoculation – wounds and existing skin lesions (Wiersinga et al., 2006), or by inhalation or aspiration of contaminated water (Harland et al., 2007).

An epidemiological survey carried out between 1997 and 2006 in north-east Thailand estimated the incidence of melioidosis to be 21.31 cases per 100,000, per annum in endemic regions, with the mortality rate being 40.5% (Limmathurotsakul et al., 2010). This high mortality rate places *B. pseudomallei* infection as the third most common cause of death in north-east Thailand, after HIV/AIDs and tuberculosis (Limmathurotsakul et al., 2010). Despite the severity of the disease, there are no available vaccines, and limited antibiotic options, as *B. pseudomallei* exhibits resistance to traditionally used antibiotics. Further study into the pathogenesis and virulence of *B. pseudomallei* is essential in working towards an effective therapy for melioidosis.

Several *B. pseudomallei* virulence factors have been identified, including the capsule, pili, flagella, LPS, quorum sensing molecules, and Type Six and Type Three Secretory Systems

(T6/T3SS). Similar to other gram-negative bacteria such as *Salmonella typhimurium*, *Shigella flexneri* and *Yersinia enterocolitica, B. pseudomallei* employs its TTSS (Sun et al., 2005) to translocate virulence effectors into the host cell (Roversi et al., 2007). *B. pseudomallei* has three TTSS gene clusters (designated TTSS1, TTSS2 and TTSS3) each of these clusters is present on the small chromosome. Previous work has shown that TTSS1 and TTSS2 are not involved in *B. pseudomallei* virulence in a hamster infection model (Warawa and Woods, 2005). TTSS3 contains the *Burkholderia* Secretion Apparatus *(bsa*) locus which shares homology with the *S. typhimurium inv/spa/prg* TTSS (Sun et al., 2005), and the *S. flexneri ipa/mxi/spa* TTSS (Ogawa and Sasakawa, 2006b).

B. pseudomallei has been shown to invade either non-phagocytic (Stevens and Galyov, 2004), or phagocytic strains (Kespichayawattana et al., 2000). Prior to host cell invasion, the bacterium employs its TTSS3 to inject effector proteins into the host cytoplasm. Within 15 m of being phagocytosed into a host cell, bacteria escape from their phagosomes into the host cell cytoplasm by lysing the phagosomal membrane using the pre-secreted effector proteins (Wiersinga et al., 2006), and continue its infectivity cycle.

Invading bacteria, viruses, fungi and parasites can initiate the autophagic response in mammalian cells to eliminate the intracellular pathogens and liberate metabolites that may have been utilised during pathogen infection, thus promoting cell survival (Orvedahl and Levine, 2008). Following infection, microbes such as *B. pseudomallei*, *Listeria monocytogenes* and *S. flexneri* have been found to escape the phagosome and then avoid autophagic capture, replicate and spread (Ogawa and Sasakawa, 2006a).

The first component of this study was to conduct a literature search to identify virulence factors employed by bacteria to escape from their confining phagosomes. Initially, a list of 22 virulence factors was compiled. Bioinformatic analysis identified five of the corresponding 22 open reading frames (ORF) as sharing significant homology with a sequence within the *B. pseudomallei* genome, namely: *BPSS1531* (*bipC*), *BPSS1532* (*bipB*), *BPSL0670*, *BPSS1394* (*bpscN*) and *BPSS0670*. The available reports at that time also identified mutants defective in the *BPSS1529* (*bipD*) and *BPSS1539* genes as being confined to the phagosome. Hence these two genes along with the five above mentioned ORFs were selected for characterisation.

Based on reports using yeast to screen for putative bacterial effectors, the initial phase of characterisation involved amplification by PCR of each of the seven sequences encoding a *B. pseudomallei* ORF for expression in *Saccharomyces cerevisiae*. The primary screen was to observe any morphological or physiological changes conferred which arise under nutrient starvation (autophagic) conditions. Yeast strains also expressed either a cytosolic, mitochondrial or nucleus targeted Rosella biosensor. Each biosensor was composed of a pH-sensitive variant of green fluorescent protein (GFP) linked to a pH-stable variant of the red fluorescent protein, DsRed. When cells are subjected to autophagic conditions, delivery of the specific target organelle (for the relevant Rosella biosensor) to the vacuole results in accumulation of red fluorescence in the vacuole. The results indicated that each of the *B. pseudomallei* proteins, when expressed in yeast under nutrient starvation, was able to produce a multiple vacuolar morphology. The deficiency of red fluorescence in the vacuoles during starvation, suggested that the autophagy of cells expressing either the cytosolic or mitochondrial of those components was impaired. On the contrary, nucleus uptake during starvation, was identified through the accumulation of red fluorescence in the vacuoles. These

results suggested that expression of each *B. pseudomallei* ORF had effects on membrane events in yeast cells.

Given their influence on vacuole morphology and organelle turnover in *S. cerevisiae*, inactivation of each of these genes in the *B. pseudomallei* genome was attempted in order to determine any phenotype of mutant bacteria on infection of mammalian cells. Using the double cross-over allelic exchange method, three deletion mutants were successfully constructed in the *B. pseudomallei* K96243 strain, namely *BPSS1532* (*bipB)*, *BPSL0670* and *BPSS1394* (*bpscN)*. Despite concerted efforts, deletion mutations in the other four genes could not be constructed.

The BipB protein is a structural component of the TTSS needle. Using the *in vivo* relative growth assay, the *BPSS1532* mutant appeared to be only partially attenuated for virulence in mice. Subsequent analysis of bacterial survival and replication in cultured murine RAW264.7 GFP-LC3 macrophage-like cells showed no significant difference to wild-type bacterium over the 6 h infection period. Consistent with this finding, the level of co-localisation between mutant bacteria and GFP-LC3 decreased over 6 h essentially in parallel to wild-type bacteria. These results suggest that mutant bacteria are able to escape the phagosome and evade intracellular killing as efficiently as wild-type bacteria.

BPSL0670 is a putative cation transporter efflux protein. The *BPSL0670* deletion mutant was also found to be partially attenuated for virulence in BALB/c mice and showed diminished survival and replication compared to wild-type bacteria following infection of cells in culture.

A two-fold increase in the co-localisation of mutant bacteria with GFP-LC3 at 6 h p.i. (compared with wild-type bacteria) correlated with its decreased survival and replication.

BpscN is a putative type three secretion associated protein and a hypothetical ATPase. The *BPSS1394 – bpscN* mutant encoded in TTSS1 was attenuated for virulence in a mouse model of infection. Additional studies using cultured RAW264.7 macrophage-like cells showed that while mutant bacteria were able to escape from phagosomes, they showed diminished survival and replication in RAW264.7 cells, and increased levels of co-localisation with the autophagy marker protein LC3. Complementation data indicated that intracellular survival and replication could be restored to about 50% of wild-type levels, confirming that the loss of function of *bpscN* strongly influences survival and replication. Collectively the data provide strong evidence that the TTSS1 *bpscN* gene plays an important role in *B. pseudomallei* pathogenesis. This is the first research crediting the TTSS1 for its role in *B. pseudomallei* virulence and justifies further research into TTSS1 effector proteins.

This research aimed to identify and characterise potential virulence factors involved in the escape of *B. pseudomallei* from the phagosome in host cells. Deletion mutants were generated for the *BPSS1532*, *BPSL0670* and *BPSS1394* ORFs in the *B. pseudomallei* genome. The *BPSS1532* and *BPSL0670* mutants were found to be partially attenuated for virulence, whilst *BPSS1394* was fully attenuated for virulence in the BALB/c melioidosis infection model.

General Declaration

In accordance with Monash University Doctorate Regulations, the following declarations are made:

I hereby declare that this thesis contains no material which has been accepted for the award of any other degree or diploma at any university or other institution and affirm that, to the best of my knowledge and belief, this thesis contains no material previously published or written by another person, except where due reference is made in the text of the thesis.

This thesis contains three results chapters, compromising of two chapters (*Chapter 3* and *4*) with unpublished data and one original paper published in a peer-reviewed journal (*Chapter 5*). The core theme of the thesis is **characterising putative effector proteins of *Burkholderia pseudomallei***. The ideas, development and writing of the chapters in the thesis were the principal responsibility of me, the candidate, working within the Department of Biochemistry & Molecular Biology under the supervision of Prof. Rodney J. Devenish, Dr. Mark Prescott and Prof. Ben Adler.

The inclusion of co-authors reflects the fact that the work came from active collaboration between researchers and acknowledges input into team-based research.

A declaration for the published work (*Chapter 5*) is provided preceding that chapter. In the case of chapters 3 and 4, I was solely responsible for the collection of data. I was primarily responsible for data analysis and interpretation. A contribution to the conception of experimental questions and interpretation of data was made by Prof. Rodney J. Devenish, Dr. Mark Prescott, Prof. Ben Adler and Dr. John D. Boyce.

Thesis Chapter	Publication Title	Publication Status	Candidate's Contribution
3	Screening putative bacterial virulence effectors in yeast	Not published	All experimentation & data collection; data analysis & interpretation; writing & editing of manuscript
4	Generating and characterising deletion mutants in *B. pseudomallei*	Not published	All experimentation & data collection; data analysis & interpretation; writing & editing of manuscript
5	Role for the *Burkholderia pseudomallei* Type Three Secretion System Cluster 1 bpscN Gene in Virulence	Published	All experimentation & data collection; data analysis & interpretation; writing & editing of manuscript

Signed: .....

Dated: .....

Acknowledgements

My PhD candidature has been a challenging and rewarding journey whereby successful experiments, expanding knowledge and close friendships constituted the highs, and failed experiments, long endless days and tremendous stress constituted the lows. This thesis represents the culmination of years of hard work which could not have been conceivable had it not been for the most brilliant supervisors, amazing staff and fellow colleagues whose guidance, wisdom and support have meant a great deal to me.

Effective supervision is pivotal in a student's path to successful completion. I was fortunate to have the opportunity to work with four of the finest supervisors in this institute. To my principal supervisor, Professor Rod Devenish, you have always been knowledgeable, patient, nurturing, tolerant and encouraging. In many ways, I strived to follow in your footsteps. As I continue my scientific journey, I know I will always consider you as my role model. Dr. Mark Prescott, I thank you for always having faith in me. On many occasions when I ran to your office in despair, you gave me advise, encouragement and direction. Professor Ben Adler and Dr. John Boyce, I appreciate you welcoming me into your lab and giving me the support I needed to complete my research, your assistance with editing and your advise have been invaluable.

I extend my sincere gratitude to all the members of the Yeast, Fluorescent and Microbiology labs. Dr. Marina Harper, I am grateful that you included and adopted me as your student. Dr. Lan Gong and Dr. Xuelei Li, I thank you for your assistance in the lab and pertinent discussions about research protocols. Dr. Dalibor Mijaljica, it was a privilege to share an office with you. You have been a great support to me and helped me to develop positive values in life and for that I thank you. Dr. Anne Pettikiriarachchi, Craig Don Paul and Alisha Lai, I have always valued your friendship. June Bug, you are a true friend and my sunshine on the rainy days. Your optimism and motivation has aspired me to persevere and never give up. Marietta, your friendship is special to me. Priya, I always enjoyed taste testing your cooking. To our late friend James Marchant, whose profound ideas are years ahead of his time, you will always be remembered as a sweet person.

To the wonderful women in SOBS, I will forever be grateful to you. Vickie Valance and Saw Eng Tan, thank you for your motherly advice and displaying excellent organisational skills in the lab. I am truly honoured to have met you. Irene Hatzinisiriou, thank you for always being obliging with imaging requests. Reenu Johnston, I am grateful for your never ending efforts to keep my name active on the Monash database. To the teaching staff, Janet Macaulay, Nirma Samarawickrema, Oanh Ho and Lina D'Agruma, I thank you for your friendship and I admire your dedication to your teaching in the under graduate program. I appreciate the efficiency by which Maxine Rebstadt, Darryl Fowler and Winston Galea processed and delivered my urgent orders.

To my friends Danielle, Ally and Denuja, you have always been there for me and I am truly thankful. To my parents, I thank you for always working hard to ensure we got the best possible education. From a young age, you taught me the value of education, and for that I will be eternally grateful. To my sister Deodrin, you are my rock, you empowered me to strive for excellence and always supported me. I sincerely thank you for your help in conferencing my thesis. To my brother Justin, you are my inspiration. You have always been obliging in lending your artistic talent to creating diagrams, formatting presentations and editing my thesis. I am forever grateful to you. I also wish to thank my grandparents, sister Cordelia and brother Jude for shining down on me from Heaven, you have always protected me. I extend my appreciation and gratitude to my brother-in-law Jude for his guidance through my journey. Lastly, to my partner Matthew, thank you for your overwhelming support in my research and understanding the demands of science. Your support, advice and encouragement has contributed to making this journey a rewarding experience.

Most importantly, I wish to thank God for granting me this experience and helping me to successfully reach the end of my PhD journey.

Publications

Journal Publications:

D'Cruze, T., Gong, L., Treerat, P., Ramm, G., Boyce, J. D., Prescott, M., Adler, B. & Devenish, R. J., 2011, Role for the *Burkholderia pseudomallei* Type Three Secretion System Cluster 1 *bpscN* Gene in Virulence. *Infect. Immun.,* 79**,** 3659-3664. **(Chapter 5)**

D'Cruze, T. & Devenish, R. J., 2011, Autophagy as a defence mechanism against bacterial pathogens. *Australian Biochemist,* 42**,** 11-13. **(Appendix)**

Conference Proceedings:

D'Cruze T., Adler, B., Prescott, M., Devenish R., 2007, Proteins influencing the extracellular pathogen *Burkholderia pseudomallei* to evade the host's immune response, *32nd Lorne Conference on Protein Structure and Function,* Lorne.

D'Cruze T., Adler, B., Prescott, M., Devenish R., 2007, Expression of *Burkholderia pseudomallei* proteins in yeast can affect vesicle trafficking and vacuolar morphology, *XXIII International Conference on Yeast Genetics & Molecular Biology,* Melbourne.

D'Cruze T., Adler, B., Prescott, M., Devenish R., 2007, Expression of *Burkholderia pseudomallei* proteins in yeast can affect vesicle trafficking and vacuolar morphology, *World Melioidosis Congress 2007,* Khon Kaen.

Abbreviations and Definitions

μg	Microgram
μL	Microlitre
μM	Micromolar
3-MA	3- Methyladenine
ALP	Alkaline phosphatase
ANOVA	Analysis of Variance
ATG/Atg	Autophagy gene/protein
ATP	Adenosine triphosphate
Bap	*Bsa* associated protein
B. abortus	*Brucella abortus*
B. cepacia	*Burkholderia cepacia*
β-gluc	**β**-glucan
Bim	*Burkholderia* intracellular motility
Bip	*Burkholderia* invasion protein
BLAST-n	Basic Local Alignment Search Tool-nucleotide
B. mallei	*Burkholderia mallei*
Bop	*Burkholderia* outer protein
bp	Base pairs
B. pseudomallei	*Burkholderia pseudomallei*
bsa	*Burkholderia* secretion apparatus
B. thailandensis	*Burkholderia thailandensis*
°C	Degrees Celsius
C. brunetii	*Coxiella brunetii*
CDT	Cytolethal distending toxin
CFU	Colony forming unit

CI	Competitive index
CIAP	Calf intestine alkaline phosphatise
CIS	Cytokine-inducible Src
CLR	C-type lectin receptors
CMI	Cell mediated immune
Cm^R	Chloramphenicol resistance
CpG	Cytosine-phosphate-guanine
CPY	Carboxypeptidase Y
DAP	Diaminopimelic acid
DMSO	Dimethyl sulfoxide
DNA	Deoxyribonucleic acid
dsRNA	Double stranded ribonucleic acid
E-value	Expected value
ECL	ElectroChemiLuminescence
E. coli	*Escherichia coli*
EM	Electron microscopy
ER	Endoplasmic reticulum
Esp	*Escherichia* secretion protein
F. tularensis	*Francisella tularensis*
g	Grams
GAS	Group A *Streptococcus*
GC	Guanine Cytosine
GFP	Green fluorescent protein
GTP	Guanosine triphosphate
h	Hour(s)
HA	Haemagglutinin

HOG	Hyperosmotic growth
HOP	Homotypic fusion and vacuole protein sorting
IFN-γ	Interferon-γ
IL	Interleukin
iNOS	Inducible nitric oxide synthase
IP	Inducible protein
Ipa	Invasion plasmid antigens
Ipg	Invasion plasmid gene
kDa	kiloDalton
kPa	Kilopascals
L	Litre
LAMP-1	Lysosomal associated membrane protein-1
LAP	LC3-associated phagocytosis
LB	Luria-Bertani broth
LC3	Light chain-3
LE	Late endosome
LipoProt	Lipoproteins
LLO	Listeriolysin O
LMA1	Low-M_r activities
L. monocytogenes	*Listeria monocytogenes*
LN	Late nucleophagy
L. pneumophilia	*Legionella pneumophilia*
LPS	Lipopolysaccharide
m	Minute(s)
M	Molar
MAPK	Mitogen-activated protein kinase

Mb	Mega base pairs
MCV	Mycobacterium-containing vacuoles
MDP	Muramyl dipeptide
MGTBE	Magnesium Tris-Borate-EDTA
MHC	Major histocompatibility complex
Mig	Monokine induced by IFN-γ
mL	Millilitre
mM	Millimolar
MNGC	Multinucleated giant cells
MOI	Multiplicity of infection
M. tuberculosis	*Mycobacterium tuberculosis*
MVB	Multivesicular body
NK	Natural killer
NLR	NOD-like receptors
ng	Nanograms
nm	Nanometre
NO	Nitric oxide
NOD	Nucleotide-binding and oligomerisation domain
NV	Nucleus-vacuole
N-WASP	Wiskott-Aldrich syndrome protein
OD_{600}	Optical density at 600 nm
OMP	Outer membrane protein
ORF	Open reading frames
PAGE	Polyacrylamide gel electrophoresis
PAMP	Pathogen-associated molecular patterns
PBS	Phosphate buffer saline

PCR	Polymerase chain reaction
PEPSY	Pathogen effector protein screening in yeast
PFA	Paraformaldehyde
PG	Peptidoglycan
P. gingivalis	*Porphymonas gingivalis*
pH	Potential of hydrogen
p.i.	Post infection
PMN	Piecemeal microautophagy of the nucleus
pmole	Picomole
PRR	Pattern recognition receptors
PVC	Prevacuolar compartment
R. conorii	*Rickettsia. conorii*
rCI	Relative competitive index
RE	Restriction enzyme
RFP	Red fluorescent protein
RIG-1	Retinoic acid-inducible gene 1
RLR	Retinoic acid-inducible gene 1 - like receptors
rmp	Revolutions per minute
RNI	Reactive nitrogen intermediate
ROI	Reactive oxygen intermediates
RPMI	Roswell Park Memorial Institute
R. rickettsia	*Rickettsia rickettsia*
RT	Room temperature
RT-PCR	Reverse transcription – polymerase chain reaction
s	Second(s)
S. cerevisiae	*Saccharomyces cerevisiae*

S. flexneri	*Shigella flexneri*
sct	Secretion and cellular translocation genes
SDS-PAGE	Sodium dodecyl sulfate-polyacrylamide gel electrophoresis
Sip	*Salmonella* invasion protein
SLO	Streptolysin O
SOCS3	Suppressor of cytokine signalling 3
Sop	*Salmonella* outer protein
SSM	*Saccharomyces* salts medium
ssRNA	Single-stranded ribonucleic acid
S. typhimurium	*Salmonella typhimurium*
TEM	Transmission electron microscopy
Tet-R	Tetracycline resistance
TLR	Toll-like receptors
TNF-α	Tumour necrosis factor α
TOR	Target of rapamycin
T6SS	Type six secretion System
TTSS	Type three secretion system
TTSS1	Type three secretion system cluster 1
TTSS2	Type three secretion system cluster 2
TTSS3	Type three secretion system cluster 3
v/v	Volume/volume
V-ATPase	Vacuolar H^+-ATPase
Vip	VPS inhibitor protein
vps	Vacuole protein sorting
w/v	Mass/volume
Yad	*Yersinia enterocolitica* auto-secreted adhesin

Y. enterocolitica	*Yersinia enterocolitica*
YEPD	Yeast extract-Peptone-Dextrose
YMM	Yeast minimal medium
Yop	*Yersinia* outer protein
Ypk	*Yersinia* protein kinase

CHAPTER ONE

INTRODUCTION

1.1 *BURKHOLDERIA PSEUDOMALLEI*

There are over 30 species belonging to the *Burkholderia* genus, with the most pathogenic being *B. pseudomallei, B. mallei,* and *B. cepacia* (Wiersinga et al., 2006). The ability of *B. pseudomallei* to invade cells, survive and replicate within phagocytes, together with its severe clinical manifestations (Stevens et al., 2004), have led to it being classified as a category B bioterrorism agent (Stevens et al., 2004) by the United States Centre for Disease Control and Prevention.

1.1.1 Geographical Distribution

B. pseudomallei is an aerobic gram-negative saprophytic bacterium (Stevens et al., 2002) found in tropical climates; capable of dwelling in soil, stagnant water and rice paddies (Jones et al., 1996). The bacterium is therefore endemic in parts of Thailand, northern Australia, Malaysia, Singapore, Vietnam, Burma (Wiersinga et al., 2006) and Indonesia (*Figure 1.1* Currie et al., 2008).

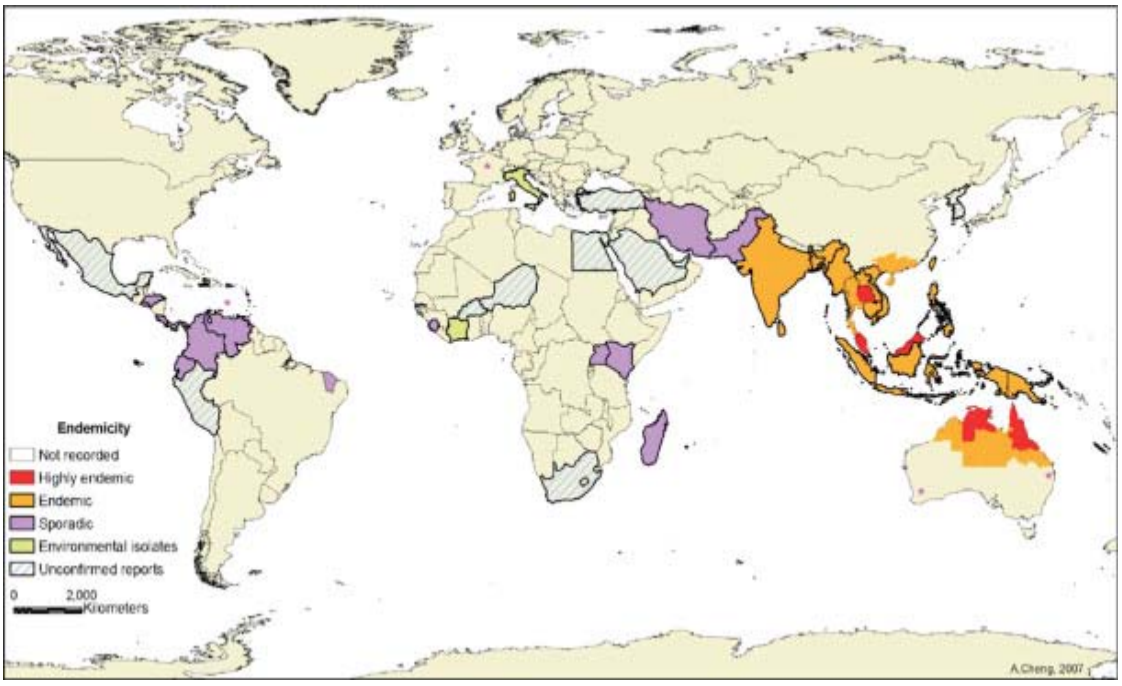

Figure 1.1: Geographical distribution of *B. pseudomallei* (Currie et al., 2008). Highly endemic areas in south-east Asia and north Australia are highlighted in red. Endemic and sporadic areas are graphed in orange and purple respectively.

1.1.2 Melioidosis

B. pseudomallei is the causative agent of melioidosis (Wiersinga et al., 2006), a disease which was first described in Burma in 1912 (Whitmore and Krishnaswami, 1912). More recently, melioidosis has emerged as an infectious disease (Stevens and Galyov, 2004) found in humans, sheep, goats and pigs (Wattiau et al., 2007). Infection is usually acquired from cutaneous inoculation through wounds and existing skin lesions (Wiersinga et al., 2006), or by inhalation of organisms, and aspiration of contaminated water (Harland et al., 2007). Since the bacteria is prevalent in tropical areas, the occurrence of melioidosis is seasonal – with most cases being reported in the rainy season (Wiersinga et al., 2006). Outbreaks are also associated with severe weather events such as cyclones and tsunamis (Novak et al., 2006).

In endemic areas where exposure to the bacteria is common, 80% of residents acquire antibodies against *B. pseudomallei* by the age of 4 years (Wiersinga et al., 2006). However, one episode of melioidosis does not guarantee future immunity against the bacterium as secondary infection is possible (Wiersinga et al., 2006). Those most susceptible to the infection also tend to have pre-existing conditions such as diabetes, renal insufficiency, cirrhosis, alcoholism or thalassemia (Apisarnthanarak et al., 2006).

1.1.2.1 Clinical Manifestations

B. pseudomallei is often referred to as the 'great mimicker' as the clinical manifestations of infection mirror those of other infections and often lead to misdiagnosis (Wiersinga et al., 2006). The clinical manifestations most often associated with *B. pseudomallei* infection include septic shock, pulmonary infections (*Figure 1.2*), skin abscesses, benign pulmonitis, acute or chronic pneumonia (Sun et al., 2005), pneumonia with septicemia, septic arthritis, prostatic abscess, cerebral abscess, meningoencephalitis, encephalomyelitis, suppurative parotitis and conjunctival ulcers (Inglis et al., 2006). The onset of acute septicemia, affecting organs throughout the body, may result in death within few days of exposure (Utaisincharoen et al., 2006).

Figure 1.2: A study carried out on patients in Sappasithiprasong Hospital, Thailand, between January 1992 and December 2001. Chest radiography data obtained from 573 melioidosis patients revealed that 88% had chest abnormalities (Veld et al., 2005).

1.1.3 Latency

B. pseudomallei is a facultative bacterium, capable of surviving in soil and water with an altered metabolism for long periods of time (Gan, 2005). The incubation period can range from two days to 26 years (Jones et al., 1996). Following infection, *B. pseudomallei* can reside in macrophages for months or years in a dormant stage (Jones et al., 1996). The longest reported period between infection and clinical manifestations is 62 years (Ngauy et al., 2005).

1.1.4 Incidence and Mortality

An epidemiological survey carried out between 1997 and 2006 in north-east Thailand estimated the incidence of melioidosis to be 21.31 cases per 100,000, per annum in endemic regions (Limmathurotsakul et al., 2010). This rate of incidence has significantly increased from the 8.0 incidence reported in the year 2000 (Limmathurotsakul et al., 2010). However, actual numbers may be higher due to misdiagnosis, since *B. pseudomallei* infection can mimic other disorders (Stevens et al., 2002). Following the December 26th tsunami in 2004, survivors in Thailand may have been at an increased risk of acquiring melioidosis. Phangnga was the worst affected of the four Thai provinces by the tsunami - within one day there were approximately 1,000 patients admitted to the general hospital with clinical manifestations of *B. pseudomallei* infections (Wuthiekanun et al., 2006). Whilst the incidence rate has increased between 1997 to 2006 in north-east Thailand, the mortality rate has decreased from 49% in 1997, to 40.5% in 2006 and has been attributed to improvements in the standard of medical care provided (Limmathurotsakul et al., 2010). Nevertheless, this high mortality rate places

B. pseudomallei infection as the third most common cause of death in north-east Thailand, after HIV/AIDs and tuberculosis (Limmathurotsakul et al., 2010).

A study carried out by the Royal Darwin Hospital in Australia over a period of 20 years – commencing in 1989, has also found that the morality rate in melioidosis patients decreased, from 30% in the first five years to 9% in the last five years of the study (Currie et al., 2010). The decrease in mortality rate in this study also attributed to earlier diagnosis and improvements in the intensive care management (Currie et al., 2010).

1.2 HOST IMMUNE RESPONSE TO INFECTION

The encountering of foreign microbes activates the host's innate and adaptive immune responses. Following *B. pseudomallei* infection, the wild-type bacterium induces an immune response that activates a number of components such as, Toll-Like Receptors (TLRs) on monocytes and granulocytes (Wiersinga et al., 2007), T-cells and Natural Killer (NK) cells.

1.2.1 Toll-Like Receptors

B. pseudomallei, like all other foreign organisms has conserved surface motifs termed Pathogen-Associated Molecular Patterns (PAMPs). The PAMPs, which generally include nucleic acids (CpG, ssRNA, dsRNA), proteins (flagellin), lipids and cell wall components (LPS, LipoProteins, PG, MDP, DAP, β-gluc), interact with membrane or

cytosolic Pattern Recognition Receptors (PRR) to activate either toll-like receptors (TLR), C-type lectin receptors (CLR), retinoic acid-inducible gene 1 (RIG-1)-like receptors (RLR) or nucleotide-binding and oligomerisation domain (NOD)-like receptors (NLR) (Delgado and Deretic, 2009).

Currently, eleven TLRs have been characterised - TLRs 1, 2, 4, 5 and 6 are associated with cell surface and recognise bacterial components, while TLRs 3, 7, 8 and 9 are associated with endocytic compartments and recognise viral components (Delgado and Deretic, 2009). *B. pseudomallei* peptidoglycan, LPS, flagellin and DNA, bind to TLR2, -4, -5 and -9 respectively (Wiersinga et al., 2006). A study by Wiersinga and colleagues (2006) found that monocytes cultured from melioidosis patients had increased TLR2 and TLR4 expression (West et al., 2008).

1.2.2 Proinflammatory Mediators

The establishment of an infection initiates several immune responses, one of which is the mass production the pro-inflammatory cytokine interferon (IFN)-γ. The induction of IFN-γ aids in the elimination of *B. pseudomallei* by activating T cells and natural killer (NK) cells, thus further promoting the cell-mediated immune response (Lazar Adler et al., 2009). Alternatively, the immune response initiated by IFN-γ may be reduced through activation of the Suppressor of Cytokine Signalling 3 (SOCS3) by cytokines and hormones associated with insulin resistance (Senn et al., 2003) and Cytokine-Inducible Src homology 2-containing protein (CIS), thus assisting the bacterium to evade intracellular killing in phagocytic cells (Ekchariyawat et al., 2005). Serum samples derived from patients with melioidosis, also show elevated

levels of the pro-inflammatory mediators IL-6, IL15, IFN-γ-inducible protein (IP)-10, monokine induced by IFN-γ (Mig), and the anti-inflammatory cytokine IL-10 (Wiersinga et al., 2006).

1.3 OVERVIEW OF LIFE CYCLE

In *in vitro* studies, *B. pseudomallei* has been shown to invade non-phagocytic cells such as epithelial cell lines, for example HeLa, CHO, A549 and VERO (Stevens and Galyov, 2004), or phagocytic cells such as macrophage cell lines, for example RAW 264.7 and J774A.1 (Kespichayawattana et al., 2000). The current view is that the bacterium constructs a macromolecular structure resembling a hollow syringe to traverse the bacterial inner and outer membranes (Zhang et al., 2006) to make contact with the host cell membrane. Hydrophilic translocators assist the integration of the hydrophobic translocators into the host cell membrane, forming a pore complex (Mueller et al., 2008). It is hypothesised that the initial contact of the needle tip with the host cell membrane triggers the Type Three Secretion System (TTSS) to secrete effector molecules (Mueller et al., 2008) into the host cell prior to infection (*Burkholderia* Secretion Apparatus (*Bsa*) in *Figure 1.3*, step **a**). Within 15 m of being phagocytosed into a host cell, *B. pseudomallei* has been shown to escape from the phagosome into the host cell cytoplasm by lysing the phagosomal membrane, using the pre-secreted effector proteins (Wiersinga et al., 2006, *Figure 1.3b*). TTSS is one of six types of secretion systems identified in bacteria and used to assist in the transport and secretion of effector molecules. There are six copies of the less

characterised Type VI Secretion System (T6SS) in *B. pseudomallei*. Recent findings has shown T6SS-1 to be critical for virulence in a hamster model (Chen et al., 2011).

Once present in the host cytoplasm, *B. pseudomallei* may initiate actin polymerisation resulting in membrane protrusion and cell-to-cell spread (*Figure* 1.3c), producing multinucleated giant cells (MNGC) by cell fusion (*Figure 1.3d*). Alternatively, the bacterium may choose to modify the phagocytic compartment and reside dormant in the host cell, thereby evading degradation (Wiersinga et al., 2006).

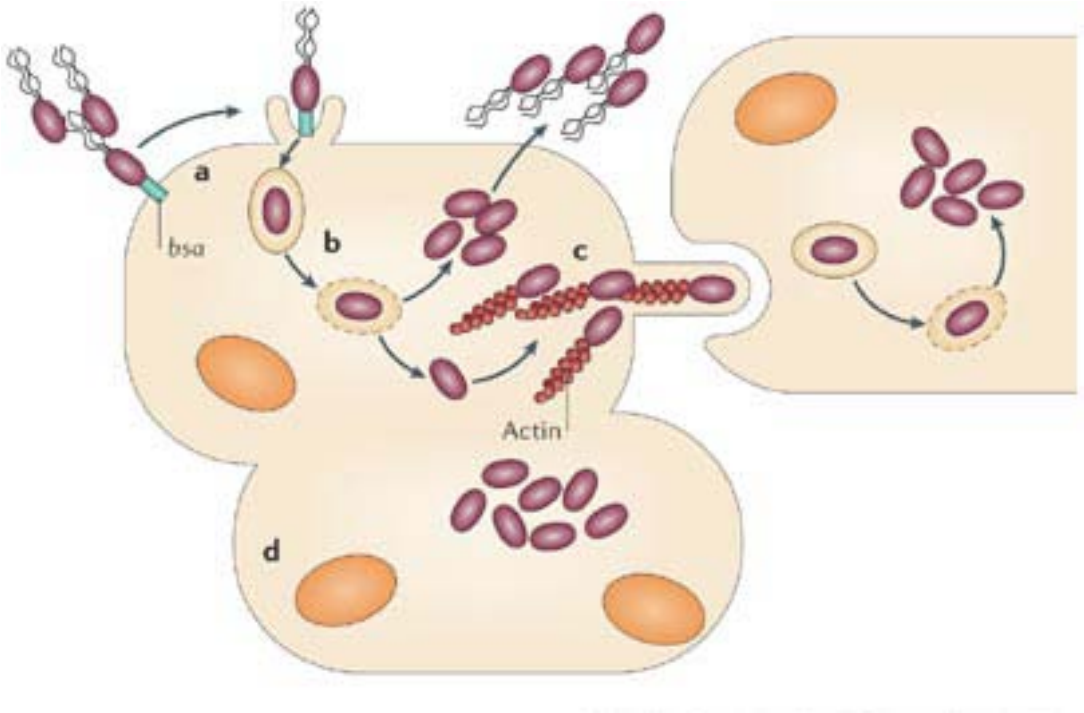

Figure 1.3: *B. pseudomallei* invasion and spread (Wiersinga et al., 2006). A: The bacterium employs the *Bsa* genes to assemble a needle-like structure which is used to secrete effector molecules into the host cytoplasm. B: Shortly after being phagocytosed into the host cell, the bacterium lysis the phagosomal membrane to continue its infectivity. C: The bacterium initiates actin polymerisation to protrude into neighbouring cells. D: MNGC are formed between adjacent *B. pseudomallei* infected cells.

1.4 TYPE III SECRETION SYSTEM

The *B. pseudomallei* genome comprises two chromosomes which have been sequenced - a large 4.07 Mb chromosome required for core functions such as cell growth and metabolism, and a smaller 3.17 Mb chromosome encoding accessory functions such as virulence (Wiersinga et al., 2006). *B. pseudomallei* has three Type Three Secretion System (TTSS) clusters encoded on the small chromosome. Similar to other gram-negative bacteria such as *S. typhimurium, S. flexneri* and *Y. enterocolitica,* the *B. pseudomallei* TTSSs (Sun et al., 2005) translocate virulence effectors into the host cell (Roversi et al., 2007).

1.4.1 Type III Secretion System Gene Clusters

The *B. pseudomallei* TTSS gene clusters (*Table 1.1*) each contain 16-18 genes (Wiersinga et al., 2006). The TTSS1 gene cluster, which was first reported in 1999, is also present in the plant pathogen *Ralstonia solanacearum,* but absent from *B. mallei* and *B. thailandensis.* TTSS2 is present in *R. solanacearum,* and the close relatives of *B. pseudomallei*, *B. mallei* and *B. thailandensis* (Wiersinga et al., 2006).

Table 1.1: TTSS gene clusters of *B. pseudomallei* (Warawa and Woods, 2005). TTSS1 encoding the *bpscN* gene is also present in the plant pathogen *R. solanacearum*. TTSS2 is present in other *Burkholderia* species. TTSS3 is present in other *Burkholderia* species and contains the *Bsa* locus.

New gene name	Previous gene name (gene annotation)		
	TTSS1	TTSS2	TTSS3
sctC	*bpscC* (BPSS1390)	*BpscC2* (a and b) (BPSS1603 and 1592)	*bsaO* (BPSS1545)
sctD	*bpscD* (BPSS1407)	*BpscD2* (BPSS1614)	*bsaM* (BPSS1547)
sctF	√ (BPSS1409)	√ (BPSS1612)	*bsaL* (BPSS1548)
sctG	*Orf*4 (BPSS1399)	√ (a and b) (BPSS1607 and 1622)	NI
sctI	*Orf5*? (BPSS1398)	*HrpJ homologue*? (BPSS1623)	*bsaK* (BPSS1549)
sctJ	*BpscJ* (BPSS1397)	*BpscJ2* (BPSS1624)	*bsaJ* (BPSS1550)
sctK	*Orf*6 (BPSS1396)	√ (BPSS1625)	√ (BPSS1551)
sctL	*bpscL* (BPSS1395)	*BpscL2* (BPSS1626)	√ (BPSS1552)
sctM	*NI*	√ (BPSS1629a)	√ (BPSS1553)
sctN	*bpscN* (BPSS1394)	*BpscN2* (BPSS1627)	*bsaS* (BPSS1541)
sctO	*Orf7*? (BPSS1393)	*HrpD homologue*? (BPSS1628)	*bsaT* (BPSS1540)
sctP	*NI*	√ (BPSS1630)	*bsaU* (BPSS1539)
sctQ	*bpscQ* (BPSS1403)	*bpscQ2* (BPSS1618)	*bsaV* (BPSS1538)
sctR	*bpscR* (BPSS1404)	*bpscR2* (BPSS1617)	*bsaW* (BPSS1537)
sctS	*BpscS* (BPSS1405)	*bpscS2* (BPSS1616)	*bsaX* (BPSS1536)
sctT	*bpscT* (BPSS1392)	*bpscT2* (BPSS1629)	*bsaY* (BPSS1535)
sctU	*bpscU* (BPSS1400)	*bpscU2* (BPSS1621)	*bsaZ* (BPSS1534)
sctV	*bpscV* (BPSS1401)	*bpscV2* (BPSS1620)	*bsaQ* (BPSS1543)
sctW	NI	NI	*bsaP* (BPSS1544)

B. pseudomallei TTSS3 contains the *Burkholderia* Secretion Apparatus *(Bsa*) locus which shares homology with the *S. typhimurium inv/spa/prg* TTSS (*Figure 1.4*; Sun et al., 2005), and the *S. flexneri ipa/mxi/spa* TTSS (Ogawa and Sasakawa, 2006b). In infected hamsters, this cluster has been shown to be necessary to facilitate *B. pseudomallei* virulence by: assisting in bacterial invasion, escape from phagosomes and intercellular spread (Wiersinga et al., 2006). The nomenclature for TTSS3 was proposed by Stevens et al. (2004). The nomenclature for the TTSS1 and 2 clusters was proposed by Rainbow et al. (2002). In 2005, Warawa and Woods (2005) attempted to unify the two different nomenclatures of Rainbow et al. (2002) and Stevens et al. (2004), by naming these genes Secretion and Cellular Translocation (*sct)* genes, followed by a subunit identifier to denote their cluster.

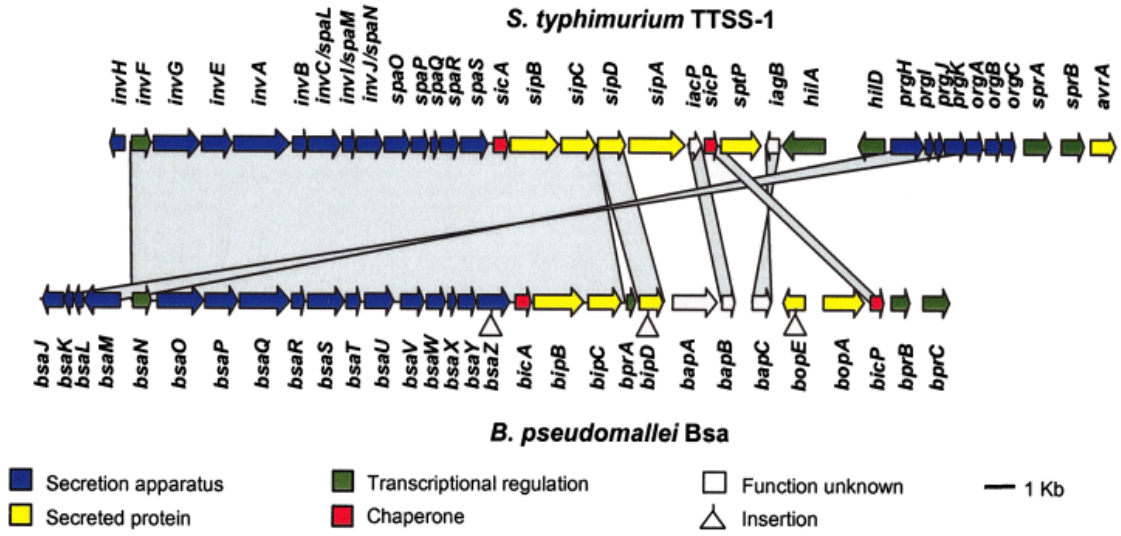

Figure 1.4: The shaded areas represent regions of homology between *B. pseudomallei Bsa* putative TTSS3 locus and *S. typhimurium inv/spa/prg* apparatus (Stevens et al., 2002). The blue, yellow, green and red arrows represent genes encoding the secretion apparatus, secretion proteins, transcriptional regulators and chaperones, respectively. The white arrows denote genes of unknown functions.

1.4.2 Secretion Apparatus

In order to infect phagocytic and non-phagocytic cells, *B. pseudomallei* initially constructs a macromolecular structure resembling a hollow syringe with a central diameter of 2-3nm, to traverse the bacterium inner and outer membranes (Zhang et al., 2006). The needle is composed of a single type of protein, BsaL, that is polymerised in a helical fashion (Zhang et al., 2006). *Figure 1.5* illustrates a proposed model structure of the *B. pseudomallei* needle complex. Bacterial secretion through the needle is activated when contact is made between the tip of the needle and the host cell membrane, triggering the TTSS to secrete effector molecules (Mueller et al., 2008). The proteins involved in this pore production are a subset of type three secretion (TTS) proteins, termed 'translocators', which inoculate other TTS 'effector' proteins into the target-cell cytosol and which serve to either inhibit or subvert host cell processes (Blocker et al., 2008).

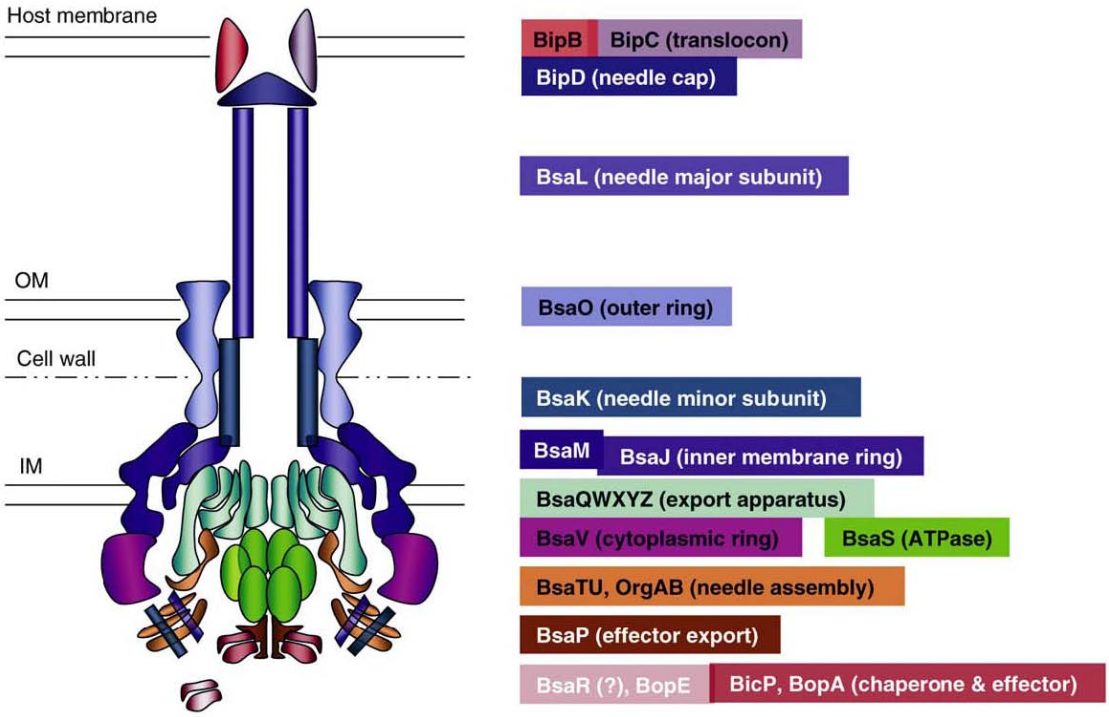

Figure 1.5: Proposed model of *B. pseudomallei* TTSS3 needle complex (Sun and Gan, 2010). The putative function and position of the proteins in the needle are derived from information on their homologous counterparts in other organisms. This study focused on BipB, BipC and BipD which is theorised to be incorporated in the distal end of the needle apparatus. The BpscN protein in TTSS1 shares homology to BsaS, a putative ATPase (highlighted in green), and is situated at the core of the needle structure.

1.5 *B. PSEUDOMALLEI* VIRULENCE PROTEINS

Effector proteins encoded in the *Bsa* locus of *B. pseudomallei* play a key role in virulence (Sun et al., 2005). Effector proteins rely on translocator proteins for their delivery into the eukaryotic cytoplasm, where they interact with host proteins (Stevens and Galyov, 2004). Several *B. pseudomallei* effector proteins share close homology with *S. typhimurium* Sip (*Salmonella* invasion protein) and Sop (*Salmonella* outer protein) proteins, namely SipB (BipB), SipC (BipC), SipD (BipD), SopA (BopA) and SopE (BopE) (Warawa and Woods, 2005). In addition, the *Bsa* Associated Protein (Bap) A, BapB and BapC are also encoded in the TTSS3 with BapB and BapC sharing homology with *S. typhimurium* IacP and IagB (Warawa and Woods, 2005). Mutants of the *B. pseudomallei BsaQ* secretion apparatus gene failed to produce a functional TTSS3 and were unable to kill mammalian cells (Sun et al., 2005). *Table 1.2* presents a summary of several *B. pseudomallei* effector proteins categorised according to their most prominent role (noting that several proteins have multiple reported functions). A more detailed discussion of each of these proteins follows.

Table 1.2: Summary of some selected essential *B. pseudomallei* virulence proteins required for bacterial invasion, survival and spread.

***B. pseudomallei* Protein**		**Description**	**Homologues**
Invasion	**BopE**	TTSS3 effector protein. Facilitates invasion by inducing rearrangements in subcortical actin cytoskeleton. Mutant did not affect actin tail formation. Mutant is not attenuated[1] (Stevens and Galyov, 2004).	*S. typhimurium:* SopE, SopE2
	BipD[2]	Translocator protein. Facilitates invasion, escape, proliferation, survival, actin-tail formation and cell-to-cell spread (Stevens et al., 2004).	*S. typhimurium:* SipD
Actin Tail Formation	**BimA**	Proline-rich putative autosecreted protein required for actin-based motility. Not involved in *Bsa*, escape or secretion of BopE (Stevens et al., 2005b).	*Y. enterocolitica:* YadA *L. monocytogenes:* ActA *S. flexneri:* IcsA
Cell-to-Cell Spread	**BopA**	Effector protein required for cell-to-cell spread. Mutant has higher co-localisation with GFP-LC3 and is attenuated (Cullinane et al., 2008, Stevens et al., 2004)	*S. flexneri:* IcsB
MNGC	**BipB**[2]	Role in Multi Nucleated Giant Cell formation, cell-to-cell spread, and invasion. May act as a translocator or effector, capable of activating caspase-1, thus leading to cell death (Suparak et al., 2005).	*S. typhimurium*: SipB *S. flexneri:* IpaB
Adherence	**PilA**	Facilitates pili formation (Essex-Lopresti et al., 2005).	
Hypothetical	**BPSS 1539**[2]	Mutant exhibits intracellular phagosomal confinement and attenuated virulence (Pilatz et al., 2006).	

[1] The level of attenuation describes the bacterium virulence capacity. BALB/c mice were infected intranasally with a lethal dose of the wild type or mutant strains. At 4 weeks post infection the mutant strain showed a low CFU count and reduced mortality in comparison to the wild type.
[2] This gene is one of seven studied in this thesis as detailed in *Chapter 3, Table 3.1.*

1.5.1 Proteins Required for Invasion

While many proteins may play a role in invasion of mammalian cells by *B. pseudomallei*, BopE and BipD are reported to be central to this process.

BopE is secreted via the *Bsa* (Stevens et al., 2004), and shares 27% identity with *S. enterica* serovar Typhimurium SopE, and 25% identity with SopE2 (Stevens et al., 2003). In the absence of both these genes *S. enterica* serovar Typhimurium is unable to be internalised (Bruno et al., 2009). The inactivation of *bopE* impaired bacterial invasion of HeLa cells (Wiersinga et al., 2006), indicating that BopE facilitates invasion.

BopE influences invasion by inducing rearrangements in the sub-cortical actin cytoskeleton of host cells in a process termed 'membrane ruffling' (Stevens and Galyov, 2004). In this context BopE acts as a guanine nucleotide exchange factor for the Rho-family GTPases that regulate the host actin network (Stevens et al., 2004), thus interfering with actin dynamics (Stevens et al., 2003). In *S. enterica* serovar Typhimurium, 'membrane ruffling' concludes with the formation of macropinocytic vesicles (Stevens and Galyov, 2004). While mutations in *bopE* were shown to reduce the invasive ability of *B. pseudomallei*, they did not adversely affect replication or the actin tail formation of bacteria that enter the host cell (Stevens et al., 2002).

BipD shares homology with *S. flexneri* IpaD (36%) and *S. enterica* serovar Typhimurium SipD (33%) (Roversi et al., 2007). In *S. flexneri*, IpaD is essential for

invasion, regulating the TTSS and modulating the host cell response following infection (Ogawa et al., 2003). A *B. pseudomallei* BipD mutant was shown to have impaired invasion, intracellular survival, actin tail formation, and reduced levels of replication (Stevens et al., 2004). BipD caps the tip of the needle structure and recruits translocon proteins BipB and BipC (Sun and Gan, 2010). BipD is required for full virulence in mice (Roversi et al., 2007) as mutations in the *bipD* gene impaired invasion of epithelial cells *in vitro* (Stevens and Galyov, 2004).

1.5.2 Proteins Required for Actin Tail Formation

BimA (*Burkholderia* Intracellular Motility A) is an auto-secreted protein required for actin tail formation and actin-based motility (Stevens et al., 2005a). BimA contains proline-rich motifs, WH2-like domains, and shares homology with the *Y. enterocolitica* auto-secreted adhesin YadA at the carboxyl terminus (Stevens and Galyov, 2004). YadA is involved in the formation of fibrilliae, bacterial adhesion to cultured epithelial cells, and bacterial attachment to host tissues (Leo et al., 2008).

BimA is localised to the pole of the bacterium where actin tail formation occurs (Stevens et al., 2005a). Mutations of the *bimA* gene abolished the actin-based motility of *B. pseudomallei* in macrophage cells (Wiersinga et al., 2006). It has been hypothesised that intra- and intercellular spread of the bacterium occurs via actin-based motility, to facilitate cell-to-cell fusion and MNGC formation (Burtnick et al., 2008).

S. flexneri, *L. monocytogenes*, *Rickettsia conorii* and *Rickettsia rickettsii* initiate actin polymerisation through the cellular Arp2/3 complex (Stevens and Galyov, 2004). This complex is also incorporated in *B. pseudomallei* actin tails (Pilatz et al., 2006). Since this complex weakly activates actin formation, most bacteria employ other cellular proteins such as Scar1 and Wiskott-Aldrich Syndrome Protein (N-WASP), activated by Rho-family GTPases such as Cdec42, to further stimulate actin formation (Stevens and Galyov, 2004). However, expression of Scar1 and N-WASP, have not displayed any influence on actin tail formation of *B. pseudomallei* when tested in PtK2 epithelial and J774A.1 macrophage cells (Pilatz et al., 2006).

1.5.3 Proteins Required for Cell-to-Cell Spread

Cell-to-cell spread of *B. pseudomallei* is attributed to BopA, a *Bsa*-encoded putative effector protein (Stevens et al., 2004). BopA shares homology with *S. flexneri* TTSS effector protein, IcsB (Ogawa and Sasakawa, 2006b) – which plays a role in camouflaging the bacteria against autophagic processes (Ogawa and Sasakawa, 2006b). The BopA deletion mutant (Cullinane et al., 2008) also showed diminished survival and invasion capabilities in RAW264.7 macrophages at the 6 h post infection stage, in comparison to the wild-type *B. pseudomallei*.

1.5.4 Proteins Required for MNGC Formation

Internalised *B. pseudomallei* can escape from the phagosome and induce cell-to-cell fusion, resulting in MNGC formation (Utaisincharoen et al., 2006). The exact mechanism by which MNGC formation is initiated is yet to be understood. The formation of MNGC is mediated by the TTSS translocator protein BipB (Suparak et

al., 2005). While BipB regulates MNGC induction, BipB-independent induction also occurs at a lesser level. A *bipB* mutant displayed reduced levels of MNGC formation, cell-to-cell spread, and induction of apoptosis following infection of J774A.1 macrophages (Suparak et al., 2005). It was hypothesised that BipB may influence apoptosis by interfering with caspase-1 activity, since its homologues, *S. typhimurium* SipB (46% amino acid identity to BipB) and *S. flexneri* IpaB have been observed to induce macrophage apoptotic death by activating caspase-1 (Suparak et al., 2005).

RpoS is a global regulatory factor, controlling the expression of genes for bacterial resistance to stressful conditions, prolonged nutrient deprivation, and virulence. An *rpoS* mutant while not having altered survival or replication, did not exhibit MNGC formation and was unable to activate iNOS in macrophages (Utaisincharoen et al., 2006), thus evading the host cell microbicidal pathway.

1.5.5 Proteins Required for Adherence

Type IV pili-mediated adherence and secretion is an important virulence mechanism for most gram-negative bacteria. Initiation of type IV pili-mediated adherence, stimulates the secretion of haemolysin, lipases and proteases (Wiersinga and van der Poll, 2009). Within the *B. pseudomallei* genome is the type IV pili-associated locus, encoding a putative pilus structural protein (PilA). A *pilA* mutant was less virulent and had reduced adherence to human epithelial cells (Wiersinga et al., 2006).

1.6 *B. PSEUDOMALLEI* DEGRADATION

Post-infection, intracellular *B. pseudomallei* may be sequestered in a membrane bound compartment (phagosome) destined for degradation. In this instance, autophagy is induced as a means of combating intracellular microbial infection (Dubuisson and Swanson, 2006). The most common methods *B. pseudomallei* may employ to evade the degradation process include induction of cell death, delaying host attack mechanisms, resisting antimicrobial activity, and inhibiting iNOS production.

1.6.1 Cell Death

Bacteria such as *S. flexneri* and *S. typhimurium* have the ability to evade macrophage killing by activating cellular caspase-1, using IpaB and SipB respectively, thus inducing rapid macrophage cell death. In this manner, these bacteria attempt to kill the macrophages and spread *in vivo* before they themselves are destroyed (Sun et al., 2005). Studies performed *in vitro,* indicate that *B. pseudomallei* also relies on the caspase-1 pathway to initiate cell death in macrophages such as J774A.1, as early as 4 h post infection (Sun et al., 2005). In THP-1 (a human monocyte-like cell line), virulent *B. pseudomallei* strains are able to induce rapid caspase-1 dependent cell lysis, while avirulent strains are not cytotoxic.

1.6.2 Delayed Cellular Attack Mechanisms

Some strains of *B. pseudomallei* were found to delay the initiation of cellular attack processes following internalisation. The production of iNOS and NO in macrophages serves to play a role in killing intracellular bacteria. It is therefore advantageous for *B. pseudomallei* to either delay or inhibit such a macrophage response, which could

prolong their own survival within cells (Utaisincharoen et al., 2006). The delayed macrophage response is potentially related to the unusual structure of *B. pseudomallei* lipopolysaccharide (LPS), which has been reported to be a poor macrophage activator (Utaisincharoen et al., 2006, West et al., 2008). *B. pseudomallei* LPS is a TLR4 ligand and is generally capable of inducing a TLR4-mediated inflammatory cytokine response (West et al., 2008). The O-antigenic polysaccharide moiety is implicated in modulating the host cell response, thus controlling the intracellular fate of *B. pseudomallei* inside macrophages (Arjcharoen et al., 2007).

Phagocytic cells have two main microbicidal pathways: the Reactive Oxygen Intermediates (ROI) including, superoxide anions, hydrogen peroxide, hydroxyl radicals and singlet oxygen, and the Reactive Nitrogen Intermediate (RNI) which include nitric oxide (Miyagi et al., 1997). Depending on the invading bacterial strain and the cell line becoming infected, a specific pathway may be activated with differing and/or detrimental effects. The RNI pathway has been shown to most actively inhibit the intracellular growth of *B. pseudomallei* (Miyagi et al., 1997).

Nitric oxide production is catalysed by inducible Nitric Oxide Synthase (iNOS) (Utaisincharoen et al., 2006). Following bacterial internalisation and macrophage activation, there is an increased level of iNOS expression and NO production. However, *B. pseudomallei* activates the negative regulators, suppressor of cytokine signalling 3 (SOCS3) and cytokine-inducible src homology 2-containing protein (CIS) that represses iNOS production (Ekchariyawat et al., 2007). Hence, *B. pseudomallei* is able to evade the cytotoxic effect of reactive NO by either

inhibiting the production of iNOS when tested in mouse J774A.1 macrophages (Sun et al., 2005).

1.6.3 Polysaccharide Capsule

During the establishment of an infection, the host innate immunity is activated, triggering the complement system. The complement cascade leads to the deposition of complement factor C3b on the bacterial surface, and opsonisation of the invading microorganisms (Reckseidler-Zenteno et al., 2005). The *B. pseudomallei* capsular polysaccharide, is hypothesised to reduce the deposition of C3b on the bacterial cell surface, thus inhibiting the activation of the complement cascade and inhibiting opsonisation. *B. pseudomallei* appeared to have less C3b deposition on its surface in comparison to *B. thailandensis*. Furthermore, it has been observed that *B. pseudomallei* can shed its capsule, thereby diverting complement activation away from the intact bacterium (Reckseidler-Zenteno et al., 2005).

1.7 TREATMENT OF *B. PSEUDOMALLEI* INFECTION

Much research has been devoted to the development of treatments for melioidosis patients. While there are no vaccines available (Sarkar-Tyson et al., 2009), a number of antibiotics have been used against melioidosis infections. Unfortunately, *B. pseudomallei* is resistant to many of the conventional antibiotics used for most gram-negative bacterial infections, such as quinolones, cephalosporins (Inglis et al., 2006), penicillin, macrolides, rifamycins, colistin and aminoglycosides (Wiersinga et

al., 2006). *B. pseudomallei* also exhibits resistance to traditionally used antibiotics such as chloramphenicol and tetracycline (Karunakaran and Puthucheary, 2007). However, *B. pseudomallei* has shown susceptibility to antibiotics such as ceftazidime, meropenem, trimethoprim-sulphamethoxazole, imipenem (Inglis et al., 2006), amoxicillin-clavulanate, doxycycline (Karunakaran and Puthucheary, 2007), ureidopenicillins and carbapenems (Wiersinga et al., 2006) .

Ceftazidime is a β-lactam antibiotic (Harland et al., 2007), recommended as an intravenous treatment for melioidosis. When used for several weeks in combination with 20 weeks oral treatment of trimethoprim-sulphamethoxazole and doxycycline (Inglis et al., 2006), ceftazidime has been shown to reduce the mortality rate by 50% (Harland et al., 2007). However, in rare cases, resistance to ceftazidime has been observed (Karunakaran and Puthucheary, 2007). In such incidents, imipenem and meropenem were shown to be as effective as ceftazidime (Inglis et al., 2006).

1.8 AUTOPHAGY

The term *autophagy* was originally developed by Christian de Duve in 1963 to describe the accumulation of lysosomes and formation of vacuoles in hepatocytes (Martinou and Kroemer, 2009). Our current understanding recognises at least three different processes that contribute to 'autophagy' in mammalian cells (*Figure 1.6*). In macroautophagy, cytoplasmic components are sequestered into double membrane-bound compartments (autophagosomes) destined for degradation resulting

from the fusion of autophagosomes with lysosomes (Ogawa and Sasakawa, 2006a). Microautophagy describes the direct engulfment of cytoplasmic contents at the lysosome surface (Uttenweiler and Mayer, 2008). Chaperone-mediated autophagy involves the direct lysosomal import of proteins which contain a particular pentapeptide motif (Martinou and Kroemer, 2009). Hereafter, this review will focus on macroautophagy referring to it as autophagy, unless otherwise specified.

The targets of autophagy may derive from cellular differentiation or result from either stress or damage by exposure to cytotoxins (Dorn et al., 2002). Autophagy is induced in response to stress related to nutrient limitation, starvation (Ogawa and Sasakawa, 2006a), or to maintain cellular amino acid levels for protein synthesis (Dorn et al., 2002). More current research has described autophagy as an important innate immune process (Ravikumar et al., 2010). The degradation of invading bacteria, viruses, fungi and parasites by autophagy in mammalian cells has been termed xenophagy and serves the purpose of not only eliminating the intracellular pathogen, but also liberating metabolites that may have been utilised during pathogen infection, thus promoting cell survival (Orvedahl and Levine, 2008).

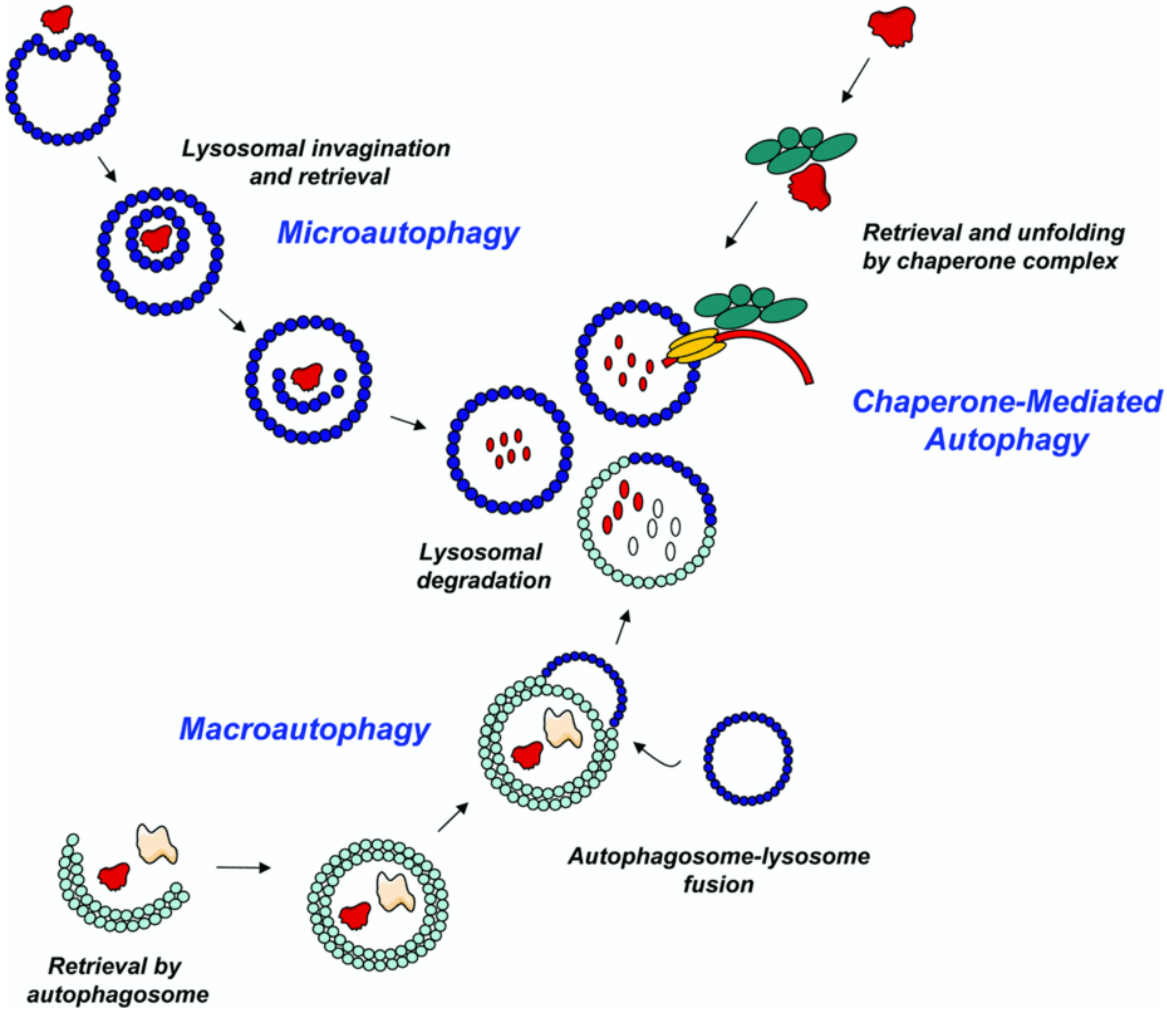

Figure 1.6: Schematic representation of chaperone-mediated, micro- and macroautophagy (Martinet et al., 2009). Microautophagy is the direct engulfment of cytoplasmic contents at the lysosomal surface. Chaperone-mediated autophagy is the direct engulfment of proteins at the lysosome surface, with the aid of chaperone complexes. Macroautophagy involves the sequestration of cytoplasmic contents into autophagosomes, destined for lysosomal fusion.

Autophagy is initiated through the Target Of Rapamycin (TOR) kinase, which under homeostatic conditions, inhibits the autophagic pathway. This multimolecular complex is subdivided into TORC1 (interacts with rapamycin) and TORC2 (Garber, 2009). Inducers such as tamoxifen, rapamycin and nutrient starvation tend to cause the dephosphorylation of TOR kinase, which in turn activates the autophagic pathway (Kirkegaard et al., 2004). Pharmacologic inhibitors of autophagy include 3-MA, wortmannin & LY294002 (Kirkegaard et al., 2004).

The initiation of autophagy gives rise to an isolation membrane which following nucleation undergoes elongation and maturation (*Figure 1.7*). The elongation step is mediated by the covalent linkage of Atg5 to Atg12, and the covalent lipidation of Atg8 (whose mammalian orthologue is microtubule-associated protein 1 light chain (LC3) (Yang et al., 2005)), by phosphatidylethanolamine, which is regulated by ubiquitin-conjugating enzymes Atg3, Atg7 and Atg10 (Kirkegaard et al., 2004).

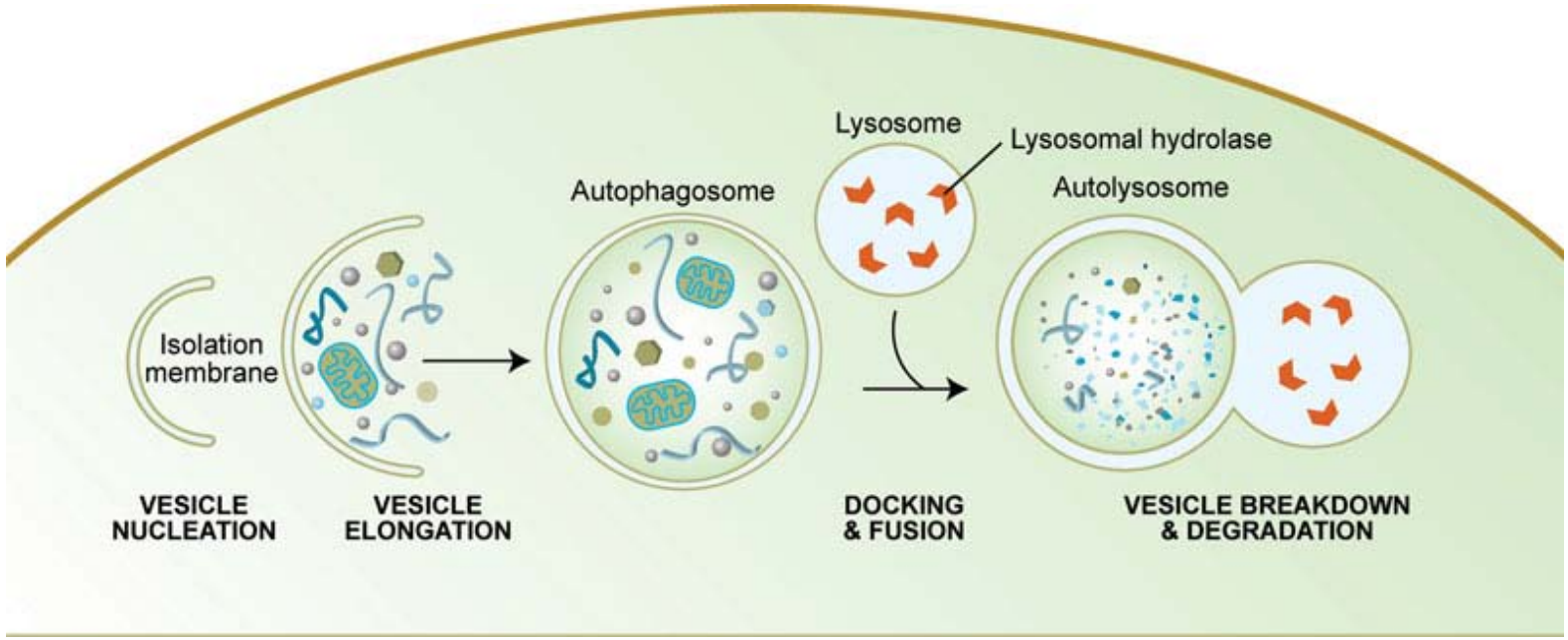

Figure 1.7: The autophagic process (Melendez and Levin, 2009). Cytoplasmic contents are sequestered in an isolation membrane which matures to exhibit autophagosomal markers. The autophagosome will mature into an autolysosome upon its fusion with lysosomes to undergo degradation.

The maturation of the autophagosome can be identified through the composition of its membrane markers. Autophagosomes will initially acquire early endocytic markers such as Rab5 and EEA1, facilitating their sequential fusion with endosomes (Duclos and Desjardins, 2000). Nascent or early autophagosomes will subsequently acquire Lysosomal Associated Membrane Protein-1 (LAMP-1) and V-ATPase to progress to late autophagosomes. The late autophagosome is a large organelle with a diameter ranging from 0.5-1.5 µm in mammalian cells (Kirkegaard et al., 2004). The late autophagosome will then mature to an autolysosome by docking and fusing with the lysosome thereby acquiring acid hydrolases that degrade the inner membrane of the autophagosome and the constituents of the compartment (Dorn et al., 2002). Such membrane interactions are regulated by Rab GTPases and their effectors, as well as SNARE proteins to facilitate docking, fusion and fission (Duclos and Desjardins, 2000).

1.9 PATHOGEN DEFENSE AGAINST AUTOPHAGY

Intracellular pathogens must find ways to either, avoid, modify or escape the lytic vacuoles, that is, phagosomes. Failure to do so, will eventuate in degradation of the pathogen (Ogawa and Sasakawa, 2006a). Following infection, microbes such as *Brucella abortus, Coxiella brunetii* and *Legionella pneumophilia* have been found to either block phagosome maturation or alter and reside within the modified phagosomal compartment. Other microbes such as *B. pseudomallei, L. monocytogenes* and *S. flexneri* having escaped the phagosome then avoid autophagic capture, to replicate, and spread (Ogawa and Sasakawa, 2006a). Group A *Streptococcus* and *Francisella tularensis* are unsuccessful in their attempts to escape degradation. *Figure 1.8* summarises the pathways (adapted from Deretic and Levine, 2009) that some pathogenic microbes may pursue.

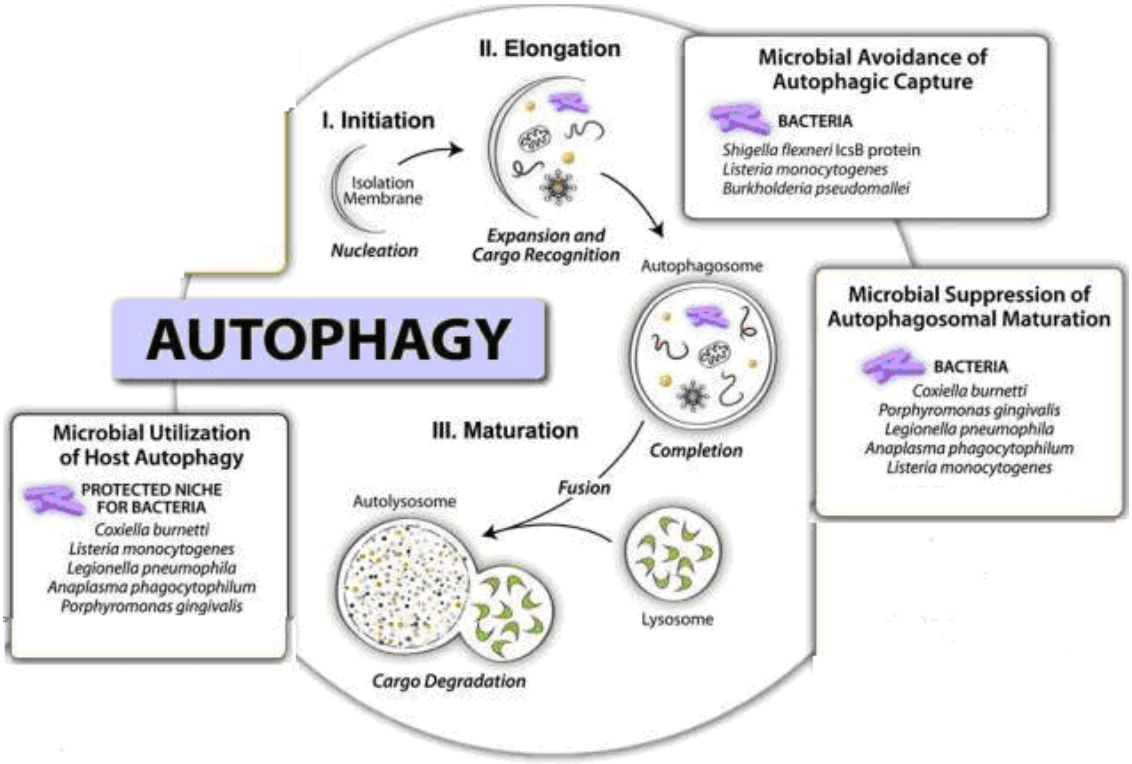

Figure 1.8: Summary of pathways internal bacteria may follow (modified from Deretic and Levine, 2009). Intracellular pathogens such as *S. flexneri*, once gaining access to the host cytoplasm, attempts to avoid autophagic capture so that they may replicate and continue to spread. Bacteria such as *L. pneumophilia* tend to suppress their phagosomal maturation to reside in their vesicle.

1.9.1 Microbial Avoidance of Capture

Bacteria can be classified by the nature of their interaction with the autophagic process, namely, avoidance of autophagic capture, suppression of autophagosomal maturation, or utilisation of host autophagy (*Figure 1.8*). Intracellular pathogens such as *S. flexneri*, *L. monocytogenes* and *B. pseudomallei*, having gained access to the host cytoplasm, attempts to avoid autophagic capture so that they may replicate and continue to spread. A classic example of avoidance is illustrated in the case of *S. flexneri*. The binding of *S. flexneri's* surface protein VirG to the autophagy protein Atg5, targets the bacterium to the autophagosome. However, the release of the TTSS effector IcsB is able to competitively bind to Atg5 thereby assisting the bacterium to avoid autophagic capture (Deretic and Levine, 2009).

However, this classification does not restrict bacteria to a single mechanism of avoidance of autophagy, for example *L. pneumophilia, Porphymonas gingivalis* and *L. monocytogenes*, whilst being able to suppress autophagosomal maturation are also able to utilise the host autophagic machinery. *Table 1.3* identifies bacteria that are able to avoid autophagic capture.

1.9.2 Suppression of Phagosomal Maturation

Following internalisation, *B. abortus*, *P. gingivalis* and *L. pneumophilia* were found to co-localise with the early endosomal marker Rab5. These microbial containing vesicles do not progress to the late endosome-like vesicular structure (Dorn et al., 2002), and so suppress phagosomal maturation. *Table 1.4* summarises the bacteria capable of suppressing phagosomal maturation.

1.9.3 Pathogens Surrendering to Autophagy

Bacteria such as Group A *Streptococcus* (GAS), *Mycobacterium tuberculosis* and *F. tularensis* are able to escape from their surround phagosome into the host cytoplasm. Following their escape, a large proportion of the bacteria is found to surrender to the autophagic machinery, leading to bacterial degradation (*Table 1.5*). In the case of GAS, 80% of the intracellular bacteria are recruited into autophagosomes.

Table 1.3: Bacteria which avoid autophagic capture.

Bacterium	Host interactions	Virulence factors	Reference
B. pseudomallei	Invades, replicates and avoids capture in host cells. BopA mutants exhibit increased co-localisation with GFP-LC3 and decreased intracellular survival and replication.	BopA, BopE	(Cullinane et al., 2008), (Stevens et al., 2003)
Rickettsia spp	Infects macrophages and endothelial cells. Escapes from the phagosome into the cytosol and possibly the nucleus where it replicates.	Phospholipases, haemolysin C, tlyC	(Balraj et al., 2009), (Ray et al., 2009), (Whitworth et al., 2005)
L. monocytogenes	Secretes pore-forming LLO into phagosome to escape confinement. Enters into the host cytoplasm to induce actin motility and cell-to-cell spread.	LLO, type C phospholipases, ActA	(Freitag et al., 2009), (Posfay-Barbe and Wald, 2009), (Desvaux and Hébraud, 2006)
S. flexneri	IcsB competitively binds to VirG, inhibiting ATG5 association and autophagic induction. Once in the cytosol, the bacterium replicates and spreads.	IcsB	(Kweon, 2008), (Ogawa and Sasakawa, 2006b), (Ogawa et al., 2003)

Table 1.4: Bacteria capable of suppressing phagosomal maturation.

Bacterium	Host interactions	Virulence factors	Reference
B. abortus	Acquires the early endosomal marker EEA1, but fails to display any late endosomal markers.	*virB*	(Sieira et al., 2009), (Duclos and Desjardins, 2000)
P. gingivalis	While being able to traffic to the autophagosome, the bacterium employs autophagic inhibitors to prevent lysosomal fusion.	Gingipain, fimbriae, LPS	(Ogawa and Sasakawa, 2006a), (Kirkegaard et al., 2004), (Hajishengallis)
L. pneumophilia	Employs secretory vesicles derived from the ER to camouflage itself and provide a protective niche.	Products secreted via T4SS	(Columbo, 2005), (Nora et al., 2009), (Dubuisson and Swanson, 2006)
C. brunetii	Bacterium is capable of surviving in acidic vacuoles in both macrophage and epithelial cell lines	Plasmids QpH1, QpRS, QpDG, QpDV or QpRS-like. LPS	(Columbo, 2005), (Ogawa and Sasakawa, 2006a), (Ghigo et al., 2009)
S. typhimurium	Capable of residing within the *Salmonella* containing vacuole (SCV), escape the SCV, or surrender to autophagy. Subversion of autophagy may also occur by killing the host macrophages via either a rapid caspase-1 dependent or a slower caspase-1 independent mechanism.	SipC	(Birmingham et al., 2006), (Duclos and Desjardins, 2000)

Table 1.5: Bacteria surrendering to autophagy.

Bacterium	Host interactions	Virulence factors	Reference
Group A *Streptococcus* (GAS)	Escapes from the endocytic pathway into the host cytoplasm in an attempt to evade degradation, but is eventually found sequestered in an autophagosome.	Streptolysin O (SLO)	(Yoshimori, 2005), (Nakagawa et al., 2004), (Ogawa and Sasakawa, 2006a), (Amano et al., 2006), (Yamaguchi et al., 2009)
F. tularensis	Escapes phagosome but re-enters the endocytic pathway to undergo autophagy	LPS, acid phosphatase AcpA, IglC, MglA	(Checroun et al., 2006), (Oyston, 2008)
M. tuberculosis	Resides in *Mycobacterium*-containing vacuoles (MCV) which are sequestered by autophagosome-like membranes.		(Columbo, 2005), (Ogawa and Sasakawa, 2006a)

1.10 GENETIC SCREENING IN YEAST OF VIRULENCE EFFECTORS

Bacterial virulence effectors may be characterised in a number of model organisms. Yeast is an ideal system to use when attempting to identify their influence on processes such as, membrane fusion/fission, vesicle trafficking and organelle turnover.

Yeast is a desirable organism to model basic disease-related processes involving cell cycle control, signal transduction, cytoskeletal dynamics and protein transport as indicated by Valdivia (2004). In comparison to higher order eukaryotes, the advantages of employing *Saccharomyces cerevisiae* as a model organism include, easy DNA transformation, highly efficient homologous recombination, and the potential to grow as either haploid or diploid cells (Lesser and Miller, 2001). Over 75% of the yeast genome is functionally annotated (Kramer et al., 2007). In addition, there are numerous reagents, including over-expression libraries and deletion strains that are available (Lesser and Miller, 2001), as well as considerable knowledge relating to conserved signalling molecules and cytoskeletal components (Hardwidge et al., 2006)

Since the biology of *S. cerevisiae* is well understood, it offers the potential to be employed as a model eukaryote in which to study the function of bacterial virulence factors (Hardwidge et al., 2006). However, until recently, little had been done to exploit the genetic tractability of yeast to determine cellular targets of effector proteins (Kramer et al., 2007). This was due to concerns of the possible divergence

between higher eukaryotes and yeast in relation to the molecular mechanisms that bacterial effectors may target (Rodriguez-Escudero et al., 2006).

While *S. cerevisiae* cannot be a physiologic model of bacterial infection of mammalian human cells, as the cell wall prevents bacterial attachment and invasion (Valdivia, 2004), it can be used to characterise the effects bacterial virulence proteins may have on conserved eukaryotic processes (Slagowski et al., 2008). Mechanisms regulating cellular processes that are affected during bacterial infections are relatively conserved from yeast to mammals, for instance, DNA metabolism, programmed cell death, cell cycle control, cytoskeletal dynamics, membrane trafficking (Valdivia, 2004), and basic signalling pathways such as those involved in GTPases or mitogen-activated protein kinase (MAPK) cascades (Rodriguez-Escudero et al., 2006). When expressed in yeast, the function of virulence factors and toxins may be characterised in phenotypic terms, as described below (*Table 1.6*).

Table 1.6: Phenotypes associated with bacterial protein expression in yeast.

Phenotype	Bacterial Protein
Inhibition of cell growth	• *Y. enterocolitica* YopO/YpkA & YopE (Nejedlik et al., 2004) • *E. coli* EspG (Siggers and Lesser, 2008) • *S. typhimurium* SigD/SopB (Rodriguez-Escudero et al., 2006) • *L. pneumophilia* proteome fragments (Slagowski et al., 2008)
Inhibition of cytoskeletal functioning	• *Y. enterocolitica* YopE (Siggers and Lesser, 2008) and YopO/YpkA (Nejedlik et al., 2004) • *S. typhimurium* SipA (Lesser and Miller, 2001)
Inhibition of DNA metabolism	• *Campylobacter* sp., *E. coli, Shigella* sp. and *H. ducreyi* CdtB (Valdivia, 2004)
Inhibition of membrane structure and functioning	• *L. pneumophilia* vipA, vipD, vipE and vipF (Shohdy et al., 2005) • *S. flexneri* IpgB2 (Kramer et al., 2007) • *Y. enterocolitica* YopE (Kramer et al., 2007) • *P. aeruginosa* ExoU (Valdivia, 2004)
Inhibition of MAP kinase signalling	• *S. flexneri* OspF (Kramer et al., 2007)

1.10.1 Growth Inhibition

Bacterial virulence factors that alter mammalian cellular processes such as actin cytoskeleton, secretory and signal transduction pathways, can also target analogous processes in yeast. Such interference can be detrimental to the cell, resulting in growth inhibition (Kramer et al., 2007). Hence, growth inhibition is an indicator of effector protein expression (*Table 1.6*).

1.10.2 Inhibition of Cytoskeletal Function

Many bacterial virulence factors target the mammalian cytoskeleton by disrupting the actin network. Since cytoskeletal dynamics are relatively conserved among eukaryotic cells, it is possible to observe the outcome of bacterial effector proteins that are expressed in yeast (Valdivia, 2004). In general, the expression of any virulence factors which interfere with host cell signalling and cytoskeleton will consequently affect yeast morphogenesis, as budding is supported by cytoskeletal structures such as actin filaments and septin collars (Rodriguez-Escudero et al., 2006). For instance, of the *Y. enterocolitica* type III secreted proteins, YopE tended to block depolarisation of the yeast actin structures and cell cycle progression (Valdivia, 2004), while YopO/YpkA disrupted the normal distribution of actin and inhibited yeast cell growth (Nejedlik et al., 2004). *S. typhimurium* SipA (SspA) was also shown to interact with yeast actin, altering polarity and inhibiting actin depolymerisation (Lesser and Miller, 2001). The loss of yeast viability paralleled the disruption of actin cytoskeletal structures (Nejedlik et al., 2004).

1.10.3 Inhibition of DNA Metabolism

In mammalian cell lines, bacteria such as *Campylobacter* spp., *E. coli*, *Shigella* spp. and *H. ducreyi* secrete a cytolethal distending toxin (CDT) that blocks cell cycle progression (Valdivia, 2004). CDT is composed of three subunits, namely, CdtA, CdtB and CdtC. CdtB showed genotoxic activity in yeast and caused cell cycle arrest through either inducing DNA damage or activating signalling pathways that sense DNA damage (Valdivia, 2004).

1.10.4 Inhibition of Membrane Structure and Function

Some bacterial virulence factors can affect the endomembrane system of mammalian cells, by, for example, arresting vesicular and endosomal trafficking, inactivating signalling lipids or degrading membranes (Valdivia, 2004).

Shohdy et al. (2005) showed that type IVB secreted effectors from *L. pneumophilia* interact with mammalian host cell components to inhibit phagolysosome formation and interfere with vacuolar trafficking pathways. This research group devised a vesicle trafficking assay, Pathogen Effector Protein Screening in Yeast (PEPSY), to identify genes that produced membrane trafficking defects as visualised by an invertase colour assay. Genes that induced a negative vacuole protein sorting (VPS) phenotype in yeast were candidate effectors, potentially capable of altering endosomal traffic in mammalian cells. Application of this screen identified four *VPS inhibitor proteins (vip)* namely, *vipA, vipD, vipE* and *vipF* that interfered with vesicle trafficking in yeast (Shohdy et al., 2005).

When expressed in yeast, *S. flexneri* IpgB2 and *Y. enterocolitica* YopE inhibited specific steps in cell wall integrity pathways (Kramer et al., 2007). Expression of *Pseudomonas aeruginosa* ExoU in yeast also resulted in a loss in cell viability and fragmented vacuolar membranes (Valdivia, 2004).

1.10.5 Inhibition of MAP Kinase Signalling

Yeast encodes mitogen-activated protein kinase (MAPK) signalling cascades such as, the mating pathway (Fus3), the invasive growth pathway (Kss1), the hyperosmotic growth (HOG) pathway, the sporulation pathway (Smk1), and a second MAPK cascade, implicated in cell wall integrity (Mlp1) (Kramer et al., 2007). *S. flexneri* TTS OspF has been shown to inhibit both yeast and mammalian MAPK phosphorylation and subsequently, inhibit signalling pathways such as those involved in cell wall biogenesis (Kramer et al., 2007).

1.10.6 Summary of Bacterial Protein Expression in Yeast

As described above, *S. cerevisiae* can be employed as a model organism to screen for and study the function of putative bacterial virulence factors. Following their identification and characterisation in yeast, genes encoding putative virulence proteins can be mutated, and the consequences in terms of infectivity and virulence can be assessed. The encoded proteins can then be further characterised for their specific roles in virulence (Lesser and Miller, 2001).

1.10.7 Yeast Vacuoles

Chapter 1.10.4 describes the ability for bacterial virulence factors to affect the functioning of the endomembrane system of mammalian cells by arresting vesicular and endosomal trafficking, inactivating signalling lipids, or degrading membranes (Valdivia, 2004). Thus, as a consequence of microbial virulence factor expression, the yeast vacuole may be anticipated to undergo physiological and morphological changes. Interruptions to the endosomal trafficking pathways by putative virulence proteins may potentially see a halt in vacuolar fusion as the yeast cell attempts to mimic mammalian cells in an attempt to circumvent autophagic degradation.

The yeast vacuole is the counterpart of mammalian lysosomes. Within the cell, this single membrane structure is generally found in low numbers (usually 1-3) with a diameter of 5-8 μm. Yeast vacuoles are versatile organelles and play a vital role in: proteolysis cleavage of proteins; turnover of macromolecules; storage of phosphates, amino acids, nutrients, ions and metals; buffering the cytoplasm pH; and maintaining water and ion homeostasis (Weisman, 2003).

Due to the many biological processes occurring within the vacuole, the vacuolar membrane is in a constant state of regulated flux with fusion and fission which is attributed to: vacuole inheritance (the segregation and migration of the vacuole towards newly forming buds); endocytic and biosynthetic membrane transport pathways; and autophagic pathways (fusion of the autophagosome to the vacuole).

The stringent regulation of such processes ensures that the vacuole maintains a proper morphology (Efe et al., 2005). Some of these pathways will now be elaborated on.

1.10.8 Screening for Mutants Defective in Vacuole Inheritance

Yeast mutants that are defective in vacuole inheritance may be screened for vacuole morphology and then can be further subdivided according to their ability to correctly localise the soluble vacuolar glycoprotein carboxypeptidase Y (CPY) to the vacuole. In the absence of a sorting signal, the CPY is secreted rather than being sorted to the vacuole. These Vacuolar Protein Sorting mutants (*vps* mutants) in *S. cerevisiae* are involved in biosynthetic transport and may be divided into six distinct classes, namely: *vps A, B, C, D, E* & *F* (Raymond et al., 1992) (*Table 1.7*).

Table 1.7: Classification of vacuole inheritance mutants (Raymond et al., 1992) and (Bowers and Stevens, 2005)

CLASS	DESCRIPTION	GENES
Class A *vps* mutants	Vacuole morphology is similar to wild-type cells, but slightly perturbed. 1-2 vacuoles per cell. Less prominent vacuolar segregation structures. CPY secretion is variable.	*vps8*, *vps10*, *vps13*, *vps29*, *vps30*, *vps35*, *vps38*, *vps55*, *vps63*, *vps70*, *vps74*
Class B *vps* mutants	Large number of small fragmented vacuoles. Defect in V-ATPase assembly. Two distinguishable subgroups: where in one group the vacuole fragments align along the mother cell to bud axis, and in the other group the fragmented vacuoles were randomly dispersed (*vps39*, *vps41* & *vps43)*. Secreted high level of CPY.	*vps5*, *vps17*, *vps39*, *vps41*, *vps43*, *vps51*, *vps52*, *vps53*, *vps54*, *vps61*, *vps64*, *vps66*, *vps69*, *vps71*, *vps72*, *vps73*, *vps75*
Class C *vps* mutants	Do not possess organised vacuoles. Defective in CPY sorting.	*vps11*, *vps16*, *vps18*, *vps33*
Class D *vps* mutants	Defects in vacuole inheritance and acidification of the vacuole. Failed to assemble membrane subunits of the V-ATPase onto the cytoplasmic surface of the vacuole. Single large vacuoles eventuated through the failure to form segregation structures, buds receive little or no vacuolar material from mother cells. No defects in CPY sorting.	*vps3*, *vps6*, *vps 8*, *vps9*, *vps15*, *vps19*, *vps21*, *vps34*, *vps45*
Class E *vps* mutants	Normal vacuolar morphology. Exaggerated prevacuolar or endosome-like organelles. Secreted modest amounts of CPY.	*vps2*, *vps4*, *vps20*, *vps22*, *vps23*, *vps24*, *vps25*, *vps27*, *vps28*, *vps31*, *vps32*, *vps36*, *vps37*, *vps44*, *vps46*, *vps60*
Class F *vps* mutants	Vacuolar morphology is intermediate between wild-type cells and vacuolar morphology of class B mutants. Characterised as large central vacuoles often surrounded by smaller vacuolar compartments. Severe CPY sorting defects.	*vps1*, *vps26*, *vps62*, *vps65*, *vps68*, *vps71*

1.11 YEAST TRAFFICKING PATHWAYS

In *S. cerevisiae*, aside from autophagy, proteins are delivered to the vacuole through the yeast secretory pathway (Stevens et al., 1982). It is in the late Golgi that soluble vacuolar proteins are sorted and targeted to the vacuole, cell surface or endosomes (Graham and Emr, 1991). There are essentially three biosynthetic pathways employed by yeast to sort newly synthesised proteins from the Golgi to the vacuole, namely: the CPY pathway which involves the movement of cargo through the endosome-like structure titled prevacuolar compartment (PVC); the alkaline phosphatase (ALP) pathway which bypasses the PVC (Wickner and Haas, 2000); and the Multivesicular-Body sorting (MVB) pathway. There are over 70 proteins involved in efficient protein trafficking from the yeast late Golgi to the vacuole. Many of these proteins have functional orthologues in higher order organisms (Bowers and Stevens, 2005).

The CPY and endocytic pathways both converge at the late endosome/MVB. While other hydrolases may take the same route – interacting with Vps10, the pathway is titled the 'CPY-pathway' due to the main cargo being transported. As illustrated by *Figure 1.9*, CPY is synthesised and transported across the ER to the Golgi (Bowers and Stevens, 2005). The protein then binds to the receptor Vps10p in the late Golgi. The CPY/Vps10p complex proceeds through the late endosome (titled LE, *Figure 1.9*) where the complex dissociates, allowing the recycling of Vps10p back to the Golgi and sorting the CPY to the vacuole where it develops to the mature form – mCPY, following cleavage (Bowers and Stevens, 2005). The CPY pathway is the default transport pathway in most yeast.

The ALP pathway also is named according to its main cargo – alkaline phosphatase, (Bowers and Stevens, 2005) and is signal mediated (Conibear and Stevens, 1997). Proteins entering the ALP pathway are sorted into classes of vesicles at the Golgi but completely bypass the PVC (*Figure 1.10*). Vesicles of the ALP and CPY pathways fuse with the vacuole via the SNARE complex (Piper et al., 1997).

Proteins may also be sorted into MVB for many cellular processes. Early and late endosomes can be distinguished on the basis of their morphological appearance. Late endosomes typically have a multivesicular appearance and are thus referred to as MVB (Katzmann et al., 2002). The contents of the MVB (such as CPY) are delivered into the vacuole through the fusion of the limiting membrane of the MVB with the vacuolar membrane (Katzmann et al., 2002).

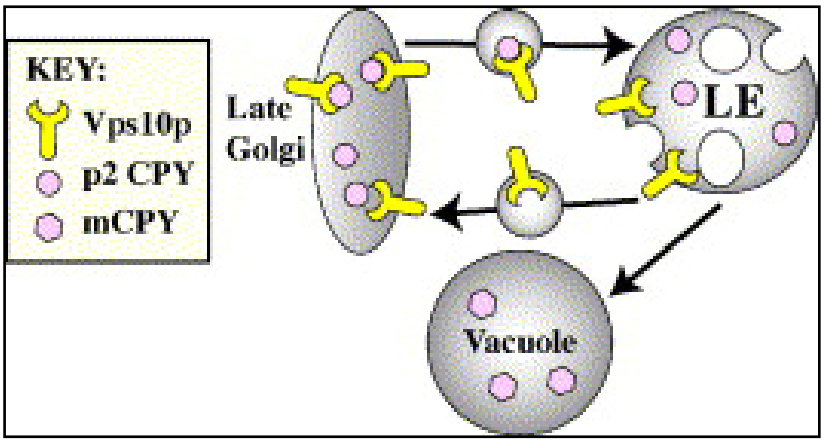

Figure 1.9: The CPY sorting pathway (Bowers and Stevens, 2005). CPY is synthesised and transported across the ER to the Golgi. The protein then binds to the receptor Vps10p in the late Golgi. The CPY/Vps10p complex proceeds through the late endosome, where the complex dissociates, allowing the recycling of Vps10p back to the Golgi and sorting the CPY to the

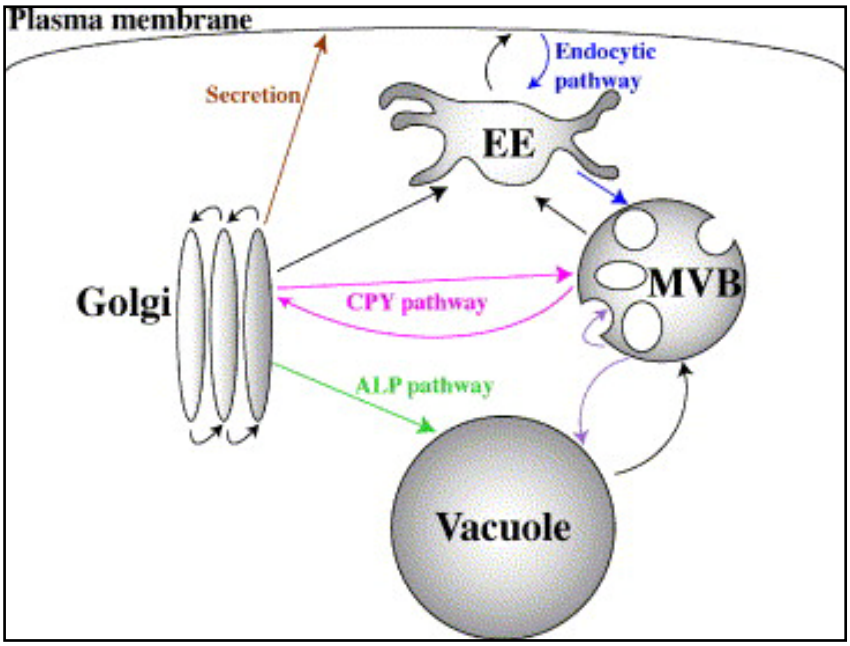

Figure 1.10: Protein trafficking pathways in *S .cerevisiae* (Bowers and Stevens, 2005). Proteins entering the ALP pathway are sorted into classes of vesicles at the Golgi but completely bypass the PVC. The contents of the MVB (such as CPY) are delivered into the vacuole through the fusion of the limiting membrane of the MVB with the vacuolar membrane.

1.12 VACUOLAR FUSION AND MEMBRANES

Vacuole fusion is divided into three distinct stages namely, “priming” which prepares the vacuoles for attachment, “docking” which includes the tethering of vacuoles for “fusion” leading to the combining of the vesicle to the vacuole (Wang et al., 2002).

The process of priming occurs on separate vacuoles in preparation for subsequent docking events (Mayer et al., 1996). The ATP-dependent priming, is initiated by Sec18p ATPase (Mayer et al., 1996) and involves the co-chaperones Sec18p/NSF, Sec17p/α-SNAP, and LMA1 (low-M_r activities) (Seeley et al., 2002). During the priming stage, the *cis*-SNARES (same membrane) also disassemble with the help of Sec18 and Sec17 (Ostrowicz et al., 2008), allowing for *trans* (between vesicles) interaction (Seeley et al., 2002). Priming allows for the release of the HOPS (Homotypic fusion and vacuole protein sorting) complex from the vacuolar membrane. Sometimes also referred to as the VPS class C complex – required for Golgi-to-vacuole protein transport (Sato et al., 2000), this group consists of six proteins (four of which belong to the VPS class C): Vps11p/Pep5p, Vps16p, Vps18p/Pep3p, Vps33p (Sec1p homologue), Vps39p/Vam6p (nucleotide exchange factor for Ypt7p) and Vps41p/Vam2p, which upon release gets transferred to Ypt7p (Price et al., 2000) catalysing the conversion to its active GTP form (Seeley et al., 2002). Ypt7p is a GTPase from the Rab/Ypt family. Vps39p and Vps41p belong to the VPS class B category.

Docking is the physical attachment of vacuole membranes. It involves two successive stages, a reversible tethering reaction and a subsequent *trans*-SNARE pairing (Ungermann and Wickner, 1998). Fusion terminates with the release of the boundary membrane into the vacuole lumen which will eventually be degraded (Wang et al., 2002).

The vacuolar membrane is a dynamic structure in a constant state of membrane fission and fusion which is dictated by the cell cycle. The balance between fission and fusion must be maintained to ensure vacuole integrity. *S. cerevisiae* relies on vacuolar H^+-ATPase (V-ATPase) to equilibrate fission and fusion (Baars et al., 2007). Fusion has been solely attributed to the physical presence of the membrane sector of the V-ATPase complex, while fission is dependent on the proton translocation function of the complex (Baars et al., 2007). In mutants lacking V-ATPase function – the cells contain a large single vacuole, whereas, multiple small vacuoles are characteristic of mutants defective in vacuolar fusion (Takeda et al., 2008).

Docked vacuoles – in preparation for fusion, have three characteristic membranes, they are, outside, boundary and vertex membranes (refer to *Figure 1.11*). In vacuole clusters, the outside membrane is defined as not being in contact with other vacuoles, while the boundary membrane does make contact with adjacent vacuoles. The vertex is the membrane connecting the boundary and outside membranes (Wang and Klionsky, 2003).

Vacuolar fusion occurs at the vertex rings around the disc of apposed boundary membranes (Wang and Klionsky, 2003), and not at the boundary membrane as reported in previous research. This vertex fusion is completed with the boundary membrane remaining in the lumen of the newly fused organelle. Several proteins essential for the docking and fusion of vacuoles are enriched at vertices.

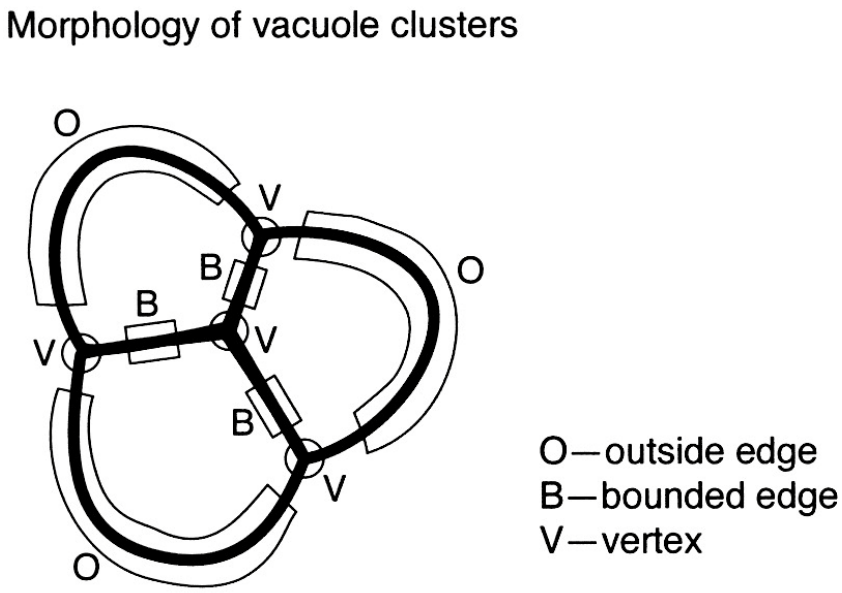

Figure 1.11: Docked vacuolar membrane (Wang and Klionsky, 2003). Following vacuolar priming, vacuoles dock in a cluster in preparation for fusion. There are three membranes namely, the outside, boundary and vertex membranes. The outside membrane does not make contact with other vacuoles, while the boundary membrane does make contact with adjacent vacuoles. The vertex is the membrane connecting the boundary and outside membranes. Fusion occurs at the vertex membrane and results with the boundary membrane remaining in the lumen.

1.13 SCOPE AND AIM OF STUDY

Following internalisation into mammalian cells, *B. pseudomallei* escapes from the phagosome to continue its infection cycle. At the commencement of this research in 2006, a literature search was performed to identify the general virulence factors employed by gram-negative bacteria to escape from their confining phagosomes. Initially, a list of 22 virulence factors was compiled. Further bioinformatics analysis identified five of the 22 open reading frames (ORF) as sharing significant homology with a sequence within the *B. pseudomallei* genome namely: *BPSS1531* (*BipC*), *BPSS1532* (*BipB*), *BPSL0670*, *BPSS1394* (*BpscN*) and *BPSS0670*. *B. pseudomallei* mutants of *BPSS1529* (*BipD*) and *BPSS1539* were identified as being confined to the phagosome. Hence these two genes along with the five ORFs identified as having a *B. pseudomallei* homologue were selected for characterisation.

In *Chapter 3*, the seven *B. pseudomallei* ORFs were expressed in *S. cerevisiae* and the cells were observed for any morphological or physiological changes which may occur under conditions when autophagy is induced. So, cells were grown under nitrogen starvation conditions to induce autophagy, then stained with FM4-64 to label the vacuole membranes and imaged. Cells expressing *B. pseudomallei* products which perturb intracellular vesicle trafficking will potentially have notable changes in the vacuolar morphology when imaged. Yeast cells expressing the *B. pseudomallei* ORFs were also co-transformed with plasmids expressing either the cytosolic, mitochondrial or nucleus targeted Rosella biosensor. This biosensor is composed of a pH-sensitive variant of GFP linked to a pH-stable variant of the RFP (Rosado et al., 2008). When cells are subjected to conditions that induce autophagy, delivery of the specifically

labelled organelle or cytosol to the vacuole results in an accumulation of red fluorescence to the vacuole as the pH-sensitive GFP is quenched in the acid vacuole but red is maintained. Yeast cells expressing the *B. pseudomallei* ORFs were observed for any influence that the expression of the encoded foreign proteins may have on cytosolic, mitochondria or nucleus turnover. These yeast cells tended to have a multi-vacuolar morphology with reduced cytosolic and mitochondrial turnover. However, there was no apparent reduction in nucleus turnover.

Given the influence specific *B. pseudomallei* ORFs had on vacuolar morphology and organelle turnover in *S. cerevisiae,* mutants of each of these ORFs in *B. pseudomallei* were attempted with the intention of determining their role in bacterial infection of mammalian cells. Using the double cross-over allelic exchange method, three deletion mutants were successfully constructed in *B. pseudomallei* namely, *BPSS1532* (*bipB)*, *BPSL0670* and *BPSS1394* (*bpscN)*. *Chapter 4* reports the characterisation of *BPSS1532* and *BPSL0670* mutants in *in vivo* studies to determine their virulence in BALB/c mice. Further *in vitro* studies were conducted to investigate the ability of these mutants to: survive and replicate in host cells, co-localise with GFP-LC3, produce actin tails and induce MNGC formation in macrophage-like RAW264.7 cells.

In *Chapter 5* a non-polar deletion mutant *BPSS1394 (bpscN)* was characterised using similar *in vivo* and *in vitro* experimental approaches. *BPSS1394* is a predicted TTSS1 ATPase. TTSS1 and TTSS2 have previously been reported to not be involved in *B. pseudomallei* virulence in a hamster infection model. This study analysed the *BPSS1394* mutant with the intention of establishing the importance of the TTSS1

BPSS1394 gene in *B. pseudomallei* pathogenesis. A virulence trial was carried out to demonstrate the importance of this gene in infection of a mouse model. Data obtained from the trial showed that the mutant bacteria was attenuated for virulence and therefore the infected mice survived for the length of the trial, whilst the mice infected with the wild-type bacteria displayed clinical manifestations of melioidosis and was therefore euthanased early in the trial. This suggests that secreted TTSS1 effectors are likely to be required for infection and virulence in human infection. Thus, further research could be carried out to elucidate the role of TTSS1 effectors, and potentially TTSS2 effectors in pathogenesis.

CHAPTER TWO

MATERIALS & METHODS

2.1 STRAINS & VECTORS

Escherichia coli strain K12 DH5α (Bethesda Research Laboratories, Rockville, USA) with the genotype: *F–, ø80dlacZΔM15, Δ(lacZYA-argF)U169, deoR, recA1, endA1, hsdR17(rK–, mK+), phoA, supE44, λ–, thi-1, gyrA96* and *relA1,* was primarily used for amplification of plasmids and transformations involving the rapid ligation vector pGEM-T (Promega, Madison, USA), pBluescriptSK phagemid (Stratagene, La Jolla, USA), and pAH19 storage vector (Hinnebusch and Fink, 1983). The K12 SM10*λpir* strain (Milton et al., 1992), with the genotype: *thi-1, thr, leu, tonA, lacY, supE, recA::RP4-2-Tc::Mu, Kmr* and λ, was used for conjugations into *B. pseudomallei* with the suicide vector pDM4 (λ*pir*-dependent, Cm^R and *sac*BR negative selection; (Milton et al., 1996)). The S17-1*λpir* strain (Simon et al., 1983) with the genotype: Tp^R, Sm^R, *recA, thi, pro, hsdR-M*$^+$*RP4: 2-Tc:Mu*: *Km,* Tn7, *λpir,* was used for conjugations in *B. pseudomallei* with the complementation vector pBHR1 (mob, rep, Cm^R and Kan^R; (Szpirer et al., 2001)).

The parental yeast *S. cerevisiae* BY4741 strain (Research Genetics, Huntsville, AL, USA) with the genotype: *MAT**a**, his3Δ1, leu2Δ0, met15Δ0* and *ura3Δ0,* was employed for all the yeast work. Strains expressing the pAH19 vector (*URA3* selectable marker) and Rosella fluorescent biosensor in the pAS1NB vector (*LEU2* selectable marker), (Rosado et al., 2008), were selected on the basis of complementation of uracil and leucine auxotrophies by the respective vector-borne *ura3* and *leu2* genes.

The *B. pseudomallei* K96243 strain (source: Dr Brenda Govan, James Cook University, Townsville, Australia) is a fully sequenced Thai clinical isolate (Holden et al., 2004). The wild-type bacterium contains a gentamicin resistance gene, which is used as an antibiotic selection marker when plated on an agar plate containing 64 μg/mL gentamicin. This concentration is sufficient for killing contaminants but not *B. pseudomallei* K96243.

2.2 GROWTH MEDIA

All materials, unless otherwise stated, were purchased from Merck (Kilsyth, Victoria, Australia). Media were autoclaved at 121°C, 405-506 kPa for 20 m. Agar plates were made by adding 1.5% w/v agar – with the exception of *B. pseudomallei* motility assay plates which required 0.4% w/v agar. Amino acid supplements and antibiotics were added to the medium after autoclaving, when it had cooled to 50°C. All yeast and bacterial cultures were grown at 28°C and 37°C respectively, broth cultures were incubated with shaking at 200 rpm.

2.2.1 Yeast Media

Table 2.1 Protocol for the preparation of YEPD

Yeast Extract Peptone Dextrose (YEPD)	
Yeast extract	1% w/v
Peptone	1% w/v
Glucose	2% w/v

Table 2.2 Protocol for the preparation of YMM

Yeast Minimal Medium (YMM)	
Yeast nitrogen base without amino acids & ammonium sulphate	0.67% w/v
Glucose	2% w/v

Table 2.3 Protocol for the preparation of SMM

***Saccharomyces* Salts Medium (SMM)**	
Yeast extract	1% w/v
$(NH_4)_2SO_4$	0.12% w/v
KH_2PO_4	0.1% w/v
$CaCl_2$	0.01% w/v
$FeCl_3$	0.0005% w/v
$MgCl_2$	0.07% w/v
NaCl	0.05% w/v

Table 2.4 Protocol for the preparation of Starvation Medium

Starvation Medium	
Yeast nitrogen base without amino acids & ammonium sulphate	0.17% w/v

Table 2.5 Protocol for the preparation of Glycerol Stock

15% Glycerol Stock Storage – Yeast & Bacterial	
Cell Suspension	300 μL
Glycerol (50% stock)	100 μL

2.2.2 Bacterial Media

Table 2.6 Protocol for the preparation of LB

Luria-Bertani Broth (LB)	
Yeast extract	1% w/v
Tryptone	1% w/v
NaCl	0.5% w/v

* Agar at 0.4% w/v added for motility assay plates
* Supplemented with ampicillin (10 μg/mL) or tetracycline (12.5 or 25 μg/mL) as required, after autoclaving

Table 2.7 Protocol for the preparation of 2 YT

2 YT Medium	
Yeast extract	1% w/v
Tryptone	1.6% w/v
NaCl	0.5% w/v

Table 2.8 Protocol for the preparation of Ashdown Medium

Ashdown Medium	
Tryptone soya broth	1% w/v
Glycerol	42% v/v
Natural red (1% v/v stock)	0.5% v/v
Crystal violet (0.1% v/v stock)	0.5% v/v

* Supplemented with gentamicin (64 μg/mL) or tetracycline (25 μg/mL) as required

Table 2.9 Protocol for the preparation of Sucrose Medium

Sucrose Medium	
Yeast extract	1% w/v
Tryptone	1% w/v
Sucrose	20% w/v

2.3 MOLECULAR BIOLOGY TECHNIQUES

2.3.1 Construction of *B. pseudomallei* Mutants

The *B. pseudomallei* deletion mutants were constructed by double cross-over allelic exchange. Primers (*Table 4.2*) were used to amplify an approximately 1 kb fragment upstream and downstream of the coding sequence to encompass approximately 100 bp of the coding sequence. The upstream fragment was flanked by *Xba*I and *Bgl*II, whilst the downstream fragment was flanked by *Bgl*II and *Xba*I. These two fragments, together with the *Bgl*II-digested tetracycline *tetA*(C) gene cassette, were introduced by a three-way ligation into pBluescriptSK phagemid. The resulting plasmid was

digested with *Xba*I, and the mutagenesis cassette recovered and ligated into *Xba*I-digested pDM4. This construct was then transformed in *E. coli* SM10 *λpir* for conjugation into *B. pseudomallei*.

2.3.2 Complementation of *B. pseudomallei* Mutants

A complementation construct was generated using primers (*Table 5.2*) to amplify a 1,374 bp fragment, spanning the entire *bpscN* coding region from *B. pseudomallei* K96243. The fragment was digested with *Dra*I and *Nco*I to be ligated into the pBHR1 mobilisation plasmid (University of Louisville, Louisville, KY, USA). The resulting pBHR1::*bpscN* plasmid was introduced into *E. coli* S17-1 and subsequently conjugated into the *B. pseudomallei bpscN* mutant strain.

2.3.3 Polymerase Chain Reaction

Polymerase chain reaction (PCR) was employed to amplify desired open reading frames (ORF) from *B. pseudomallei* genomic DNA and as a diagnostic measure to determine the presence and orientation of cloned ORFs. PCR amplifications from the GC-rich *B. pseudomallei* genomic DNA were carried out using either the LA Taq (TaKaRa, Shiga, Japan) or KOD (Novagen, Madison, USA) polymerase with GC-rich specific buffers provided by the manufacturers.

Table 2.10 Protocol for the preparation of PCR mixture for Takara polymerase

PCR mixture for *TaKaRa LA Taq*	
Template	1 μg
Primer 1	0.2-1 μM final conc.
Primer 2	0.2-1 μM final conc.
dNTP (2.5 mM each)	8 μL
2XGC buffer (5 mM Mg^{+2})	25 μL
TaKaRa LA Taq	0.5 μL
Sterilised water	up to 50 μL

Table 2.11 Protocol for the preparation of PCR mixture for KOD polymerase

PCR mixture for KOD	
Template	10-500 pg/1 μL
Primer 1	0.4 μM final conc.
Primer 2	0.4 μM final conc.
dNTP (2 mM each)	0.2 mM
KOD $MgSO_4$ (25 mM)	1.5 mM
DMSO	1.25 uL
10 X KOD buffer *	2.5 μL
KOD (2.5 U/μL)	0.02 U/μL
Sterilised water	up to 25 μL

* (1.2 M Tris-HCl, 100 mM KCl, 60 mM $(NH_4)_2SO_4$, 1% Triton X-100, 0.01% BSA, pH 8.0)

PCR Cycle Conditions

Table 2.12 PCR cycle conditions for Takara and KOD polymerase

TaKaRa LA Taq			KOD		
Cycle	**Temperature**	**Time**	**Cycle**	**Temperature**	**Time**
1	94°C	5 m	**1**	94°C	2 m
2-30	94°C	30 s	**2-35**	94°C	20 s
	55°C	30 s		58°C	30 s
	72°C	90 s		70°C	4 m
Hold	72°C	7 m	**Hold**	72°C	7 m
Pause	4°C		**Pause**	4°C	

2.3.4 Agarose Gel Electrophoresis

A quantity of DNA product derived from either PCR amplification, restriction enzyme digestion or purification processes, was run on 1% agarose gels in the MGTBE running buffer (*Table 2.13*) at pH 8.0. Gels were run at 90 V for 90 m. A *Hin*dIII-digested MassRuler (Promega, Madison, WI, USA) was run as a standard, allowing for the size and concentration of DNA samples to be quantified. As required, gel slices containing single DNA bands were excised for further manipulation and purified using a gel extraction kit (Qiagen, Alameda, Province, Canada).

Table 2.13 Protocol for the preparation of MGTBE 10X Buffer

MGTBE 10X Buffer	
Tris	107.7 g w/v
EDTA	8.4 g w/v
Boric acid	55.5 g w/v
Water	Up to 1 L

* Autoclave mixture

2.3.5 DNA Restriction Digests

DNA products that were to be linearised or contained the same restriction site at the 5' and 3' were subjected to restriction endonuclease digestion with a single enzyme. Products flanked by two different restriction sites required double digestion. All restriction enzymes used were obtained from Promega, and used in reactions containing optimal buffers (60mM Tris-HCl, 500mM-1.5M NaCl, 60mM $MgCl_2$ and 10mM DTT) provided by the manufacturer. Unless otherwise stated, all restriction digests were incubated at 37°C for 3 h.

Table 2.14 Protocol for the preparation of digestion mixture for Single enzyme digest

Single Digestion	
DNA (80 ng/µL)	5 µL
RE 10X Buffer	3 µL
Restriction Enzyme (10 u/µL)	3 µL
Acetylated BSA (10 µg/µL)	1 µL
Sterilised water	19 µL

Table 2.15 Protocol for the preparation of digestion mixture for Double enzyme digest

Double Digestion	
DNA (80 ng/μL)	20 μL
RE 10X Buffer	6 μL
Restriction Enzyme 1 (10 u/μL)	2 μL
Restriction Enzyme 1 (10 u/μL)	2 μL

All vectors that underwent restriction enzyme (RE) digestion were subsequently dephosphorylated with Calf Intestine Alkaline Phosphatise (CIAP, Promega), to prevent re-ligation. The dephosphorylation mixture was incubated at 37°C for 1 h.

Table 2.16 Protocol for the preparation of Dephosphorylation mixture

Dephosphorylation	
DNA RE digest sample	30 μL
Alkaline Phosphatase 10X Reaction Buffer*	6 μL
CIAP (0.01 μ/μl)	2 μL
Sterilised water	12 μL

* (50mM Tris-HCl pH 9.3, 1mM $MgCl_2$, 0.1mM $ZnCl_2$, 1mM spermidine)

Enzyme restriction and dephosphorylation samples were subsequently purified using PCR purification kits (Qiagen), according to the manufacturer's protocol.

2.3.6 DNA Ligation

Ligation mixtures adhered to a vector-insert ratio of 1:3. Ligations were performed using LigaFast Rapid T4 DNA ligase (Promega) at 37°C for 30 m – 1 h. DNA of ligation reactions was subsequently transformed into competent *E. coli* DH5α and amplified.

Table 2.17 Protocol for the preparation of Ligation mixture for T4 DNA Ligase

Ligation Reaction Mixture	
Vector DNA	33 ng
Insert DNA	100 ng
2X Rapid Ligation Buffer	2.5 µL
T4 DNA Ligase	0.5 µL

* 60mM Tris-HCl pH 7.8, 20mM $MgCl_2$, 20mM DTT, 2mM ATP and 10% PEG

Bacterial plasmids were extracted from *E. coli* using the commercially available Wizard Plus SV Miniprep DNA Purification System (Promega).

2.3.7 DNA Sequencing

Nucleotide sequencing utilised a procedure based on the use of Big Dye (*Table 2.18)* (Applied Biosystems, Carlsbad, CA, USA) as supplied by Micromon (Monash University). The Micromon protocol and clean-up procedures are available at: (http://www.micromon.monash.org/dna-seq-reaction-param.html).

Table 2.18 Protocol for the preparation of Sequencing Reaction mixture

Sequencing Reaction Mixture	
Template DNA	300 ng
Primer	3 pmole
Buffer 5X*	3.5 µL
Big Dye	1 µL

***** (400mM Tris pH 9.0, 10mM MgCl2)

Table 2.19 Sequencing conditions for Big Dye

Sequencing Conditions for Big Dye		
Cycle	**Temperature**	**Time**
1	96 °C	60 s
2-30	96 °C	10 s
	50 °C	5 s
	60 °C	4 m
Hold	5 °C	2 m
Pause	4 °C	

2.4 TRANSFORMATIONS & CONJUGATION

2.4.1 Chemically Made Competent *E. coli*

The *E. coli* DH5α used for plasmid amplification, and SM10 conjugation strains were made chemically competent using rubidium chloride treatment (Glover, 1985), prior to being transformed with DNA. Cells from an overnight bacterial culture were harvested (13,000g for 15 m at 4°C) and resuspended in 1/3 volume of RF1 solution for 1 h on ice. At all times the suspension was maintained either on ice or at 4°C. The cells were then pelleted by centrifugation again and resuspended in 1/12.5 volume of RF2 solution for 15 m on ice. The suspension was dispersed into sterile 1.5 mL microcentrifuge tubes suspended in a dry ice – ethanol bath. Once cells were frozen the tubes were stored at -80°C.

Table 2.20 Protocol for the preparation of RF1 solution

RF1 Solution – 40 mL	
RbCl (100 mM)	0.48 g
$MnCl_2$ (50 mM)	0.40 g
K acetate (30 mM pH 7.5)	1.2 mL
$CaCl_2.2H_2O$ (10 mM)	0.06 g
Glycerol (15% w/v)	6 mL

* pH to 5.8 with 0.2 M acetic acid

Table 2.21 Protocol for the preparation of RF2 solution

RF2 Solution – 20 mL	
RbCl (10 mM)	0.02 g
MOPS (10mM)	0.4 mL
$CaCl_2.2H_2O$ (75mM)	0.22g
Glycerol (15%w/v)	3 mL

* pH to 6.8 with NaAc

* Both RF1 and RF2 solutions were sterilised with a 25mm filter (Pall Life Science, Port Washington, NY, USA).

2.4.2 Transformation of *E. coli*

In accordance with the high-efficiency protocol (NEB, 2007), 100 ng of plasmid DNA (1 – 5 μL) was incubated with 50 μL of competent *E. coli* DH5α on ice for 30 m. The mixture was heat-shocked at 42°C for 60 s, and returned to ice for a further 5 m. The cells were then inoculated into 250 μL LB and underwent recovery for 1 h, with shaking at 240 rpm at 37°C. 60 μL of the suspension was subsequently plated onto LB agar containing specific antibiotics to select for specific plasmids.

2.4.3 Chemically Competent *S. cerevisiae*

The *S. cerevisiae* strain BY4741 was made competent using the commercially available *S.c* EasyComp Transformation Kit (Invitrogen, Carlsbad, CA, USA). 1 mL of an overnight culture was harvested by centrifugation (1,500 rpm for 2 m) and the pellet resuspended in 1 mL of solution 1 as provided by the manufacturer. Cells were pelleted by centrifugation again and resuspended in 100 μL of solution 2 as provided

by the manufacturer. The cell suspension was then dispersed into sterile 1.5 mL microcentrifuge tubes and stored at -80°C.

2.4.4 Transformation of *S. cerevisiae*

A mixture comprising 100 ng of vector DNA, 5 μL of competent *S. cerevisiae* cells and 50 μL of solution 3 (*S.c* EasyComp Transformation Kit; Invitrogen), was incubated for 1 h, with shaking at 120 rpm at 30°C. The entire cell suspension was subsequently plated on a yeast minimal medium plate supplemented with 30 μL of relevant amino acids (0.002% w/v).

2.4.5 Conjugation between *E. coli* and *B. pseudomallei*

Deletion mutants were constructed by double cross-over allelic exchange in *B. pseudomallei* K96243. Mutagenesis constructs were cloned so as to incorporate a tetracycline resistance cassette into the *λpir*-dependent pDM4 suicide vector which carries a gene for chloramphenicol resistance, and was introduced into the *E. coli* K-12 SM10 *λpir* strain. The SM10 strain was used as the donor strain to allow mobilisation of the pDM4 plasmid into *B. pseudomallei* K96243.

Overnight cultures of the SM10 containing pDM4 and wild-type *B. pseudomallei* strains were sub-cultured to mid-log phase. 500 μL of both cultures were spotted together on LB agar plates which were then incubated overnight at 37°C, allowing for conjugation between *E. coli* and *B. pseudomallei,* and the transfer of the pDM4 vector into *B. pseudomallei*. The conjugants were resuspended in 200 μL phosphate buffered

saline (PBS) pH7.2 and plated on LB agar containing 64 μg/mL gentamicin to select for the *B. pseudomallei*; and 25 μg/mL tetracycline to select for cells carrying the mutated gene. Plates were incubated overnight at 37°C. The following day, transformants were selected and further characterised for their antibiotic profile by patching them onto LB agar plates containing either 64 μg/mL gentamicin and 25 μg/mL tetracycline, or 64 μg/mL gentamicin and 50 μg/mL chloramphenicol. Patches showing both tetracycline and chloramphenicol resistance were denoted single cross-over mutants. Patches showing both tetracycline resistance and chloramphenicol sensitivity were denoted double cross-over mutants.

2.4.6 Resolving Single-Crossover *B. pseudomallei* Mutants

Single-crossover mutants were resolved according to the method of Logue et al (2009), based on a *sacB* counter-selection protocol which acts through activation of the *sacB* gene encoded in pDM4. Following overnight growth and sub-culturing in LB supplemented with 20% sucrose, transconjugants were plated onto 2YT agar. The resulting colonies were characterised for their antibiotic profile as described in *Chapter 2.4.5* above.

2.5 ANALYSIS OF PROTEIN EXPRESSION IN YEAST

2.5.1 Yeast Whole Cell Lysates

Overnight cultures of yeast expressing *B. pseudomallei* proteins were grown to mid-log phase, and cells harvested at the equivalent of 5 mg of dry weight cells (OD_{650} of 1.0 represents approximately 430 μg/mL) and then resuspended in 1 mL distilled water, 75 μL of 3.7 M NaOH and 11 μL of 2-mercaptoethanol. The suspension was incubated on ice for 10 m, after which 90 μL of 80% TCA was added followed by a further 10 m incubation on ice. The suspension was then centrifuged at 13,000 rmp for 90 s and the pellet was washed with 1 mL cold acetone twice. The pellet was resuspended in 150 μL of 5% SDS and boiled for 5 m. After cooling, the suspension was centrifuged at 13,000 rpm for 90 s and the resulting supernatant transferred to a sterile 1.5 mL microfuge tube and mixed with an equal volume of 2X sample SDS/PAGE buffer (25% (v/v) 0.5 M stacking buffer with a pH of 6.8, 20% (v/v) glycerol, 40% (v/v) 20% SDS, 10% (v/v) 2-mercaptoethanol, 5% (v/v) water and bromophenol blue), in preparation for gel loading.

2.5.2 Sodium Dodecyl Sulfate-PolyAcrylamide Gel Electrophoresis

Protein lysates were run on SDS-PAGE gels comprising a 10% resolving gel (2 mL water, 1.25 mL of 3 M Tris resolving buffer pH 8.8, 1.67 mL Bis/Acrylamide, 25 μL of 20% SDS, 25 μL ammonium peroxidisulphate and 10 μL TEMED) and a 4% stacking gel (1.5 mL water, 625 μL of 0.5M Tris stacking buffer pH 6.8, 12.5 μL of 20% SDS, 325 μL Bis-Acrylamide, 12.5 μL ammonium peroxidisulphate and 5 μL TEMED). Gels were run in running buffer (250 mM Tris, 1.92 M glycine and 1%

SDS) at 120 V for 90 m and subsequently prepared for either Western Immuno-Blotting analysis or ElectroChemiLuminescence detection.

2.5.3 Western Immuno-Blotting and ElectroChemiLuminescence (ECL) Detection

Protein samples resolved on SDS-Polyacrylamide gels were transferred to PVDF membranes (Pall Life Science) at 90 V, for 1 h at 4°C. Membranes were then blocked in 5% skim milk and probed with the primary mouse anti-HA monoclonal antibody (Lithgow Lab, Monash University, Melbourne) and fluorescent secondary goat anti-mouse HRP-conjugated antibodies (Pierce, Rockford, MA, USA). Membranes were imaged on a Typhoon Trio imager using Image Quant software (GE Healthcare Life Sciences, Uppsala, Sweden). Protein bands expressing low signal required ECL detection. Membranes to be analysed through ECL (reagents provided by Amersham, Piscataway, NJ, USA) were probed with an additional SuperSignal West Femto (Pierce) and x-ray imaged with 1 m exposure.

2.6 OBSERVING YEAST ORGANELLE MORPHOLOGY AND TURNOVER

Vacuolar morphology in yeast strains expressing *B. pseudomallei* proteins was observed by confocal laser scanning microscopy following 4 h incubation in starvation medium (Rosado et al., 2008) and 1 h incubation with 1 μL of FM4-64 (Invitrogen, (Vida and Emr, 1995)). In a similar manner, organelle turnover was observed in cells transformed with Rosella biosensors, targeted to specific cellular compartments (Rosado et al., 2008). Strains were grown under non-starved (control)

or nitrogen-starved conditions to induce organelle turnover by autophagy. Cells were mounted with 0.2% (w/v) low melting point agarose and imaged using the FITC and TRITC channels, on an Olympus FV500 Confocal Laser Scanning Microscope (Nowikovsky et al., 2009).

2.7 ANALYSIS OF BACTERIAL GROWTH

The growth of mutant bacterial strains was compared to wild-type *B. pseudomallei* by optical density at 600 nm (OD_{600}). *B. pseudomallei* strains were grown in 5 mL LB with and without tetracycline 25 μg/mL for 5 h with shaking (200 rpm) at 37°C. At this point, an OD_{600} reading was made and 100 μL of cells were then subcultured into a fresh 5 mL LB for overnight growth. The following day, all cultures were inoculated into fresh 20 mL LB at an OD_{600} of 0.05 and allowed to grow for 12 h at 37°C with shaking at 200 rpm. OD_{600} was measured at 20 m intervals.

2.8 TISSUE CULTURE OF MOUSE MACROPHAGE CELLS

The mouse macrophage cell lines RAW 264.7 and RAW 264.7 stablely transfected with LC3-GFP (Cullinane et al., 2008) were cultured in Roswell Park Memorial Institute (RPMI) medium supplemented with 10% (v/v) of heat-inactivated fetal calf serum (Invitrogen), grown at 37°C with 5% CO_2. At 15 h prior to *B. pseudomallei* infection, the relevant cell lines were seeded at 1.0 x 10^5 cells/well into 24-well trays.

RAW 264.7 cells were used for viable cell counts in survival assays and actin visualisation while GFP-LC3 transfected macrophages were used in autophagy related assays to identify the co-localisation of *B. pseudomallei* with GFP-LC3.

2.9 *B. PSEUDOMALLEI* SURVIVAL ASSAY

The ability of mutant and wild-type *B. pseudomallei* to survive and replicate within RAW 264.7 macrophage cells was measured by viable cell counts. Strains were grown overnight in LB medium with relevant antibiotics and subcultured for 3 h to reach mid-log phase. Macrophage cells were infected for 1 h at a multiplicity of infection (MOI) of 6:1, by using 20 μL of a $5x10^8$ bacteria/mL culture. At 1 h post infection, cells were washed with PBS and placed in fresh RPMI medium containing 100 μg/mL ceftazidime and 800 μg/mL kanamycin to kill extracellular bacteria. At 2 h, 4 h and 6 h post infection, wells were washed four times with 500 μL PBS to remove any extracellular bacteria. 50 μL of the final wash was plated on LB agar 'wash plates' and incubated at 37°C for two days. The RAW 264.7 macrophages were incubated with 200 μL of 0.1% Triton X-100 for 10 m to lyse the cells. 100 μL of the bacterial lysis solution was plated on LB agar 'lysis plates' and grown at 37°C for two days.

Numbers of bacterial colonies growing on 'wash plates' and 'lysis plates' were tallied and statistically analysed using T-tests and one-way ANOVA.

2.10 *B. PSEUDOMALLEI* INFECTION ASSAY

The intracellular infectivity of mutant and wild-type *B. pseudomallei* was determined visually within macrophage RAW 264.7 cells expressing LC3-GFP. Cells were grown as a monolayer in 24-well trays containing cover slips. In a similar manner to the survival assay, both bacterial strains were grown overnight in LB supplemented with 25 μL/mL tetracycline for the mutant strain and 64 μL/mL gentamicin for the wild-type strain, and subcultured to mid-log phase. Macrophages were infected for 1 h with mutant and wild-type *B. pseudomallei* at an MOI of 6:1. At this time the wells were washed four times with PBS and replaced with fresh RPMI containing ceftazidime (100 μg/mL) and kanamycin (800 μg/mL). At 2 h, 4 h and 6 h post-infection the macrophages were washed four times with PBS to remove extracellular bacteria. The PBS was replaced with 500 μL of 100% methanol and incubated at 37°C for 10 m to permeabilise the cells. The adhered infected macrophages on the cover slips were immunofluorescently-labelled.

2.10.1 Immunofluorescent Labelling

Where required, antibody solutions and washes were made with 1% (w/v) BSA PBS. The cells were incubated with the primary rabbit anti-*B. pseudomallei* outer membrane antibody (Cullinane et al., 2008) at a dilution of 1:100 for 1 h. Following three 10 m washes with shaking at 100 rpm at room temperature, the cells were incubated with the secondary goat anti-rabbit IgG Texas Red antiserum (Molecular Probes, Eugene, OR, USA) at a 1:250 dilution, for a further 1 h. Once again the wells were washed three times at 10 m intervals before cover slips containing the infected macrophages were mounted on glass slides. Internalised *B. pseudomallei* and

cytoplasmic LC3 were visualised by confocal microscopy using the green FITC and red TRITC channels. The green channel detects cytoplasmic LC3 while the red channel detects the *B. pseudomallei*. The images were scored for the internalised bacteria and compared to internalised bacteria co-localised with LC3. This ratio of co-localisation was identified for the wild-type and mutant strains in triplicate experiments and subsequently statistically analysed with T-tests.

2.11 *B. PSEUDOMALLEI* ACTIN-BASED MOTILITY

Intracellular *B. pseudomallei* employs actin-based motility to facilitate its spread within mammalian cells. *B. pseudomallei* strains were grown overnight in LB and sub-cultured to mid-log phase. The bacterial strains were inoculated into 24-well trays containing glass cover slips and macrophage RAW 264.7 cells, at an MOI of 6:1. At 1 h post-infection, the wells were washed and the medium replaced with fresh RPMI supplemented with the antibiotics ceftazidime (100 μg/mL) and kanamycin (800 μg/mL). At time points 2 h, 4 h, 6 h and 8 h post-infection, the cells were washed three times with PBS and then fixed with 4.5% PFA for 15 m at 37°C. The PFA was then replaced with PBS in preparation for immunofluorescent labelling and actin staining.

2.11.1 Immunofluorescent Labelling and Actin Staining

All antibody solutions and washes used 1% BSA PBS. As outlined in *Chapter 2.10.1*, cells were labelled with primary rabbit anti-*B. pseudomallei* outer membrane antibody (Cullinane et al., 2008) and secondary goat anti-rabbit IgG Texas Red antiserum (Molecular Probes). Following immunofluorescent labelling, wells were incubated for 1 h with Phalloidin Alexa Fluor 488 at a dilution 1:100 (Molecular Probes) to stain intracellular actin. After washing the wells three times with PBS, the cover slips were mounted on glass slides. Internalised *B. pseudomallei* and intracellular actin were visualised by confocal microscopy.

2.12 CONFOCAL LASER SCANNING MICROSCOPY

The Olympus FV-500 confocal microscope in the Department of Biochemistry & Molecular Biology (Monash University, Melbourne) was used for all imaging. Yeast cells expressing organelle targeted biosensors utilised the FITC and TRITC lasers. Likewise, the same channels were utilised for *B. pseudomallei in vitro* infectivity assays in RAW 264.7 LC3-GFP cells. The 488 laser was used to visualise intracellular actin in macrophage cells.

2.13 TRANSMISSION ELECTRON MICROSCOPY

RAW264.7 cells were infected with wild-type or mutant *B. pseudomallei* strains at a MOI of 6. At 2, 4 and 6 h p.i., cells were fixed for 2 h with 2.5% glutaraldehyde in

0.1 M cacodylate buffer, pH 7.2. At this time, cells were harvested and postfixed for an additional 1 h in 1% (w/v) osmium tetroxide, followed by 1 h in 2% (w/v) uranyl acetate. Samples were then dehydrated, embedded in Epon resin, sliced to 70 nm sections and stained with lead citrate and uranyl acetate. Images were obtained using a Hitachi H-7500 Transmission Electron Microscope. A minimum of 150 cross-sections was imaged in each experiment and bacteria scored according to the presence and number of visible membranes in which they were encapsulated.

2.14 ANIMAL COMPETITION ASSAYS

In order to determine the *in vivo* growth rate of *B. pseudomallei*, an *in vivo* competition analysis of the wild-type and mutant strain was performed. As a means of comparison, an *in vitro* analysis was also performed simultaneously. Overnight cultures of wild-type *B. pseudomallei* and mutant strains grown in LB-supplemented with relevant antibiotics, were sub-cultured for 90 m to early-log phase, OD_{600nm} of 0.2 (corresponding to 2 x 10^8 bacteria/mL). Equal volumes of both cultures were combined, serial dilutions of the combined mixture made to 10^{-5} and 100 μL were spread onto three LB agar plates. These plates represented bacterial inputs.

For the *in vitro* growth analysis, 10 μL of the 10^{-2} dilution – corresponding to 4 x 10^4 bacteria, were inoculated in LB and the culture incubated at 37°C with shaking at 200 rpm for 18 h. 100 μL of the culture was subsequently spread onto LB agar, denoted *in vitro* growth plates.

For the *in vivo* competitive assay, six eight-week old female BALB/c mice were intra-nasally infected with 20 μL of the 10^{-2} dilution and housed at room temperature for 24 h in filtered sealed cages. At this time point, mice were killed in an ethically approved manner (Monash University Animal Ethics Committee approval # SOBS/M/2008/2), with their spleens removed and homogenised in 3 mL PBS. Homogenate was spread onto three LB agar, denoted as *in vivo* plates.

All LB plates were incubated at 37°C for a minimum of 24 h until visible colonies were apparent. At this point, 100 colonies from each plate, input, *in vitro* and *in vivo*, were picked randomly and patched onto non-selective LB agar and LB- tetracycline-25 μg/mL, and grown overnight at 37°C. The presence and absence of patches on these plates identified the mutant strain and wild-type *B. pseudomallei* respectively. The colonies on all plates were enumerated and statistically analysed with a one-sided *z* test, to obtain a competitive index (CI) – ratio of mutant to wild-type bacteria in each individual study, and a relative competitive index (rCI) – difference between the *in vitro* CI and *in vivo* CI (Harper et al., 2004). Mutant strains displaying an rCI <0.10 were considered attenuated in the mice model.

2.15 ANIMAL VIRULENCE ASSAYS

In order to determine the level of attenuation, wild-type *B. pseudomallei* and mutant strains were grown in LB media supplemented with relevant antibiotics overnight. Strains were sub-cultured in fresh medium with appropriate antibiotics and grown for 4 h to mid-log phase OD_{600nm} of 0.8 (corresponding to 5 x 10^8 bacteria). Groups of seven, 6 to 8 week–old, female BALB/c mice were infected intranasally with 20 μL of wild-type or mutant at doses of 2 x 10^7 CFU or 2 x 10^5 CFU. Mice were housed at room temperature in filter sealed cages, observed for ten days and euthanased if moribund, in accordance with animal ethics requirements (Monash University Animal Ethics Committee approval # SOBS/M/2008/2). Survival data were displayed as Kaplan-Meier curves, and the difference in overall survival was assessed using Fisher's exact test, and the difference in time to death was analysed using Log-rank Mantel-Cox test (Hiscox et al., 2011).

CHAPTER THREE

SCREENING PUTATIVE BACTERIAL VIRULENCE EFFECTORS IN YEAST

3.1 Introduction

Autophagy is a cellular process whereby cytosolic components maybe sequestered into double membrane vesicles, autophagosomes, and destined for lysosomal degradation. This process of autophagy is also employed to combat microbial infections, whereby pathogens can be enveloped in autophagosomes and directed to the lysosomes.

Following infection of phagocytic and non-phagocytic cells, some intracellular pathogens such as *S. flexneri, R. prowazekii* and *B. pseudomallei* have been found to evade autophagy, an innate degradation response mechanism. Gong et al. (2011) described *B. pseudomallei* lacking the BopA protein to have delayed escape from phagosomes. As described in *Chapter 1*, these bacteria employ a variety of virulence factors, such as secreted proteins and toxins, to escape the phagosome/endosome, to subsequent autophagic capture or to suppress autophagosomal maturation.

Of particular interest are the secreted bacterial proteins that assist microbes to escape the autophagic pathway by disrupting the membrane encapsulating them. It was postulated that *B. pseudomallei* may utilise similar effector proteins to also escape phagosomal confinement.

A literature search was performed to identify the virulence factors employed by bacteria to escape from their confining phagosomes. Initially, a list of 22 virulence

factors was compiled. A BLAST-p search was performed for each sequence against the *B. pseudomallei* genome using Wasabi (Seemann, 2012). BLAST-p results revealing hits with low E-values (such as, less than 10^{-66}), high identity (more than 20%), high positive matches (more than 40%) and low gap values were denoted as putative *B. pseudomallei* homologues. Using these criteria the bioinformatics analysis identified five sequences within the *B. pseudomallei* genome as sharing significant homology with one of the 22 virulence factor open reading frames (ORF). *Table 3.1A & B* summarises the available information concerning the five virulence factors having a homologue within the *B. pseudomallei* genome.

B. pseudomallei virulence is largely attributed to proteins encoded in the *Bsa* (Burkholderia Secretion Apparatus) locus, found on the TTSS3 gene cluster (Wiersinga et al., 2006). TTSS3 is proposed to secrete BicA, BipB, BipC, BprA, BipD, BapA, BapB, BapC, BopE and BopA into a target cell prior to infection (Stevens et al., 2002), although definite evidence showing secretion is available only for BopE (Stevens et al., 2003). The BLAST-p searches found substantial homology with two of these TTSS3 proteins namely BipB and -C.

Other work concerning putative effectors of *B. pseudomallei*, showed an insertion disruption mutant of BipD in the *B. pseudomallei* 576 strain to have impaired invasion, endosomal confinement and reduced proliferation (Stevens et al., 2004). Pilatz et al. (2006), found that the insertion disruption mutant BPSS1539 in the *B. pseudomallei* E8 strain was confined to intracellular vacuoles and displayed attenuated virulence. As deletion mutants of *BPSS1529* (*bipD)* and *BPSS1539* had not

been generated in the *B. pseudomallei* K96243 strain, both were also selected for characterisation experiments in this study, along with the five ORFs described in *Table 3.1*.

Shohdy et al. (2005) utilised yeast as a method for screening potential *L. pneumophilia* candidate effectors on the basis of their potential for altering endosomal traffic (*Chapter 1.10.4*). Sequences encoding the seven *B. pseudomallei* ORFs (*Table 3.1*) were expressed in the yeast *S. cerevisiae BY4741* strain, with the intention of observing any morphological or physiological differences which may arise under nutrient starvation (autophagy induction) conditions. Given the importance of vesicle traffic in autophagy and the gene product descriptions in *Table 3.1*, it was hypothesised that most of these proteins may affect the autophagy process in yeast by perturbing vesicle trafficking. Cellular changes which influence the rate of vesicle fusion to the vacuole may result in an altered vacuolar morphology.

Table 3.1A: Sequence homology between selected virulence factors and the *B. pseudomallei* genome.

Protein	Organism	Description	*B. pseudomallei* Homologue	Genome Location	Positive (%)[3]	Putative function in *B. pseudomallei*	Reference
Ipa C	*S. flexneri*	Forms membrane pores. Required for epithelia cell entry and phagosome escape.	BPSS 1531 Bip C	*Bsa* (TTSS3) locus of chromosome 2.	44	Putative cell invasion protein.	(Ogawa et al., 2003)
Ipa B	*S. flexneri*	Chaperoned by IpgC to form an invasion-mediating protein complex.	BPSS 1532 Bip B	*Bsa* (TTSS3) locus of chromosome 2.	42	Putative cell invasion protein. Predicted to be located in the bacterial inner membrane.	(Ogawa et al., 2003), (Guichon et al., 2001)
Haemolysin	*R. prowazekii*	Bacterial protein exotoxin. It may be involved in the disruption of phagosome membrane	BPSL 0670	Chromosome 1	53	Putative cation transporter efflux protein. Predicted to be located in the bacterial cytoplasm.	(Whitworth et al., 2005)
HrcN	*X. axonopodis*	Escape from endosomal vacuole. Also shares homology to *BsaS*.	BPSS 1394 BpscN	Cluster 1 of the TTSS on chromosome 2.	83	Putative type three secretion associated protein SctN. Predicted to be located in the bacterial cytoplasm.	(Whitworth et al., 2005)

[3] The percentage of similarity and exact identity between two amino acid sequences.

Table 3.1B: Sequence homology between selected virulence factors and the *B. pseudomallei* genome.

Protein	Organism	Description	*B. pseudomallei* Homologue	Genome Location	Positive (%)[4]	Putative function in *B. pseudomallei*	Reference
AP003013	*Mesorhizobium loti*	Multidrug efflux protein	BPSS 0670	Chromosome 2	65	Putative transporter protein. Predicted to be located in the bacterial inner membrane.	(Kaneko et al., 2000)
			BPSS 1529 BipD	*Bsa* (TTSS3) locus of chromosome 2.		Type three effector protein.	(Stevens et al., 2004)
			BPSS 1539	*Bsa* (TTSS3) locus of chromosome 2.		Unknown.	(Pilatz et al., 2006)

[4] The percentage of similarity and exact identity between two amino acid sequences.

Overview of Experimental Strategy

DNA cassettes encoding the seven ORFs listed in *Table 3.1* were amplified by PCR. In addition, the phosphoglycerate mutase *BPSL0443* ORF was amplified to act as a negative control. Phosphoglycerate mutase is a non-secreted protein involved in carbohydrate transport and metabolism, and not therefore in determining the infectivity of *B. pseudomallei.*

Yeast strains expressing each of the individual *B. pseudomallei* ORFs were subjected to nutrient and nitrogen starvation. Under such conditions, autophagy is induced in yeast cells as a means of obtaining nutrients and surviving starvation stress. As described in *chapter 1*, this process requires the intracellular trafficking of cellular components in membrane bound vesicles which subsequently fuse with the vacuole to undergo degradation.

Yeast strains expressing the *B. pseudomallei* ORFs were also co-transformed with plasmids expressing the cytosolic-, mitochondrial- or nucleus- targeted Rosella biosensors (Rosado et al., 2008, Devenish et al., 2008). These cells were grown under nitrogen starvation conditions to induce autophagy, stained with FM4-64 to label the vacuole membranes, and imaged by confocal microscopy to determine the localisation of the biosensor. Each biosensor is composed of a pH-sensitive variant of green fluorescent protein (GFP) linked to a pH-stable variant of the red fluorescent protein, DsRed. Under autophagic conditions, the delivery of organelles (pH $\geq$ 7.0) to the acidic vacuole (pH 4.8) results in highly diminished or no detectable fluorescence of

the GFP component. The accumulation of red fluorescence in the vacuole that may be observed is indicative of autophagic uptake of the labelled compartment. Following nitrogen starvation for 4, 6 or 20 h, the autophagic turnover of the cytosol, mitochondria, or nucleus can be observed respectively (Rosado et al., 2008, Devenish et al., 2008).

3.2 Results:

Cloning *B. pseudomallei* Genes into the *S. cerevisiae*

The *B. pseudomallei* genome has a 65% G+C content, making PCR amplification and cloning particularly challenging. For this reason, primers were designed to have minimum GC base content which in turn ensures the lowest possible annealing temperature for amplification. Each primer was designed to introduce nested *Spe*I and *BamH*I restriction sites at the 5' end of the DNA cassette and nested *BamH*I, *Not*I and *Hind*III restriction sites at the 3' end. Nucleotides encoding a single haemagglutinin (HA) epitope tag were included between the *Not*I and *Hind*III sites to facilitate possible detection of protein expression (*Figure 3.1*).

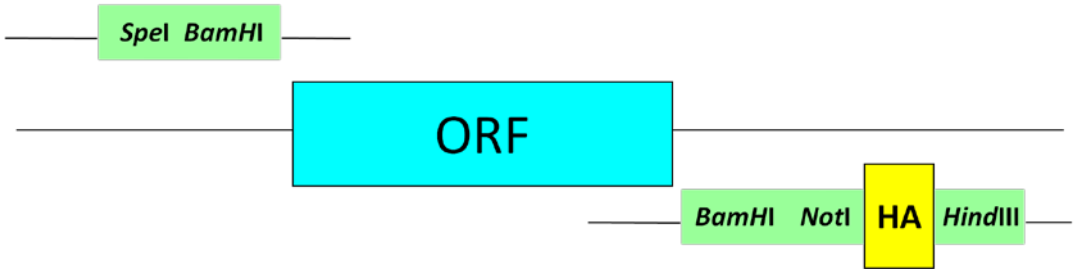

Figure 3.1: The standard template utilised for the design of *B. pseudomallei* genomic DNA primers. *Spe*1 and *BamH*1 were introduced at the 5' end of the cassette whilst the *BamH*I, *Not*I and *Hind*III were introduced at the 3' end. An HA epitope tag was cloned between the *Not*I and *Hind*III sites.

Each target ORF was amplified from *B. pseudomallei* K96243 genomic DNA using TAK (TaKaRa, Shiga, Japan) and KOD (EMD & Merck, Darmstadt, Germany) polymerases with GC-specific buffers specified by the manufacturers (*Chapter 2.3.1*). All cloned PCR products were sequenced to confirm the absence of PCR-derived infidelities (data not shown). The PCR products were cloned into the pAH19 yeast expression vector and transformed into the BY4741 strain (*Chapter 2.1*).

Vacuolar Morphology of Strains Expressing *B. pseudomallei* ORF

The yeast strains expressing *B. pseudomallei* proteins were subjected to nitrogen starvation for 4 h. Wild-type BY4741 yeast expressing the empty pAH19 vector or *BPSL0443* were also grown under the same conditions and served as negative controls. After 4 h cytoplasmic components will be sequestered into vesicles subject to vacuolar degradation (Rosado et al., 2008).

Yeast strains expressing the empty pAH19 vector or a *B. pseudomallei* protein, under growing or starvation conditions were then stained with FM4-64 and imaged (*Figure 3.2A & B*). When subjected to nitrogen starvation, the empty vector control strain and the strain expressing *BPSL0443* exhibited a single vacuole phenotype. By contrast, the seven strains expressing a putative *B. pseudomallei* effector protein produced a multi-vacuole phenotype, with an increase in vacuole number following 4 h starvation (*Figure 3.3*). Under growing conditions all strains showed a high percentage of single vacuoles (65 - 95%). During starvation conditions the 70 – 75% of cells expressing the empty pAH19 vector or *BPSL0670* maintained a single vacuole phenotype whilst strains expressing the *B. pseudomallei* effector protein only produced single vacuoles in 5 – 10% cells and, multiple vacuoles in approximately 90% of the cells.

From the repertoire of *B. pseudomallei* proteins being studied, cells expressing truncated BPSS1529 or BPSS1532 proteins were retested to verify the phenotype produced by the full length effector proteins. The DNA cassette encoding the *BPSS1529* and *BPSS1532* ORFs was amplified so as to introduce truncations at either

the N or C-terminal end. Thus the *BPSS1529ΔC* was cloned with 20% of the nucleotides deleted from the C-terminus. Two truncations of *BPSS1532* were constructed each with 50% deletion at either the C or N-terminus (*Figure 3.4*). It was anticipated that such truncations may result in loss of 'function' of the full-length protein when expressed in yeast, resulting in a wild-type single vacuole phenotype.

Confocal images of strains expressing *BPSS1529ΔC*, *BPSS1532ΔN* or *BPSS1532ΔC* (*Figure 3.5*) revealed that in the absence of expression of the full-length protein, a single vacuole phenotype was observed under starvation conditions. *Figure 3.6* shows the number of vacuoles produced by expression of the full length BPSS1529 and BPSS1532 as opposed to the truncated versions, under starvation conditions. The full-length proteins produced single vacuoles in only 10-20% of the imaged cells, whereas the truncated proteins yielded single vacuoles in 60-70% of the cells – similar to the control empty vector strain. Thus the multi-vacuole phenotype can be attributed to the expression of full-length *B. pseudomallei* proteins.

As another means of verifying that the multiple vacuole phenotype was dependent on the expression of a putative effector protein, a strain expressing the *BPSL0443* ORF was tested for vacuole phenotype under conditions of nitrogen starvation. BPSL0443 encodes a cytosolic phosphoglycerate mutase, not involved in bacterial invasion of host cells, and therefore its expression would not be expected to affect vacuolar morphology. When grown under starvation conditions, this strain produced a predominantly single vacuole phenotype (*Figure 3.3*). This result suggests that not all *B. pseudomallei* proteins will interfere with vesicle transport and vacuole fusion, and

further supports the conclusion that the multiple vacuole phenotype observed for expression of putative *B. pseudomallei* effector proteins, derives from their perturbation of vesicular transport and/or vacuole fission/fusion in yeast.

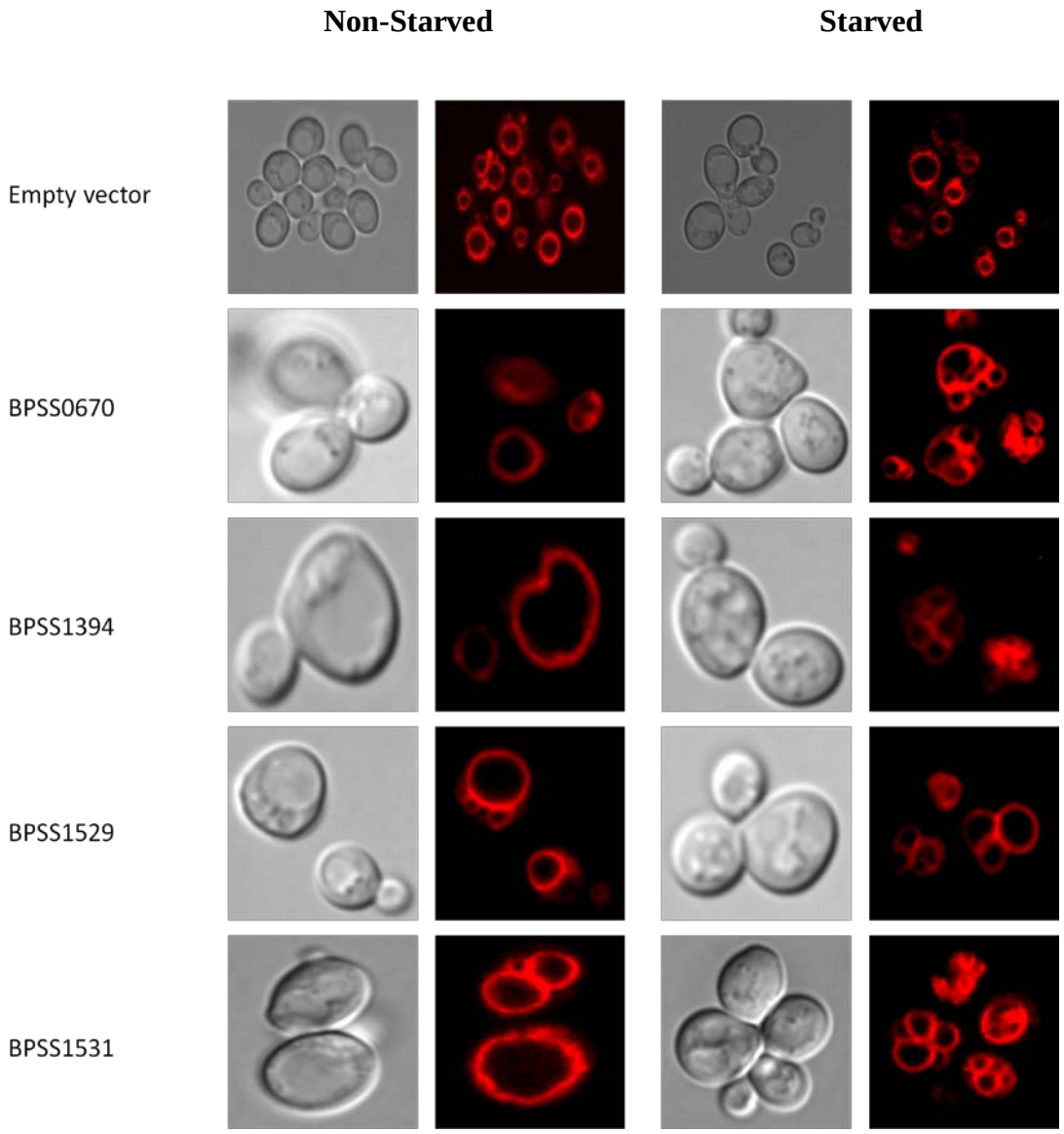

Figure 3.2A: Expression of *B. pseudomallei* proteins in BY4741 produces a multiple vacuole phenotype under starvation conditions. The empty pAH19 vector expressed in BY4741 served as a negative control. Cells were either starved or not starved for 4 h and then stained with FM4-64.

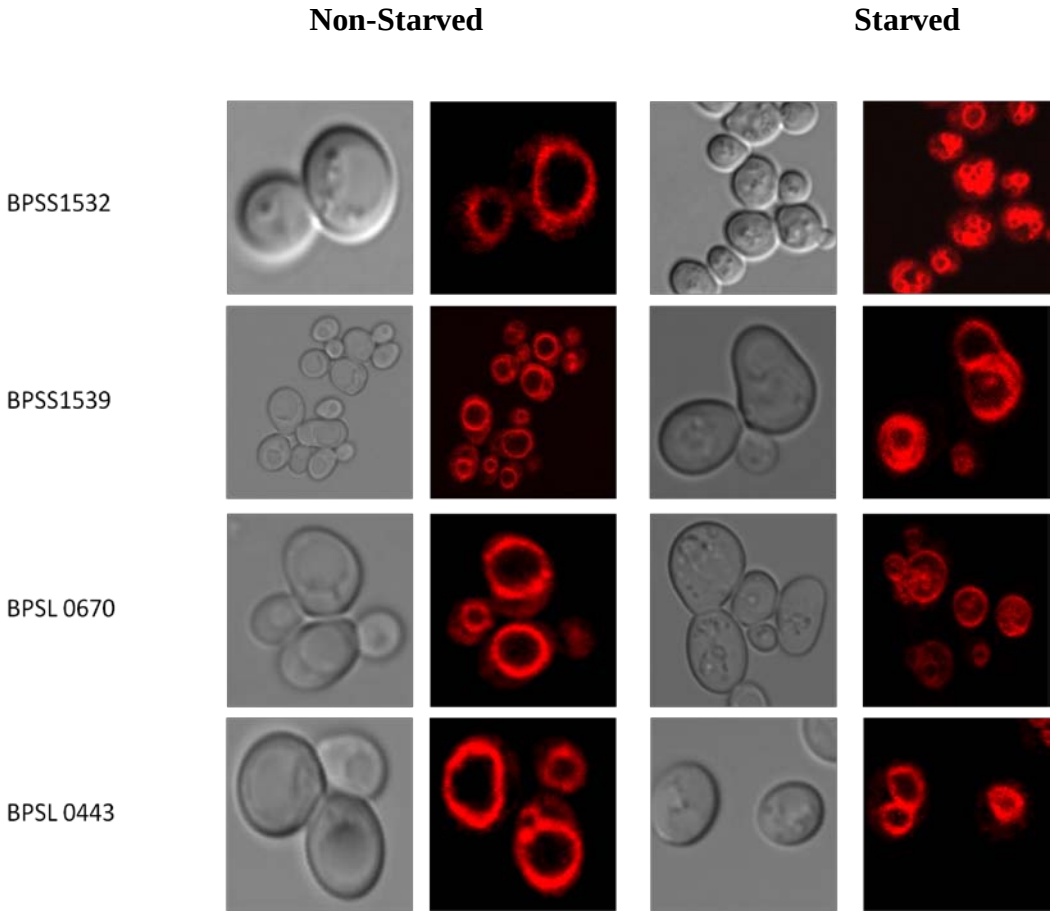

Figure 3.2B: Expression of *B. pseudomallei* proteins in BY4741 produces a multiple vacuole phenotype under starvation conditions. The empty pAH19 vector expressed in BY4741 served as a negative control. Cells were either starved or not starved for 4 h and then stained with FM4-64.

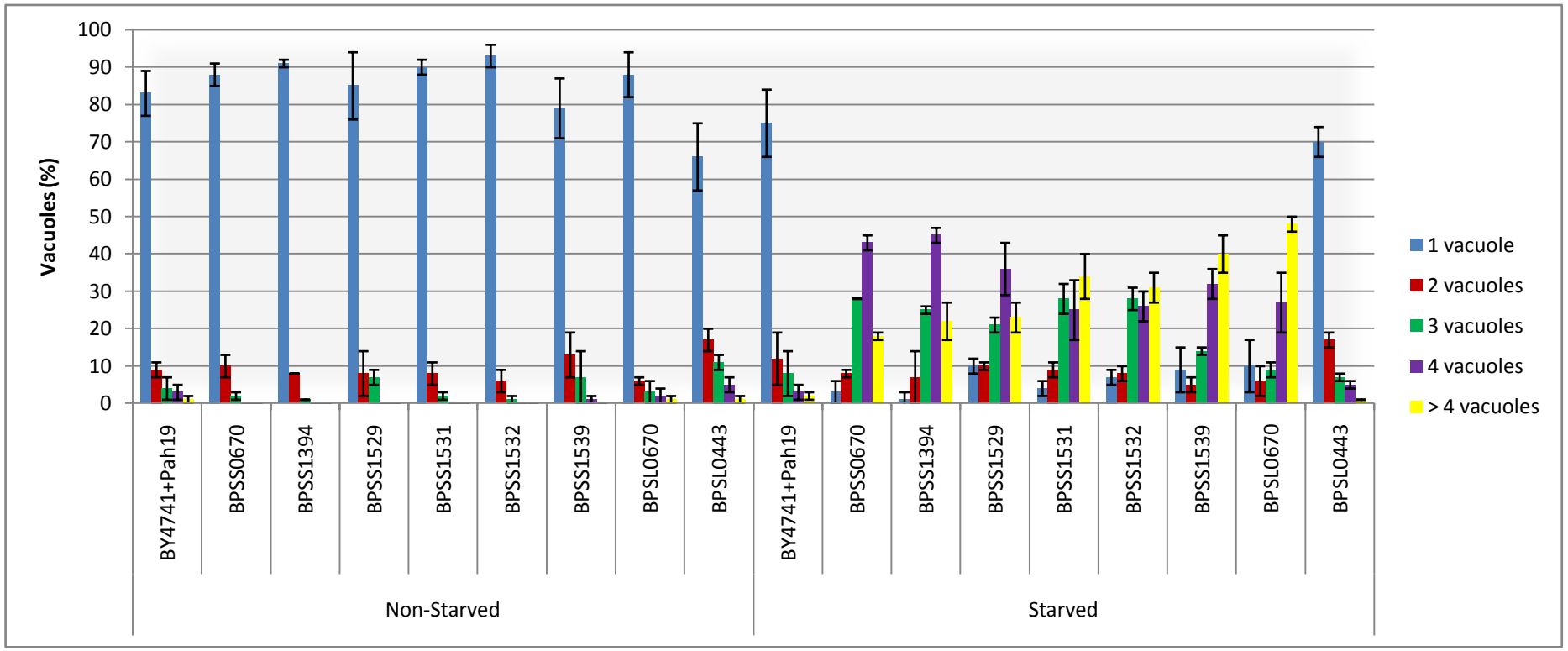

Figure 3.3: Enumeration of vacuoles in yeast strains expressing *B. pseudomallei* proteins. The empty pAH19 vector expressed in BY4741 served as a negative control. Cells were either starved, or not starved, for 4 h and then stained with FM4-64. 150 cells were scored in each of three replicate experiments.

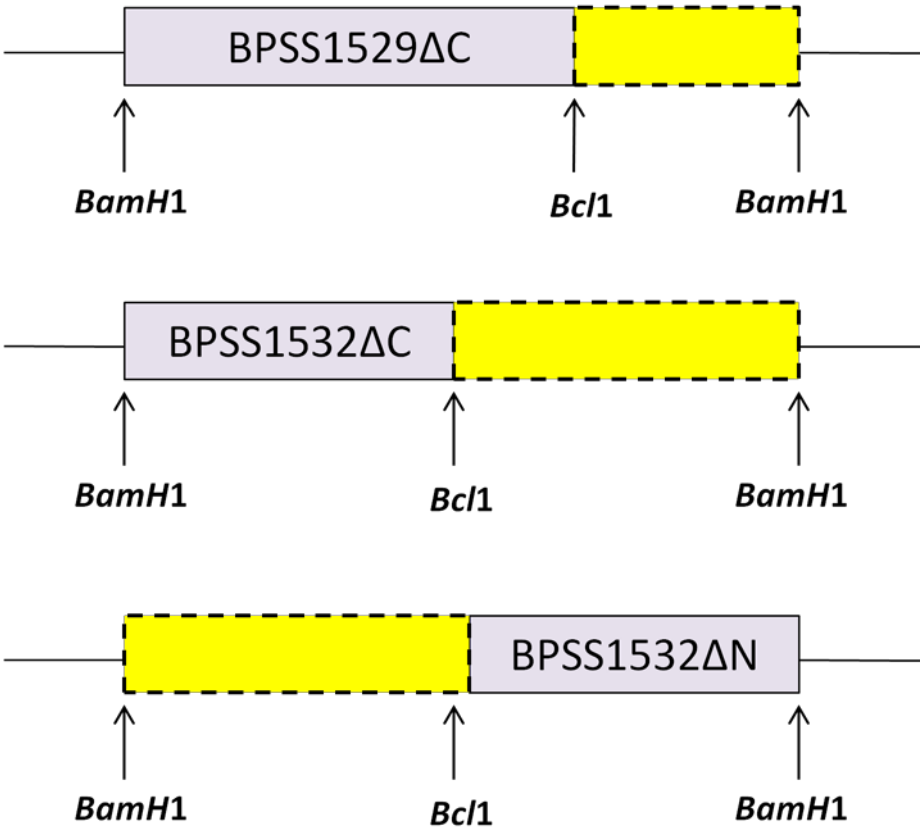

Figure 3.4: The truncated versions of the *BPSS1529* and *BPSS1532* ORFs. The *Bcl*I site within either ORF was used to clone truncated fragments. The *BPSS1529ΔC* was cloned with 20% of the nucleotides deleted from the C-terminus. Two truncations of *BPSS1532* were constructed each with 50% deletion at either the C or N-terminus. This figure is not to scale.

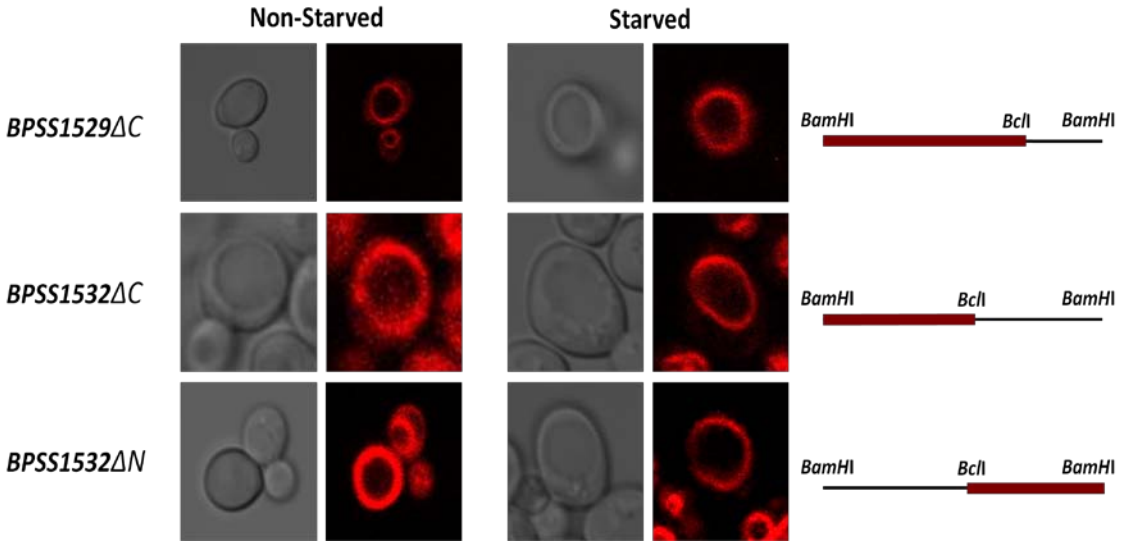

Figure 3.5: Expression of the truncated versions of *B. pseudomallei* protein BPSS1529 and BPSS1532. Cells were either starved, or not starved, for 4 h and then stained with FM4-64. The truncated sections are diagrammatically shown on the right.

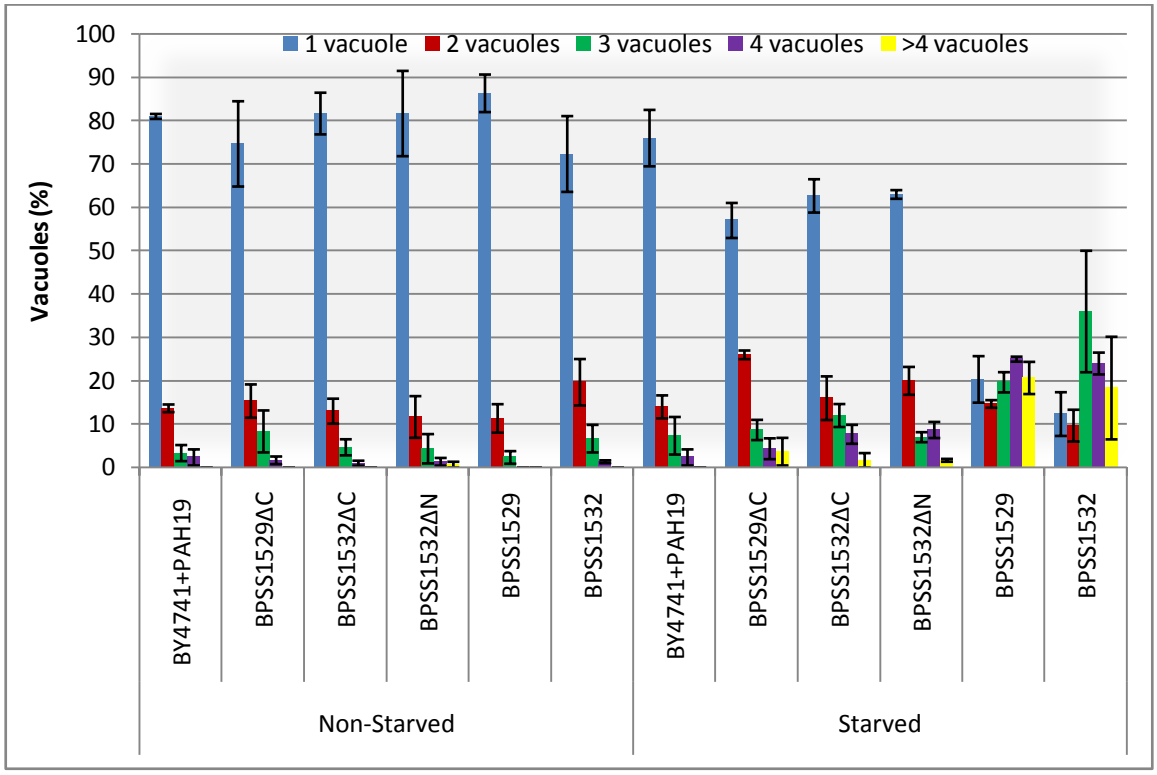

Figure 3.6: Enumeration of vacuoles in yeast strains expressing truncations of the *B. pseudomallei* proteins. The empty pAH19 vector expressed in BY4741 served as a negative control. Cells were either starved, or not starved, for 4 h and then stained with FM4-64. 150 cells were scored in each of five replicate experiments.

Cytosolic Turnover in Cells expressing *B. pseudomallei* Proteins

As detailed in *Chapter 1*, autophagy is a cellular response to microbial infection, stress, nutrient starvation or chemical inducers (Ravikumar et al., 2010). In these experiments, autophagy was induced through nitrogen starvation. Under such conditions in yeast, some cytoplasm and/or organelle turnover can be observed using fluorescent biosensors. Depending on the time period of starvation, various organelles will be turned over. The 4 h starvation period used in these experiments was sufficient to initiate autophagy of the cytosol (Rosado et al., 2008, Devenish et al., 2008).

Yeast strains expressing the selected *B. pseudomallei* ORFs were transformed with the vector pAS1NB expressing the cytosolic Rosella biosensor (Rosado et al., 2008). When subjected to nitrogen starvation conditions, cytosolic turnover is noted as the accumulation of red fluorescence in the vacuole along with the absence of green fluorescence in the vacuole. Such a phenotype can be observed in the control strains – wild-type cells expressing pAH19 empty vector or *BPSL0443* (*Figures 3.7A & B*). In contrast, for each of the other *B. pseudomallei* proteins a lack of red fluorescence was observed in the vacuole. Note that the multi-vacuole phenotype observed using FM4-64 staining was confirmed in these experiments as fluorescent material is apparently excluded from the multiple vacuoles. This finding suggests that yeast strains expressing the *B. pseudomallei* proteins, have delayed cytosolic turnover when subjected to 4 h of nutrient starvation.

The truncated versions of BPSS1529 and BPSS1532 were also tested for cytosolic turnover (*Figure 3.8*). In the absence of the full length *B. pseudomallei* proteins, red vacuoles were observed, indicating that the yeast cells sequester cytosolic components for degradation, following 4 h of nutrient starvation. These results indicate that the phenotype of delayed cytosolic turnover can be solely attributed to the effects on vesicle trafficking/vacuole fission/fusion caused by expression of the particular set of *B. pseudomallei* proteins being tested. A single vacuole phenotype for the truncation proteins of BPSS1529 and BPSS1532 is indicated by the green fluorescent image under starved conditions.

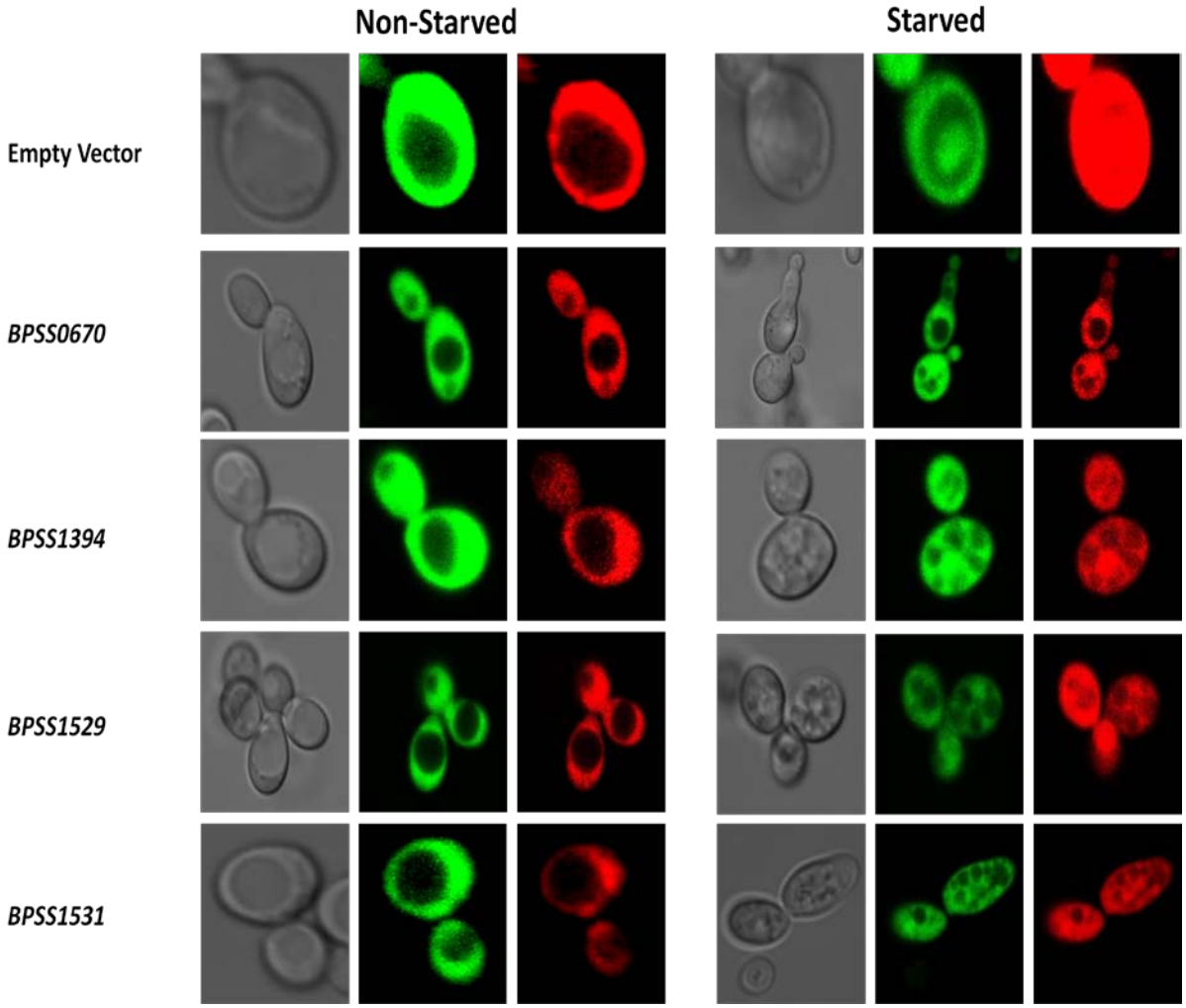

Figure 3.7A: *B. pseudomallei* proteins inhibit cytosolic autophagy in yeast under starvation conditions. Expression of the *B. pseudomallei* proteins with co-expression of the cytosolic biosensor in the BY4741 strain, either starved or not starved for 4 h. The empty pAH19 vector and *BPSL0443* expressed in BY4741 served as a negative control.

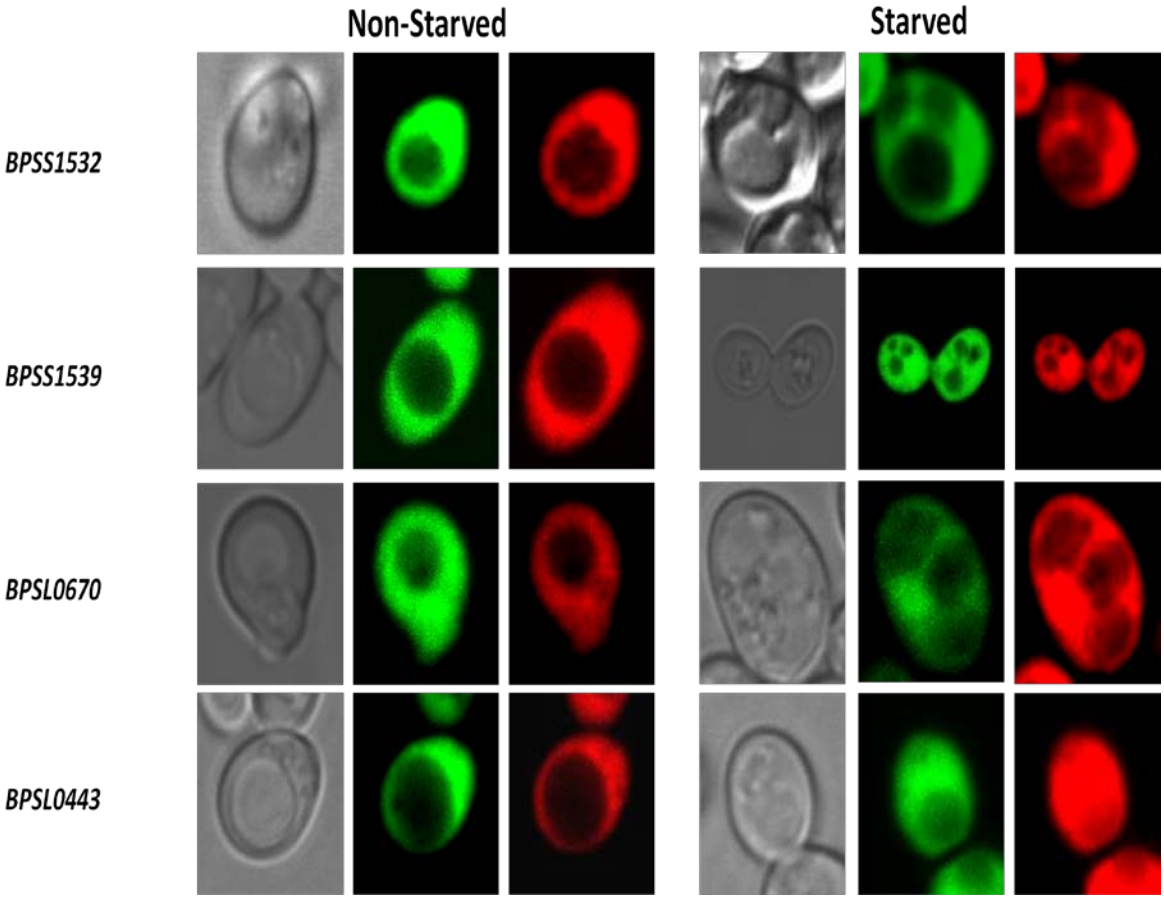

Figure 3.7B: *B. pseudomallei* proteins inhibit cytosolic autophagy in yeast under starvation conditions. Expression of the *B. pseudomallei* proteins with co-expression of the cytosolic biosensor in the BY4741 strain, either starved or not starved for 4 h. The empty pAH19 vector and *BPSL0443* expressed in BY4741 served as a negative control.

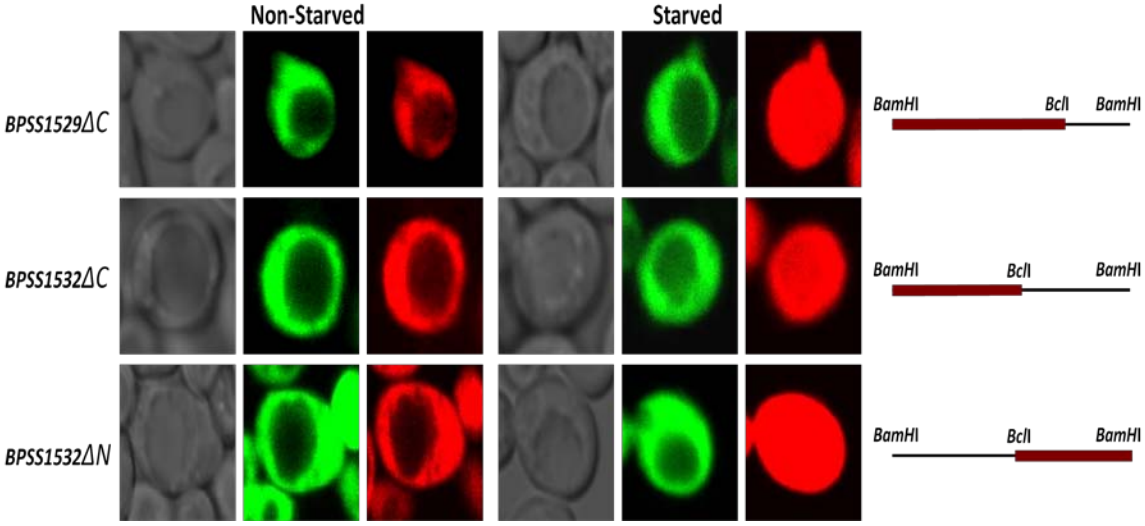

Figure 3.8: Expression of truncated versions of the *B. pseudomallei* proteins in yeast allows cytosolic autophagy to occur under starvation conditions. Expression of the truncated BPSS1529 and BPSS1532 *B. pseudomallei* proteins with co-expression of the cytosolic biosensor in the BY4741 strain, either starved or not starved for 4 h. The truncated sections are diagrammatically shown on the right.

Mitochondrial Turnover in cells expressing *B. pseudomallei* Proteins

Given the influence of the putative *B. pseudomallei* effectors on cytosolic turnover, the *B. pseudomallei* proteins were then tested for their influence on mitochondrial turnover by autophagy. After 6 h of nutrient starvation, *S. cerevisiae* BY4741 recruits mitochondria into the autophagic process (Rosado et al., 2008). Yeast strains expressing the *B. pseudomallei* ORFs were co-transformed with the pAS1NB vector expressing the mitochondrial Rosella biosensor. In cells subjected to nutrient starvation exceeding 6 h, recruitment of mitochondria for autophagic degradation is shown by diffuse red fluorescence coupled with the absence of green fluorescence in the vacuole. This diffuse red fluorescence can be observed in the control strain cells carrying the pAH19 empty vector or *BPSL0443* (*Figures 3.9A & B*). Cells grown under the same conditions and expressing the *B. pseudomallei* ORFs, showed little if any evidence of mitochondria turnover whilst maintaining the multi-vacuolar phenotype, as illustrated in *Figure 3.9A & B*.

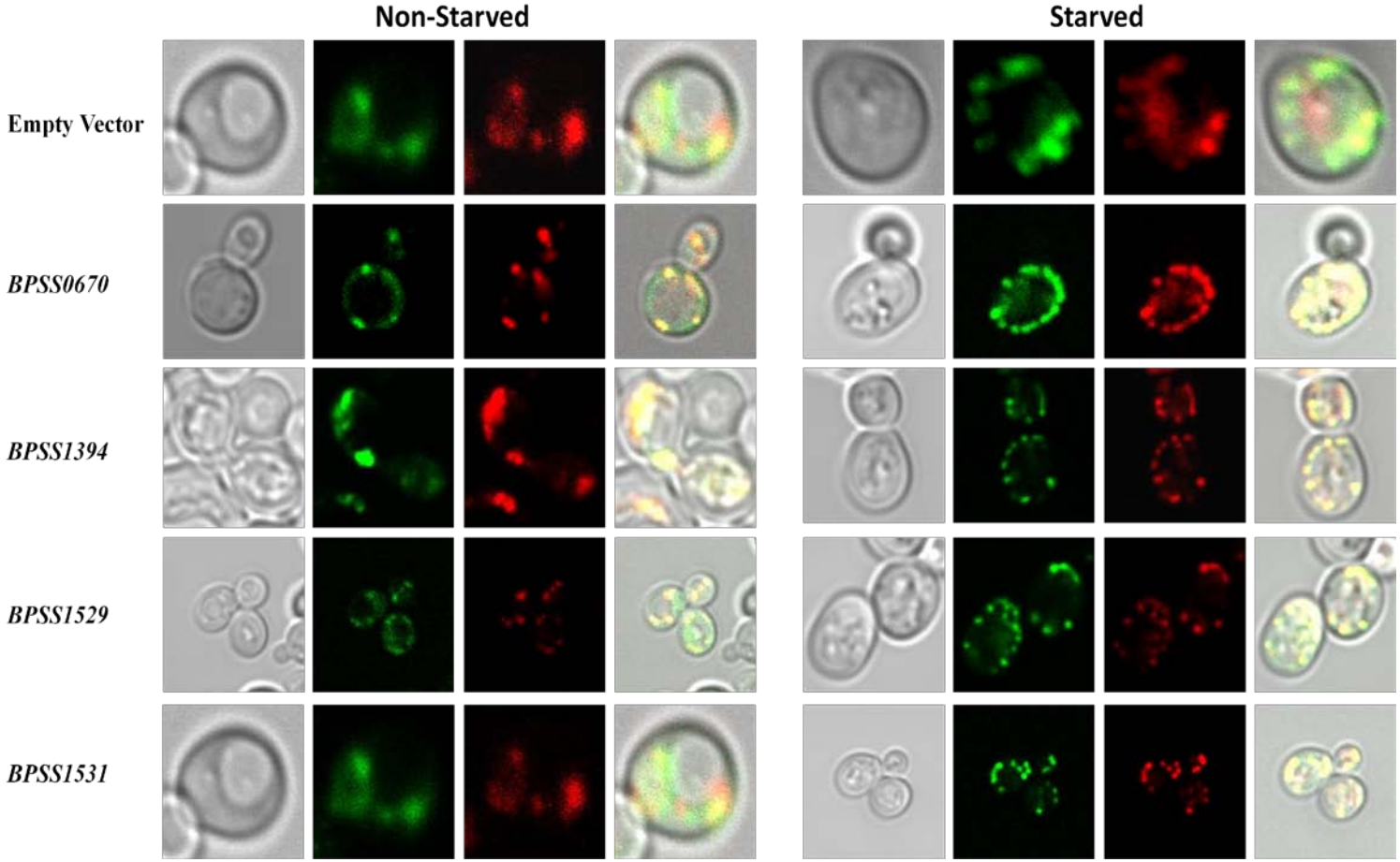

Figure 3.9A: *B. pseudomallei* proteins inhibit mitochondria autophagy in yeast under starvation conditions. Expression of the *B. pseudomallei* proteins with co-expression of the mitochondrion biosensor in the *BY4741* strain, either starved or not starved for 6 h. The empty pAH19 vector and *BPSL0443* expressed in BY4741 served as a negative control.

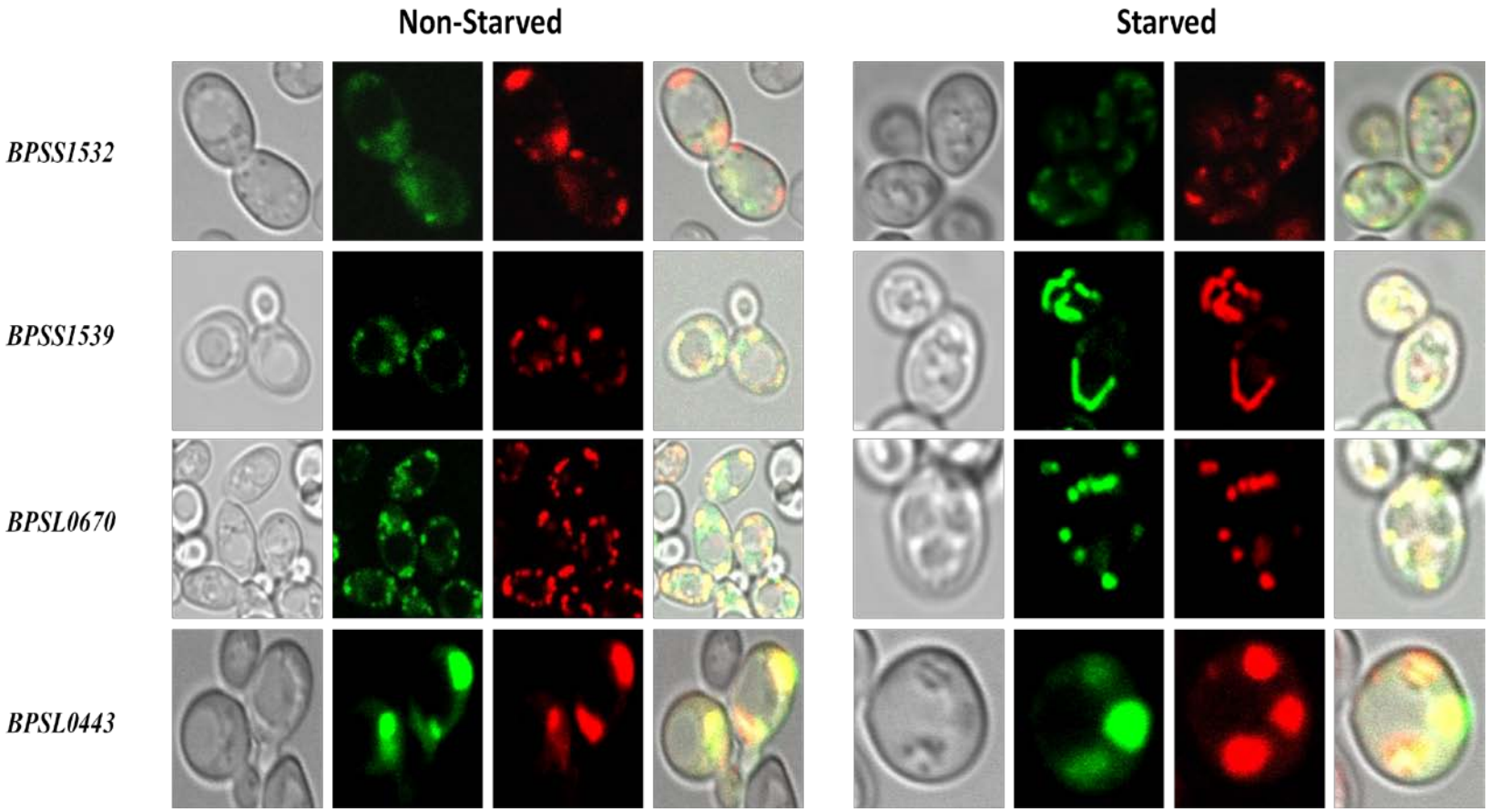

Figure 3.9B: *B. pseudomallei* proteins inhibit mitochondria autophagy in yeast under starvation conditions. Expression of the *B. pseudomallei* proteins with co-expression of the mitochondrion biosensor in the BY4741 strain, either starved or not starved for 6 h. The empty pAH19 vector and *BPSL0443* expressed in BY4741 served as a negative control.

Nucleus Turnover in Cells Expressing *B. pseudomallei* Proteins

The expression of these *B. pseudomallei* ORFs evidentially perturbed cytosolic and mitochondrial turnover. These organelles can undergo macroautophagy but can also be turned over by microautophagy (*Chapter 1.8*). Turnover of the nucleus in yeast is dependent solely on a microautophagic process. Turnover of the yeast nucleus can be detected during prolonged nutrient starvation exceeding 20 h using NAB35-Rosella (Mijaljica et al., 2007, Rosado et al., 2008, Devenish et al., 2008). Yeast strains expressing the *B. pseudomallei* ORFs were co-transformed with the pAS1NB vector expressing the nucleus biosensor. The autophagic turnover of nucleus membrane is observed as diffuse red fluorescence in the vacuole and the absence of green fluorescence in the vacuole. Such turnover is apparent in the control strains cells carrying the pAH19 empty vector or expressing BPSL0443. Turnover of the nucleus was evident in the red flaring of fluorescence from the nucleus into the adjacent multiple vacuole structures in cells expressing the *B. pseudomallei* ORFs (*Figure 3.10A & B*). The presence of red fluorescence in the vacuole, illustrates that the process of nucleus autophagy is not inhibited in the presence of the *B. pseudomallei* proteins.

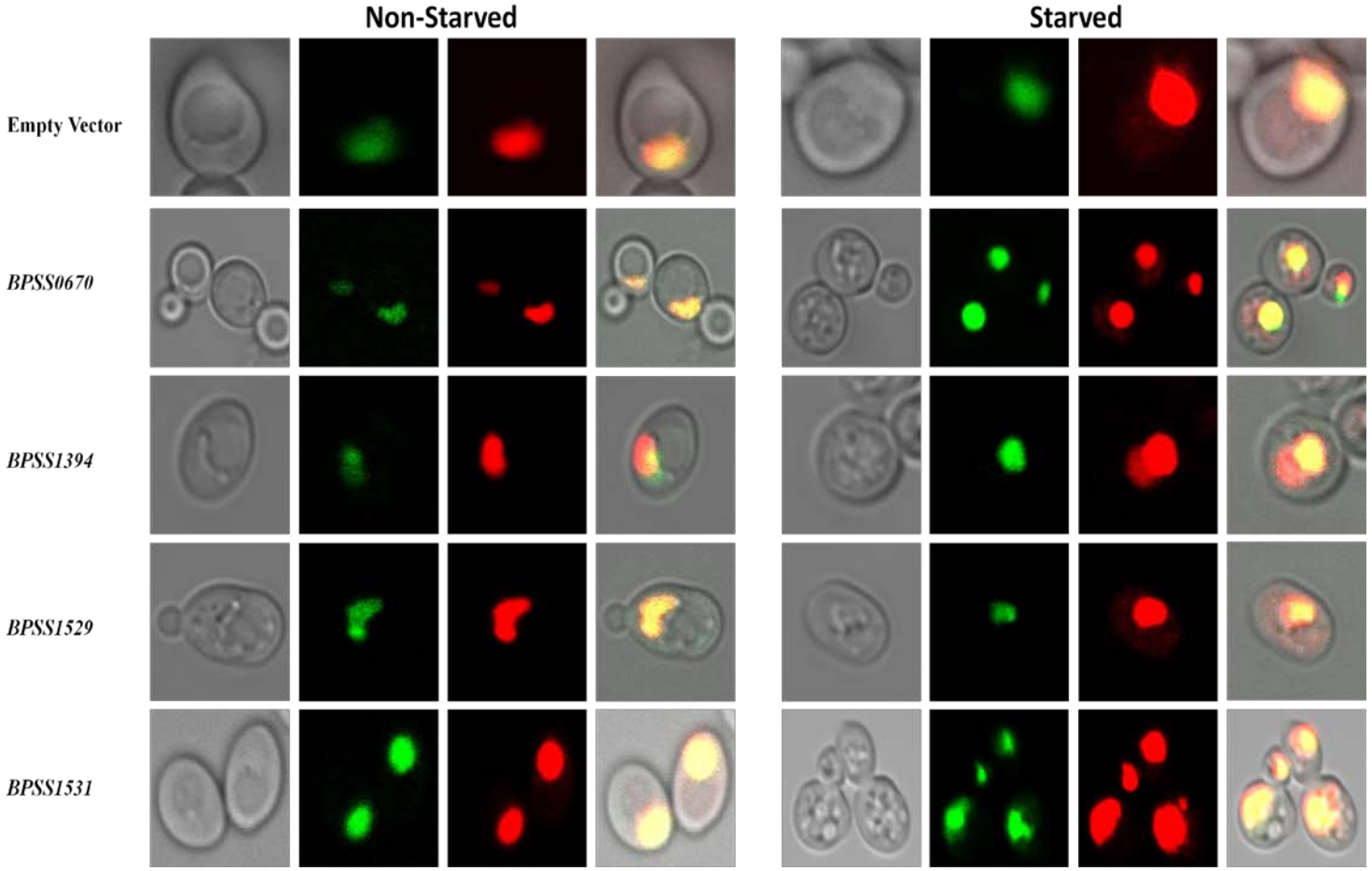

Figure 3.10A: *B. pseudomallei* proteins do not inhibit nucleus autophagy under starvation conditions. Expression of the *B. pseudomallei* proteins with co-expression of the nucleus biosensor in the BY4741 strain, either starved or not starved for 20 h. The empty pAH19 vector and *BPSL0443* expressed in BY4741 served as a negative control.

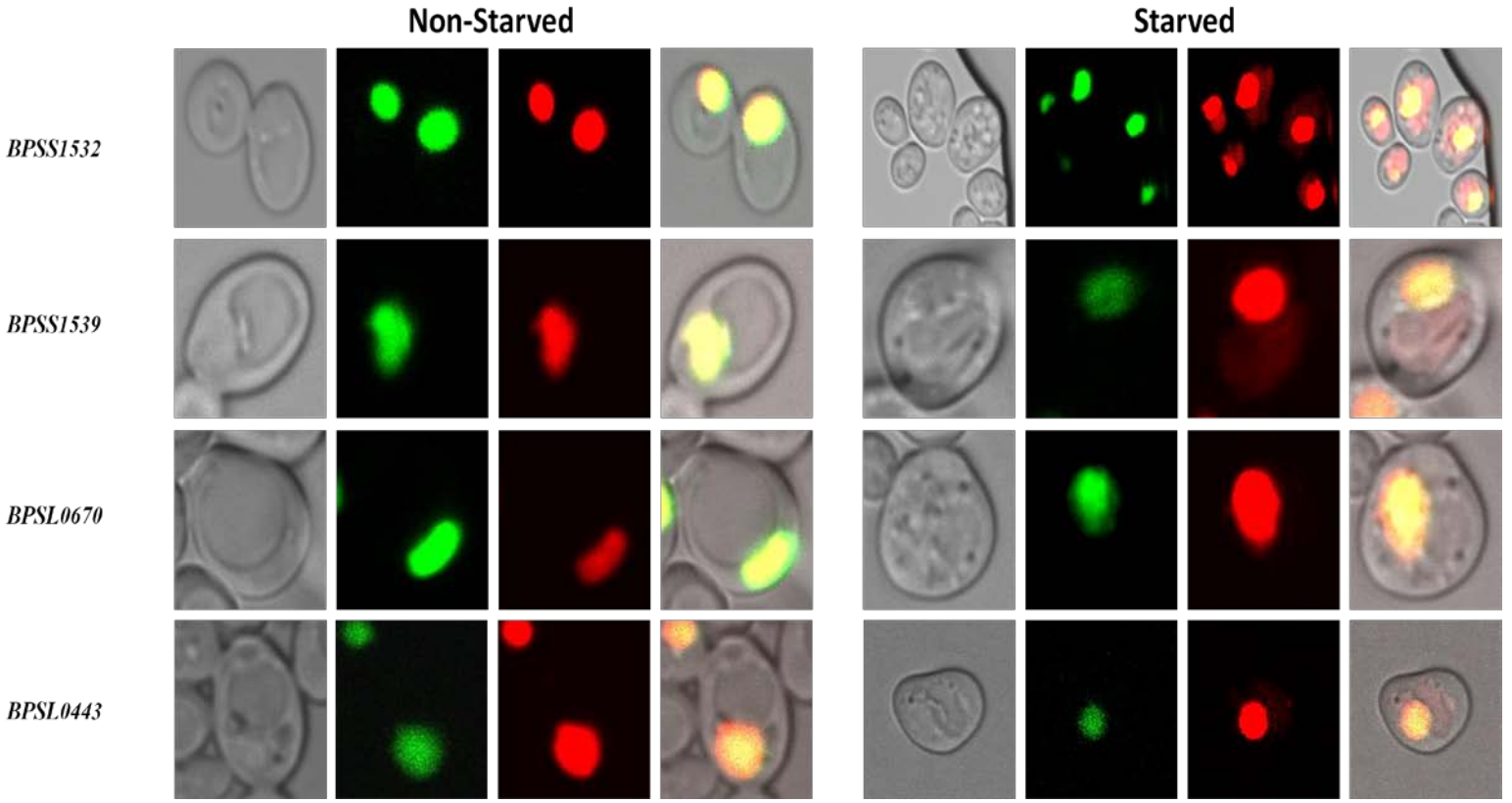

Figure 3.10B: *B. pseudomallei* proteins do not inhibit nucleus autophagy under starvation conditions. Expression of the *B. pseudomallei* proteins with co-expression of the nucleus biosensor in the BY4741 strain, either starved or not starved for 20 h. The empty pAH19 vector and *BPSL0443* expressed in BY4741 served as a negative control.

3.3 Discussion

Five of the *B. pseudomallei* proteins tested in this study were selected on the basis of bioinformatics analysis as sharing high similarity to virulence factors employed by *S. flexneri, R. prowazekii, M. loti* and *X. axonopodis.* In the afore-mentioned bacteria, these factors were shown to contribute to bacterial evasion of microbial degradation. Hence, these proteins were chosen on the basis of their role as prospective effector proteins in autophagy evasion. When expressed in *S. cerevisiae* under autophagy inducing conditions, each of the selected *B. pseudomallei* proteins produced a phenotype that was atypical of normal yeast physiology.

3.3.1 Vacuolar Phenotype

Expression of each of the *B. pseudomallei* proteins in yeast under nitrogen starvation conditions resulted in a multiple vacuole phenotype. Such a phenotype may be attributed to impairment of the inability of the vacuoles to fuse. In *Chapter 1.12* vacuole fusion was described as involving "priming" which prepares the vacuoles for attachment, and "docking" which includes the tethering of vacuoles for "fusion" thereby leading to the fusion of the vesicle with the vacuole (Wang et al., 2002). Priming allows for the release of the HOPS (Homotypic fusion and vacuole protein sorting) complex from the vacuolar membrane. Mutants that have a defect in the HOPS complex (also referred to as Class C *vps*) may produce a fragmented/multiple vacuole phenotype (see *Chapter 1.10.8*). The expressed *B. pseudomallei* proteins may interact with the HOPS complex directly, or lead to perturbation of its function to produce the multiple vacuole phenotype observed. Mutants defective in members of either class B or class C vacuolar protein sorting complex have been shown to

eventuate in fragmented vacuoles (Raymond et al., 1992). Studies of mutants in the class B *vps* family – in particular *vps39, vps41* and *vps43,* have been found to produce a large number of small fragmented vacuoles which are randomly dispersed (*Figure 3.11*) (Raymond et al., 1992, Bowers and Stevens, 2005). Images presented in *Figures 3.2A* & *B* show a distribution of vacuoles within the yeast cell which is consistent with the class B *vps* mutant phenotype.

Other speculations for the multiple vacuole phenotype include the interaction of the *B. pseudomallei* proteins with enolases and Bor1p. Decker and Wickner (2006) have identified a role for yeast enolase, a cytosolic glycolytic enzyme, in vacuole fusion. Deletion of either the gene encoding non-essential Eno1p, or reduction in the expression level of the essential Eno2p caused fragmented vacuoles *in vivo,* which was attributed to insufficient fusion. The deletion of both genes resulted in a more dramatic vacuolar fragmentation phenotype which is exacerbated by the prevention of normal protein sorting to the vacuole, leading to the inability of the vacuoles to fuse *in vitro* (Decker and Wickner, 2006).

Human band 3 which binds glycolytic enzymes to membranes of mammalian erythrocytes has sequence homology to yeast Bor1p (Decker and Wickner, 2006). It localises to the vacuole and is required for the localisation of enolases and vacuolar fusion proteins, to the vacuole. Thus, loss of Bor1p results in the mislocalisation of enolases and vacuolar fusion proteins (Decker and Wickner, 2006). Since the cellular localisation of any of the *B. pseudomallei* proteins expressed in yeast is unknown, one

can only speculate on their possible intracellular interactions with Bor1p or Eno1p and Eno2p to influence vacuolar fragmentation or perturbation of their localisation.

Figure 3.11: Confocal imaging of *S. cerevisiae* strain *SF383-9D* class B mutant *vps41* exhibiting fragmented vacuoles that are randomly dispersed (Raymond et al., 1992).

3.3.2 Influence on Autophagy

In yeast, cytosol and mitochondria may be sequestered into double membrane structures destined for macroautophagy, or they may be directly engulfed by invagination of the vacuole membrane – microautophagy. The former process is a bulk degradation process which requires recruitment of the organelle and fusion of the autophagosome at the vacuolar membrane. In the presence of the putative *B. pseudomallei* effector proteins, macroautophagy of the cytosol and mitochondria is stalled or significantly reduced. By contrast, the presence of the *B. pseudomallei* proteins appears to have little influence on nucleus turnover (*Figure 3.10A & B*). One partially characterised form of nuclear turnover uses the unique process of Piecemeal Microautophagy of the Nucleus (PMN). This process involves specific interactions at the nucleus-vacuole (NV) junctions where blebs are pinched from the nucleus to be released into the vacuole (Roberts et al., 2003), and does not require fusion of autophagosomes with the vacuolar membranes. The form of nuclear autophagy detected by the use of the NAB35 biosensor is denoted Late Nucleophagy (LN) which occurs after 20 h of nitrogen starvation, whereby turnover of the nucleus is observed as diffuse red fluorescence in the vacuole (Rosado et al., 2008). The mechanism is undefined but does not require all the components for macroautophagy and presumably also occurs by a microautophagic pathway.

Characterisation of the expression of the putative *B. pseudomallei* effector proteins in yeast suggests a potential role in vesicle trafficking, as they influence vacuolar phenotype and autophagic uptake of the cytosol and mitochondria (by macroautophagy) in *S. cerevisiae*. On this basis an attempt was made to inactivate

each of these genes in the *B. pseudomallei* genome in order to determine whether mutant bacteria were defective in, infection and survival, in mammalian cells.

CHAPTER FOUR

GENERATION AND CHARACTERISATION OF DELETION MUTANTS IN *B. PSEUDOMALLEI*

4.1 Introduction

In *Chapter 3*, seven ORFs within the *B. pseudomallei* genome were selected as potential bacterial effectors which play a role in the bacteria's ability to evade phagosomal or autophagic degradation. Sequences encoding the seven *B. pseudomallei* ORFs were expressed in the yeast *S. cerevisiae* BY4741 strain. Cells were characterised for their vacuolar morphology phenotype under nutrient starvation (autophagic) conditions. Expression of the *B. pseudomallei* ORFs induced a multiple vacuole phenotype. These cells also exhibited a decrease in cytosolic and mitochondrial turnover by autophagy. It is therefore apparent that, the proteins encoded by each of the ORFs can exert an influence on vacuolar morphology and organelle turnover in *S. cerevisiae*. Therefore, it was decided to attempt inactivation of each ORF in the *B. pseudomallei* genome in order to determine the effects of bacterial infection on mammalian cells.

The generation of a deletion mutant for each ORF was attempted by double cross-over allelic exchange. Deletion mutants were derived in such a manner so as to result in a substantial number of nucleotides being removed from any individual ORF and to ensure that a functional product cannot be expressed. Being irreversible, deletion mutants are preferred for specific gene characterisation. In contrast, insertional mutants arise from the insertion of a vector construct within an ORF and create a disruption of the target ORF. In such mutants, there is a possibility for disruption of the expression of downstream genes (Stevens et al., 2004), therefore hindering the true characterisation of the target gene. Insertional mutations are potentially reversible, since a recombination event leading to the elimination of the inserted vector may restore the wild-type genome sequence.

Using the double cross-over allelic exchange method (Logue et al., 2009), deletion mutants were successfully constructed in *B. pseudomallei* K96243 for *BPSS1532* (*bipB)*, *BPSL0670* and *BPSS1394* (*bpscN)*, as outlined in *Table 4.1*. This chapter reports on the *BPSS1532* and *BPSL0670* mutants. The *BPSS1394* mutant is reported on in the following chapter. Several attempts were made to construct double cross-over deletion mutations of the other four ORFs, but these were unsuccessful and were abandoned.

Table 4.1: Table describing the *B. pseudomallei* double cross-over deletion mutants to be characterised

***B. pseudomallei* ORF**	**Description**	**Mutant Description**	**Reference**
***BPSS1532* BipB**	Putative cell invasion protein. Type three secretion system associated protein. Predicted to be located in the bacterial inner membrane.	A polar insertional mutant had reduced MNGC formation and cell-to-cell spreading, and was attenuated for virulence in BALB/c mice. Deletion mutant not previously published.	(Suparak et al., 2005). Characterisation of deletion mutant reported in this chapter.
BPSL0670	Putative cation transporter efflux protein. Predicted to be located in the bacterial cytoplasm.	Deletion mutant not previously published.	Characterisation of deletion mutant reported in this chapter.
***BPSS1394* BpscN**	Putative type three secretion associated protein SctN. Predicted to be located in the bacterial cytoplasm.	Deletion mutant not previously published.	Characterisation of deletion mutant reported in *Chapter 5*

Overview of Experimental Strategy

The *BPSS1532* and *BPSL0670* deletion mutants were constructed by double cross-over allelic exchange. Mutagenesis constructs were generated by amplifying approximately 1 kb upstream and downstream of the target gene to encompass approximately 100 bp of the 5' and 3' coding sequence respectively. The primers for the upstream and downstream fragments were designed to incorporate *Xba*I and *Bgl*II restriction sites (*Table 4.2*). For the upstream construct, the 5' primer contained an *Xba*I restriction site, and the 3' primer contained a *Bgl*II site. For the downstream construct, the 5' primer contained a *Bgl*II restriction site, and the 3' primer contained an *Xba*I site. *Figure 4.1A* illustrates the template design of the mutagenesis constructs. Following PCR amplification, both fragments were introduced by a three-way ligation into *Xba*I-digested pBluescriptSK vector (*Figure 4.1B*). The pBluescriptSK clones were digested with *Bgl*II in preparation for insertional ligation of a tetracycline *tetA*(C) gene cassette (*Figure 4.1C*). The resulting plasmid was digested with *Xba*I to release the gene deletion cassette that was then ligated into *Xba*I-digested pDM4 vector (*Figure 4.1D*), for subsequent introduction into the *B. pseudomallei* genome by conjugation.

The *BPSS1532* and *BPSL0670* deletion mutants were characterised *in vivo* for their virulence in female BALB/c mice aged 6 – 8 weeks. Competition assays (*Materials and Methods, Chapter 2.14*) were performed to determine the relative Competitive Index (rCI), whereby an rCI less than 0.10 was deemed partial attenuation and an rCI of less than 0.05 as complete attenuation. In addition, the mutants were characterised for their ability to survive and replicate intracellularly in mouse macrophage-like RAW 264.7 cells (Cullinane et al., 2008). Further *in vitro* studies were carried out in

RAW 264.7 cells stably expressing LC3-GFP to facilitate determination of the degree of mutant co-localisation with the autophagic marker LC3, and their ability to spread via actin motility.

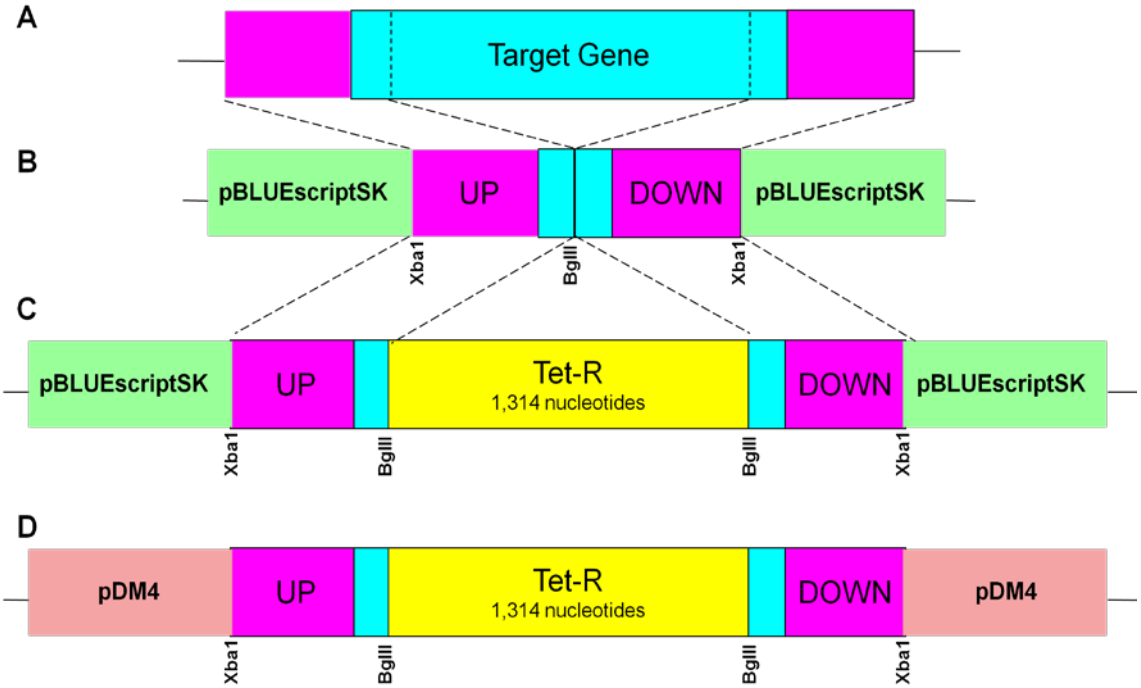

Figure 4.1: The standard template utilised for the design of constructs for creating *B. pseudomallei* mutants. Mutagenesis constructs were generated by amplifying approximately 1 kb upstream (titled UP) and downstream (titled DOWN) of the target gene to encompass approximately 100 bp of the 5' coding sequence and 3' coding sequence respectively (A). For the UP construct, the 5' primer specified an *Xba*I restriction site, and the 3' primer specified a *Bgl*II site. For the DOWN construct, the 5' primer specified a *Bgl*II restriction site, and the 3' primer specified an *Xba*I site. Following PCR amplification both fragments were introduced by a three-way ligation into *Xba*I-digested pBluescriptSK vector (B). The pBluescriptSK clones were digested with *Bgl*II in preparation for insertional ligation of a tetracycline *tetA(C)* gene cassette (C). The resulting plasmid was digested with *Xba*I to release the gene deletion cassette that was then ligated into *Xba*I-digested pDM4 vector (D).

Table 4.2: Mutagenesis primers used to generate *BPSS1532* and *BPSL0670* deletion mutants

Primer	Sequence[a]	Description
mutBipB-U5'	GGGCGA**TCTAGA**CGCGGACAAC	Forward primer upstream of *BPSS1532;* specifying an *Xba*I site
mutBipB-U3'	GTACGC**AGATCT**CGACAGCGTGCCGAG	Reverse primer upstream of *BPSS1532*; specifying a *Bgl*II site
mutBipB-D5'	ATGTAC**AGATCT**AAGCTGCTCGGCGATC	Forward primer downstream of *BPSS1532;* specifying a *Bgl*II site
mutBipB-D3'	CCGCGT**TCTAGA**GCTTGAGCTC	Reverse primer downstream of *BPSS1532*; specifying a *Xba*I site
mutBpsl0670-U5'	GGCGCT**TCTAGA**GCGCGAGATGGCGATG	Forward primer upstream of *BPSL0670;* specifying an *Xba*I site
mutBpsl0670-U3'	CAGACG**AGATCT**CAGCGAGCGTTTTTC	Reverse primer upstream of *BPSL0670*; specifying a *Bgl*II site
mutBpsl0670-D5'	AACGAA**AGATCT**GGCACCGATTTCTCCGAC	Forward primer downstream of *BPSL0670;* specifying a *Bgl*II site
mutBpsl0670-D3'	CGACGC**TCTAGA**GGCGGCCCGGCCGTTTC	Reverse primer downstream of *BPSL0670*; specifying a *Xba*I site
3325	AGGTCGAGGTGGCC	Forward primer at 5' of *tetA(C)* cassette
4629	ATTTGCCGACTACCTTGGTG	Reverse primer at 3' of *tetA(C)* cassette
5116	ATCAGGGACAGCTTCAAGGA	Reverse primer embedded at nucleotide position 182 of *tetA(C)* cassette
5424	GCTGTCGGAATGGACGATAT	Forward primer embedded at nucleotide position 1,081 of *tetA(C)* cassette

[a] Bold type face indicates nucleotides specifying restriction sites.

4.2 Results

BPSS1532 and *BPSL0670* Mutagenesis

Genomic DNA was extracted and purified from *B. pseudomallei* K96243 to serve as the template for PCR amplifications (*Chapter 2.3*). The *BPSS1532* mutagenesis construct was generated using mutBipB-U5' and mutBipB-U3' primers (*Table 4.2*) to amplify a 900 bp fragment spanning 804 bp upstream of the *BPSS1532* coding sequence, plus 96 bp of the 5' coding sequence, flanked by *Xba*I and *Bgl*II restriction sites. The mutBipB-D5' and mutBipB-D3' primers (*Table 4.2*) were used to amplify a 960 bp fragment encompassing 162 bp at the 3' end of the coding sequence and 798 bp downstream of the ORF, flanked by *Bgl*II and *Xba*I restriction sites. PCR products of the expected size were amplified for *BPSS1532* (*Figure 4.2*). The intensity of the bands in lanes 4 and 5 suggested that the amplification of DNA produced for the downstream fragment was much less efficient than for the upstream fragment. Low DNA yields from PCR amplification are common, when using the GC-rich template of *B. pseudomallei*, the GC content for the *BPSS1532* and *BPSL0670* ORFs is 70% and 64% respectively. In an attempt to increase the DNA yield of PCR products, conditions were optimised by varying the concentrations of additions such as betaine, DMSO and magnesium, varying the annealing temperature, varying primer and template concentrations, and using alternative polymerases. These alternative conditions did not significantly increase DNA yield for the PCR amplification of the BPSS1532 downstream fragment (data not shown).

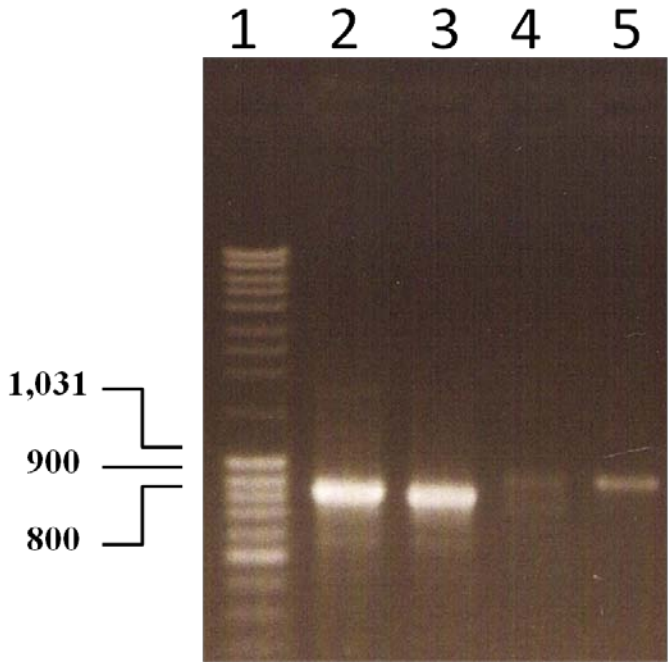

Figure 4.2: PCR amplification of *BPSS1532* mutagenesis constructs. Lane 1: Fermentas MassRuler DNA Ladder. The positions of relevant size markers (bp) are shown on the left. Lanes 2 and 3 display independent PCR amplification products for the *BPSS1532* upstream fragment. Lanes 4 and 5 display independent PCR amplification products for the *BPSS1532* downstream fragment.

Following purification by QIAGEN PCR clean-up kits, the upstream and downstream fragments were introduced following three-way ligation into the *Xba*I-digested pBluescriptSK vector. Colonies produced from transformation of this ligation reaction into *E. coli* DH5α cells were screened by PCR using the mutBipB-U5' and mutBipB-D3' mutagenesis primers. This primer pair should amplify a 1,860 bp product if the up and down fragments assemble correctly. Four colonies had produced a fragment of the correct size (*Figure 4.3*). DNA from the pBluescriptSK::BPSS1532 clone "E" (*Figure 4.3, lane 6*), was digested with *Bgl*II to introduce the *Bgl*II digested tetracycline *tetA(C)* gene cassette (1,314 bp). The resulting mutagenesis construct, consisting of the upstream fragment, *tetA(C)* cassette and downstream fragment resulted in a 3,174 bp product. The pBluescriptSK::BPSS1532::*tetA(C)* clone was then digested with *Xba*I to liberate the 3,174 bp product, which was ligated into the *Xba*I-digested pDM4 vector (7,107 bp)**,** for transformation into *E. coli* SM10 *λpir* cells. The pDM4::BPSS1532::*tetA(C)* clones were verified by restriction digests (*Figure 4.4*), and by nucleotide sequencing. Digestion of a correctly assembled construct with *Bgl*II is expected to yield an 8,967 bp vector/construct fragment and a *tetA(C)* insert fragment of 1,314 bp. Digestion with *Xba*I will result in a vector backbone fragment of 7,107 bp and a mutagenesis construct fragment of 3,174 bp. Clone "C" highlighted in lanes 3 and 8 (*Figure 4.4*) produced the expected banding profile. The correct sequence identity of clone C was also confirmed by nucleotide sequencing (data not shown).

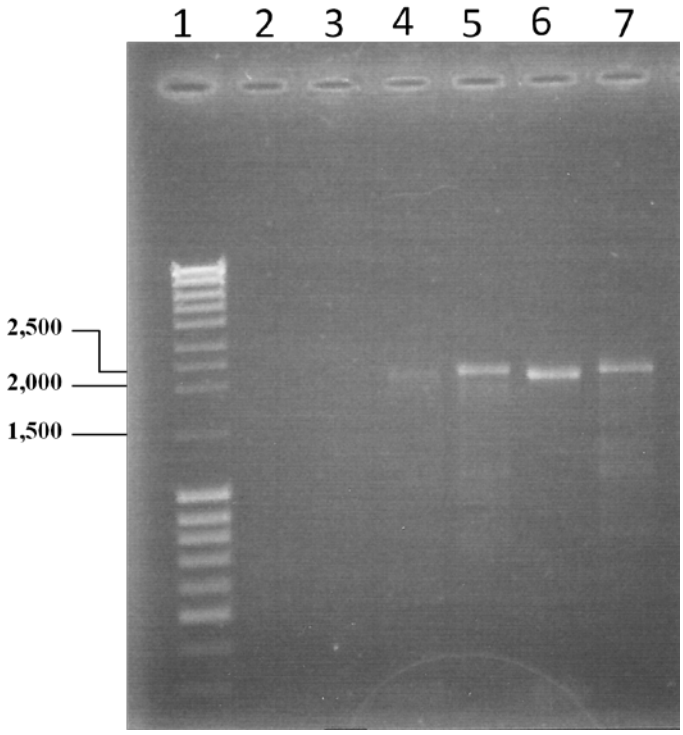

Figure 4.3: PCR amplification of pBluescriptSK::BPSS1532 clones using primer pair mutBipB-U5' and mutBipB-D3'. Lane 1: Fermentas MassRuler DNA Ladder. The positions of relevant size markers (bp) are shown on the left. Lanes 2 through to 7 display PCR amplification products from DNA of pBluescriptSK::BPSS1532 clones A to F.

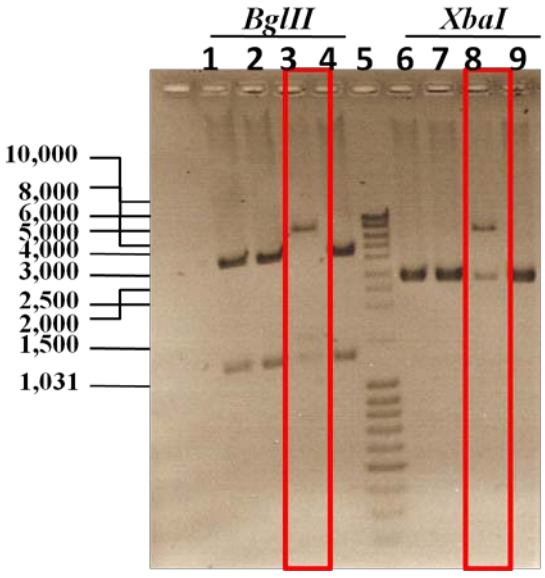

Figure 4.4: Restriction enzyme digestion analysis of four clones of the pDM4::BPSS1532::*tetA(C)* plasmid. Lanes 1 to 4 display restriction digestion products of clones A, B, C and D with *Bgl*II enzyme. Lane 5: Fermentas MassRuler DNA Ladder. The positions of relevant size markers (bp) are shown on the left. Lanes 6 to 9 display restriction digestion products of clones A, B, C and D with *Xba*I enzyme. Clone C is highlighted in lanes 3 and 8 as producing the expected banding profile.

In a similar manner, the *BPSL0670* mutagenesis construct was generated. Primers mutBpsl0670-U5' and mutBpsl0670-U3' (*Table 4.2*) were used to produce a 976 bp fragment encompassing 916 bp upstream of the coding sequence and 60 bp of the 5' end of the ORF. The downstream fragment was amplified with primers mutBpsl0670-D5' and mutBpsl0670-D3' (*Table 4.2*) to generate a 987 bp fragment spanning 780 bp downstream of the ORF and including 207 bp at the 3' end of the coding sequence (*Figure 4.5*). These two fragments were introduced by a three-way ligation into the *Xba*I-digested pBluescriptSK vector. Following transformation of this ligation reaction into *E. coli* DH5α cells, two colonies were screened by PCR using the mutBpsl0670-U5' and mutBpsl0670-D3' mutagenesis primers. This primer pair should amplify a 1,963 bp product if the up and down fragments have assembled correctly (*Figure 4.6*). DNA of the pBluescriptSK::BPSL0670 clone "B" showed a product band of appropriate size (*Figure 4.6, lane 3*). DNA was then digested with *Bgl*II for the introduction of the *Bgl*II tetracycline *tetA(C)* gene cassette (1,314 bp). The resulting mutagenesis construct, consisting of the upstream fragment, *tetA(C)* cassette and downstream fragment formed a 3,277 bp product. Digestion with *Xba*I was used to liberate the 3,277 bp product, which was then ligated into *Xba*I-digested pDM4 vector, for transformation into *E. coli* SM10 *λpir* cells.

DNA from four pDM4:BPSL0670:*tetA(C)* clones was verified by PCR screening (*Figure 4.7*). Clone C produced the appropriate PCR product profile (*Figure 4.7, lanes 8 – 10*) and was used for transformation. The correct sequence identity of clone C was also confirmed by nucleotide sequencing (data not shown).

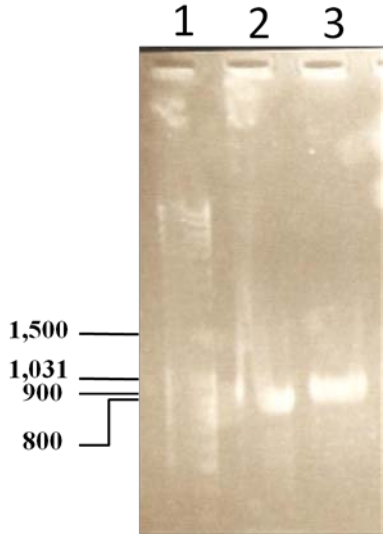

Figure 4.5: PCR amplification of *BPSL0670* mutagenesis constructs. Lane 1: Fermentas MassRuler DNA Ladder. The positions of relevant size markers (bp) are shown on the left. Lane 2 displays *BPSL0670* upstream fragment. Lane 3 displays *BPSL0670* downstream fragment.

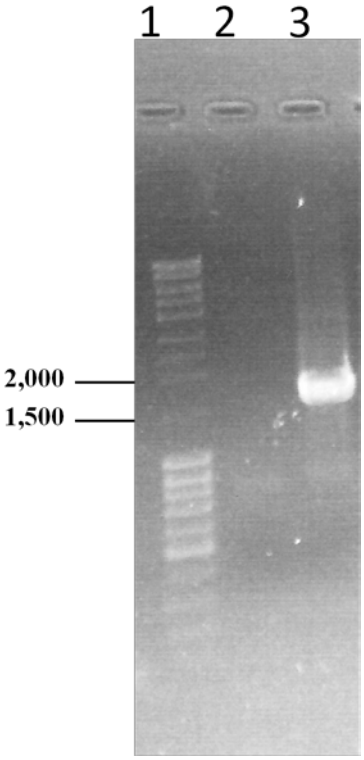

Figure 4.6: PCR amplification of pBluescriptSK::BPSL0670 clones using primer pair mutBpsl0670-U5' and mutBpsl0670-D3'. Lane 1 showing Fermentas MassRuler DNA Ladder. The positions of relevant size markers (bp) are shown on the left. Lanes 2 and 3 display PCR amplification products from DNA of pBluescriptSK::BPSL0670 clones A and B.

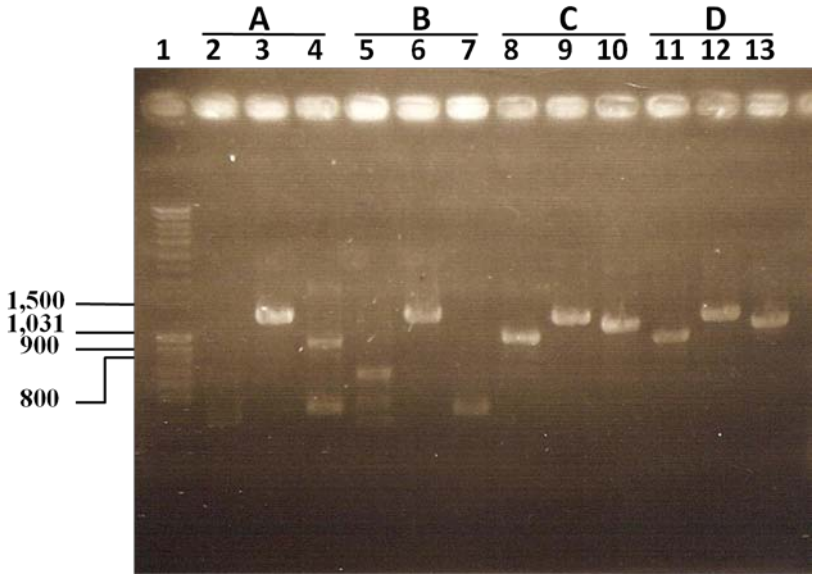

Figure 4.7: PCR screening of pDM4:BPSL0670:*tetA(C)* clones. Lane 1: Fermentas MassRuler DNA Ladder. The positions of relevant size markers (bp) are shown on the left. Lanes 2 – 4: Clone A; lanes 5 – 7: Clone B; lanes 8 – 10: Clone C; lanes 11 – 13: Clone D. Amplification with primer pairs: was as follows: mutBpsl0670-U5' and 5116 (lane 2, 5, 8 and 11); 3325 and 4629 (lanes 3, 6, 9 and 12); and 5424 and mutBpsl0670-D3' (lanes 4, 7, 10 and 13). Amplification with each primer pair should produce products of the following sizes: mutBpsl0670-U5' and 5116, 867 bp; tetracycline primers 3325 and 4629, 1,314 bp; and 5424 and mutBpsl0670-D3', 987 bp. Clone C produced the appropriate PCR product profile

E. coli SM10 cells expressing the pDM4 mutagenesis constructs were grown overnight in LB medium at 37°C with shaking at 200 rpm, in preparation for conjugation with *B. pseudomallei*. The *E. coli* and wild-type *B. pseudomallei* were subcultured and grown to mid-log phase to reach an OD_{600} 0.6. Equal volumes of both cultures, were spotted together on LB agar plates and grown overnight at 37°C. Transconjugants were selected by plating on LB agar containing tetracycline (25 µg/mL) and gentamicin (64 µg/mL). Transconjugants were screened by patching onto LB agar containing chloramphenicol (40 µg/mL). Single cross-over transconjugants retaining the pDM4 plasmid displayed resistance to chloramphenicol. Double cross-over transconjugants displayed chloramphenicol sensitivity. Putative deletion mutants were initially confirmed with PCR amplification using either the BipB-5' and BipB-3' or Bpsl0670-5' and Bpsl0670-3' primer pair, and internal primers (*Table 4.3*). Subsequently putative mutants were subjected to DNA sequencing which verified the correct sequence of the *BPSS1532* and *BPSL0670* deletion mutations in the *B. pseudomallei* genome (data not shown).

Putative *BPSS1532* deletion mutants were screened with the BipB-5' and BipB-3' primers (*Table 4.3*). PCR amplification of wild-type *B. pseudomallei* DNA template with this primer pair should produce a 1,174 bp fragment. Using these same primers on a double cross-over deletion mutant DNA template should yield a larger 1,711 bp fragment. This increase in fragment size is attributed to the presence of the inserted *tetA(C)* cassette. Template DNA of single cross-over mutants would yield products of both the wild-type band and the larger deletion mutant band. PCR amplification products were produced as expected for wild-type DNA template (*Figure 4.8B, lane*

1), two independent double cross-over mutant DNA templates (*Figure 4.8B, lanes 2* and *3*) which produced a larger 1,711 bp product and a single cross-over DNA template (*Figure 4.8B, lane 4*).

The *BPSS1532* double cross-over mutant DNA templates were also PCR screened with internal primer pair internalBipB-5' and internalBipB-3' (*Table 4.3*). These primers were designed to amplify 877 bp within the deleted region of the *BPSS1532* mutagenesis construct. Therefore, use of this primer pair will produce a fragment for the wild-type and single cross-over DNA template, but will not yield any product with the double cross-over DNA template. The 877 bp fragment was present in the wild-type (*Figure 4.8B, lane 5*) and single cross-over (*Figure 4.8B, lanes 8*) DNA templates, but absent with both of the double cross-over DNA templates (*Figure 4.8B, lanes 6* and *7*). Therefore, the PCR screening confirmed the identity of the *BPSS1532* double cross-over mutant.

In a similar manner, putative *BPSL0670* deletion mutants were PCR screened with the Bpsl0670-5' and Bpsl0670-3' primer set (*Table 4.3*). Amplification with these primers using the wild-type *B. pseudomallei* template will produce the full length *BPSL0670* ORF of 906 bp (*Figure 4.9A*). Using these primers on the double cross-over deletion mutant DNA template will yield a larger 1,604 bp fragment (*Figure 4.9A*) to account for the additional *tetA(C)* cassette. A single cross-over mutant template will yield both the wild-type band and the larger mutant band (*Figure 4.9B, lane 5*). Amplification with the wild-type genome produced a 906 bp fragment

(*Figure 4.9B, lane 2*). As expected, amplification with two double cross-over mutant templates (*Figure 4.9B, lanes 3* and *4*) produced a larger 1,604 bp product.

A subsequent screen with the internal primer pair internalBpsl0670-5' and internalBpsl0670-3' (*Table 4.3*), designed to amplify 570 bp within the deleted region of the *BPSL0670* mutagenesis construct, was then carried out (see *Figure 4.9B, lanes 6 – 9*). The use of this primer pair will produce a 570 bp fragment for both the wild-type and single cross-over template, but will not yield any product using the double cross-over template. The 570 bp fragment was observed in the PCR amplification products for wild-type (*Figure 4.9B, lane 6*) and single cross-over template (*Figure 4.9B, lane 9*), but absent for both of the double cross-over templates (*Figure 4.9B, lanes 7* and *8*). Therefore, the PCR screening confirmed the identity of the *BPSL0670* double cross-over mutant.

Table 4.3: Primers used to verify *BPSS1532* and *BPSL0670* deletion mutants.

Primer	Sequence	Description
BipB-5'	ATGGATCCAAACATGTCATCG GGAGTGCAGGGCGGAC	Forward primer of *BPSS1532* coding region.
BipB-3'	TTAGGATCCCACTGCGCGGGC GTTACGCAGGATCAG	Reverse primer of *BPSS1532* coding region
internalBipB-5'	AGGCGGCGGCCGACGCGGCC GAGCAGGCC	Forward primer within deletion section of *BPSS1532*.
internalBipB-3'	ATCGCGCCGGCGAGCTCGGCC TTCTGCTGAT	Reverse primer within deletion section of *BPSS1532*.
Bpsl0670-5'	ATGGATCCAAACATGAACGA TTCGTATCCCAGTCG	Forward primer of *BPSL0670* coding region.
Bpsl0670-3'	TCAGGATCCGTCTTCGCCCGC CGAGCCGCTGCGCCG	Reverse primer of *BPSL0670* coding region.
internalBpsl0670-5'	GAGCCCGACTCGCGGGCCGA GCTTCTC	Forward primer within deletion section of *BPSL0670*.
internalBpsl0670-3'	GATCTCGGTCAGCGCGCGCAC GCGGTAG	Reverse primer within deletion section of *BPSL0670*.

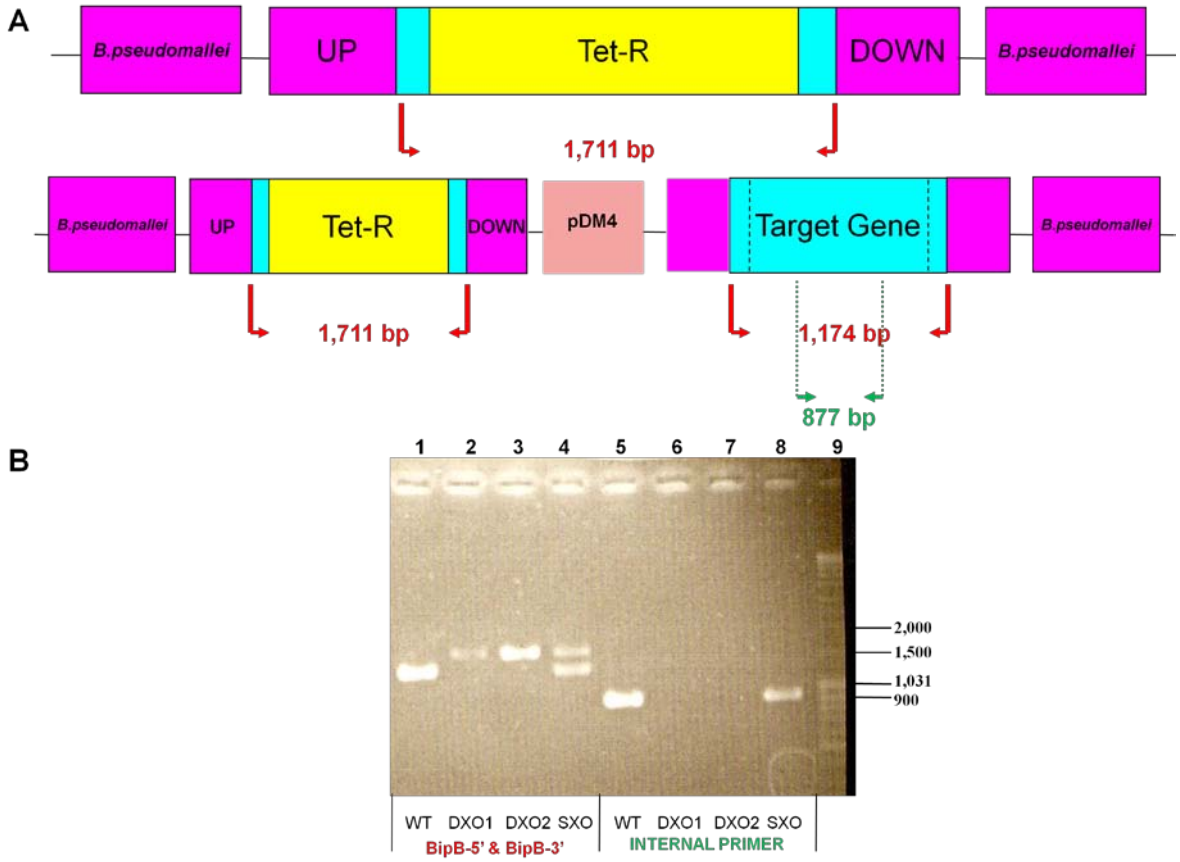

Figure 4.8: Panel A illustrates the expected configuration of the *BPSS1532* double cross-over deletion and single cross-over insertional mutations integrated in the *B. pseudomallei* genome. The positions of primer pairs are shown as depicted by the red arrows – illustrating the 5' and 3' primers specific for ORF sequence, and the dotted green arrows – highlighting the positions of the internal primers.

Panel B displays the PCR products of *B. pseudomallei* wild-type and *BPSS1532* mutant templates amplified with the BipB-5' and BipB-3' primer pair (lanes 1 – 4) and the internal primer pair (lanes 5 – 8). Wild-type template (lanes 1 and 5); double cross-over *BPSS1532* mutant template (lanes 2, 3 and 6, 7) and single cross-over mutant template (lanes 4 and 8). Lane 9 shows the Fermentas MassRuler DNA Ladder. The positions of relevant size markers (bp) are shown on the right.

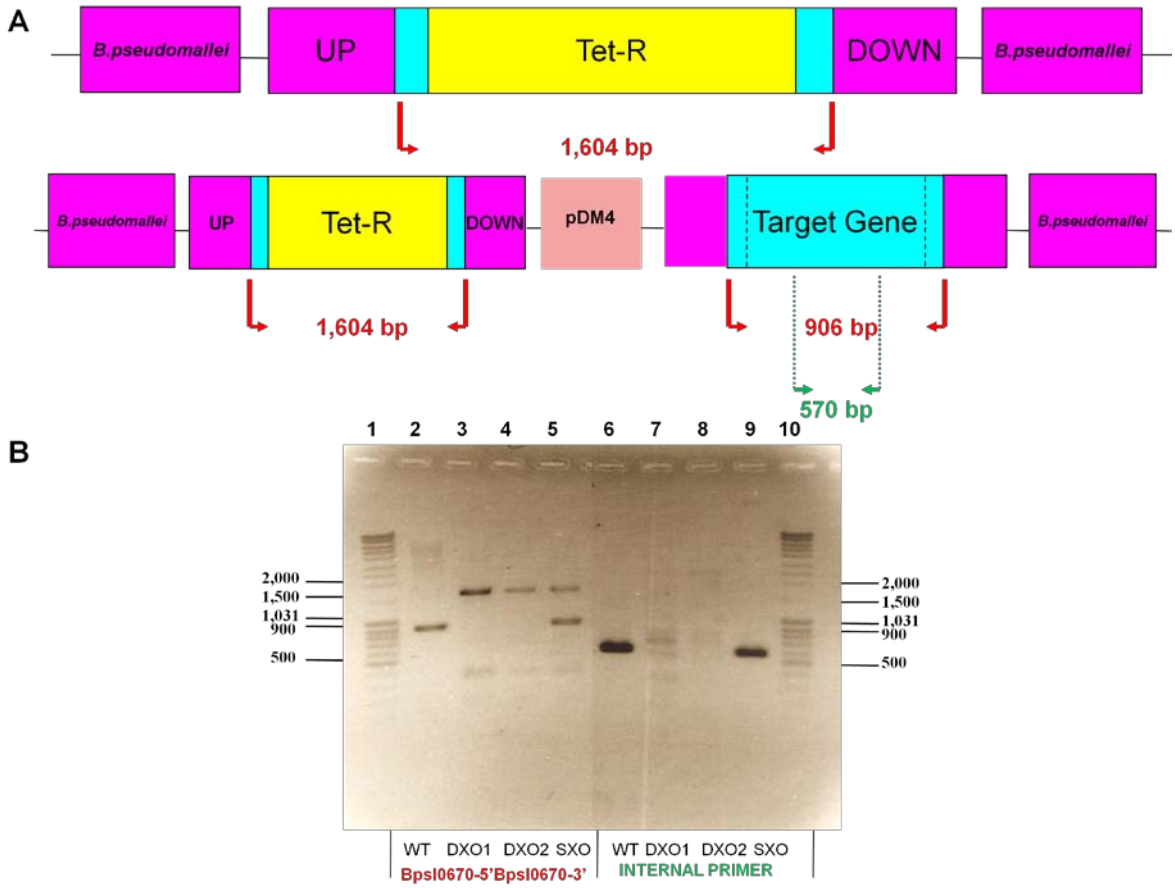

Figure 4.9: Panel A illustrates the expected size configuration of the *BPSL0670* double cross-over deletion and single cross-over insertional mutants integrated in the *B. pseudomallei* genome. The position of primer pairs are shown as depicted by the red arrows – illustrating the 5' and 3' primer specific for ORF sequence, and the dotted green arrows – highlighting the positions of the internal primers.

Panel B displays the PCR products of *B. pseudomallei* wild-type and *BPSL0670* mutant templates amplified with the Bpsl0670-5' and Bpsl0670-3' primer pairs (lanes 2 – 5) and the internal primer pair (lanes 6 – 9). Lanes 1 and 10 show the Fermentas MassRuler DNA Ladder. The positions of relevant size markers (bp) are shown on the left and right. Wild-type template (lanes 2 and 6); double cross-over *BPSL0670* mutant template (lane 3, 4 and 7, 8) and single cross-over mutant template (lanes 5 and 9).

The *BPSS1532* and *BPSL0670* Mutants are Partially Attenuated for Growth in BALB/c Mice:

The *BPSS1532* and *BPSL0670* mutants were examined for their ability to grow *in vivo* in 6 – 8 week old BALB/c mice. Mice were co-infected intranasally with an inoculum containing equal volumes of wild-type *B. pseudomallei* and the mutant strain cultures grown to the same cell density (*Materials and Methods Chapter 2.14*). The *in vivo* relative growth assays were used to calculate the ratio of mutant bacteria retrieved from mouse spleen in comparison to the *in vitro* analysis. Statistical analysis using a one sided *z* test categorised mutants with rCI < 0.1 as highly attenuated for virulence and, 0.1 < rCI < 1.0 as partially attenuated for virulence. In five independent experiments the rCI for the *BPSS1532* mutant was determined as: 1.02, 0.21, 0.03, 0.47 and 0.52, and the rCI for the *BPSL0670* mutant was determined to be: 0.72, 0.63, 0.90, 0.40 and 0.64, indicating partial attenuation for virulence *in vivo* (*Figure 4.10*) ($p<0.001$). Only mutants showing high attenuation for growth were subjected to further *in vivo* testing for virulence (*Materials and Methods, Chapter 2.14*).

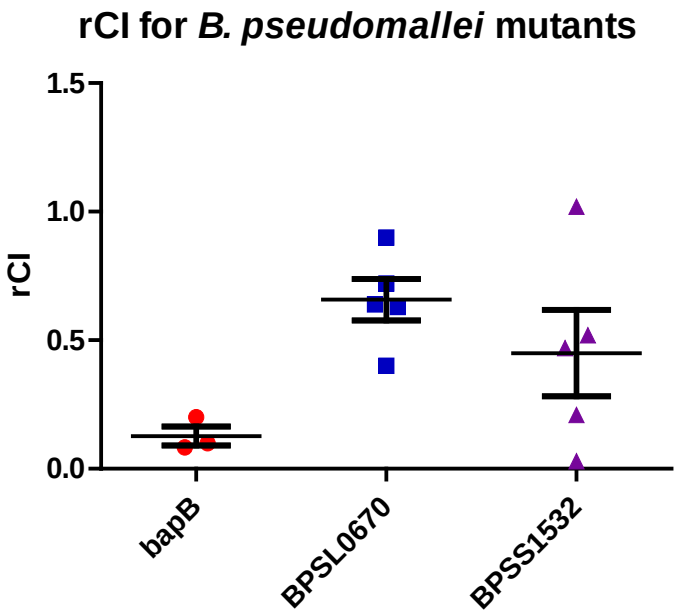

Figure 4.10: Scatter plot of *in vivo* relative growth assays for mutants *BPSL0670*, *BPSS1532* and control *bapB* (Treerat et al., unpublished). The experiment was carried out in three to five BALB/c mice aged between 6 – 8 weeks. Error bars show SEM.

The *BPSS1532* Mutant has a Delayed Replication Rate in RAW264.7 Cells, whilst the *BPSL0670* Mutant has Diminished Survival and Replicative Abilities.

Given the partial attenuation of the *BPSS1532* and *BPSL0670* mutants as determined by the *in vivo* relative growth assays, these strains were examined for their growth characteristics in LB broth *in vitro*. The *in vitro* growth rates of both mutants, were similar to that of wild-type *B. pseudomallei* (*Figure 4.11*), suggesting that the ability of the mutant strains to survive in mice is not attributed to its growth rate.

As described previously, wild-type *B. pseudomallei* is able to survive and replicate in macrophage RAW 264.7 cells over six hours p.i. (Cullinane et al., 2008). Accordingly, the survival and replication of mutant strains in macrophage cells were determined. Wild-type *B. pseudomallei* and mutant bacteria were used to infect macrophage RAW264.7 cells for 1 h at an MOI of 6 (*Materials and Methods, Chapter 2.9*). Following macrophage lysis, samples were plated on LB and the intracellular bacteria enumerated. Lysates prepared at 2 h p.i. from cells infected with either wild-type *B. pseudomallei* or the *BPSS1532*, mutant produced similar CFU numbers. At 4 h p.i. the CFU for the *BPSS1532* mutant had increased, but not to the same extent as wild-type, suggesting slightly delayed replication of the mutant in comparison to the wild-type bacterium. At 6 h p.i., again the numbers of mutant bacterial colonies increased, but not to the same extent as for wild-type bacteria (*Figure 4.12A*).

The *BPSL0670* mutant bacteria were allowed to infect macrophage RAW264.7 cells for 1 h at an MOI of 6. At 2, 4 and 6 h p.i. the macrophage cells were lysed and the bacteria retrieved were enumerated. At 2 h p.i. the numbers of mutant and wild-type

bacteria were similar. However, at 4 h p.i. there was a distinct decrease in the recovery of mutant bacteria. Compared to the wild-type, the *BPSL0670* mutant showed a statistically significant decrease ($p = 0.004$). At 6 h p.i. there was an even more pronounced difference in numbers ($p = 0.0003$) of mutant in comparison to wild-type bacteria (*Figure 4.12B*). This study clearly demonstrated decreased survival of the mutant *BPSL0670* over the 6 h infection period.

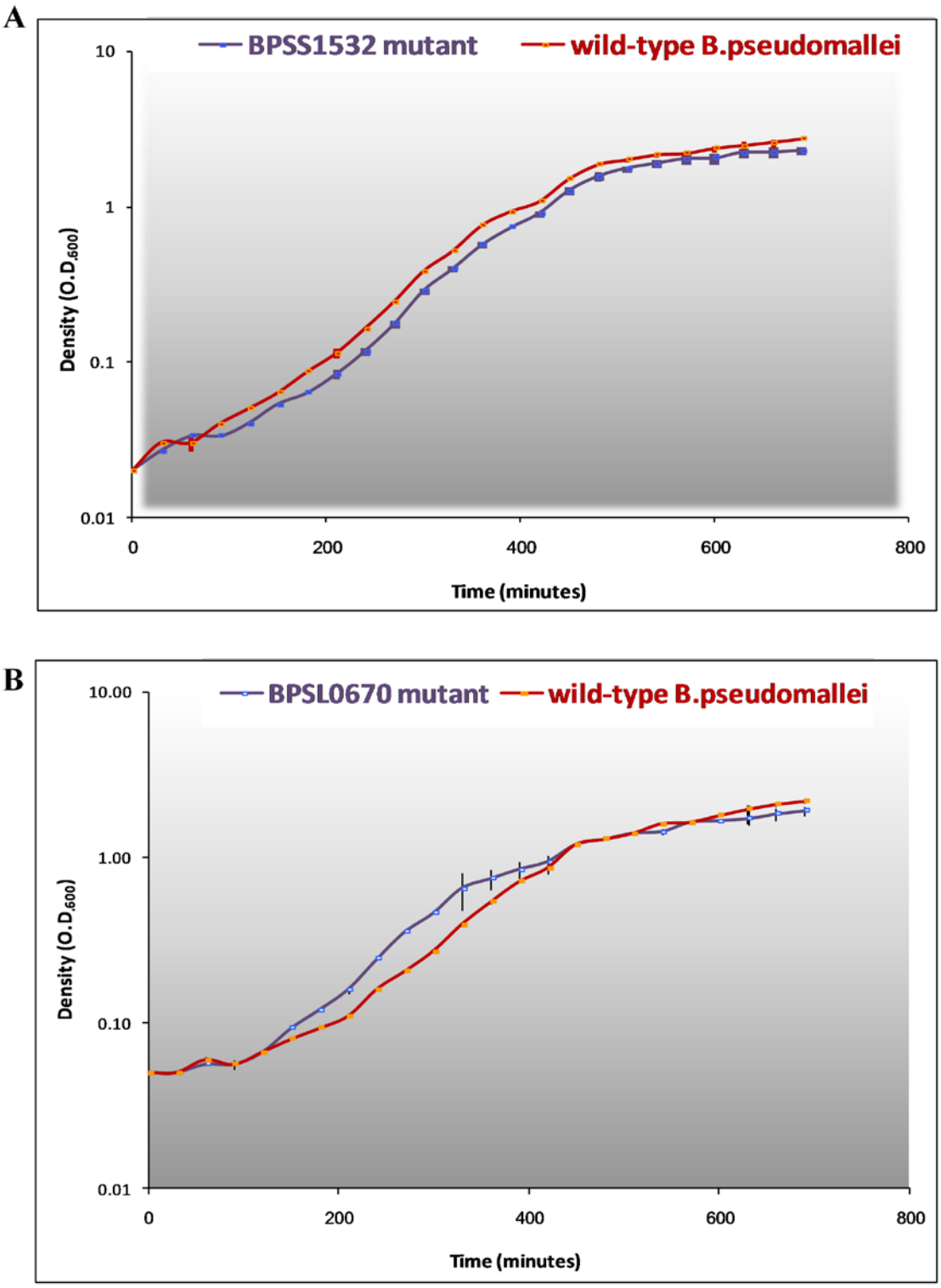

Figure 4.11: Growth curves for each mutant strain compared to the wild-type *B. pseudomallei*. Panel A: *BPSS1532* mutant; Panel B: *BPSL0670* mutant. Error bars represent the SEM for three independent experiments.

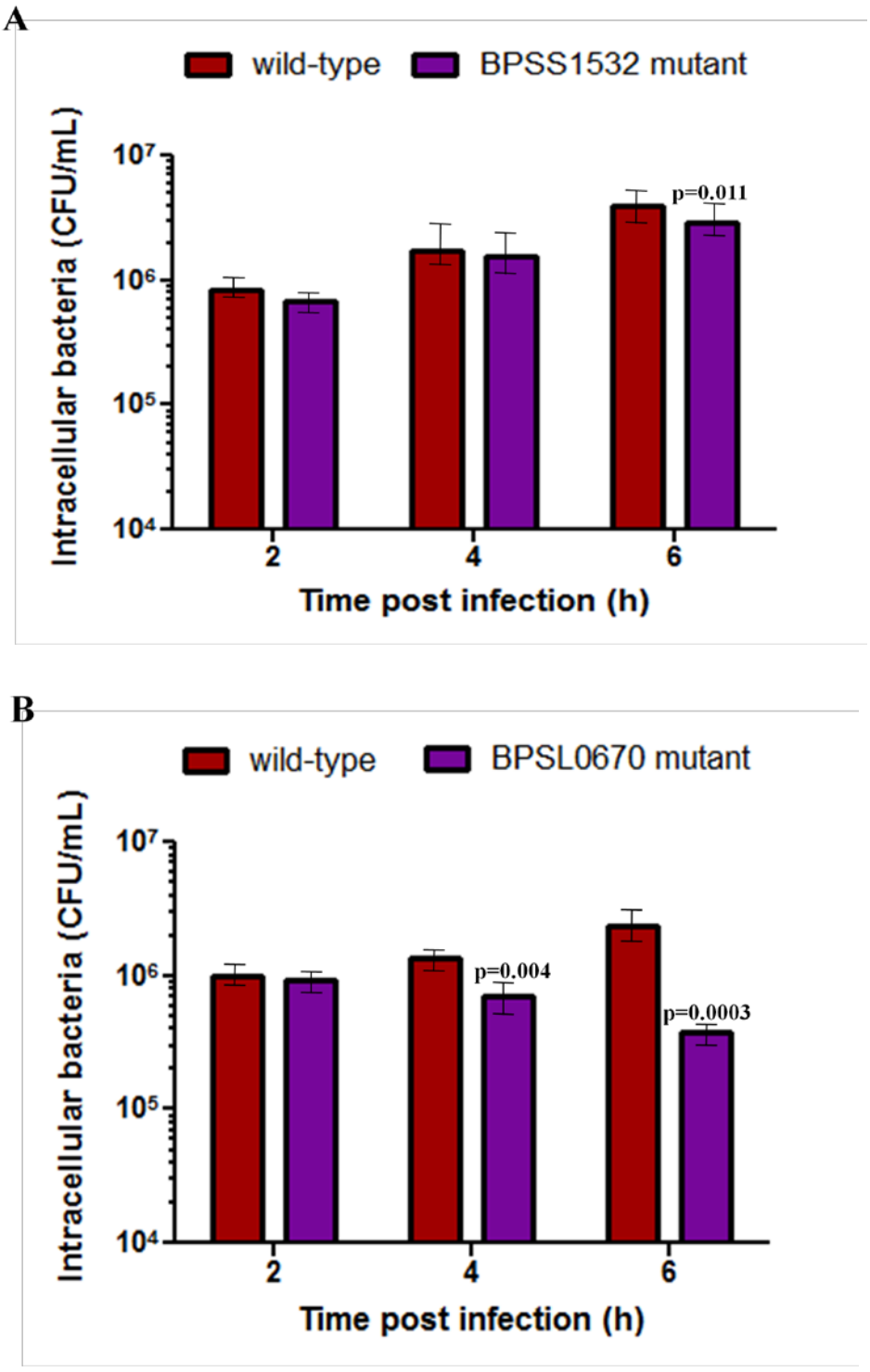

Figure 4.12: Mutant survival and replication within RAW264.7 macrophage-like cells. Panel A: *BPSS1532* mutant; Panel B: *BPSL0670* mutant. Statistical significance ($p<0.02$) is apparent for *BPSS1532* mutant at 6 h p.i., and *BPSL0670* mutant at 4 and 6 h p.i. in comparison to the wild-type. Error bars represent the SEM from nine biological replicates.

Mutant Co-Localisation with LC3-GFP as a Measure of Phagosomal Escape

Recent research at Monash University, has explored the interaction between *B. pseudomallei* and host autophagic processes. Application of a combination of imaging technologies, principally confocal microscopy and EM, to the analysis of infected macrophage RAW264.7 cells stably expressing LC3-GFP has revealed that the intracellular bacteria are subject to LC3-associated phagocytosis (LAP) rather than canonical autophagy (Gong et al., 2011). However, the bacterial killing associated with LAP is generally low. In the case of *B. pseudomallei*, 75 % of the wild-type bacteria at 6 h p.i., have escaped degradation in phagosomes, and continue to survive in the cytosol (*Chapter 5*).

Given the survival and replication data obtained for the *BPSS1532* mutant, it was hypothesised that this strain would be able to evade intracellular degradation with similar efficiency to wild-type cells. To test this hypothesis, the *BPSS1532* mutant strain was allowed to infect macrophage RAW264.7 cells stably transfected with LC3-GFP at an MOI of 6. At 2 h, 4 h and 6 h p.i., samples were fixed and analysed for co-localisation of the mutant bacteria with LC3-GFP (*Figure 4.13A*). There was a decrease in co-localisation for the *BPSS1532* mutant, similar to that observed for wild-type bacteria at all time points (*Figure 4.13A*). Scoring of bacterial co-localisation with LC3-GFP puncta (*Figure 4.13B*) revealed that the mutant strain was able to evade intracellular killing as effectively as the wild-type bacteria.

The *BPSL0670* mutant showed a decrease in intracellular survival over 6 h following infection of macrophage RAW264.7 cells. This decrease in CFU numbers was hypothesised to be attributed to intracellular killing by LAP in the macrophage cells. To test this hypothesis, RAW264.7 LC3-GFP cells were infected with *BPSL0670* mutant bacteria at an MOI of 6. At 2 h and 4 h p.i., the mutant bacteria showed a statistically significant decrease in LC3 co-localisation, compared to the wild-type. However, over the next two hours co-localisation of the mutant bacteria did not decrease further whereas at 6 h p.i. the co-localisation with LC3 for wild-type bacteria was less than at 4 h p.i. (*Figure 4.14B*). Although the percentage of bacteria co-localised with GFP was low, overall these data are consistent with decreased survival and replication for *BPSL0670* mutant bacteria (*Figure 4.12B*).

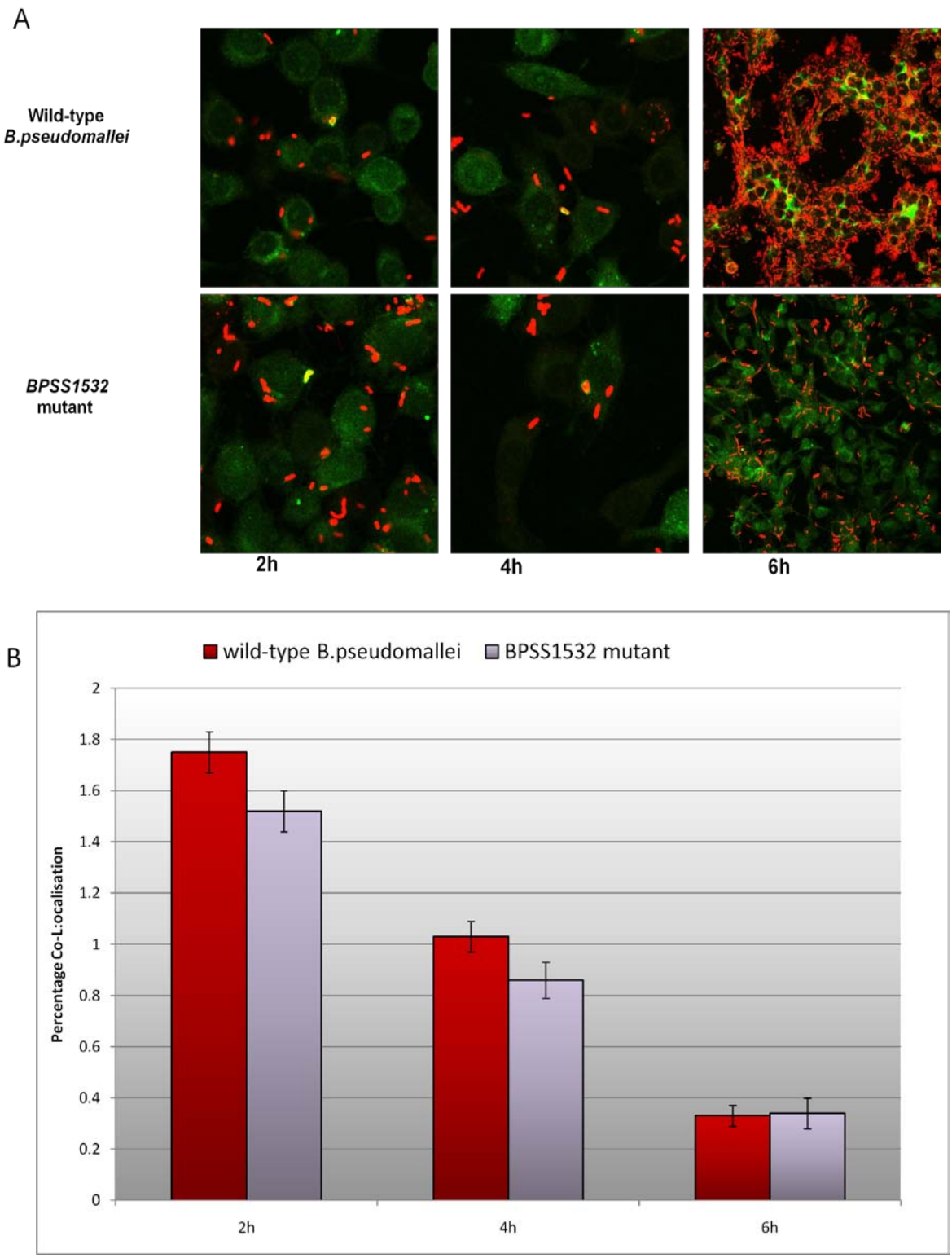

Figure 4.13: Co-localisation of wild-type and *BPSS1532* mutant bacteria with LC3-GFP. (A) Bacterial co-localisation with LC3-GFP was defined by the presence of labelled bacteria (red fluorescence) which were fully overlaid by intense green (yellow fluorescence) or fully contained within a green ring. Scale bar = 10 μm. (B) Quantitative analysis of bacterial co-localisation with LC3-GFP. The experiment was performed in biological triplicates and data are presented as the mean ± SEM.

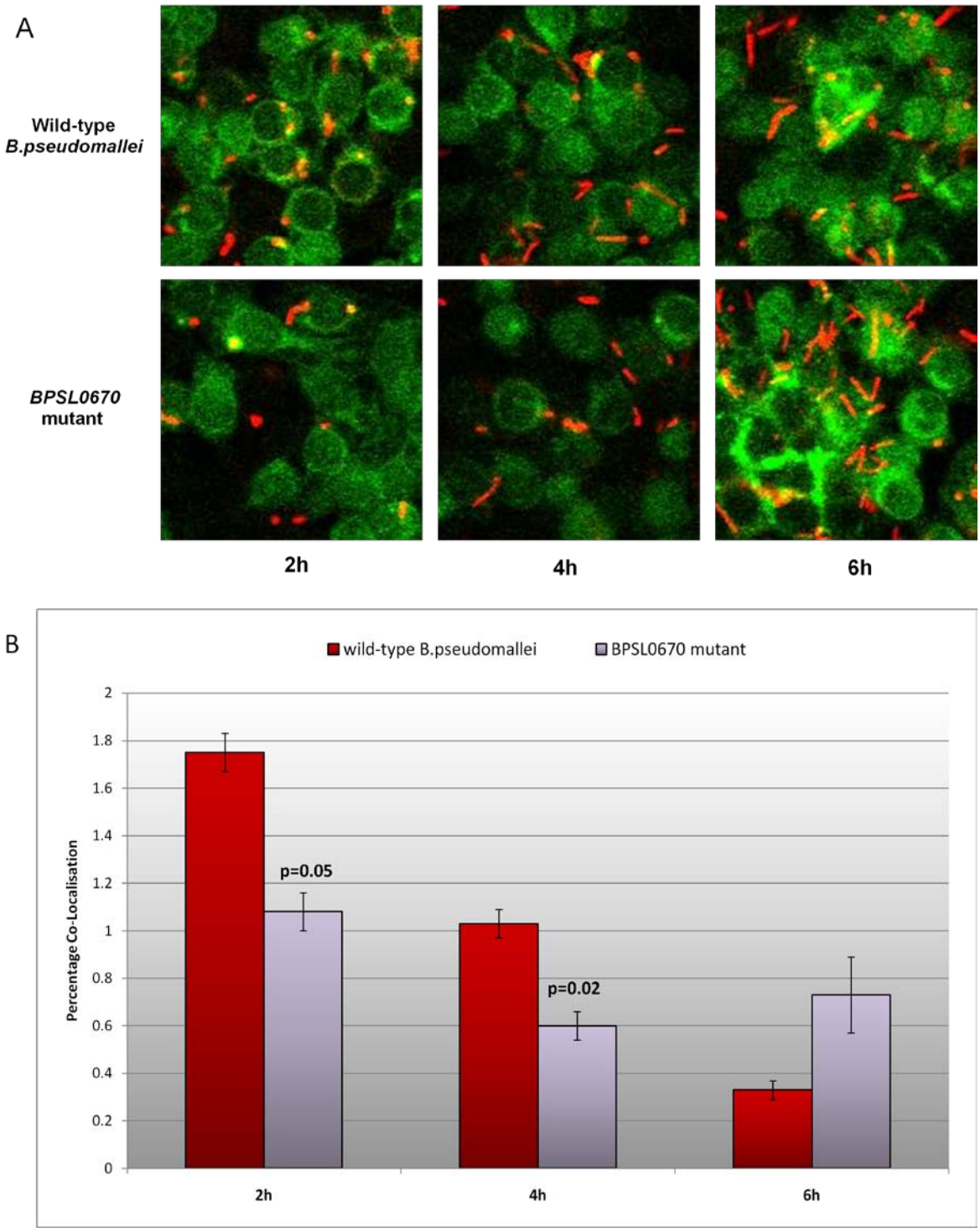

Figure 4.14: Co-localisation of wild-type and *BPSL0670* mutant bacteria with LC3-GFP. (A) Bacterial co-localisation with LC3-GFP was defined by the presence of labelled bacteria (red fluorescence) which were fully overlaid by intense green (yellow fluorescence) or fully contained within a green ring. Scale bar = 10 μm. (B) Quantitative analysis of bacterial co-localisation with LC3-GFP. The experiment was performed in biological triplicates. The experiment was performed in biological triplicates and data are presented as the mean ± SEM.

The *BPSS1532* and *BPSL0670* Mutants Maintain the Ability to Polymerise Actin Tails

Following infection and escape from phagosomes, wild-type *B. pseudomallei* are able to polymerise an actin tail by manipulating the host actin. Employing actin-based motility, *B. pseudomallei* is then able to form membrane protrusions into adjacent cells continuing its cell-to-cell spread (Stevens et al., 2006). To determine whether the ability to form actin tails was altered in mutant bacteria, RAW264.7 LC3-GFP cells were infected with mutant bacteria and after 6 h were fixed, immune-histochemically stained and imaged.

At 6 h p.i. actin tails were observed in the *BPSS1532* and *BPSL0670* mutant strains (*Figure 4.15*). This phenotype appeared identical to that of the wild-type strain. Thus it seems unlikely that a change in actin tail phenotype contributes to the partial attenuation phenotype observed for both mutants in the *in vivo* competition assay. In addition, the staining of the nucleus shows a clumping phenotype suggesting the formation of MNGC at 6 h p.i., similar to the wild-type.

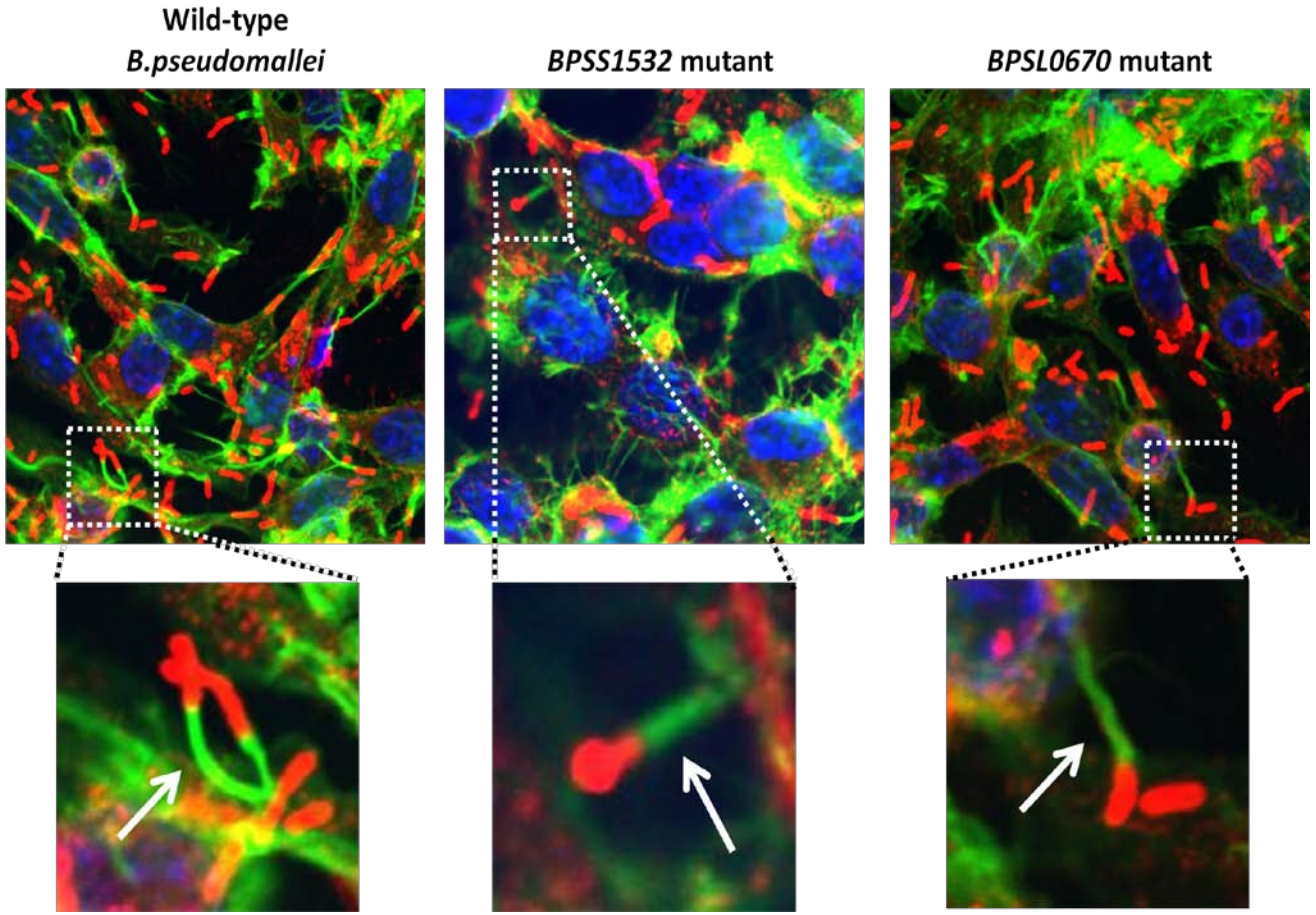

Figure 4.15: RAW264.7 LC3-GFP macrophage-like cells were infected with *B. pseudomallei* wild-type, *bipB* or *BPSL0670* mutant bacteria and viewed at 6 h p.i. Bacteria were labelled with primary rabbit anti–*B. pseudomallei* OMP and secondary goat anti–rabbit IgG Texas Red antiserum. Actin was stained with Phalloidin Alexa Fluor 488. Nuclei were stained with DAPI. Bacteria (red fluorescence) have actin tails (green fluorescence) protruding at one pole. Nucleus (blue fluorescence).

4.3 Discussion

The double cross-over allelic exchange method was employed to generate deletion mutations of *BPSS1532* and *BPSL0670* in the *B. pseudomallei* K96243 strain. This chapter has focused on the derivation of the *BPSS1532* and *BPSL0670* deletion mutants and their phenotypic characterisation.

4.3.1 Double Cross-Over Deletion Mutant *BPSS1532*

Firstly, mutant bacteria were tested for attenuation of virulence *in vivo*. Using the *in vivo* relative growth assay, the *BPSS1532* mutant appeared to be only partially attenuated for virulence in mice. This suggests that the mutant is able to survive the immune response initiated in mice. Subsequent analysis of bacterial survival and replication in cultured murine RAW264.7 LC3-GFP macrophage-like cells showed no significant difference from wild-type bacteria over the 6 h infection period. Consistent with this finding, the level of co-localisation between mutant bacteria and LC3-GFP decreased over 6 h essentially in parallel with wild-type bacteria. These results suggest that mutant bacteria are able to escape the phagosome and evade intracellular killing as efficiently as wild-type bacteria.

The only other *BPSS1532* mutant of which there are published data was reported by Suparak et al. (2005). However, they generated a single cross-over insertional polar *BPSS1532* mutant that was attenuated for virulence and had reduced cell-to-cell spread and MNGC formation. The virulence trial performed by Suparak et al. was conducted over 42 days using BALB/c mice that were infected intranasally. Mice

infected with the wild-type strain all died within 5 – 11 days, whereas 5 of 6 mice infected with the mutant strain survived until the termination of the experiments. By comparison, for the deletion mutant reported here an assay was conducted, whereby BALB/c mice were co-infected with wild-type and mutant bacteria for 18 h. This study found the *BPSS1532* mutant to be only partially attenuated for growth *in vivo*. On this basis it was decided not to proceed to an *in vivo* test of virulence using the mouse model over a longer time frame.

Suparak et al. (2005) assessed the ability of their *BPSS1532* mutant to form MNGC in J774A.1 murine macrophage-like cells. They found reduced MNGC formation in cells infected by the mutant bacteria in comparison to wild-type bacteria at time points up to 12 h post infection. At 24 h they observed an increased level of MNGC formation following infection with mutant bacteria, which were still less than that in cells infected by wild-type bacteria. RT-PCR was used to establish that this mutant had a polar effect that disrupted expression of downstream *bipC* and *bipD* genes. A *bipD* mutant is unable to escape from endocytic vacuoles/phagosomes (Stevens et al., 2002, Gong et al., 2011), a requirement of cell-to-cell spread. It is therefore possible that the reduced level of MNGC formation and cell-to-cell spread observed, were due to the disruption of the *bipC* and *bipD*. The BipB protein is a structural component situated at the tip of the TTSS needle (Sun and Gan, 2010). Disruption of the *bipB* gene may result in inaccurate assembly of the needle tip and subsequent hindrance to protein secretion through the needle. Suparak et al. (2005) assessed the effect of their *BPSS1532* mutant on the secretion of effector proteins by analysing the detection of BopE in whole-cell and secreted protein fractions. BopE was detected in their sample (data not shown). The effector secretion “phenotype” of the *BPSS1532* deletion

mutant has not been determined, but future experiments could test this by determining the ability of mutant bacteria to secrete BopE. The unhindered secretion of BopE will verify that the TTSS is still functional in the deletion mutant.

4.3.2 Double Cross-Over Deletion Mutant *BPSL0670*

The *BPSL0670* deletion mutant was also found to be partially attenuated for virulence in BALB/c mice and showed diminished survival and replication compared to wild-type bacteria following infection of cells in culture. A two-fold increase in the co-localisation of mutant bacteria with LC3-GFP at 6 h p.i. (compared with wild-type bacteria) correlated with its decreased survival and replication. Inactivation of the *BPSL0670* gene had no apparent influence on the ability of mutant bacteria to polymerise actin tails, or the formation of MNGC.

There are few clues in the literature as to the function of the *BPSL0670* gene product. The *B. pseudomallei BPSL0670* gene shares 42.9% identity to the *S. enterica* serovar Typhimurium *corC* gene – a component of the CorA system. The CorA magnesium transport system of *S. enterica* serovar Typhimurium mediates the influx and efflux of magnesium by means of the products of four genes: *corA*, *corB*, *corC* and *corD*. Gibson et al. (1991) found that mutations of the *corC* gene had minimal effects on cation influx (threefold increase in cobalt uptake), but more drastic effects on cation efflux, specifically in the case of magnesium. Magnesium transport systems were transcribed a thousand fold higher upon *S. enterica* serovar Typhimurium infection of epithelial cells, due to the lack of intravacuolar magnesium. However, the absence of a functional CorA system had no apparent effect on the invasion efficiency or

short-term survival of *S. typhimurium* in eukaryotic cells (Smith et al., 1998). If the *BPSL0670* gene product functions as a cation transporter efflux protein then its deletion does not significantly affect bacterial invasion or intracellular growth under the conditions tested. The magnesium concentration in the soil where *B. pseudomallei* grows is undetermined. Future experiments could determine whether *BPSL0670* mutant bacteria may display altered infectivity or growth phenotype in medium of varying magnesium concentrations.

CHAPTER FIVE

ROLE FOR THE *BURKHOLDERIA PSEUDOMALLEI* TYPE THREE SECRETION SYSTEM CLUSTER 1 *BpscN* GENE IN VIRULENCE

5.1 Declaration

In the case of *Chapter 5*, the nature and extent of my contribution to the work was the following:

Nature of Contribution	Extent of Contribution (%)
All laboratory work, data collection and analysis, discussion and interpretation of data with supervisors; co-editing of paper.	**75%**

The following co-authors contributed to the work:

Name	Nature of Contribution	Extent of Contribution (%)
Lan Gong	Interpretation of data with co-authors. Assistance in TEM and Confocal imaging.	
Puthayalai Treerat	Discussion and assistance in animal work.	**5%**
Georg Ramm	Explanation and assistance in TEM imaging	
John D. Boyce	Discussion and interpretation of data with co-authors; co-editing.	
Mark Prescott	Co-supervisor of project; discussion and interpretation of data with co-authors.	
Ben Adler	Co-supervisor of project; discussion and interpretation of data with co-authors; co-editing. Assistance in animal experiments.	
Rodney J. Devenish	Main supervisor of project; discussion and interpretation of data with co-authors; co-editing	

Signed: .....

Dated: .....

Declaration by Co-Authors:

The undersigned hereby certify that:

1. The above declaration correctly reflects the nature and extent of the candidate's contribution to this work, and the nature of the contribution of each of the co-authors.
2. They meet the criteria for authorship in that they have participated in the conception, execution, or interpretation, of at least that part of the publication in their field of expertise.
3. They take public responsibility for their part of the publication, except for the responsible author who accepts overall responsibility for the publication.
4. There are no other authors of the publication according to these criteria.
5. Potential conflicts of interest have been disclosed to (a) granting bodies, head of the responsible academic unit.
6. The original data will be stored in the Department of Biochemistry and Molecular Biology, Monash University, Clayton Campus, Victoria, Australia, and will be held for at least five years from the date indicated below.

Name	**Signature**	**Date**
Lan Gong		
Puthayalai Treerat		
Georg Ramm		
John D. Boyce		
Mark Prescott		
Ben Adler		
Rodney J. Devenish		

5.2 Introduction

This chapter presents the generation and characterisation of a Type III Secretion System cluster 1 (TTSS1) *BPSS1394 – BpscN*, deletion mutant in the form of a published journal article (D'Cruze et al., 2011). The *Introduction Chapter (Chapter 1.4.1*) gives an overview of the TTSS gene clusters in *B. pseudomallei*. *Table 1.1* of that chapter indicates that the *BPSS1394* gene is located in TTSS1 and illustrates its homology with the TTSS3 gene *BsaS*, a putative ATPase. The positioning of the *BsaS* protein at the core of the *B. pseudomallei* needle structure (*Introduction Chapter Figure 1.5*) suggests that it has a pivotal role in the functioning of the TTSS3. It was hypothesised therefore, that a *BPSS1394* deletion mutant, given the homology of the *BPSS1394* gene to the *BsaS* gene, would have a deleterious effect on the function of the *B. pseudomallei* secretion apparatus.

The functions of genes within the TTSS1 and TTSS2 clusters are essentially uncharacterised. Warawa and Woods (2005) reported that TTSS1 and TTSS2 were not involved in the virulence of *B. pseudomallei* in hamsters. However, the results reported in this chapter identify a role for the *BPSS1394* gene in virulence of infection in mice. To the best of my knowledge, this is the first study that suggests a role for TTSS1 (and potentially TTSS2) in the infectivity and pathogenicity of *B. pseudomallei* in mice.

INFECTION AND IMMUNITY, Sept. 2011, p. 3659–3664 Vol. 79, No. 9
0019-9567/11/$12.00 doi:10.1128/IAI.01351-10
Copyright © 2011, American Society for Microbiology. All Rights Reserved.

Role for the *Burkholderia pseudomallei* Type Three Secretion System Cluster 1 *bpscN* Gene in Virulence▽

Tanya D'Cruze,[1,3] Lan Gong,[1,3] Puthayalai Treerat,[2,3] Georg Ramm,[1] John D. Boyce,[2,3] Mark Prescott,[1] Ben Adler,[2,3]* and Rodney J. Devenish[1,3]

Departments of Biochemistry and Molecular Biology[1] and Microbiology[2] and Australian Research Council Centre of Excellence in Structural and Functional Microbial Genomics,[3] Monash University, Clayton, Victoria 3800, Australia

Received 22 December 2010/Returned for modification 19 January 2011/Accepted 30 June 2011

***Burkholderia pseudomallei*, the causal agent of melioidosis, employs a number of virulence factors during its infection of mammalian cells. One such factor is the type three secretion system (TTSS), which is proposed to mediate the transport and secretion of bacterial effector molecules directly into host cells. The *B. pseudomallei* genome contains three TTSS gene clusters (designated TTSS1, TTSS2, and TTSS3). Previous research has indicated that neither TTSS1 nor TTSS2 is involved in *B. pseudomallei* virulence in a hamster infection model. We have characterized a *B. pseudomallei* mutant lacking expression of the predicted TTSS1 ATPase encoded by *bpscN*. This mutant was significantly attenuated for virulence in a respiratory melioidosis mouse model of infection. In addition, analyses *in vitro* showed diminished survival and replication in RAW264.7 cells and an increased level of colocalization with the autophagy marker protein LC3 but an unhindered ability to escape from phagosomes. Taken together, these data provide evidence that the TTSS1 *bpscN* gene product plays an important role in the intracellular survival of *B. pseudomallei* and the pathogenesis of murine infection.**

Burkholderia pseudomallei, the causal agent of melioidosis, is endemic in southeastern Asia and northern Australia (3), with recently diagnosed sporadic cases in southeastern Africa (1), the Americas, New Caledonia, and Mauritius (4). *B. pseudomallei* infection can present with acute or chronic clinical manifestations, including septic shock, pulmonary infections, benign pulmonitis, pneumonia (21), prostatic abscesses, cerebral abscesses, meningoencephalitis, encephalomyelitis, suppurative parotitis, and conjunctival ulcers (10).

Several *B. pseudomallei* virulence factors have been identified, including the capsule, pili, flagella, lipopolysaccharide, quorum-sensing molecules, and type six and type three secretory systems (6). The type three secretion system (TTSS) is one of six types of secretion systems identified in bacteria and mediates the secretion of effector molecules directly into host cells (24). Structurally, TTSS consist of a membrane-spanning needle which employs hydrophilic and hydrophobic translocators to deliver bacterial effectors directly into the host cell cytoplasm (16). The current view is that the hydrophilic translocators assist the integration of the hydrophobic translocators into the host cell membrane, forming a pore complex (16). It is hypothesized that the initial contact of the needle tip with the host cell membrane triggers the TTSS to secrete effector molecules (16). *B. pseudomallei* has been shown to assemble a syringe-like TTSS structure, which is proposed to inject critical virulence effectors into the host cell cytoplasm (17).

B. pseudomallei has three TTSS gene clusters (designated TTSS1, TTSS2, and TTSS3), and each of these clusters is present on the small chromosome (20). The TTSS1 gene cluster, which was first reported in 1999 by Winstanley et al. (25), shows homology to a TTSS in the plant pathogen *Ralstonia solanacearum* but is absent from the related *Burkholderia* species *B. mallei* and *B. thailandensis* (24). In contrast, TTSS2, while showing homology to a TTSS present in *R. solanacearum*, is also present in *B. mallei* and *B. thailandensis* (24). TTSS3 shows homology to a TTSS found in *Salmonella enterica* serovar Typhimurium, *Shigella flexneri* (21), *B. mallei*, and *B. thailandensis*. The TTSS1 and TTSS2 loci encode 16 to 18 proteins, the functions of which remain mostly uncharacterized. Previous work has shown that TTSS1 and TTSS2 are not involved in *B. pseudomallei* virulence in a hamster infection model (23).

In this paper, we report the construction and characterization of a *B. pseudomallei* mutant lacking expression of the predicted TTSS1 ATPase (*bpscN*, *BPSS1394*). The hydrolysis of ATP by TTSS-associated ATPases is the key energizer of the TTSS (5, 12). It has been proposed that TTSS ATPases form ring structures associated with the secretion apparatus at the inner bacterial membrane. ATP hydrolysis functions to drive TTSS function by promoting the initial docking of TTSS substrates to the secretion apparatus, unfolding effector proteins prior to secretion, and releasing effectors from their cognate chaperones (12). Here we show that the *bpscN* mutant is attenuated for virulence in a mouse model of infection. Furthermore, additional studies using cultured RAW264.7 macrophage-like cells show that while mutant bacteria are able to escape from phagosomes, they show diminished survival and replication in RAW264.7 cells and show increased levels of colocalization with the autophagy marker protein LC3. Collectively, our data provide strong evidence that the TTSS1 *bpscN* gene plays an important role in *B. pseudomallei* pathogenesis.

* Corresponding author. Mailing address: Department of Microbiology, Monash University, Clayton Campus, VIC 3800, Australia. Phone: 61-3-9902-9177. Fax: 61-3-9902-9222. E-mail: ben.adler@monash.edu.

▽ Published ahead of print on 18 July 2011.

MATERIALS AND METHODS

Bacterial strains and vectors. The *Escherichia coli* K-12 DH5α strain (Bethesda Research Laboratories, Rockville, MD) was used primarily for propagation of the pBluescriptKS phagemid (Stratagene, La Jolla, CA) (Table 1) and its

TABLE 1. Strains and plasmids used in this study

Strain or plasmid	Description	Reference
B. pseudomallei strains		
K96243	Virulent Thai clinical isolate	9
K96243Δ*bpscN::tetA*(C)	*bpscN* deletion mutant, Tet^r	This study
K96243Δ*bpscN::tetA*(C)/pBHR1	*bpscN* deletion mutant, Tet^r, containing the original pBHR1 plasmid	This study
K96243Δ*bpscN::tetA*(C)/pBHR1comp	*bpscN* deletion mutant, Tet^r, containing the pBHR1 plasmid with the inserted *bpscN* complementation construct	This study
E. coli strains		
K-12 DH5α	For propagation of pBluescriptKS phagemid; F$^-$ ϕ80d*lacZ*ΔM15 Δ(*lacZYA-argF*)*U169 deoR recA1 endA1 hsdR17*(r_K^- m_K^+) *phoA supE44* λ$^-$ *thi-1 gyrA96 relA1*	13
K-12 SM10λ*pir*	For propagation of λ*pir*-dependent plasmid pDM4; *thi-1 thr leu tonA lacY supE recA::RP4-2*-Tc::Mu Km^r λ′	15
S17-1λ*pir*	Tp^r Sm^r *recA thi pro hsdR-M$^+$RP4-2*-Tc:Mu:Km Tn*7* λ*pir*	19
Plasmids		
pBluescriptKS phagemid	*lacZ rep* pMB1 Amp^r	18
pBluescript::*bpscN::tetA*(C)	pBluescriptKS phagemid vector containing the *bpscN* mutagenesis construct	This study
pDM4	λ*pir* dependent, Cm^r, *sacBR* negative selection	15
pDM4::*bpscN::tetA*(C)	pDM4 vector containing the *bpscN* mutagenesis construct	This study
pBHR1	mob, rep, Cm^r, Kan^r	22
pBHR1comp	pBHR1 plasmid containing the *bpscN* complementation construct	This study

derivatives. The *E. coli* K-12 SM10λ*pir* strain (15) was used as the donor strain to allow mobilization of the λ*pir*-dependent plasmid pDM4 (14) (Table 1) into *B. pseudomallei* strain K96243 (9).

Construction of a *B. pseudomallei bpscN* mutant. The *bpscN* deletion mutant was constructed by double-crossover allelic exchange. Primers bpscN-U5′ and bpscN-U3′ (Table 2) were used to amplify a 1,203-bp fragment spanning 972 bp upstream of the *bpscN* coding sequence plus 231 bp of the 5′ coding sequence flanked by XbaI and BglII restriction sites. Primers bpscN-D5′ (containing a BglII site) and bpscN-D3′ (containing an XbaI site) were used to amplify a 981-bp fragment spanning 105 bp of the 3′ end of the coding sequence and 876 bp of downstream sequence flanked by BglII and XbaI restriction sites. These two fragments, together with the BglII-digested tetracycline *tetA*(C) gene cassette, were introduced by three-way ligation into the pBluescriptKS phagemid. The resulting plasmid was digested with XbaI, and the *bpscN* mutagenesis cassette was recovered and ligated into XbaI-digested pDM4. This construct was then introduced by transformation into *E. coli* SM10 λ*pir*. For mobilization into *B. pseudomallei*, overnight cultures of *E. coli* and *B. pseudomallei* were subcultured, grown to mid-log phase, spotted together onto Luria-Bertani (LB) agar plates, and grown overnight at 37°C. Transconjugants were subsequently selected on LB agar containing tetracycline (25 μg/ml) and gentamicin (64 μg/ml). Transconjugants were screened for chloramphenicol sensitivity (40 μg/ml), and mutants were confirmed by PCR using primers specific for the *tetA*(C) gene (Tet-5424, Table 2) and sequences upstream and flanking the mutagenesis site (bpscN-D3′O, Table 2). The identity of the PCR product was confirmed by DNA sequencing.

Complementation of a *B. pseudomallei bpscN* mutant. The *bpscN* complementation construct was generated using primers cbpscN-5′ and cbpscN-3′ (Table 2) to amplify a 1,374-bp fragment, spanning the entire *bpscN* coding region from *B. pseudomallei* K96243. The fragment was digested with DraI and NcoI and ligated into the pBHR1 plasmid (23), which was kindly provided by J Warawa (University of Louisville, Louisville, KY). The resulting pBHR1comp plasmid was introduced into *E. coli* S17-1 and subsequently conjugated into the *bpscN* mutant *B. pseudomallei* strain.

Mouse relative *in vivo* growth assays. Relative *in vivo* growth assays were carried out with BALB/c mice. Overnight cultures of wild-type *B. pseudomallei* and the *bpscN* mutant, grown in LB supplemented with appropriate antibiotics, were subcultured for 90 min to an optical density at 600 nm (OD_{600}) of 0.2. For *in vitro* growth analysis, the cultures were combined, a 10-μl aliquot of an appropriate dilution (containing 4×10^4 CFU and designated the input culture) was inoculated into LB broth and grown for 18 h at 37°C with shaking (200 rpm), and an appropriate volume of a serial dilution was spread onto LB agar plates. For *in vivo* growth analysis, groups of five 6- to 8-week-old female BALB/c mice were infected intranasally with 20 μl of the same input culture. After 24 h, mice were euthanized in accordance with animal ethics requirements, their spleens were removed and homogenized in phosphate-buffered saline (PBS), and the homogenate was spread onto LB agar plates. After incubation at 37°C for 24 h, 100 colonies from each experimental set of plates (bacteria recovered *in vitro* and *in vivo*) were patched onto LB agar and LB agar with tetracycline (25 μg/ml) to identify the proportions of wild-type and *bpscN* mutant bacteria. The relative competitive index (rCI) was determined by dividing the number of tetracycline-resistant bacteria derived from the *in vivo* growth assay by the number of tetracycline-resistant bacteria derived from the *in vitro* growth assay (8). The statistical significance of a reduced rCI was determined using a one-sided *z* test as described previously (8).

Mouse virulence assays. Wild-type or mutant *B. pseudomallei* bacteria were subcultured in fresh medium with appropriate antibiotics and grown for 4 h to mid-log phase, to an OD_{600} of 0.8 (corresponding to 5×10^8 CFu/ml). Groups of seven 6- to 8-week-old, female BALB/c mice were infected intranasally with 20 μl of wild-type or mutant bacteria at a dose of 2×10^7 or 2×10^5 CFU. Mice were observed for 10 days and euthanized if moribund, in accordance with

TABLE 2. Primers used in this study

Primer	Sequence 5′→3′	Description
bpscN-U5′	TGCGGCTCTAGACGCGGACCGCGAC	Forward primer upstream of *bpscN*; specifying an XbaI site
bpscN-U3′	CGCCACAGATCTATCACGCGTGAAACCGAC	Reverse primer upstream of *bpscN*; specifying a BglII site
bpscN-D5′	GACGAGAGATCTGCGAAGGCCGACGCGATTC	Forward primer downstream of *bpscN*; specifying a BglII site
bpscN-D3′	ACGATCTCTAGAGTGCCGTGCAGCGTC	Reverse primer downstream of *bpscN*; specifying an XbaI site
tet-5424	GCTGTCGGAATGGACGATAT	Forward primer at 3′ end of *tetA*(C)
bpscN-D3′O	TACCGAGGACGACGCCGATC	Reverse primer downstream of *bpscN* and outside the region used to make the mutagenesis construct
cbpscN-5′	CGC GGG TTT AAA GGC ATG AGC GCG G	Forward primer for complementation of *bpscN*; specifying a DraI site
cbpscN-3′	TCA CCA TGG GTT CGC CCC GCT CAA C	Reverse primer for complementation of *bpscN*; specifying an NcoI site

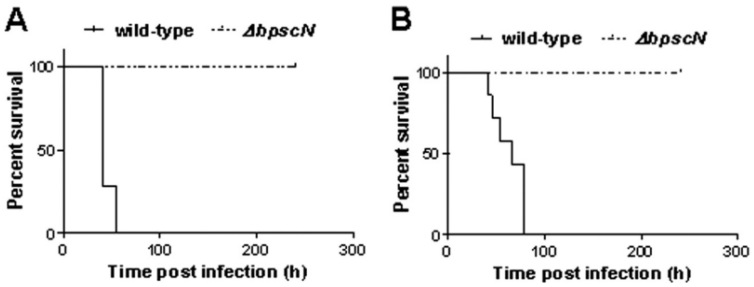

FIG. 1. Kaplan-Meier survival curves for mice infected with either 2×10^7 CFU (A) or 2×10^5 CFU (B) of wild-type or *bpscN* mutant *B. pseudomallei*.

animal ethics requirements. Survival data were displayed as Kaplan-Meier curves, the difference in overall survival was assessed using Fisher's exact test, and the difference in time to death was analyzed using the log-rank Mantel-Cox test.

Survival and replication of *B. pseudomallei* in RAW 264.7 cells. The ability of wild-type and *bpscN* mutant bacteria to survive and replicate intracellularly was investigated in the mouse macrophage-like cell line RAW 264.7 (2). Cells were maintained in RPMI 1640 medium supplemented with 10% (vol/vol) heat-inactivated fetal calf serum (Invitrogen, Carlsbad, CA) at 37°C with 5% CO_2. At 15 h prior to *B. pseudomallei* infection, cells were seeded at 1.0×10^5/well into 24-well trays.

B. pseudomallei strains were grown overnight in LB medium containing appropriate antibiotics and subcultured for 3 h to reach mid-log phase. RAW 264.7 macrophage-like cells were infected for 1 h at a multiplicity of infection (MOI) of 6. At 1 h postinfection (p.i.), cells were washed with PBS, pH 7.2, and replenished with fresh RPMI containing 100 μg/ml ceftazidime and 800 μg/ml kanamycin to kill extracellular bacteria. At 2 h, 4 h, and 6 h p.i., wells were washed to remove extracellular bacteria and lysed with 0.1% (vol/vol) Triton X-100 for 10 min. An aliquot of the bacterial lysate was plated on LB agar and grown at 37°C for 2 days, and CFU were enumerated.

Transmission electron microscopy (TEM). RAW264.7 cells were infected with wild-type or mutant *B. pseudomallei* strains at an MOI of 6. At 2, 4, and 6 h p.i., cells were fixed for 2 h with 2.5% glutaraldehyde in 0.1 M cacodylate buffer, pH 7.2. At this time, cells were harvested and postfixed for an additional 1 h in 1% (wt/vol) osmium tetroxide, followed by 1 h in 2% (wt/vol) uranyl acetate. Samples were then dehydrated, embedded in Epon resin, sliced into 70-nm sections, and stained with lead citrate and uranyl acetate. Images were obtained using a Hitachi H-7500 transmission electron microscope. A minimum of 150 cross sections was imaged in each experiment, and bacteria were scored according to the presence and number of visible membranes in which they were encapsulated.

Fluorescence microscopy. Strains were grown overnight in LB broth supplemented with appropriate antibiotics and subcultured to mid-log phase. RAW264.7 cells stably transfected with LC3-GFP (green fluorescent protein) (2) were infected with *B. pseudomallei* for 1 h in 24-well trays containing coverslips, at an MOI of 6. Wells were then washed with PBS and replenished with fresh RPMI containing ceftazidime (100 μg/ml) and kanamycin (800 μg/ml) to kill extracellular bacteria. At 2 h, 4 h, and 6 h p.i., the cells were fixed with methanol for 10 min, washed with PBS, and incubated with rabbit antiserum against *B. pseudomallei* (2) at a dilution of 1:100 for 1 h. Following washes, the cells were further incubated with goat anti-rabbit IgG Texas Red antiserum (Molecular Probes, Eugene, OR) at a 1:250 dilution for a further 1 h. Internalized *B. pseudomallei* and cytoplasmic LC3 were visualized with an Olympus FV-500 confocal laser scanning microscope by using the fluorescein isothiocyanate and tetramethyl rhodamine isothiocyanate channels to monitor green and red fluorescence emissions, respectively. The images were scored for the numbers of bacteria within RAW 264.7 cells and colocalized with LC3-GFP.

RESULTS

The *bpscN* mutant is highly attenuated for virulence in BALB/c mice. In order to investigate the role of TTSS1 in *B. pseudomallei* virulence, we constructed, in the K96243 background, a *bpscN* (the predicted TTSS1 ATPase) mutant strain. Reverse transcription-PCR performed on RNA isolated from *bpscN* mutant bacteria successfully led to the amplification of transcripts of the downstream gene *BPSS1393* (data not shown), indicating that no polarity effects arose due to the *tetA*(C) insertion in *bpscN*. To determine the ability of the mutant to grow *in vivo*, relative growth assays were carried out with 6- to 8-week-old BALB/c mice coinfected with wild-type and mutant *B. pseudomallei* bacteria. In three independent experiments, the rCI of the *bpscN* mutant was determined to be 0.00, 0.00, and 0.06, respectively, indicating a highly reduced growth rate *in vivo* ($P < 0.001$).

The *bpscN* mutant was then tested for virulence in BALB/c mice, which were challenged intranasally with wild-type or mutant bacteria at a dose of 2×10^7 or 2×10^5 CFU and monitored for 10 days (Fig. 1). All mice infected with 2×10^5 CFU of the wild-type strain showed signs of acute illness within 24 h and were euthanized by 78 h. Similarly, mice infected with 2×10^7 CFU of the wild-type strain were moribund at 24 h and were euthanized by 54 h. However, all of the mice infected with either the large or the small dose of the mutant strain showed no signs of disease for the 10 days of the trial (Fig. 1). Therefore, the *bpscN* deletion mutant is highly attenuated for virulence in BALB/c mice.

To confirm the *in vivo* results, we constructed a second, independent *bpscN* deletion mutant; this mutant had rCI values of 0.09, 0.02, and 0.09 and was also attenuated for virulence in BALB/c mice (data not shown). Bacteria recovered from the spleens of mice infected with the second *bpscN* mutant were tested by PCR and confirmed as retaining the mutation.

The *bpscN* mutant has diminished survival and replicative capacity in RAW264.7 cells. As the *bpscN* mutant was highly attenuated for virulence in BALB/c mice, we hypothesized that mutant bacteria have an increased susceptibility to killing by macrophages. In order to address this hypothesis, we infected murine macrophage-like RAW264.7 cells with wild-type bacteria, mutant bacteria, mutant bacteria harboring the empty pBHR1 vector, or mutant bacteria harboring the *bpscN* complementation construct. There was no difference in the growth rate in LB broth among any of the four strains (data not shown).

Wild-type bacteria were able to survive and multiply in macrophages over the 6 h of the experiment, as observed previously (2). However, compared with wild-type bacteria, *bpscN* mutant bacteria and *bpscN* mutant bacteria harboring the empty pBHR1 vector showed a statistically significant decrease in the number of intracellular bacteria at 4 h ($P < 0.001$) and

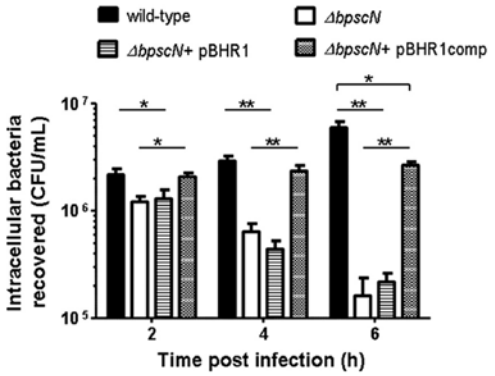

FIG. 2. Bacterial survival and replication within RAW264.7 macrophage-like cells infected at an MOI of 6 with wild-type *B. pseudomallei*, the *bpscN* mutant, the *bpscN* mutant expressing the empty pBHR1 plasmid, or the *bpscN* mutant complemented (comp) with an intact *bpscN* gene. Error bars indicate the standard error of the mean of nine biological replicates. *, $P < 0.05$; **, $P < 0.001$.

at 6 h ($P < 0.001$) p.i (Fig. 2). The mutant complemented with an intact copy of *bpscN* showed a statistically significant increase in the number of intracellular bacteria at 4 h and 6 h p.i ($P < 0.001$) compared to the *bpscN* mutant (Fig. 2).

The *bpscN* mutant is able to escape from phagosomes. As the *bpscN* mutant showed a reduced ability to survive and replicate in RAW 264.7 cells, we investigated whether this outcome resulted from a reduced ability of the mutant to escape from phagosomes. We first used TEM to determine the location of intracellular bacteria at different times after infection. Thin sections of infected macrophage cells were scored for the presence of bacteria and whether they existed free in the cytoplasm or were confined within single membrane compartments (phagosomes). At 2 h p.i., 84% of the wild-type and 66% of the mutant bacteria were found in single membrane compartments, with the remainder free in the cytosol. At 4 h and 6 h p.i., the number of bacteria within single membrane compartments decreased, while the number of bacteria free in the cytosol increased. Thus, at 6 h p.i., 75% and 91% of the wild-type and mutant bacteria, respectively, were found free in the cytosol (Fig. 3). Therefore, *bpscN* mutant bacteria are able

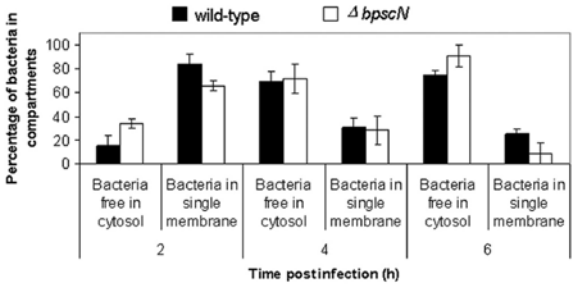

FIG. 3. TEM analysis of the intracellular locations of wild-type and *bpscN* mutant *B. pseudomallei* bacteria in infected RAW264.7 macrophage-like cells. Bacteria were scored as free in the cytoplasm or encapsulated in a single membrane. At least 100 bacteria were scored for both strains in triplicate experiments. Error bars represent the standard error of the mean of biological triplicates.

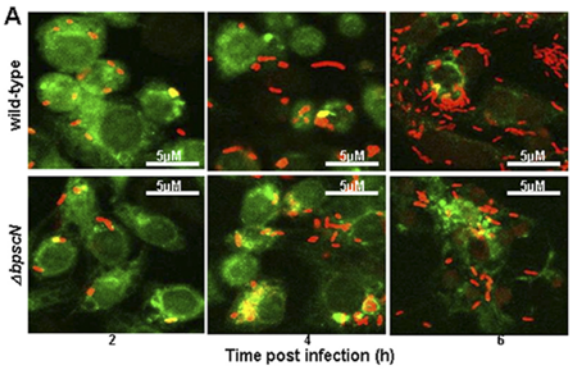

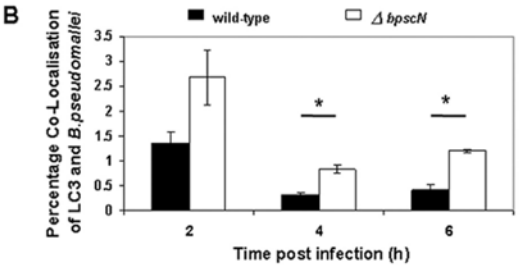

FIG. 4. Colocalization of wild-type and *bpscN* mutant bacteria with LC3-GFP. RAW264.7 macrophage-like cells stably expressing LC3-GFP were infected with wild-type or *bpscN* mutant *B. pseudomallei* bacteria and viewed at 2, 4, and 6 h p.i. (A) Bacterial colocalization with LC3-GFP was defined by the presence of labeled bacteria (red) (yellow fluorescence) which were fully overlaid by intense green or fully contained within a green ring. Scale bars, 5 μm. (B) Quantitative analysis of bacterial colocalization with LC3-GFP. The experiment was performed in biological triplicates, and data are presented as the mean ± the standard error of the mean. *, $P < 0.01$.

to escape from the phagosome at levels similar to those of the wild-type strain. Notably, only a single multiple-membrane structure (encapsulating the *bpscN* mutant) predicted to be an autophagosome was observed across all of the samples analyzed.

The *bpscN* mutant shows increased colocalization with LC3-GFP. To complement the findings of TEM analysis and in view of our recent observations that the TTSS3 genes *bopA* and *bipD* are critical for escape from LC3-associated phagocytosis (7), we analyzed the colocalization of wild-type and *bpscN* mutant bacteria with LC3-GFP. LC3 has been an accepted marker of autophagy; however, our recent data suggest that LC3 is recruited directly to phagosomal membranes, where it contributes to phagosomal maturation and increased bacterial killing (7). At all of the time points measured, the *bpscN* mutant showed an approximately 2-fold increase in colocalization with LC3 compared to that of the wild-type strain (Fig. 4B). This difference was statistically significant at both 4 h and 6 h p.i. ($P < 0.01$).

DISCUSSION

The TTSS1 gene *bpscN* (23) encodes a protein with 63.5% amino acid identity to *R. solanacearum* HrcN, which is a predicted TTSS-associated ATPase (17). TTSS ATPases are pre-

dicted to facilitate the initial docking of the TTSS substrates to the secretion apparatus and through ATP hydrolysis provide the proton motive force for subsequent expulsion of these proteins through the TTSS (12). In the plant pathogen *Xanthomonas campestris* pv. vesicatoria, HrcN has 31% amino acid identity to the bacterial F_0F_1 ATPase β subunit. HrcN is proposed to drive ATP binding and hydrolysis and therefore would be involved in the translocation and secretion of effector TTSS proteins (12). *B. pseudomallei* TTSS1 mutant strains are significantly less virulent in the infection of tomatoes, suggesting a potential role for *B. pseudomallei* TTSS1 in pathogenesis and virulence in plants (11). In contrast, Warawa and Woods (23) had earlier reported that TTSS1 and TTSS2 were not involved in the virulence of *B. pseudomallei* in hamsters. Hence, we aimed to clarify the importance of *B. pseudomallei* TTSS1 for pathogenesis in mammals using the well-characterized BALB/c mouse melioidosis model.

Given the requirement of the ATPase as an energizer of the TTSS secretion process, we generated a *bpscN* deletion mutant in the expectation that loss of ATPase function would result in specific loss of TTSS1 function. The *bpscN* mutant showed a growth rate *in vitro* in LB medium equivalent to that of wild type bacteria (data not shown) but significantly reduced growth relative to that of the wild type *in vivo*. Furthermore, the *bpscN* mutant showed significantly reduced virulence in the BALB/c melioidosis model. All of the mice infected with the mutant strain remained healthy for the duration of the experiment ($P < 0.0001$). Thus, we conclude that *bpscN* plays an important role in the virulence of *B. pseudomallei* and that the reduction in virulence is not due to diminished growth rate of the mutant *per se*. On this basis, we determined the importance of *bpscN* for the intracellular survival of *B. pseudomallei*.

The intracellular survival and replication of *bpscN* mutant bacteria in RAW 264.7 macrophage-like cells were decreased significantly at 2 h, 4 h, and 6 h p.i. Indeed, at 6 h p.i., the reduction in intracellular survival was 46-fold. This finding suggests that effectors of TTSS1 are critical for intracellular survival and replication. Following complementation with an intact copy of *bpscN* in multicopy plasmid pBHR1, intracellular survival and replication were restored to approximately 50% of wild-type levels, confirming that *bpscN* is important for intracellular survival. The exact reason for the lack of complete restoration of intracellular replication is unknown, but it may be due to gene dosage effects resulting in the overproduction of the ATPase relative to other components of the TTSS1 apparatus. Next, we analyzed at what stage of macrophage infection the *bpscN* mutant strain was susceptible to increased killing. To determine the intracellular location of wild-type and mutant bacteria, we performed TEM, which showed that both wild-type and mutant bacteria were either free in the macrophage cytosol or encapsulated in single-membrane phagosomes. A high proportion of both mutant and wild-type bacteria was found within phagosomes at 2 h p.i., but this number decreased at 4 h and 6 h; there was a concomitant increase in bacteria free in the cytosol at these times. There was no statistically significant difference in the extent of phagosomal escape of mutant compared with wild-type bacteria over time. Analysis of the ability of both strains to form actin tails revealed that both wild-type and *bpscN* mutant bacteria were able to polymerize actin at 6 h p.i. (data not shown). This observation provides supporting evidence that both strains are able to escape from the phagosomes into the cytosol and subsequently initiate actin polymerization. Therefore, TTSS1 does not appear to be involved in phagosome escape, consistent with previous data showing that this role is mediated by TTSS3 effectors (2).

Given the similar levels of phagosomal escape observed for mutant and wild-type bacteria, we analyzed whether mutant bacteria may be killed more efficiently in the phagosomes. We have recently shown that LC3 recruitment to phagosomes stimulates bacterial killing (7). The *bpscN* mutant bacteria showed an increased level of colocalization with LC3, consistent with the mutant bacteria being more susceptible to LC3-associated phagocytosis and therefore having increased susceptibility to intracellular killing. These data are consistent with a role for TTSS1 in subverting normal phagosomal maturation, possibly by slowing the recruitment of LC3. As TEM analysis identified only a single bacterium enclosed within a multimembrane structure, the *bpscN* mutant is not susceptible to canonical autophagy (the encapsulation of cytoplasmic bacteria by a double-membrane autophagosome), in agreement with recent finding that TTSS3 mutants are not susceptible to autophagy (6).

In conclusion, we have shown that the TTSS1 gene *bpscN* is involved in the infectivity and pathogenicity of *B. pseudomallei* in mice. Our results differ from those reported by Warawa and Woods (23), who showed that the TTSS1 and TTSS2 clusters are not critically required for *B. pseudomallei* virulence in the hamster model. Thus, it appears that there may be differences in the gene complements required for virulence in these two animal models. Moreover, we cannot exclude the possibility that survival and replication may differ in other cell types, such as epithelial cells or fibroblasts. Given the importance of the *bpscN* gene in mouse infection, it is likely that secreted TTSS1 effectors are required for infection and virulence. Further research on elucidating the role of the TTSS1 effectors and potentially TTSS2 in pathogenesis is therefore warranted.

ACKNOWLEDGMENTS

This research was supported by the Australian Research Council and the National Health and Medical Research Council, Australia.

REFERENCES

1. **Borgherini, G., et al.** 2006. Melioidosis: an imported case from Madagascar. J. Travel Med. **13:**318–320.
2. **Cullinane, M., et al.** 2008. Stimulation of autophagy suppresses the intracellular survival of *Burkholderia pseudomallei* in mammalian cell lines. Autophagy **4:**744–753.
3. **Currie, B. J.** 2008. Advances and remaining uncertainties in the epidemiology of *Burkholderia pseudomallei* and melioidosis. Trans. R. Soc. Trop. Med. Hyg. **102:**225–227.
4. **Currie, B. J., D. A. B. Dance, and A. C. Cheng.** 2008. The global distribution of *Burkholderia pseudomallei* and melioidosis: an update. Trans. R. Soc. Trop. Med. Hyg. **102**(Suppl. 1):S1–S4.
5. **Galán, J. E., and A. Collmer.** 1999. Type III secretion machines: bacterial devices for protein delivery into host cells. Science **284:**1322–1328.
6. **Galyov, E. E., P. J. Brett, and D. DeShazer.** 2010. Molecular insights into *Burkholderia pseudomallei* and *Burkholderia mallei* Pathogenesis. Annu. Rev. Microbiol. **64:**495–517.
7. **Gong, L., et al.** 2011. The *Burkholderia pseudomallei* type III secretion system and BopA are required for evasion of LC3-associated phagocytosis. PLoS One **6:**e17852.
8. **Harper, M., A. D. Cox, F. St. Michael, I. W. Wilkie, J. D. Boyce, and B. Adler.** 2004. A heptosyltransferase mutant of *Pasteurella multocida* produces a truncated lipopolysaccharide structure and is attenuated in virulence. Infect. Immun. **72:**3436–3443.

9. **Holden, M. T. G., et al.** 2004. Genomic plasticity of the causative agent of melioidosis, *Burkholderia pseudomallei*. Proc. Natl. Acad. Sci. U. S. A. **101:** 14240–14245.
10. **Inglis, T. J., D. B. Rolim, and J. L. Rodriguez.** 2006. Clinical guideline for diagnosis and management of melioidosis. Rev. Inst. Med. Trop. Sao Paulo **48:**1–4.
11. **Lee, Y., Y. Chen, X. Ouyang, and Y.-H. Gan.** 2010. Identification of tomato plant as a novel host model for *Burkholderia pseudomallei*. BMC Microbiol. **10:**28.
12. **Lorenz, C., and D. Buttner.** 2009. Functional characterization of the type III secretion ATPase HrcN from the plant pathogen *Xanthomonas campestris* pv. vesicatoria. J. Bacteriol. **191:**1414–1428.
13. **Mason, C. A., and J. E. Bailey.** 1989. Effects of plasmid presence on growth and enzyme activity of *Escherichia coli* DH5α. Appl. Microbiol. Biotechnol. **32:**54–60.
14. **Milton, D., R. O'Toole, P. Horstedt, and H. Wolf-Watz.** 1996. Flagellin A is essential for the virulence of *Vibrio anguillarum*. J. Bacteriol. **178:**1310–1319.
15. **Milton, D. L., A. Norqvist, and H. Wolf-Watz.** 1992. Cloning of a metalloprotease gene involved in the virulence mechanism of *Vibrio anguillarum*. J. Bacteriol. **174:**7235–7244.
16. **Mueller, C. A., P. Broz, and G. R. Cornelis.** 2008. The type III secretion system tip complex and translocon. Mol. Microbiol. **68:**1085–1095.
17. **Rainbow, L., A. Hart, and C. Winstanley.** 2002. Distribution of type III secretion gene clusters in *Burkholderia pseudomallei*, *B. thailandensis* and *B. mallei*. J. Med. Microbiol. **51:**374–384.
18. **Short, J. M., J. M. Fernandez, J. A. Sorge, and W. D. Huse.** 1988. Lambda ZAP: a bacteriophage lambda expression vector with *in vivo* excision properties. Nucleic Acids Res. **16:**7583–7600.
19. **Simon, R., U. Priefer, and A. Pühler.** 1983. A broad host range mobilization system for *in vivo* genetic engineering: transposon mutagenesis in Gram negative bacteria. Nat. Biotech. **1:**784–791.
20. **Sun, G. W., and Y.-H. Gan.** 2010. Unraveling type III secretion systems in the highly versatile *Burkholderia pseudomallei*. Trends Microbiol. **18:**561–568.
21. **Sun, G. W., J. Lu, S. Pervaiz, W. P. Cao, and Y.-H. Gan.** 2005. Caspase-1 dependent macrophage death induced by *Burkholderia pseudomallei*. Cell. Microbiol. **7:**1447–1458.
22. **Szpirer, C. Y., M. Faelen, and M. Couturier.** 2001. Mobilization function of the pBHR1 plasmid, a derivative of the broad-host-range plasmid pBHR1. J. Bacteriol. **183:**2101–2110.
23. **Warawa, J., and D. E. Woods.** 2005. Type III secretion system cluster 3 is required for maximal virulence of *Burkholderia pseudomallei* in a hamster infection model. FEMS Microbiol. Lett. **242:**101–108.
24. **Wiersinga, W. J., T. van der Poll, N. White, N. Day, and S. Peacock.** 2006. Melioidosis: insights into the pathogenicity of *Burkholderia pseudomallei*. Nat. Rev. Microbiol. **4:**272–280.
25. **Winstanley, C., B. A. Hales, and C. A. Hart.** 1999. Evidence for the presence in *Burkholderia pseudomallei* of a type III secretion system-associated gene cluster. J. Med. Microbiol. **48:**649–656.

Editor: J. B. Bliska

CHAPTER SIX

DISCUSSION AND FUTURE DIRECTIONS

6.0 CONCLUSIONS AND FUTURE DIRECTIONS

6.1 INTRODUCTION

This project set out to use knowledge of virulence factors employed by other bacteria to circumvent their degradation, to identify possible *B. pseudomallei* virulence factors. As described in *Chapter 3* bioinformatics analysis identified five putative homologues of virulence factors for other bacteria, within the *B. pseudomallei* genome. In addition, two other ORFs within the *B. pseudomallei* genome were selected for analysis, as previous research suggested that the respective mutants had impaired functioning of the TTSS3. Of the seven ORFs studied, five were putative TTSS associated proteins. These ORFs were selected on the basis that the corresponding *B. pseudomallei* mutants having defective TTSS3 would be unable to escape from the phagosome, form actin tails or replicate within macrophage cell lines. It was hypothesised that these genes may play a role in assisting *B. pseudomallei* to evade autophagic degradation.

6.2 INSIGHTS FROM EXPRESSION OF *B. PSEUDOMALLEI* ORFs IN YEAST

The research presented in this thesis has identified that putative virulence factors encoded in the K96243 *B. pseudomallei* genome, may interact with the vesicle trafficking pathways, including autophagic pathways. The ORFs were initially characterised by expression in the yeast *S. cerevisiae*. For the purpose of this research, yeast was used as a “diagnostic” for the ORF-encoded proteins having an effect on vesicle traffic, for example formation of the autophagosome or its fusion with the

vacuole, or membrane interactions as evidenced by changes in vacuole morphology and numbers.

Expression of all seven ORFs in the yeast model produced a multiple vacuolar morphology, which may be attributed to the influence these putative effector proteins have on vacuole membrane fusion and fission. In addition, the expression of these ORFs had an apparent influence on organelle turnover during starvation conditions. There was an evident decrease in macroautophagic turnover, as illustrated by the reduced red cytosolic and mitochondrial fluorescence in the vacuole. However, the process of nucleophagy was not hindered, as evident through the red nuclear-derived fluorescence in the vacuole. Overall these result suggests that whilst the presence of the *B. pseudomallei* ORFs may influence the "vesicle-based" trafficking of cargo to the vacuole (as seen by the lack of cytoplasm and mitochondrial turnover), it does not affect a process (nucleophagy) where discrete vesicles are not formed and trafficked to the vacuole.

Given the influence of these putative effector ORFs when expressed in yeast, the decision was made to generate a deletion mutant for each ORF in the *B. pseudomallei* genome. Deletion mutants were successfully constructed for the *BPSS1532*, *BPSL0670* and *BPSS1394* ORFs. Using *in vivo* relative growth assays, the *BPSS1532* and *BPSL0670* mutants appeared to be partially attenuated for virulence in mice. In the same experiment, the *BPSS1394* mutant exhibited attenuation for virulence with *in vitro* experiments showing a reduced ability to survive and replicate in RAW 264.7 cells. In an attempt to identify the method by which the bacteria are degraded, TEM

was performed. Data from the images acquired, indicated the mutant and wild-type bacteria were confined in single membrane structures characteristic of LC3-associated phagocytosis (LAP) (see *Chapter 6.3*), rather than double membrane structures typical of canonical autophagy.

6.3 BACTERIA EVADING AUTOPHAGY

Chapter 1.8 reviews the role for autophagy as a cellular homeostatic mechanism for the removal of obsolete or damaged organelles. In recent years, a significant focus of the autophagy field has been its role in immunity, particularly, the degradation of invading bacteria, viruses, fungi and parasites (Orvedahl and Levine, 2008), termed xenophagy. The degradation of intracellular pathogens serves a dual purpose in liberating metabolites that may have been utilised during pathogen infection (Orvedahl and Levine, 2008).

Canonical phagocytosis dictates that invading pathogens encapsulated in a phagosome are trafficked to the lysosome for degradation. Some pathogens such as *S. aureus, P. gingivalis* and *L. pneumophilia* have devised ways to manipulate the membrane trafficking pathways in order to delay their degradation or increase the longevity of their replicative niches (Ogawa et al., 2011). *Figure 6.1* illustrates the mechanisms by which pathogens may attempt to circumvent degradation by either escaping from the host phagosome, preventing acquisition of autophagic markers or stalling the auto/phagolysosome maturation. *S. flexneri* employs virulence factors to escape the host phagosome and continue its infectivity (Ogawa et al., 2005). In the case of

C. burnetii, the bacterium reside in an acidic vacuole that gradually acquires the autophagic marker LC3 (Colombo et al., 2006). The *C. burnetii*-containing vacuole interacts with autophagosomes to delay the arrival of hydrolytic enzymes (Lerena et al., 2010) by delaying fusion with the lysosome (Deretic and Levine, 2009). Some bacteria, such as *S. pyogenes* and *M. tuberculosis*, after escaping phagosomes can be effectively cleared by autophagy (Nakagawa et al., 2004). Similar to *S. flexneri*, *B. pseudomallei* employs virulence factors such as BopA (Cullinane et al., 2008) to escape from the phagosome into host cytosol, thereby maintaining the infection.

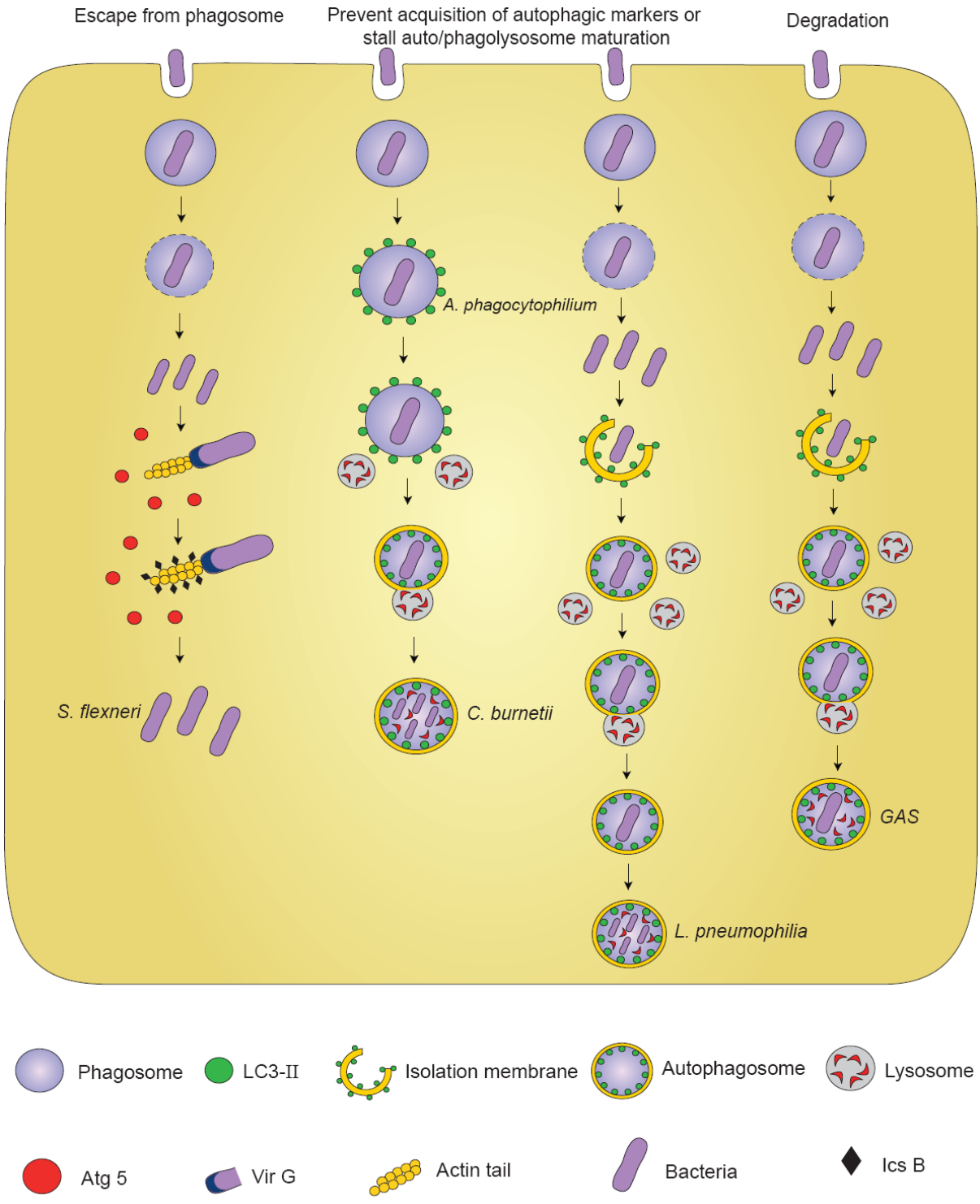

Figure 6.1: How pathogens interact with autophagy (D'Cruze and Devenish, 2011). Intracellular pathogens may escape into the cytosol and continue to spread, or suppress phagosomal maturation, to reside in their phagosome. Alternatively, pathogens may succumb to degradation.

6.4 LC3-ASSOCIATED PHAGOCYTOSIS

Since the commencement of my studies, a new bacterial degradation pathway has emerged which is distinct from canonical macroautophagy, namely LC3-associated phagocytosis (LAP). The LAP degradation pathway differs from canonical autophagy, in the sense that the bacterium may remain within a phagosome to which are recruited autophagy proteins such as LC3. The bacterium can then be killed within a single-membrane structure (Sanjuan et al., 2009). Research carried out at Monash University has identified that *B. pseudomallei* can be degraded by the LAP pathway. While bacterium can co-localise with GFP-LC3, potentially indicative of being within an autophagosome, EM analysis revealed that intracellular *B. pseudomallei* either reside in a single membrane compartment (phagosomes; *Figure 6.2*) or are free in the cytosol (Gong et al., 2011). *Figure 6.3* summaries the pathways *B. pseudomallei* may follow, following infection into macrophages. Post infection, the bacterium may escape from the phagosome to enter the host cytosol. At this point, the bacterium may continue to be infective residing in the host cytoplasm, or potentially be sequestered within an autophagosome (A) to be degraded through the action of the canonical autophagic pathway. Alternatively, the bacterium-containing phagosome may be encapsulated in an autophagosome and the bacterium degraded by the canonical autophagic pathway (B). The LAP pathway (C) illustrates the recruitment of LC3 onto the membrane of bacteria-containing phagosomes then subsequent fusion with lysosomes and degradation of bacteria. Phagosomes containing bacteria may directly fuse with lysosomes to give rise to canonical phagolysosomal degradation (D).

TEM data acquired at Monash University (Gong et al., 2011) have identified only very rare instances of *B. pseudomallei* encapsulated within multiple membrane structures following infection in RAW 264.7 cells. Hence the current view is that *B. pseudomallei* cells that are unable to escape from the phagosome will most likely be subjected to LAP rather than canonical autophagy. However, since 75% of wild-type bacteria escape the phagosomes (at 6 h p.i) (D'Cruze et al., 2011) and evade the LAP, a significant question remains to be answered. Why are the bacteria that escape to the cytosol not targeted and degraded by canonical autophagy?

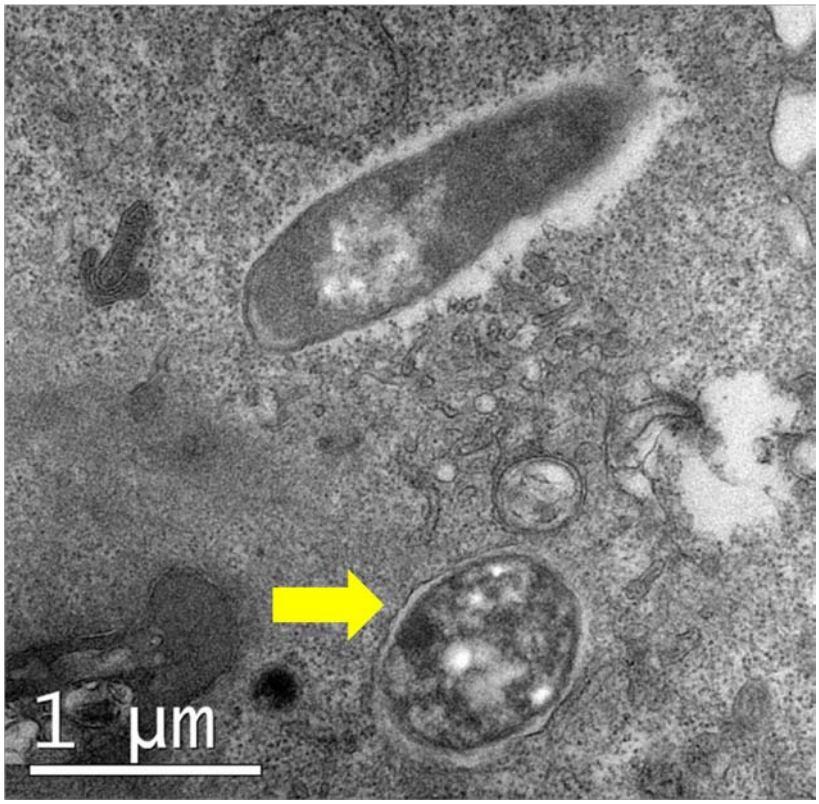

Figure 6.2: Transmission electron micrograph of RAW264.7 cells at 2 h p.i. with *B. pseudomallei* (magnification x600). Intracellular bacteria are observed almost exclusively within single-membrane compartments (yellow arrow) and not double-membrane autophagic compartments (D'Cruze, unpublished).

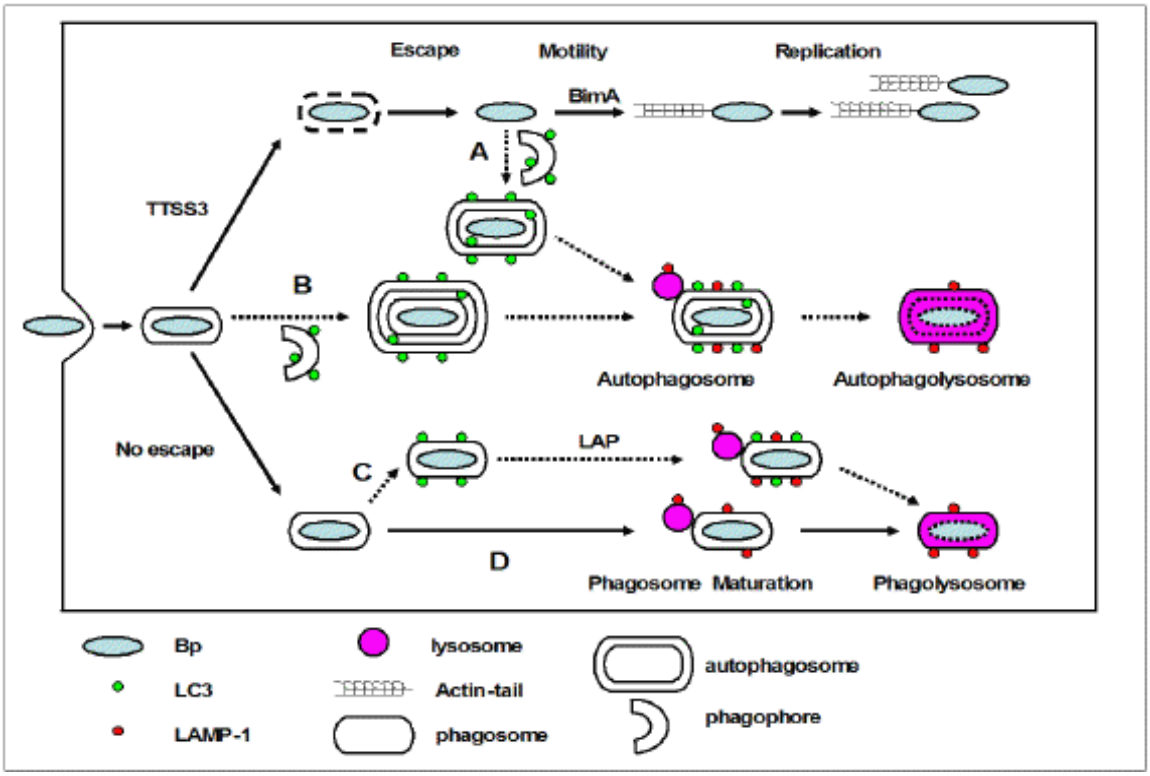

Figure 6.3: *B. pseudomallei* clearance whereby cytosolic *B. pseudomallei* can become encapsulated by the phagophore, subsequently leading to lysosomal fusion (A), bacteria encapsulated in the phagosome becomes enveloped by the phagophore to induce lysosomal degradation (B), membrane-bound bacteria recruits LC3 for subsequent fusion with the lysosome (C), or the membrane-bound bacteria may directly converge with lysosome to undergo phagolysosome (D) (Gong et al., 2011).

6.5 UBIQUITINATION

Another emerging paradigm in autophagic targeting of intracellular bacteria is ubiquitination-mediated autophagy. Following internalisation into host cells, some bacteria that either escape into the cytosol or damage their endosomal membrane may potentially be ubiquitinated and targeted for autophagy. The current model (as illustrated in *Figure 6.4*), whilst lacking biochemical evidence, hypothesises the ubiquitin (Ub) to be deposited directly onto the bacterium, and protein adaptors such as p62 or NDP52, to simultaneously bind to both the Ub and LC3, thereby linking it to the autophagic membranes (Fujita and Yoshimori, 2011).

Recent studies have described *S. pyogenes*, *L. monocytogenes* and *M. marinum* as co-localising with poly-Ub to eventually result in autophagic degradation. A second scenario is observed during infection of HeLa cells by *S. flexneri*, which results in the internalised bacterium being encapsulated by the host membrane vacuole. In order to gain access to the host cytosol, the bacterium ruptures the surrounding vacuolar membrane. The vacuolar remnants induce an inflammatory response and can be observed to co-localise with inflammasome components and caspase-1 (Dupont et al., 2009). These authors provided evidence that proteins associated with the membrane remnants undergo polyubiquitination, thereby targeting them to autophagy and subsequently reducing the inflammation response and enhancing bacterial survival.

Some bacteria such as *L. monocytogenes* and *S. enterica* serovar Typhimurium, have evolved mechanisms to benefit from their interaction with the ubiquitin system. *L. monocytogenes* employs the bacterial toxin Listeriolysin O (LLO) to escape from

the phagosome into the host cytoplasm. The host immune response is to eliminate the LLO by subjecting the toxin to ubiquitination and proteolysis. However, down regulation of LLO is advantageous for some strains that tend to either over express LLO or produce LLO with mutations, as over production of the toxin by some strains increases the toxicity of the host cell and potentially produces virulence defects (Steele-Mortimer, 2011). Preliminary data suggest that *S. Typhimurium* encodes two effectors, SseL and AvrA, with deubiquitinase activity to down regulate the immune signalling thereby giving rise to an anti-inflammatory effect, and thus promoting bacterial survival (Steele-Mortimer, 2011). AvrA which is translocated by TTSS1 shares homology with *Y. enterocolitica* YopJ, an effector that negatively regulates NFκB and MAPK signalling. In this manner, AvrA acts to deubiquitinate IκBα and β-catenin to produce an anti-inflammatory effect (Steele-Mortimer, 2011).

Deubiquitinases work to reverse the ubiquitination process, thereby potentially interfering with signalling intermediates, thus promoting intracellular bacterial survival. The *tssM* deubiquitinase of *B. mallei* shares 100% identity to the *tssM* gene of *B. pseudomallei* (Tan et al., 2010). The *tssM* deubiquitinase encoded by *B. pseudomallei* T6SS gene cluster 1 (Burtnick et al., 2011) was reported to modulate the host innate immune response (Tan et al., 2010). Mice infected with the *tssM* mutant provoked a hyper inflammatory host response resulting in faster death (Tan et al., 2010). Current research at Monash University is also focusing on the cellular response to a *B. pseudomallei tssM* mutant. It is hypothesised that the deubiquitinase activity of TssM may facilitate *B. pseudomallei* survival by assisting the bacterium to avoid canonical autophagy (Gong et al., 2011).

The *B. pseudomallei* K96243 genome encodes six T6SS gene clusters; TssM is encoded by T6SS gene cluster 1 (Burtnick et al., 2011). T6SS are also encoded in the genomes of *V. cholerae, P. aeruginosa, E. coli* and *B. mallei* (Bingle et al., 2008). Despite being first described in 2006 (Pukatzki et al., 2006) the function of T6SS in infection remains largely uncharacterised and clearly warrants further investigation.

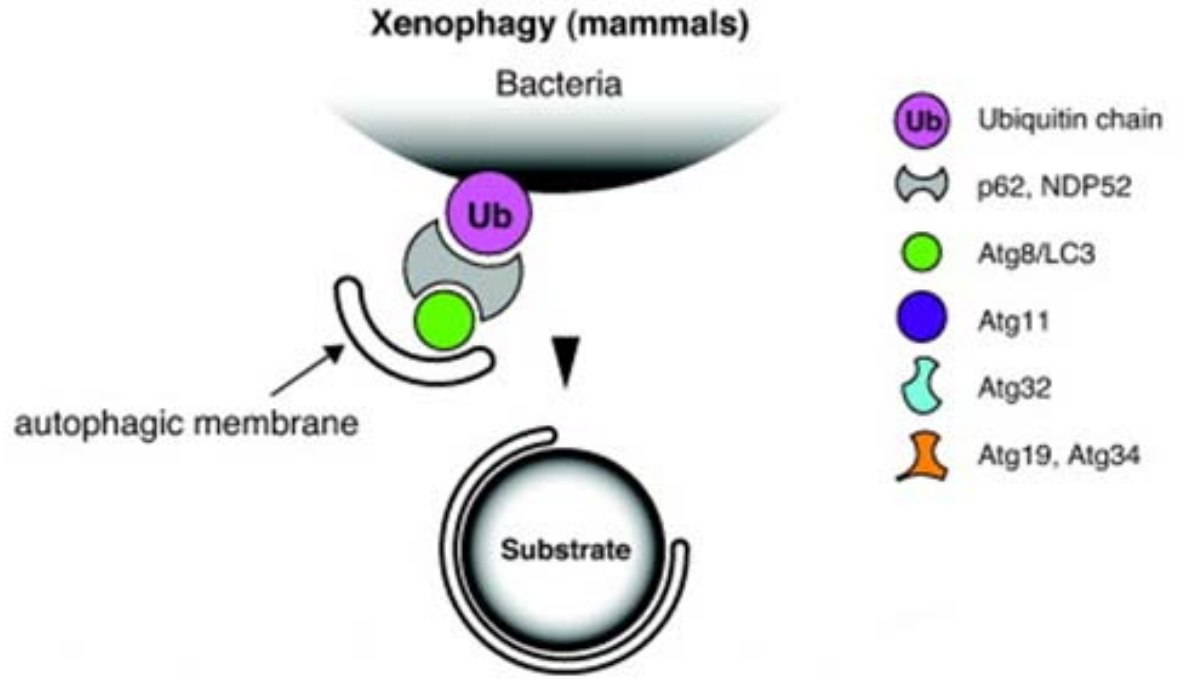

Figure 6.4: Diagrammatic representation of ubiquitination-mediated autophagy (adapted from Fujita and Yoshimori, 2011). Following the ubiquitination of bacteria, protein adaptors such as p62 or NDP52, simultaneously bind to both the Ub and LC3, thereby linking it to the autophagic membranes. Consequently, the bacterium undergoes degradation.

6.6 GENETICALLY MANIPULATING *B. PSEUDOMALLEI*

The discovery of novel vaccines and therapeutic targets is dependent on the ability to manipulate bacterial genomes (Mima et al., 2011). Molecular manipulation of the *B. pseudomallei* genome is often arduous for reasons including the GC content of the genome and the consequent difficulty in PCR amplification of genomic fragments, and the need to introduce foreign DNA by conjugation, as direct transformation of the *B. pseudomallei* K96243 strain is presently not achievable. Kang et al. (2011) have devised a system which they assert, will more readily produce gene inactivation in the genome of some *B. pseudomallei* strains. The system employs phage λ-Red proteins to transform DNA fragments into the naturally transformable *B. pseudomallei* 1026b strain (Kang et al., 2011). However, this group was unable to transform the non-naturally transformable *B. pseudomallei* K96243 strain or *B. mallei* ATCC2334 strain. Research carried out at Monash University uses the K96243 strain, principally because of its fully sequenced and annotated genome.

In the future, should it prove possible to optimise the electrotransformation protocol of Kang et al., to accommodate transformations of the K96243 genome, this system can potentially be utilised to construct the other *B. pseudomallei* mutants, which this project initially aimed to achieve. In addition to generating mutants in the *BPSS1531, BPSS1529, BPSS1539* and *BPSS0670* genes, future application of the phage λ-Red protein system could be targeted to generating double and triple mutants of the *BpscN* in clusters 2 and 3 of the TTSS, for functional characterisation. Considering the importance of the TTSS1, future experiments can therefore attempt to more readily construct mutants of other ORFs encoded in TTSS clusters 1 and 2.

6.7 CONCLUDING REMARKS

The research presented in this thesis establishes a strong foundation upon which future projects can build. Future *B. pseudomallei* research at Monash University will continue to focus on the ways in which *B. pseudomallei* may be eliminated from infected host cells, thereby facilitating possible therapy treatments for melioidosis. Such knowledge will further assist in reducing the mortality rate of melioidosis.

APPENDIX

Autophagy as a Defence Mechanism Against Bacterial Pathogens

Tanya D'Cruze and Rodney Devenish*

Department of Biochemistry and Molecular Biology, and ARC Centre of Excellence for Structural and Functional Microbial Genomics, Monash University, Clayton, VIC 3800

**Corresponding author: rod.devenish@monash.edu*

Autophagy occurs in all eukaryotic cells and is important in the context of cellular homeostasis for the removal of damaged or non-functional organelles and the destruction of certain long-lived proteins and other macromolecules (1). More recently, autophagy has become increasingly viewed as an important component of the eukaryotic innate immune system (1,2). The degradation of invading bacteria, viruses, fungi and parasites by autophagy in mammalian cells has been termed xenophagy and serves the purpose of not only eliminating the intracellular pathogen, but also liberating metabolites that may have been utilised during pathogen infection, thus promoting cell survival (3). This review will consider autophagy as a defence mechanism against bacterial pathogens and briefly survey the mechanisms employed by bacteria to circumvent autophagic degradation, with a particular focus on the evasion of autophagy.

After gaining entry to the cell, intracellular pathogens attempt to escape from phagosomes or endosomes into the cytosol where they endeavour to continue the infection cycle unhindered by host cell protective mechanisms. Bacterial recognition resulting from either the cytosolic location, the secretion of bacterial products or phagosomal membrane damage can induce autophagy (4,5,6). In this context, induction of autophagy results in the clearance of some bacterial pathogens (**Table 1**). Other bacteria are able to manipulate autophagy for their own benefit and appear to effectively replicate within autophagosome-like vesicles, while others are able to evade autophagy (**Table 1**). However, within and across these groupings there are many 'variations on a theme' and in some cases the autophagic response may vary depending on the cell type infected. We next briefly survey the three groupings of bacterial pathogen interactions with autophagy.

Table 1. Microbial interaction with autophagy. *Adapted from (5)*

Bacteria	Interaction with host autophagy	Biological factors and outcomes
Streptococcus pyogenes (GAS)	Induction	Bacterial clearance
Salmonella typhimurium	Induction	Bacterial clearance
Rickettsia conorii	Induction	Bacterial clearance
Mycobacterium tuberculosis	Induction	IFNγ treatment enhances clearance
Vibrio cholerae (exotoxin)	Induction	Limits cytotoxicity, enhances survival
Legionella pneumophilia	Manipulation	Autophagosome maturation delayed
Anaplasma phagocytophilium	Manipulation	Autophagy harnessed for replication
Brucella abortus	Manipulation	Autophagy harnessed for replication
Coxiella burnetii	Manipulation	Autophagosome maturation delayed
Listeria monocytogenes	Evasion	Dependent on ActA, PLC
Shigella flexneri	Evasion	Bacterial escape, dependent on IcsB
Burkholderia pseudomallei	Evasion	Bacterial escape

Bacterial Pathogen Interactions with Autophagy

Group A Streptococcus (GAS) and *Mycobacterium tuberculosis* are examples of bacterial pathogens that can be cleared by autophagy. During the early stages of *GAS* infection, the bacterium secretes a pore-forming cytolysin to disrupt the surrounding phagosome and gain access to the host cytosol. Once in the cytosol, the bacterium can be sequestered into autophagosomes and subsequently undergo degradation (7) (**Fig. 1**). *M. tuberculosis* persists within phagosomal compartments by interfering with phagosome maturation and reducing acidification in mycobacterium-containing vacuoles (MCVs) (8). Subsequently, MCVs can be sequestered by autophagosome-like membranes formed by the fusion of autophagosomes with MCVs; lysosomal degradation of the sequestered bacteria then ensues (9).

Legionella pneumophilia, Coxiella burnetii and *Anaplasma phagocytophilium* manipulate autophagy to their own advantage. Following ingestion by macrophages, *L. pneumophilia* resides in vacuoles, rather than in phagosomes. These compartments gradually acquire acidic lysosomal characteristics, but continue to remain a favourable environment for bacterial replication (**Fig. 1**). It has been proposed that *L. pneumophilia* interacts with autophagy in order to delay the maturation of the vacuole in which it resides, thereby facilitating its later survival in the harsher lysosomal environment (6). Upon infection by phagocytosis, *C. burnetti* is confined to an acidic vacuole that eventually acquires the autophagic marker LC3. The infective non-replicative bacteria, termed small cell variant (SCV), differentiates into the replicative large cell variant (LCV) when exposed to an autolysosomal environment. This nutrient-rich environment is believed to be conducive for bacterial replication (10). This pathogen actively interacts with autophagosomes early after infection to delay the arrival of hydrolytic enzymes

facilitating vacuole development (11) (**Fig. 1**). After entry into host cells, *A. phagocytophilium* is diverted from the endosomal pathway and replicates in a membrane-bound compartment having features of early autophagosomes (**Fig. 1**). Stimulation of autophagy by use of the pharmacological inducer rapamycin favours infection. Thus autophagy is subverted to establish bacteria in an early autophagosome-like compartment segregated from lysosomes in order to facilitate their proliferation (12).

Once in the cytosol, *Listeria monocytogenes* (13) and *Shigella flexneri* (14) employ known virulence factors, ActA and IcsB respectively, to evade autophagy. *L. monocytogenes* can escape from phagosomes into the cytosol through the combined action of a pore-forming toxin listeriolysin O (LLO) and a phospholipase C. Once within the cytosol, bacteria mediate actin polymerisation and intracellular motility via the bacterial protein ActA. Evasion of autophagy is critically dependent on ActA-mediated, actin-based motility as well as the expression of other factors. Those bacteria that produce insufficient LLO to affect escape from the phagosome can be targeted by autophagy, resulting in the formation of LC3+ single-membrane 'spacious Listeria-containing phagosomes' (SLAPs) (15). However, these compartments do not facilitate degradation of bacteria, but rather their replication, thereby enabling the infection to persist.

S. flexneri, once escaped from the phagosome, also induces actin polymerisation at one pole of the bacterial cell. Actin polymerisation is mediated by the bacterial VirG (IcsA) protein, but VirG is specifically targeted by the autophagic membrane protein Atg5 and induces autophagy (14). However, the bacteria secrete an effector protein, IcsB, which binds to VirG and competitively inhibits the interaction of VirG with Atg5, thus abrogating the induction of autophagy (**Fig. 1**). *S. flexneri icsB* mutants are significantly more susceptible to clearance by autophagy. Therefore, *S. flexneri* actively avoids the induction of autophagy and enhances its own intracellular survival by the secretion of IcsB (14).

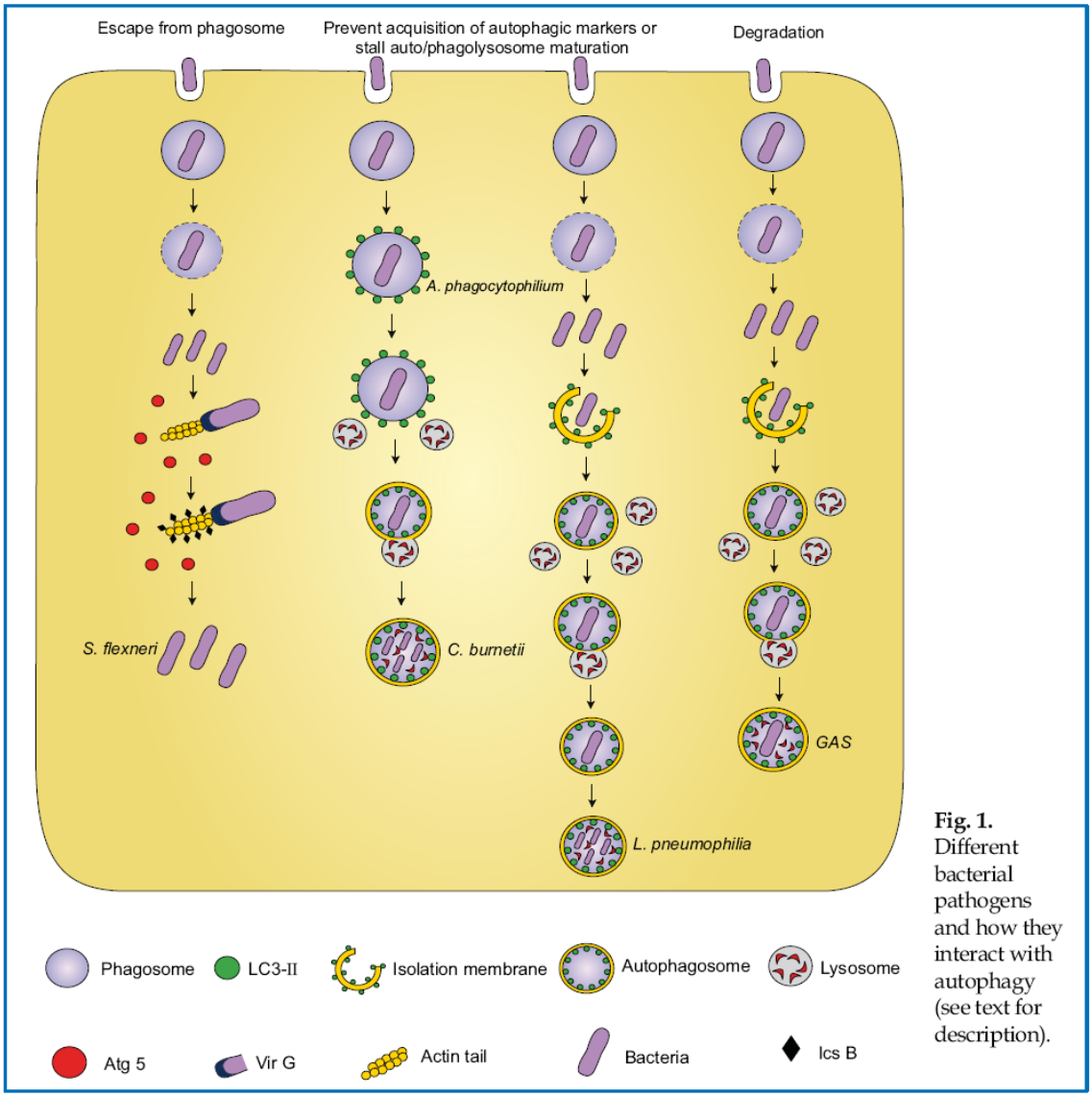

Fig. 1. Different bacterial pathogens and how they interact with autophagy (see text for description).

Burkholderia pseudomallei Evades Autophagy by a Different Mechanism

Burkholderia pseudomallei is the causative agent of melioidosis, a serious invasive disease of humans and animals, with a very high mortality rate (16), that is endemic in tropical areas, including northern Australia. This pathogen can invade and survive within phagocytic cells. Within 15 minutes of internalisation by phagocytosis, *B. pseudomallei* escapes into the cytoplasm by a process that is critically dependent on a type III secretion system (T3SS) designated T3SS3. The T3SS3 delivers proteins secreted directly from the bacterial cell into the eukaryotic 'host' cell undergoing infection and that help the bacteria establish the infection. *B. pseudomallei* mutants having defective T3SS3 are unable to escape from phagosomes, form actin tails or replicate within macrophage cell lines (17). In investigating the susceptibility of *B. pseudomallei* to autophagy, we have shown that, in response to infection of the macrophage cell line RAW 264.7, only a subset of bacteria co-localised with the autophagy marker protein LC3 (18). When cells were treated with rapamycin, bacterial co-localisation with LC3 was significantly increased and bacterial survival reduced. Thus, autophagy was implicated as part of the host defence system against *B. pseudomallei* infection, although the mechanism by which most invading bacteria avoided host autophagic attack remained obscure. An ongoing collaborative program of research conducted within the ARC Centre of Excellence in Structural and Functional Microbial Genomics at Monash University is directed towards understanding the mechanism by which *B. pseudomallei* evades host cell autophagy.

Once within the cytoplasm, *B. pseudomallei* stimulates actin polymerisation and the formation of an actin 'tail' at one pole of the bacterial cell, facilitating intracellular motility. This actin-based motility is mediated by BimA, a T3SS3 effector protein that has very low similarity to *S. flexneri* VigG and lacks the VirG-binding domain targeted by Atg5 (14). Moreover, while the *B. pseudomallei* BopA protein shows 23% amino acid identity to *S. flexneri* IcsB, our data suggest that *B. pseudomallei* proteins do not interact in a manner comparable to their *S. flexneri* counterparts (Cullinane, M., Allwood, E., Prescott, M., Devenish, R.J., Adler, B., and Boyce, J.D., unpublished data). Thus, we propose that *B. pseudomallei* evades autophagy by an alternative mechanism to one based on BimA functioning in a manner equivalent to *S. flexneri* VirG. In support of this proposal is the observation that a *B. pseudomallei bimA* mutant does not exhibit increased susceptibility to autophagy (Cullinane, M., Allwood, E., Prescott, M., Devenish, R.J., Adler, B., and Boyce, J.D., unpublished data). Nevertheless, BopA is involved in modulating the host cell response to infection, as *bopA* mutant bacteria showed increased co-localisation with LC3 and reduced intracellular survival (18).

Recently it was shown that LC3, normally considered a marker of the autophagsome, can be recruited directly to bacteria-containing phagosomes via a process designated LC3-associated phagocytosis (LAP) (19). This finding led us to assess the nature of the compartment in which intracellular *B. pseudomallei* is sequestered. Through an extensive analysis of electron microscopic images of infected cells, we demonstrated that intracellular bacteria are either free in the cytosol or sequestered in single-membrane phagosomes (**Fig. 2**), but only very rarely contained in double-membrane autophagosomes, suggesting that LC3 is recruited to *B. pseudomallei*-containing phagosomes (20). In addition, *B. pseudomallei* mutants defective in phagosome escape show increased LC3 co-localisation. The same mutant bacteria also showed decreased intracellular survival (20), so we determined bacteria co-localisation with LC3 and the lysosome marker LAMP-1, which serves as a measure of the maturation of bacteria-containing LC3+ phagosomes by fusion with lysosomes. The percentage of bacteria co-localised with both markers was significantly higher for the mutants, suggesting that LC3 recruitment is associated with enhanced levels of phagolysosome maturation.

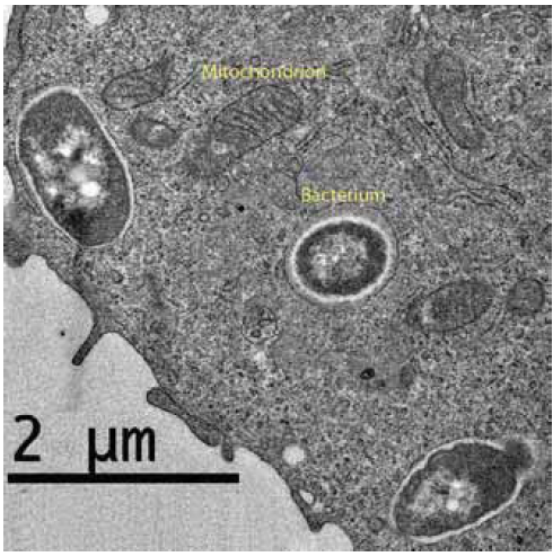

Fig. 2. Transmission electron micrograph of a RAW264.7 cell at 6 h post-infection with *Burkholderia pseudomallei* strain K96243 (magnification x600). Intracellular bacteria are observed within single-membrane compartments (labelled Bacterium), and not double-membrane autophagic compartments. Within the cell, typical organelles such as a mitochondrion can be identified. The scale bar is indicated.

Collectively, our data support the hypothesis that LC3 recruitment to *B. pseudomallei*-containing phagosomes stimulates fusion of phagosomes with lysosomes, leading to killing of the bacteria contained within. Nevertheless, most bacteria can escape from phagosomes and once free in the cytoplasm are rarely targeted by autophagosomes. The means by which *B. pseudomallei* evades autophagy remains unknown. Current studies focus on whether ubiquitin signalling is involved, and on the contribution of other TTSS virulence factors, in the evasion of autophagy.

References

1. 1. Ravikumar, B., Sarkar, S., Davies, J.E., *et al.* (2010) *Physiol. Rev.* **90**, 1383-1435

References continued on page 16

References continued from page 13

2. Schmid, D., and Munz, C. (2007) *Immunity* **27**, 11-21
3. Orvedahl, A., and Levine, B. (2009) *Cell Death Differ.* **16**, 57-69
4. Deretic, V., and Levine, B. (2009) *Cell Host Microbe* **5**, 527-549
5. Hussey, S., Travassos, L.H., and Jones, N.L. (2009) *Semin. Immunol.* **21**, 233-241
6. Lerena, M.C., Vázquez, C.L., and Colombo, M.I. (2010) *Cell Microbiol.* **12**, 10-18
7. Nakagawa, I., Amano, A., Mizushima, N., Yamamoto, A., Yamaguchi, H., Kamimoto, T., Nara, A., Funao, J., Nakata, M., Tsuda, K., Hamada, S., and Yoshimori, T. (2004) *Science* **306**, 1037-1040
8. Vergne, I., Chua, J., Lee, H.H., Lucas, M., Belisle, J., and Deretic, V. (2005) *Proc. Natl Acad. Sci. USA* **102**, 4033-4038
9. Gutierrez, M.G., Munafó, D.B., Berón, W., and Colombo, M.I. (2004) *J. Cell Sci.* **117**, 2687-2697
10. Colombo, M.I., Gutierrez, M.G., and Romano, P.S. (2006) *Autophagy* **2**, 162-164
11. Romano, P.S., Gutierrez, M.G., Berón, W., Rabinovitch, M., and Colombo, M.I. (2007) *Cell Microbiol.* **9**, 891-909
12. Niu, H., Yamaguchi, M., and Rikihisa, Y. (2008) *Cell Microbiol.* **10**, 593-605
13. Meyer-Morse, N., Robbins, J.R., Rae, C.S., Mochegova, S.N., Swanson, M.S., Zhao, Z., Virgin, H.W., and Portnoy, D. (2010) *PLoS One* **5**, e8610
14. Ogawa, M., Yoshimori, T., Suzuki, T., Sagara, H., Mizushima, N., and Sasakawa, C. (2005) *Science* **307**, 727-731
15. Birmingham, C.L., Canadien, V., Kaniuk, N.A., Steinberg, B.E., Higgins, D.E., and Brumell, J.H. (2008) *Nature* **451**, 350-354
16. Wiersinga, W.J., van der Poll, T., White, N.J., Day, N.P., and Peacock, S.J. (2006) *Nat. Rev. Microbiol.* **4**, 272-282
17. Stevens, M.P., Wood, M.W., Taylor, L.A., Monaghan, P., Hawes, P., Jones, P.W., Wallis, T.S., and Galyov, E.E. (2002) *Mol. Microbiol.* **46**, 649-659
18. Cullinane, M., Gong, L., Li, X., Lazar-Adler, N., Tra, T., Wolvetang, E., Prescott, M., Boyce, J.D., Devenish, R.J., and Adler, B. (2008) *Autophagy* **4**, 744-753
19. Sanjuan, M.A., Milasta, S., and Green, D.R. (2009) *Immunol. Rev.* **227**, 203-220
20. Gong, L., Cullinane, M., Treerat, P., Ramm, G., Prescott, M., Adler, B., Boyce, J.D., and Devenish, R.J. (2011) *PLoS One* **6**, e17852

***Australian Biochemist* is online!**
Showcase on Research
Great Expectations
Technical Features
Students' Page
Coverage of all issues from 2000 to the present
http://www.asbmb.org.au/magazine.html

BIBLIOGRAPHY

AMANO, A., NAKAGAWA, I. & YOSHIMORI, T. 2006. Autophagy in Innate Immunity against Intracellular Bacteria. *J. Biochem.,* 140**,** 161-166.

APISARNTHANARAK, A., APISARNTHANARAK, P. & MUNDY, L. M. 2006. Computed Tomography Characteristics of *Burkholderia pseudomallei* Liver Abscess. *Clin. Infect. Dis.,* 42**,** 989-993.

ARJCHAROEN, S., WIKRAIPHAT, C., PUDLA, M., LIMPOSUWAN, K., WOODS, D., SIRISINHA, S. & UTAISINCHAROEN, P. 2007. Fate of a *Burkholderia pseudomallei* Lipopolysaccharide Mutant in the Mouse Macrophage cell line RAW 264.7: Possible Role for the O-antigenic polysaccharide moiety of Lipopolysaccharide in Internalization and Intracellular Survival. *Infect. Immun.,* 75**,** 4298-4304.

BAARS, T. L., PETRI, S., PETERS, C. & MAYER, A. 2007. Role of the V-ATPase in Regulation of the Vacuolar Fission Fusion Equilibrium. *Mol. Biol. Cell,* 18**,** 3873-3882.

BALRAJ, P., RENESTO, P. & RAOULT, D. 2009. Advances in *Rickettsia* Pathogenicity. *Ann. N. Y. Acad. Sci.,* 1166**,** 94-105.

BINGLE, L. E. H., BAILEY, C. M. & PALLEN, M. J. 2008. Type VI secretion: A Beginner's Guide. *Curr. Opin. Microbiol.,* 11**,** 3-8.

BIRMINGHAM, C. L., SMITH, A. C., BAKOWSKI, M. A., YOSHIMORI, T. & BRUMELL, J. H. 2006. Autophagy Controls *Salmonella* Infection in Response to Damage to the *Salmonella*-containing Vacuole. *J. Biol. Chem.,* 281**,** 11374-11383.

BLOCKER, A. J., DEANE, J. E., VEENENDAAL, A. K. J., ROVERSI, P., JULIE L. HODGKINSON, JOHNSON, S. & LEA, S. M. 2008. What's the Point of the Type III Secretion System Needle? *PNAS,* 105**,** 6507-6513.

BOWERS, K. & STEVENS, T. H. 2005. Protein Transport from the Late Golgi to the Vacuole in the Yeast *Saccharomyces cerevisiae*. *Biochim. Biophys. Acta,* 1744**,** 438-454.

BRUNO, V. M., HANNEMANN, S., LARA-TEJERO, M., FLAVELL, R. A., KLEINSTEIN, S. H. & GALAN, J. E. 2009. *Salmonella Typhimurium* Type III Secretion Effectors Stimulate Innate Immune Responses in Cultured Epithelial Cells. *Plos pathog.,* 5**,** 1-11.

BURTNICK, M. N., BRETT, P. J., HARDING, S. V., NGUGI, S. A., RIBOT, W. J., CHANTRATITA, N., SCORPIO, A., MILNE, T. S., DEAN, R. E., FRITZ, D. L., PEACOCK, S. J., PRIOR, J. L., ATKINS, T. P. & DESHAZER, D. 2011. The Cluster 1 Type VI Secretion System Is a Major Virulence Determinant in *Burkholderia pseudomallei*. *Infect. Immun.,* 79**,** 1512-1525.

BURTNICK, M. N., BRETT, P. J., NAIR, V., WARAWA, J. M., WOODS, D. E. & GHERARDINI, F. 2008. *Burkholderia pseudomallei* Type III Secretion System Mutants Exhibit Delayed Vacuolar Escape Phenotypes in RAW 264.7 Murine Macrophages. *Infect. Immun.,* 76**,** 2991-3000.

CHECROUN, C., WEHRLY, T. D., FISCHER, E. R., HAYES, S. F. & CELLI, J. 2006. Autophagy-Mediated Reentry of *Francisella tularensis* into the Endocytic Compartment after Cytoplasmic Replication. *PNAS,* 103**,** 14578-14583.

CHEN, Y., WONG, J., SUN, G. W., LIU, Y., TAN, G.-Y. G. & GAN, Y.-H. 2011. Regulation of Type VI Secretion System during *Burkholderia pseudomallei* Infection. *Infect. Immun.,* 79**,** 3064-3073.

COLOMBO, M. I., GUTIERREZ, M. G. & ROMANO, P. S. 2006. The Two Faces of Autophagy. *Autophagy,* 2**,** 162-164.
COLUMBO, M. 2005. Pathogens and Autophagy: Subverting to Survive. *Cell Death Differ.,* 12**,** 1481-1483.
CONIBEAR, E. & STEVENS, T. H. 1997. Multiple Sorting Pathways Between the Late Golgi and the Vacuole in Yeast. *Biochim. Biophys. Acta,* 1404**,** 211-230.
CULLINANE, M., GONG, L., LI, X., LAZAR-ADLER, N., TRA, T., WOLVETANG, E., PRESCOTT, M., BOYCE, J. D., DEVENISH, R. J. & ADLER, B. 2008. Stimulation of Autophagy Suppresses the Intracellular Survival of *Burkholderia pseudomallei* in Mammalian Cell Lines. *Autophagy,* 4**,** 744-753.
CURRIE, B. J., DANCE, D. A. B. & CHENG, A. C. 2008. The Global Distribution of *Burkholderia pseudomallei* and Melioidosis: An Update. *Trans. Royal. Soc. Trop. Med. Hyg.,* 102**,** S1-S4.
CURRIE, B. J., WARD, L. & CHENG, A. C. 2010. The Epidemiology and Clinical Spectrum of Melioidosis: 540 Cases from the 20 Year Darwin Prospective Study. *PLoS Negl. Trop. Dis.,* 4**,** e900.
D'CRUZE, T. & DEVENISH, R. J. 2011. Autophagy as a Defence Mechanism against Bacterial Pathogens. *Australian Biochemist,* 42**,** 11-13.
D'CRUZE, T., GONG, L., TREERAT, P., RAMM, G., BOYCE, J. D., PRESCOTT, M., ADLER, B. & DEVENISH, R. J. 2011. Role for the *Burkholderia pseudomallei* Type Three Secretion System Cluster 1 *bpscN* Gene in Virulence. *Infect. Immun.,* 79**,** 3659-3664.
DECKER, B. L. & WICKNER, W. T. 2006. Enolase Activates Homotypic Vacuole Fusion and Protein Transport to the Vacuole in Yeast. *J. Biol. Chem.,* 281**,** 14523-14528.
DELGADO, M. & DERETIC, V. 2009. Toll-like Receptors in Control of Immunological Autophagy. *Cell Death Differ.,* 16**,** 976-983.
DERETIC, V. & LEVINE, B. 2009. Autophagy, Immunity, and Microbial Adaptations. *Cell Host Microbe,* 5**,** 527-549.
DESVAUX, M. & HÉBRAUD, M. 2006. The Protein Secretion Systems in *Listeria*: Inside Out Bacterial Virulence. *FEMS Microbiol. Rev.,* 30**,** 774-805.
DEVENISH, R. J., PRESCOTT, M., TURCIC, K. & MIJALJICA, D. 2008. Chapter 9: Monitoring Organelle Turnover in Yeast Using Fluorescent Protein Tags. *Meth. Enzymol.,* 451**,** 109-131.
DORN, B. R., DUNN, W. A. & PROGULSKE-FOX, A. 2002. Bacterial Interactions with the Autophagic Pathway. *Cell. Microbiol.,* 4**,** 1-10.
DUBUISSON, J.-F. & SWANSON, M. S. 2006. Mouse Infection by *Legionella,* A Model to Analyze Autophagy. *Autophagy,* 2**,** 179-182.
DUCLOS, S. & DESJARDINS, M. 2000. Subversion of a Young Phagosome: The Survival Strategies of Intracellular Pathogens. *Cell. Microbiol.,* 2**,** 365-377.
DUPONT, N., LACAS-GERVAIS, S., BERTOUT, J., PAZ, I., FRECHE, B., VAN NHIEU, G. T., VAN DER GOOT, F. G., SANSONETTI, P. J. & LAFONT, F. 2009. *Shigella* Phagocytic Vacuolar Membrane Remnants Participate in the Cellular Response to Pathogen Invasion and Are Regulated by Autophagy. *Cell Host Microbe,* 6**,** 137-149.
EFE, J. A., BOTELHO, R. J. & EMR, S. D. 2005. The Fab1 Phosphatidylinositol Kinase Pathway in the Regulation of Vacuole Morphology. *Curr. Opin. Cell Biol.,* 17**,** 402-408.

EKCHARIYAWAT, P., PUDLA, S., LIMPOSUWAN, K., ARJCHAROEN, S., SIRISINHA, S. & UTAISINCHAROEN, P. 2005. *Burkholderia pseudomallei*-Induced Expression of Suppressor of Cytokine Signaling 3 and Cytokine-Inducible Src Homology 2-Containing Protein in Mouse Macrophages: a Possible Mechanism for Suppression of the Response to Gamma Interferon Stimulation. *Infect. Immun.,* 73**,** 7332-7339.

EKCHARIYAWAT, P., PUDLA, S., LIMPOSUWAN, K., ARJCHAROEN, S., SIRISINHA, S. & UTAISINCHAROEN, P. 2007. Expression of Suppressor of Cytokine Signaling 3 (SOCS3) and Cytokine-Inducible Src Homology 2-Containing Protein (CIS) Induced in *Burkholderia pseudomallei*-Infected Mouse Macrophages Requires Bacterial Internalization. *Microb. Pathog.,* 42**,** 104-110.

ESSEX-LOPRESTI, A. E., BODDEY, J. A., THOMAS, R., SMITH, M. P., HARTLEY, M. G., ATKINS, T., BROWN, N. F., TSANG, C. H., PEAK, I. R. A., HILL, J., BEACHAM, I. R. & TITBALL, R. W. 2005. A Type IV Pilin, PilA, Contributes to Adherence of *Burkholderia pseudomallei* and Virulence *In Vivo*. *Infect. Immun.,* 73**,** 1260-1264.

FREITAG, N. E., PORT, G. C. & MINER, M. D. 2009. *Listeria monocytogenes*-from Saprophyte to Intracellular Pathogen. *Nat. Rev. Micro.,* 7**,** 623-628.

FUJITA, N. & YOSHIMORI, T. 2011. Ubiquitination-Mediated Autophagy Against Invading Bacteria. *Curr. Opin. Cell Biol.,* 23**,** 492-7.

GAN, Y.-H. 2005. Interaction between *Burkholderia pseudomallei* and the Host Immune Response: Sleeping with the Enemy? *J. Infect. Dis.,* 192**,** 1845-1850.

GARBER, K. 2009. Targeting mTOR: Something Old, Something New. *J. Natl. Cancer Inst.,* 101**,** 288-90.

GHIGO, E., PRETAT, L., DESNUES, B., CAPO, C., RAOULT, D. & MEGE, J.-L. 2009. Intracellular Life of *Coxiella burnetii* in Macrophages. *Ann. N. Y. Acad. Sci.,* 1166**,** 55-66.

GIBSON, M. M., BAGGA, D. A., MILLER, C. G. & MAGUIRE, M. E. 1991. Magnesium transport in Salmonella typhimurium: the influence of new mutations conferring Co2+ resistance on the CorA Mg2+ transport system. *Molecular Microbiology,* 5**,** 2753-2762.

GLOVER, D. M. 1985. *DNA Cloning: a practical approach,* Oxford, IRL Press Limited.

GONG, L., CULLINANE, M., TREERAT, P., RAMM, G., PRESCOTT, M., ADLER, B., BOYCE, J. D. & DEVENISH, R. J. 2011. The *Burkholderia pseudomallei* Type III Secretion System and BopA Are Required for Evasion of LC3-Associated Phagocytosis. *PLoS ONE,* 6**,** e17852.

GRAHAM, T. R. & EMR, S. D. 1991. Compartmental Organization of Golgi-Specific Protein Modification and Vacuolar Protein Sorting Events Defined in a Yeast Sec18 (NSF) mutant. *J. Cell Biol.,* 114**,** 207-218.

GUICHON, A., HERSH, D., SMITH, M. & ZYCHLINSKY, A. 2001. Structure-Function Analysis of the *Shigella* Virulence Factor IpaB. *J. Bacteriol.,* 183**,** 1269-1276.

HAJISHENGALLIS, G. 2009. *Porphyromonas gingivalis*-Host Interactions: Open War or Intelligent Guerilla Tactics? *Microbes Infect.,* 11**,** 637-645.

HARDWIDGE, P. R., DONOHOE, S., AEBERSOLD, R. & FINLAY, B. B. 2006. Proteomic Analysis of the Binding Partners to Enteropathogenic *Escherichia coli* Virulence Proteins Expressed in *Saccharomyces cerevisiae*. *Proteomics,* 6**,** 2174-2179.

HARLAND, D. N., CHU, K., HAQUE, A., NELSON, M., WALKER, N. J., SARKAR-TYSON, M., ATKINS, T. P., MOORE, B., BROWN, K. A., BANCROFT, G., TITBALL, R. W. & ATKINS, H. S. 2007. Identification of a LolC Homologue in *Burkholderia pseudomallei* a Novel Protective Antigen for Melioidosis. *Infect. Immun.,* 75**,** 4173-4180.

HARPER, M., COX, A. D., ST. MICHAEL, F., WILKIE, I. W., BOYCE, J. D. & ADLER, B. 2004. A Heptosyltransferase Mutant of *Pasteurella multocida* Produces a Truncated Lipopolysaccharide Structure and is Attenuated in Virulence. *Infect. Immun.,* 72**,** 3436-3443.

HINNEBUSCH, A. G. & FINK, G. R. 1983. Positive Regulation in the General Amino Acid Control of *Saccaromyces cerevisiae*. *PNAS,* 80**,** 5374-5378.

HISCOX, T. J., CHAKRAVORTY, A., CHOO, J. M., OHTANI, K., SHIMIZU, T., CHEUNG, J. K. & ROOD, J. I. 2011. Regulation of Virulence by the RevR Response Regulator in *Clostridium perfringens*. *Infect. Immun.,* 79**,** 2145-2153.

HOLDEN, M. T. G., TITBALL, R. W., PEACOCK, S. J., CERDEÑO-TÁRRAGA, A. M., ATKINS, T., CROSSMAN, L. C., PITT, T., CHURCHER, C., MUNGALL, K., BENTLEY, S. D., SEBAIHIA, M., THOMSON, N. R., BASON, N., BEACHAM, I. R., BROOKS, K., BROWN, K. A., BROWN, N. F., CHALLIS, G. L., CHEREVACH, I., CHILLINGWORTH, T., CRONIN, A., CROSSETT, B., DAVIS, P., DESHAZER, D., FELTWELL, T., FRASER, A., HANCE, Z., HAUSER, H., HOLROYD, S., JAGELS, K., KEITH, K. E., MADDISON, M., MOULE, S., PRICE, C., QUAIL, M. A., RABBINOWITSCH, E., RUTHERFORD, K., SANDERS, M., SIMMONDS, M., SONGSIVILAI, S., STEVENS, K., TUMAPA, S., VESARATCHAVEST, M., WHITEHEAD, S., YEATS, C., BARRELL, B. G., OYSTON, P. C. F. & PARKHILL, J. 2004. Genomic plasticity of the causative agent of melioidosis, *Burkholderia pseudomallei*. *PNAS,* 101**,** 14240-14245.

INGLIS, T., ROLIM, D. & RODRIGUEZ, J. 2006. Clinical Guideline for Diagnosis and Management of Melioidosis. *Rev. Inst. Med,* 48**,** 1-4.

JONES, A., BEVERIDGE, T. & WOODS, D. 1996. Intracellular Survival of *Burkholderia pseudomallei*. *Infect. Immun.,* 64**,** 782-790.

KANEKO, T., NAKAMURA, Y., SATO, S., ASAMIZU, E., KATO, T., SASAMOTO, S., WATANABE, A., IDESAWA, K., ISHIKAWA, A., KAWASHIMA, K., KIMURA, T., KISHIDA, Y., KIYOKAWA, C., KOHARA, M., MATSUMOTO, M., MATSUNO, A., MOCHIZUKI, Y., NAKAYAMA, S., NAKAZAKI, N., SHIMPO, S., SUGIMOTO, M., TAKEUCHI, C., YAMADA, M. & TABATA, S. 2000. Complete Genome Structure of the Nitrogen-fixing Symbiotic Bacterium *Mesorhizobium loti*. *DNA Res.,* 7**,** 331-338.

KANG, Y., NORRIS, M. H., WILCOX, B. A., TUANYOK, A., KEIM, P. S. & HOANG, T. T. 2011. Knockout and Pullout Recombineering for Naturally Transformable *Burkholderia thailandensis* and *Burkholderia pseudomallei*. *Nat. Protocols,* 6**,** 1085-1104.

KARUNAKARAN, R. & PUTHUCHEARY, S. D. 2007. *Burkholderia pseudomallei*: *In Vitro* Susceptibility to Some New and Old Antimicrobials. *Scand. J. Infect. Dis.,* January**,** 1-4.

KATZMANN, D. J., ODORIZZI, G. & EMR, S. D. 2002. Receptor Downregulation and Multivesicular-Body Sorting. *Nat. Rev.,* 3**,** 893- 905.

KESPICHAYAWATTANA, W., RATTANACHETKUL, S., WANUN, T., UTAISINCHAROEN, P. & SIRISINHA, S. 2000. *Burkholderia pseudomallei* Induces Cell Fusion and Actin-Associated Membrane Protrusion: a Possible Mechanism for Cell-to-Cell Spreading. *Infect. Immun.*, 68**,** 5377-5384.

KIRKEGAARD, K., TAYLOR, M. P. & JACKSON, W. T. 2004. Cellular Autophagy: Surrender, Avoidance and Subversion by Microorganisms. *Nat. Rev.*, 2**,** 301-314.

KRAMER, R. W., SLAGOWSKI, N. L., EZE, N. A., GIDDINGS, K. S., MORRISON, M. F., SIGGERS, K. A., STARNBACK, M. N. & LESSER, C. F. 2007. Yeast Functional Genomic Screens Lead to Identification of a Role for a Bacterial Effector in Innate Immunity Regulation. *Plos Pathog.*, 3**,** 179-190.

KWEON, M.-N. 2008. Shigellosis: The Current Status of Vaccine Development. *Curr. Opin. Infect. Dis.*, 21**,** 313-318.

LAZAR ADLER, N., GOVAN, B., CULLINANE, M., HARPER, M., ADLER, B. & BOYCE, J. 2009. The Molecular and Cellular Basis of Pathogenesis in Melioidosis: How Does *Burkholderia pseudomallei* Cause Disease? *FEMS Microbiol. Lett.*, 33**,** 1079-99.

LEO, J. C., ELOVAARA, H., BRODSKY, B., SKURNIK, M. & GOLDMAN, A. 2008. The *Yersinia* adhesin YadA binds to a collagenous triple-helical conformation but without sequence specificity. *Protein Eng. Des. Sel.*, 21**,** 475-484.

LERENA, M. C., VÁZQUEZ, C. L. & COLOMBO, M. I. 2010. Bacterial Pathogens and the Autophagic Response. *Cell. Microbiol.*, 12**,** 10-18.

LESSER, C. F. & MILLER, S. I. 2001. Expression of Microbial Virulence Proteins in *Saccharomyces cerevisiae* Models Mammalian Infection. *EMBO J.*, 20**,** 1840-1849.

LIMMATHUROTSAKUL, D., WONGRATANACHEEWIN, S., TEERAWATTANASOOK, N., WONGSUVAN, G., CHAISUKSANT, S., CHETCHOTISAKD, P., CHAOWAGUL, W., DAY, N. P. J. & PEACOCK, S. J. 2010. Increasing Incidence of Human Melioidosis in Northeast Thailand. *Am. J. Trop. Med. Hyg.*, 82**,** 1113-1117.

LOGUE, C.-A., PEAK, I. R. A. & BEACHAM, I. R. 2009. Facile Construction of Unmarked Deletion Mutants in *Burkholderia pseudomallei* Using SacB Counter-Selection in Sucrose-Resistant and Sucrose-Sensitive Isolates. *J. Microbiol. Methods*, 76**,** 320-323.

MARTINET, W., AGOSTINIS, P., VANHOECKE, B., DEWAELE, M. & DEÂ MEYER, G. R. Y. 2009. Autophagy in Disease: A Double-Edged Sword with Therapeutic Potential. *Clin. Sci.*, 116**,** 697-712.

MARTINOU, J.-C. & KROEMER, G. 2009. Autophagy: Evolutionary and Pathophysiological Insights. *Biochim. Biophys. Acta*, 1793**,** 1395-1396.

MAYER, A., WICKNER, W. & HAAS, A. 1996. Sec18p (NSF)-Driven Release of Sec17p ([alpha]-SNAP) Can Precede Docking and Fusion of Yeast Vacuoles. *Cell*, 85**,** 83-94.

MELENDEZ, A. & LEVIN, B. 2009. Autophagy in *C. elegans*. *WorkBook*, August**,** 1-26.

MIJALJICA, D., PRESCOTT, M. & DEVENISH, R. J. 2007. Nibbling Within the Nucleus: Turnover of Nuclear Contents. *Cell. Mol. Life Sci.*, 64**,** 581-8.

MILTON, D., O'TOOLE, R., HORSTEDT, P. & WOLF-WATZ, H. 1996. Flagellin A is Essential for the Virulence of *Vibrio anguillarum*. *J. Bacteriol.,* 178**,** 1310-1319.

MILTON, D. L., NORQVIST, A. & WOLF-WATZ, H. 1992. Cloning of a Metalloprotease Gene Involved in the Virulence Mechanism of *Vibrio anguillarum*. *J. Bacteriol.,* 174**,** 7235-7244.

MIMA, T., KVITKO, B. H., RHOLL, D. A., PAGE, M. G. P., DESARBRE, E. & SCHWEIZER, H. P. 2011. *In vitro* activity of BAL30072 against *Burkholderia pseudomallei*. *Int. J. Antimicrob. Agents,* 38**,** 157-159.

MIYAGI, K., KAWAKAMI, K. & SAITO, A. 1997. Role of Reactive Nitrogen and Oxygen Intermediates in Gamma Interferon-Stimulated Murine Macrophage Bactericidal Activity against *Burkholderia pseudomallei*. *Infect. Immun.,* 65**,** 4108-4113.

MUELLER, C. A., BROZ, P. & CORNELIS, G. R. 2008. The Type III Secretion System Tip Complex and Translocon. *Mol. Microbiol.,* 68**,** 1085-1095.

NAKAGAWA, I., AMANO, A., MIZUSHIMA, N., YAMAMOTO, A., YAMAGUCHI, H., KAMIMOTO, T., NARA, A., FUNAO, J., NAKATA, M., TSUDA, K., HAMADA, S. & YOSHIMORI, T. 2004. Autophagy Defends Cells Against Invading Group A *Streptococcus*. *Science,* 306**,** 1037-1040.

NEB. 2007. *Enhancing Transformation Efficiencies* [Online]. NEB Expressions. Available: http://www.neb.com/nebecomm/tech_reference/competent_cells/transformationtips.asp [Accessed 2007].

NEJEDLIK, L., T. PIERFELICE & J. R. GEISER 2004. Actin Distribution is Disrupted Upon Expression of *Yersinia* YopO/YpkA in Yeast. *Yeast,* 21**,** 759-768.

NGAUY, V., LEMESHEV, Y., SADKOWSKI, L. & CRAWFORD, G. 2005. Cutaneous Melioidosis in a Man Who Was Taken as a Prisoner of War by the Japanese during World War II. *J. Clin. Microbiol.,* 43**,** 970-972.

NORA, T., LOMMA, M., GOMEZ-VALERO, L. & BUCHRIESER, C. 2009. Molecular Mimicry: An Important Virulence Strategy Employed by *Legionella pneumophila* to Subvert Host Functions. *Future Microbiol.,* 4**,** 691-701.

NOVAK, R. T., GLASS, M. B., GEE, J. E., GAL, D., MAYO, M. J., CURRIE, B. J. & WILKINS, P. P. 2006. Development and Evaluation of a Real-Time PCR Assay Targeting the Type III Secretion System of *Burkholderia pseudomallei*. *J. Clin. Microbiol.,* 44**,** 85-90.

NOWIKOVSKY, K., DEVENISH, R. J., FROSCHAUER, E. & SCHWEYEN, R. J. 2009. Chapter 17 Determination of Yeast Mitochondrial KHE Activity, Osmotic Swelling and Mitophagy. *In:* WILLIAM, S. A. & ANNE, N. M. (eds.) *Methods in Enzymology.* Academic Press.

OGAWA, M., MIMURO, H., YOSHIKAWA, Y., ASHIDA, H. & SASAKAWA, C. 2011. Manipulation of Autophagy by Bacteria for Their Own Benefit. *Microbiol. Immunol.,* 55**,** 459-71.

OGAWA, M. & SASAKAWA, C. 2006a. Bacterial Evasion of the Autophagic Defense System. *Curr. Opin. Microbiol.,* 9**,** 62-68.

OGAWA, M. & SASAKAWA, C. 2006b. Intracellular Survival of *Shigella*. *Cell. Microbiol.,* 8**,** 177-184.

OGAWA, M., SUZUKI, T., TATSUNO, I., ABE, H. & SASAKAWA, C. 2003. IcsB, Secreted via the Type III Secretion System, is Chaperoned by IpgA and Required at the Post-Invasion Stage of *Shigella* Pathogenicity. *Mol. Microbiol.,* 48**,** 913-931.

OGAWA, M., YOUIMORI, T., SUZUKI, T., SAGARA, H., MIZUSHIMA, N. & SASAKAWA, C. 2005. Escape of Intracellular *Shigella* from Autophagy. *Science,* 307.

ORVEDAHL, A. & LEVINE, B. 2008. Eating the Enemy Within: Autophagy in Infectious Diseases. *Cell Death Differ.,* 16**,** 57-69.

OSTROWICZ, C. W., MEIRINGER, C. T. A. & UNGERMANN, C. 2008. Yeast Vacuole Fusion: A Model System for Eukaryotic Endomembrane Dynamics. *Autophagy,* 4**,** 1-15.

OYSTON, P. C. F. 2008. *Francisella tularensis*: Unravelling the Secrets of an Intracellular Pathogen. *J. Med. Microbiol.,* 57**,** 921-930.

PILATZ, S., BREITBACH, K., HEIN, N., FEHLHABER, B., SCHULZE, J., BRENNEKE, B., EBERL, L. & STEINMETZ, I. 2006. Identification of *Burkholderia pseudomallei* Genes Required for the Intracellular Life Cycle and *In Vivo* Virulence. *Infect. Immun.,* 74**,** 3576-3586.

PIPER, R., BRYANT, N. & STEVENS, T. 1997. The Membrane Protein Alkaline Phosphatase is Delivered to the Vacuole by a Route that is Distinct from the VPS-Dependent Pathway. *J. Cell Biol.,* 138**,** 531-45.

POSFAY-BARBE, K. M. & WALD, E. R. 2009. Listeriosis. *Seminars in Fetal and Neonatal Medicine,* 14**,** 228-233.

PRICE, A., SEALS, D., WICKNER, W. & UNGERMANN, C. 2000. The Docking Stage of Yeast Vacuole Fusion Requires the Transfer of Proteins from a cis-SNARE Complex to a Rab/Ypt Protein. *J. Cell Biol.,* 148**,** 1231-1238.

PUKATZKI, S., MA, A., STURTEVANT, D., KRASTINS, B., SARRACINO, D., NELSON, W., HEIDELBERG, J. & MEKALANOS, J. 2006. Identification of a Conserved Bacterial Protein Secretion System in *Vibrio cholerae* Using the Dictyostelium Host Model System. *PNAS,* 103**,** 1528-33.

RAINBOW, L., HART, A. & WINSTANLEY, C. 2002. Distribution of Type III Secretion Gene Clusters in *Burkholderia pseudomallei*, *B. thailandensis* and *B. mallei*. *J. Med. Microbiol.,* 51**,** 374-384.

RAVIKUMAR, B., SARKAR, S., DAVIES, J. E., FUTTER, M., GARCIA-ARENCIBIA, M., GREEN-THOMPSON, Z. W., JIMENEZ-SANCHEZ, M., KOROLCHUK, V. I., LICHTENBERG, M., LUO, S., MASSEY, D. C. O., MENZIES, F. M., MOREAU, K., NARAYANAN, U., RENNA, M., SIDDIQI, F. H., UNDERWOOD, B. R., WINSLOW, A. R. & RUBINSZTEIN, D. C. 2010. Regulation of Mammalian Autophagy in Physiology and Pathophysiology. *Physiol. Rev.,* 90**,** 1383-1435.

RAY, K., MARTEYN, B., SANSONETTI, P. J. & TANG, C. M. 2009. Life on the Inside: The Intracellular Lifestyle of Cytosolic Bacteria. *Nat. Rev. Micro.,* 7**,** 333-340.

RAYMOND, C. K., HOWALD-STEVENSON, I., VATER, C. A. & STEVENS, T. H. 1992. Morphological classification of the Yeast Vacuolar Protein Sorting Mutants: Evidence for a Prevacuolar Compartment in Class E *vps* Mutants. *Mol. Biol. Cell,* 3**,** 1389-1402.

RECKSEIDLER-ZENTENO, S., DEVINNEY, R. & WOODS, D. 2005. The Capsular Polysaccharide of *Burkholderia pseudomallei* Contributes to

Survival in Serum by Reducing Complement Factor C3b Deposition. *Infect. Immun.*, 73**,** 1106-1115.
ROBERTS, P., MOSHITCH MOSHKOVITZ, S., KVAM, E., O'TOOLE, E., WINEY, M. & GOLDFARB, D. 2003. Piecemeal Microautophagy of Nucleus in *Saccharomyces cerevisiae*. *Mol. Biol. Cell,* 14**,** 129-41.
RODRIGUEZ-ESCUDERO, I., ROTGER, R., CID, V. J. & MOLINA, M. 2006. Inhibition of Cdc42-Dependent Signalling in *Saccharomyces cerevisiae* by Phosphatase-Dead SigD/SopB from *Salmonella typhimurium*. *Microbiology,* 152**,** 3437-3452.
ROSADO, C. J., MIJALJICA, D., HATZINISIRIOU, I., PRESCOTT, M. & DEVENISH, R. J. 2008. Rosella: A Fluorescent pH-Biosensor for Reporting Vacuolar Turnover of Cytosol and Organelles in Yeast. *Autophagy,* 4**,** 205-13.
ROVERSI, P., JOHNSON, S., FIELD, T., DEANE, J. E., GALYOV, E. E. & LEA, S. M. 2007. Expression, Purification, Crystalization and Preliminary Crystallographic Analysis of BipD, a Component of the *Burkholderia Pseudomallei* Type III Secretion System. *Acta Cryst.,* F62**,** 861-864.
SANJUAN, M. A., MILASTA, S. & GREEN, D. R. 2009. Toll-Like Receptor Signaling in the Lysosomal Pathways. *Immun. Rev.,* 227**,** 203-220.
SARKAR-TYSON, M., SMITHER, S. J., HARDING, S. V., ATKINS, T. P. & TITBALL, R. W. 2009. Protective Efficacy of Heat-Inactivated *B. thailandensis, B. mallei* or *B. pseudomallei* Against Experimental Melioidosis and Glanders. *Vaccine,* 27**,** 4447-4451.
SATO, T. K., REHLING, P., PETERSON, M. R. & EMR, S. D. 2000. Class C Vps Protein Complex Regulates Vacuolar SNARE Pairing and Is Required for Vesicle Docking/Fusion. *Mol. Cell,* 6**,** 661-671.
SEELEY, E. S., KATO, M., MARHOLIS, N., WICKNER, W. & EITZEN, G. 2002. Genomic Analysis of Homotypic Vacuole Fusion. *Mol. Biol.,* 13**,** 782-794.
SEEMANN, T. 2012. *Wasabi* [Online]. Melbourne: Victorian Bioinformatics Consortium. Available: http://vbc.med.monash.edu.au/wasabi [Accessed 2006].
SENN, J. J., KLOVER, P. J., NOWAK, I. A., ZIMMERS, T. A., KONIARIS, L. G., FURLANETTO, R. W. & MOONEY, R. A. 2003. Suppressor of Cytokine Signaling-3 (SOCS-3), a Potential Mediator of Interleukin-6-Dependent Insulin Resistance in Hepatocytes. *J. Biol. Chem.,* 278**,** 13740-13746.
SHOHDY, N., EFE, J. A., EMR, S. D. & SHUMAN, H. A. 2005. Pathogen Effector Protein Screening in Yeast Identifies *Legionella* Factors that Interfere with Membrane Trafficking. *PNAS,* 102**,** 4866-4871.
SIEIRA, R., AROCENA, G. M., BUKATA, L., COMERCI, D. J. & UGALDE, R. A. 2009. Metabolic Control of Virulence Genes in *Brucella*: HutC Coordinates virB Expression and the Histidine Utilization Pathway by Direct Binding to Both Promoters. *J. Bacteriol.***,** JB.01124-09.
SIGGERS, K. A. & LESSER, C. F. 2008. The Yeast *Saccharomyces cerevisiae*: A Versatile Model System for the Identification and Characterization of Bacterial Virulence Proteins. *Cell Host & Microbe,* 4**,** 8-15.
SIMON, R., PRIEFER, U. & PUHLER, A. 1983. A Broad Host Range Mobilization System for *In Vivo* Genetic Engineering: Transposon Mutagenesis in Gram Negative Bacteria. *Nat. Biotech.,* 1**,** 784-791.
SLAGOWSKI, N. L., KRAMER, R. W., MORRISON, M. F., LABAER, J. & LESSER, C. F. 2008. A Functional Genomic Yeast Screen to Identify Pathogenic Bacterial Proteins. *Plos Pathog.*, 4**,** 96-107.

SMITH, R. L., KACZMAREK, M. T., KUCHARSKI, L. M. & MAGUIRE, M. E. 1998. Magnesium Transport in *Salmonella typhimurium*: Regulation of MgtA and MgtCB During Invasion of Epithelial and Macrophage Cells. *Microbiology,* 144**,** 1835-1843.

STEELE-MORTIMER, O. 2011. Exploitation of the Ubiquitin System by Invading Bacteria. *Traffic,* 12**,** 162-169.

STEVENS, J. M., GALYOV, E. E. & STEVENS, M. P. 2006. Actin-Dependent Movement of Bacterial Pathogens. *Nat. Rev. Microbiol.,* 4**,** 91-101.

STEVENS, J. M., ULRICH, R. L., TAYLOR, L. A., WOOD, M. W., DESHAZER, D., STEVENS, M. P. & GALYOV, E. E. 2005a. Actin-Binding Proteins from *Burkholderia mallei* and *Burkholderia thailandensis* can Functionally Compensate for the Actin-Based Motility Defect of a *Burkholderia pseudomallei* BimA Mutant. *J. Bacteriol.,* 187**,** 7857-62.

STEVENS, M., FRIEBEL, A., TAYLOR, L., WOOD, M., BROWN, P., HARDT, W.-D. & GALYOV, E. 2003. A *Burkholderia pseudomallei* Type III Secreted Protein, BopE, Facilitates Bacterial Invasion of Epithelial Cells and Exhibits Guanine Nucleotide Exchange Factor Activity. *J. Bacteriol.,* 185**,** 4992-4996.

STEVENS, M. & GALYOV, E. 2004. Exploitation of host cells by *Burkholderia pseudomallei*. *Int. J. Med. Microbiol.,* 293**,** 549-555.

STEVENS, M., HAQUE, A., ATKINS, T., HILL, J., WOOD, M., EASTON, A., NELSON, M., UNDERWOOD-FOWLER, C., TITBALL, R., BANCROFT, G. & GALYOV, E. 2004. Attenuated Virulence and Protective Efficacy of a *Burkholderia pseudomallei Bsa* Type III Secretion Mutant in Murine Models of Melioidosis. *Microbiology,* 150**,** 2669-2676.

STEVENS, M., STEVENS, J., JENG, R., TAYLOR, L., WOOD, M., HAWES, P., MONAGHAN, P., WELCH, M. & GALYOV, E. 2005b. Identification of a Bacterial Factor Required for Actin-Based Motility of *Burkholderia pseudomallei*. *Mol. Microbiol.,* 56**,** 40-53.

STEVENS, M., WOOD, M., TAYLOR, L., MONAGHAN, P., HAWES, P., JONES, P., WALLIS, T. & GALYOV, E. 2002. An Inv/Mxi-Spa-Like Type III Protein Secretion System in *Burkholderia pseudomallei* Modulates Intracellular Behaviour of the Pathogen. *Mol. Microbiol.,* 46**,** 649-659.

STEVENS, T., ESMON, B. & SCHEKMAN, R. 1982. Early Stages in the Yeast Secretory Pathway are Required for Transport of Carboxypeptidase Y to the Vacuole. *Cell,* 30**,** 439-448.

SUN, G. W. & GAN, Y.-H. 2010. Unraveling Type III Secretion Systems in the Highly Versatile *Burkholderia pseudomallei*. *Trends in Microbiol.,* 18**,** 561-568.

SUN, G. W., LU, J., PERVAIZ, S., CAO, W. P. & GAN, Y.-H. 2005. Caspase-1 Dependent Macrophage Death Induced by *Burkholderia pseudomallei*. *Cellular Microbiol.,* 7**,** 1447-1458.

SUPARAK, S., KESPICHAYAWATTANA, W., HAQUE, A., EASTON, A., DAMNIN, S., LERTMEMONGKOLCHAI, G., BANCROFT, G. J. & KORBSRISATE, S. 2005. Multinucleated Giant Cell Formation and Apoptosis in Infected Host Cells Is Mediated by *Burkholderia pseudomallei* Type III Secretion Protein BipB. *J. Bacteriol.,* 187**,** 6556-6560.

SZPIRER, C. Y., FAELEN, M. & COUTURIER, M. 2001. Mobilization Function of the pBHR1 Plasmid, a Derivative of the Broad-Host-Range Plasmid pBHR1. *J. Bacteriol.,* 183**,** 2101-2110.

TAKEDA, K., CABRERA, M., ROHDE, J., BAUSCH, D., JENSEN, O. N. & UNGERMANN, C. 2008. The Vacuolar V1/V0-ATPase is Involved in the Release of the HOPS Subunit Vps41 from Vacuoles, Vacuole Fragmentation and Fusion. *FEBS Lett.,* 582**,** 1558-1563.

TAN, K. S., CHEN, Y., LIM, Y.-C., TAN, G.-Y. G., LIU, Y., LIM, Y.-T., MACARY, P. & GAN, Y.-H. 2010. Suppression of Host Innate Immune Response by *Burkholderia pseudomallei* through the Virulence Factor TssM. *J. Immun.,* 184**,** 5160-5171.

TREERAT, P., ALWIS, P., D'CRUZE, T., CULLINANE, M., VADIVELU, J., DEVENISH, R. J., PRESCOTT, M., ADLER, B. & BOYCE, J. D. unpublished. Importance of the Type III secretion system genes *bapA, bapB* and *bapC* in the virulence of *Burkholderia pseudomallei*.

UNGERMANN, C. & WICKNER, W. 1998. Vam7p, a Vacuolar SNAP-25 Homolog, is Required for SNARE Complex Integrity and Vacuole Docking and Fusion. *EMBO J.,* 17**,** 3269-32-76.

UTAISINCHAROEN, P., ARJCHAROEN, S., LIMPOSUWAN, K., TUNGPRADABKUL, S. & SIRISINHA, S. 2006. *Burkholderia pseudomallei* RpoS Regulates Multinucleated Giant Cells Formation and Inducible Nitric Oxide Synthase Expression in Mouse Macrophage Cell Line (RAW 264.7). *Microb. Pathog.,* 40**,** 184-189.

UTTENWEILER, A. & MAYER, A. 2008. Microautophagy in the Yeast *Saccharomyces cerevisiae*. *Methods Mol. Biol.,* 445**,** 245-59.

VALDIVIA, R. J. 2004. Modeling the Functin of Bacterial Virulence factors in *Saccharomyces cerevisiae*. *Eukaryotic Cell,* 3**,** 827-834.

VELD, D. H. I. T., WUTHIEKANUN, V., CHENG, A. C., CHIERAKUL, W., CHAOWAGUL, W., BROUWER, A. E., WHITE, N. J., DAY, N. P. J. & PEACOCK, S. J. 2005. The Role and Significance of Sputum Cultures in the Diagnosis of Melioidosis *Am. J. Trop. Med. Hyg.,* 73**,** 657-661.

VIDA, T. A. & EMR, S. D. 1995. A New Vital Stain for Visualizing Vacuolar Membrane Dynamics and Endocytosis in Yeast. *J. Cell Biol.,* 128**,** 779-92.

WANG, C.-W. & KLIONSKY, D. 2003. The Molecular Mechanism of Autophagy. *Mol. Med.,* 9**,** 65-76.

WANG, L., SEELEY, E. S., WICKNER, W. & MERZ, A. J. 2002. Vacuole Fusion at a Ring of Vertex Docking Sites Leaves Membrane Fragments within the Organelle. *Cell,* 108**,** 357-369.

WARAWA, J. & WOODS, D. E. 2005. Type III Secretion System Cluster III is Required for Maximal Virulence of *Burkholderia pseudomallei* in a Hamster Infection Model. *FEMS Microbiol. Lett.,* 242**,** 101-108.

WATTIAU, P., HESSCHE, M. V., NEUBAUER, H., ZACHARIAH, R., WERNEY, U. & IMBERECHTS, N. 2007. Identification of *Burkholderia pseudomallei* and Related Bacteria by Multiple-Locus Sequence Typing-Derived PCR and Real-Time PCR. *J. Clin. Microbiol.,* 45**,** 1045-1048.

WEISMAN, L. S. 2003. Yeast Vacuole Inheritance and Dynamics. *Annu. Rev. Genet.,* 37**,** 435-460.

WEST, T. E., ERNST, R., JANSSON-HUTSON, M. & SKERRETT, S. 2008. Activation of Toll-like receptors by Burkholderia pseudomallei. *BMC Immunology,* 9**,** 46.

WHITMORE, A. & KRISHNASWAMI, C. 1912. An Account of the Discovery of a Hitherto Undiscovered Infective Disease Occuring Among the Population of Rangoon. *Indian Med. Gaz.,* 47**,** 262-267.

WHITWORTH, T., POPOV, V., YU, X.-J., WALKER, D. & BOUYER, D. 2005. Expression of the *Rickettsia prowazekii* Pld or TlyC Gene in *Salmonella enterica* serovar *Typhimurium* Mediates Phagosomal Escape. *Infect. Immun.,* 73**,** 6668-73.

WICKNER, W. & HAAS, A. 2000. Yeast Homotypic Vacuole Fusion: A Window on Organelle Trafficking Mechanisms. *Annu. Rev. Biochem,* 69**,** 247-75.

WIERSINGA, J., WIELAND, C. W., DESSING, M. C., CHANTRATITA, N., CHENG, A. C., LIMMATHUROTSAKUL, D., CHIERAKUL, W., LEENDERTSE, M., FLORQUIN, S., VOS, A. F. D., WHITE, N., DONDORP, A. M., DAY, N. P., PEACOCK, S. J. & POLL, T. V. D. 2007. Toll-like receptor 2 impairs host defence in gram-negative sepsis caused by *Burkholderia pseudomallei* (melioidosis). *PLoS Medicine,* 4**,** 121-144.

WIERSINGA, W. J., POLL, T. V. D., WHITE, N., DAY, N. & PEACOCK, S. 2006. Melioidosis: Insights into the Pathogenicity of *Burkholderia pseudomallei*. *Nat. Rev. Microbiol.,* 4**,** 272-280.

WIERSINGA, W. J. & VAN DER POLL, T. 2009. Immunity to Burkholderia pseudomallei. *Curr. Opin. Infect. Dis.,* 22**,** 102-108 10.1097/QCO.0b013e328322e727.

WUTHIEKANUN, V., CHIERAKUL, W., RATTANALERTNAVEE, J., LANGA, S., SIRODOM, D., WATTANAWAITUNECHAI, C., WINOTHAI, W., WHITE, N. J., DAY, N. & PEACOCK, S. J. 2006. Serological Evidence for Increased Human Exposure to *Burkholderia pseudomallei* following the Tsunami in Southern Thailand. *J. Clin. Microbiol.,* 44**,** 239-240.

YAMAGUCHI, H., NAKAGAWA, I., YAMAMOTO, A., AMANO, A., NODA, T. & YOSHIMORI, T. 2009. An Initial Step of *GAS*-Containing Autophagosome-Like Vacuoles Formation Requires Rab7. *Plos Pathog.,* 5**,** e1000670-e1000670.

YANG, Y.-P., LIANG, Z.-Q., GU, Z.-L. & QIN, Z.-H. 2005. Molecular Mechanism and Regulation of Autophagy. *Acta Pharmacol. Sinica,* 26**,** 1421-34.

YOSHIMORI, T. 2005. Autophagy vs. Group A *Streptococcus*. *Autophagy,* 2**,** 154-155.

ZHANG, L., WANG, Y., PICKING, W. L., PICKING, W. D. & DE GUZMAN, R. N. 2006. Solution Structure of Monomeric BsaL, the Type III Secretion Needle Protein of *Burkholderia pseudomallei*. *J. Mol. Biol.,* 359**,** 322-330.

“As the circle of light increases, so does the circumference of darkness around it.”

Albert Einstein

Erratum

- Page 93, paragraph 3, lines 8-10 should read:
  Under autophagic conditions, the delivery of organelles (≥ pH 7.0) to the acidic vacuole (pH 4.8) results in highly diminished or no detectable fluorescence of the GFP component.
- Figures 3.7, 3.9 and 3.10 used confocal microscopy fluorescence to illustrate the influence *B. pseudomallei* proteins exert on specific organelles, in yeast *BY4741* during non-starved and starved conditions. Below is a schematic representation.

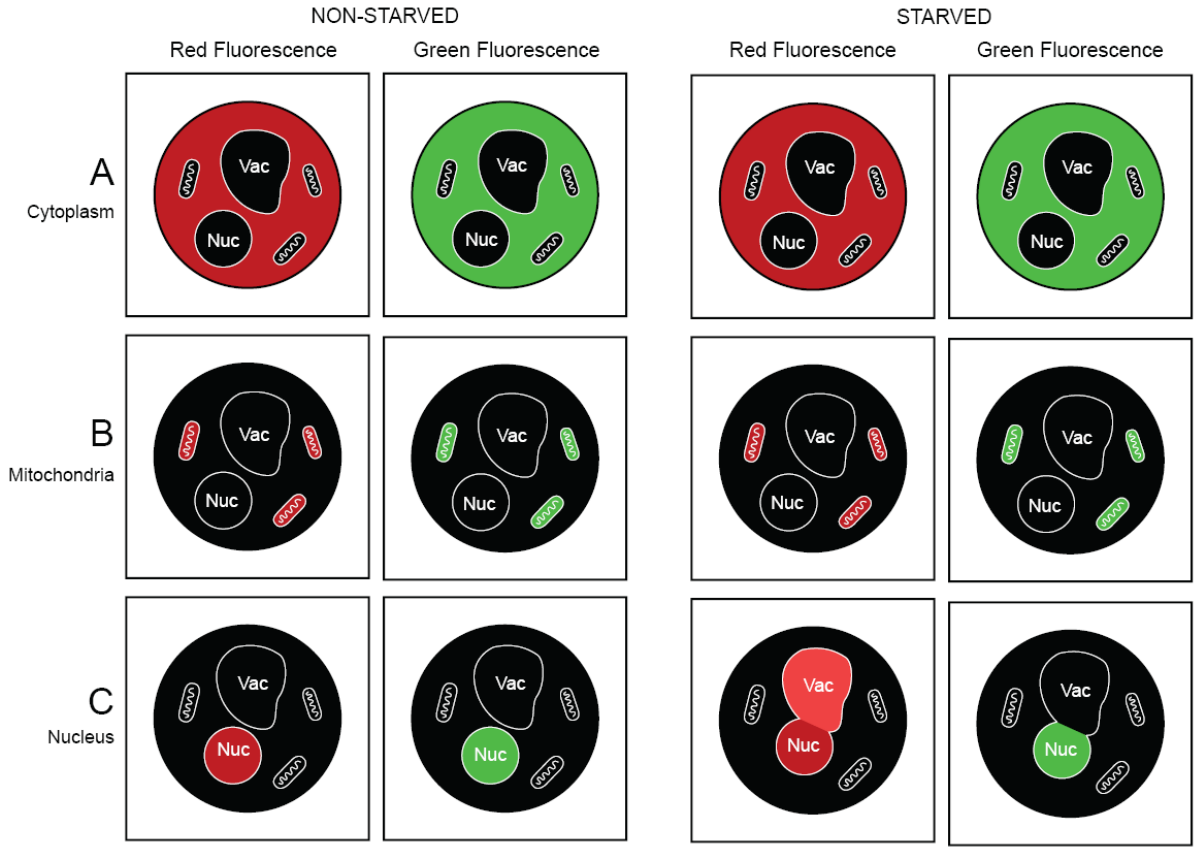

Panel A: The biosensor located in the cytosol exhibits red and green fluorescence. Under non-starvation conditions little autophagy takes place, so the biosensor is not delivered to the vacuole and it does not show any fluorescence. When subjected to 4 h starvation, wild-type cells tend to undergo cytosolic autophagy as evident by red fluorescence in the vacuole, with the absence of green fluorescence (Figure 3.7A). However, if the expression of a *B. pseudomallei* protein inhibits cytosolic autophagy in yeast under starvation conditions, then red fluorescence is not observed in the vacuole (see Figures 3.7A & B).

Panel B: Under non-starved conditions the biosensor targeted to mitochondria exhibits red and green fluorescence. When subjected to 6 h starvation, wild-type cells tend to undergo mitochondrial autophagy as evident by diffuse red fluorescence in the vacuole, with the absence of green fluorescence (Figure 3.9A). However, if the expression of a *B. pseudomallei* protein inhibits mitochondrial autophagy under starvation conditions, then red fluorescence is not observed in the vacuole (see Figures 3.9A & B).

Panel C: Under non-starved conditions the biosensor targeted to the nucleus exhibits red and green fluorescence. When subjected to 20 h starvation, wild-type cells tend to undergo partial nuclear autophagy as evident by "blebs" of diffuse red fluorescence in the vacuole, with the absence of green fluorescence (Figure 3.10A). If the expression of a *B. pseudomallei* protein does not inhibit nuclear autophagy under starvation conditions, then diffuse red fluorescence is observed in the vacuole, with the absence of green fluorescence (see Figures 3.10A & B).

- Page 148, Figure 4.13. Survival assays show the CFU numbers of wild-type bacteria and BPSS1532 mutant bacteria to be similar at 6 h post infection, as depicted in Figure 4.12 (page 145). The image presented in Figure 4.13A for the 6h time point was selected for its fluorescence intensity, and is not the best representation of bacterial numbers. A better representative image is presented in Figure E.1A.

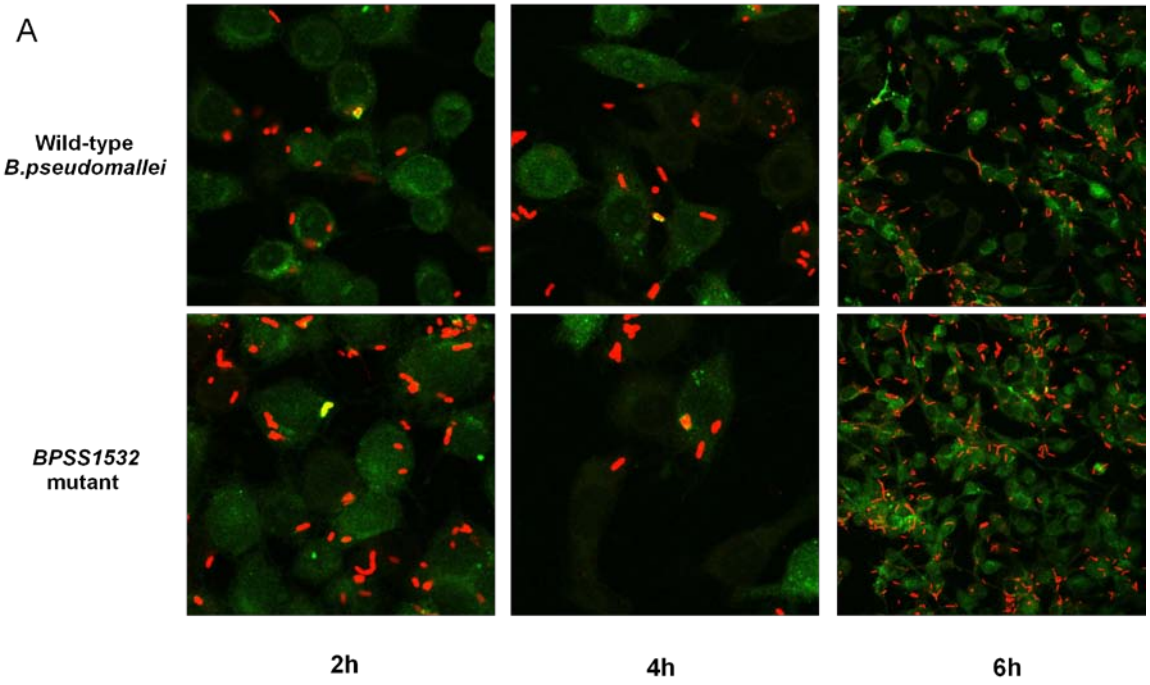

Figure E.1A: Co-localisation of wild-type and *BPSS1532* mutant bacteria with LC3-GFP. (A) Bacterial co-localisation with LC3-GFP was defined by the presence of labelled bacteria (red fluorescence) which were fully overlaid by intense green (yellow fluorescence) or fully contained within a green ring.

- As described in *Chapter 1*, pathogenic bacteria employ a variety of virulence factors, such as secreted proteins and toxins, to escape the phagosome/endosome, to escape subsequent autophagic capture or to suppress autophagosomal maturation.

  Of particular interest are the secreted bacterial proteins that assist pathogenic bacteria to escape the autophagic pathway by disrupting the membrane encapsulating them. It was postulated that *B. pseudomallei* may utilise similar effector proteins to also escape phagosomal confinement.

  Based on these criteria (see also page 88), 22 proteins of interest were identified (listed in Table E1).

Table E.1: Summary of some virulence factors employed by pathogenic bacteria to escape autophagy.

Protein	Organism	Gene Accession	Description	*Burkholderia* Protein
IpaA	*Shigella flexneri*	AAP78988 (*ipaA* gene)	Effector protein secreted by TTSS. Promotes depolymerisation of actin filaments. Modulates entry of bacteria into epithelial cells.	
IpaB		AAM89546 (*ipaB* gene)	Regulates TTSS. Chaperoned by IpgC to form an invasion-mediating protein complex. Forms membrane pores. The binding of IpaB to the cystine protease caspase-1 (Casp-1) induces macrophage apoptosis.	BPSS1532
Ipa C		AY206439 (*ipaC* gene)	TTSS. Forms membrane pores. Integrates into host plasma membrane. Required for epithelia cell entry and phagosome escape. Chaperoned by IpgC.	BPSS1531
Ipa D		AF330514 (*ipaD* gene)	Regulates TTSS. Modulates host cell plasma membrane. Required for epithelia cell entry and phagosome escape.	
Ics B		AY206439 (*icsB* gene)	TTSS. Aids in lysis of the secondary phagosome. Chaperoned by IpgA protein which assists in stabilisation and secretion. Binds to VirG protein to inhibit autophagy. Has similar sequence to *Burkholderia pseudomallei* BopA.	
Ipg C		AY206439 (*ipgC* gene)	Chaperones IpaB and IpaC. Prevents IpaB degradation prior to its secretion.	
Vir A		NC_004851 (*virA* gene)	Promotes invasion of host cell. Induces local microtubule degradation	
IcsA Vir G		NC_004851 (*virG* gene)	In mutant cells VirG binds to ATG5 to cause autophagy, in normal *Shigella* IcsB protein competitively binds to VirG to inhibit autophagy therefore enabling escape. Allows for actin based motility.	BPSS0962 BPSS1631
Mgl A	*Francisella tularensis*	AF045772 (*mglA* gene)	Regulates IglC, IglA, pdpA, pdpD. Mutant bacteria cannot escape from the phagosome.	
Igl C		AY293579 (*iglC* gene)	Together with MglA, disrupts the phagolysosome. Mutant bacteria are incapable of intracellular replication and unable to escape from phagosome. Regulated by MglA. Phagosomes with the IglC and MglA mutants, will acquire the lysosomal enzyme cathepsin D, and proceed down the autophagy pathway.	

Protein	Organism	Gene Accession	Description	*Burkholderia* Protein
LLO	*Listeria monocytogenes*	AY168094 (*hyl* gene)	Pore-forming cytolysin. Expressed in the phagosomal compartment to aid in escape from primary phagosome. The production of LLO is modulated by the stress protein Clp-caseinolytic proteins. May be replaced by PFO, ALO or ILO	
PI-PLC		AY168068 (*plcA* gene)	Secretory protein. Expressed in phagosomal compartment. Activates protein kinase C (PKC) cascade which promotes escape from primary phagosome.	
PC-PLC		DQ118415 (*plcB* gene)	Secretory protein. Aids in escape from primary phagosome	
PlcA		NC_002973 (*plcA* gene)	Phospholipase C. Membrane active toxin. Works with PlcB and cytolysin to disrupt phagosomal membrane	
PlcB		NC_002973 (*plcB* gene)	Phospholipase C. Membrane active toxin. Works with PlcA and cytolysin to disrupt phagosomal membrane.	
Svp A		(*svpA* gene)	Surface-Virulence-associated-protein (SvpA). Facilitates the bacterial escape from phagosomes within macrophages. Required for intracellular survival. Mutant bacteria remained confined to phagosomes.	
Sip B	*Salmonella enterica*	AE017220 (*sipB* gene)	*Salmonella* Invasion Protein B (SipB) is homologous for IpaB. Required for invasion of epithelial cells and interacts with Casp-1 to trigger macrophage apoptosis.	
Hemolysin	*Rickettsia prowazekii*	Y11778 (*tlyA* & tlyC gene)	Bacterial protein exotoxin. Optimally active at low pH. It may be involved in the disruption of phagosome membrane.	BPSS0670 BPSS1394
Tc-Tox	*Trypanosoma cruzi*		Transmembrane pore-forming protein involved in vacuole disruption, facilitating the parasite escape. This hemolyosin is active at low pH.	
PFO	*Clostridium perfringens*	AY304477 (*pfo* genes)	Can replace LLO. Cholesterol-dependent cytolysin that oligomerises to form pores, aiding in escape from phagosome. Exerts a toxic effect on the host cells by damaging the plasma membrane, preventing further intracellular proliferations.	
ALO	*Bacillus anthracic*		Can replace LLO in mediating escape from the primary phagosome. However, ALO exerts a toxic effect on the host cells by damaging the plasma membrane. Has 87% similarity to PFO, and 64% similarity to LLO.	
ILO	*Listeria ivanovii*	X60461 (*ilo* gene)	Amino acid sequence of LLO and ILO is very similar. It is not cytotoxic, promoting normal intracellular multiplications. Can functionally replace LLO for efficient phagosomal escape.	